Table of Contents

Acknowledgements

A.A.Balkema Publishers

Order Form:

Hoek, E., P.K.Kaiser & W.F.Bawden:
Support of underground excavations in hard rock
1995, 28 cm, 232 pages

☐ Hard cover edition (90 5410 186 5)   Dutch fl.95 / US $45.00 / UK £32
☐ Student edition (paper back) (90 5410 187 3)   Dutch fl.45/ US $19.50/ UK £16

A comprehensive volume dealing with the design of rockbolts, dowels, cables bolts and shotcrete for underground excavations in hard rock. Many practical examples are given and extensive use is made of user-friendly software developed specifically for this application (available separate). Topics covered include rock mass classification systems, shear strength of discontinuities, analysis of structurally controlled failures, in situ and included stresses, estimating rock mass strength, support design for overstressed rock as well as discussions on different types of underground support.

Please fill out the following to order the book:

Personal Information (Please print)

Name:	
Address:	
City:	
Zipcode:	
Country:	
Telephone:	
Telefax:	
e-mail:	

Type of payement

☐ pro-forma invoice (postage will be charged extra)
☐ Travellers cheque
☐ Personal cheque (drawn on a bank in USA or UK)
☐ Credit card (Deliveries are made only to the address of the account or credit card holder)

Card Type and Number: …………………/……………………………
Expiry Date: ……………………………………………………………

Signature: …………………………………………………………………

Bankers: ING Bank, Schiekade, Rotterdam. Account No.: 69.52.62.904

1

Development of rock engineering

1.1 Introduction

We tend to think of rock mechanics as a modern engineering discipline and yet, as early as 1773, Coulomb included results of tests on rocks from Bordeaux in a paper read before the French Academy in Paris (Coulomb (1776), Heyman (1972)). French engineers started construction of the Panama Canal in 1884 and this task was taken over by the US Army Corps of Engineers in 1908. In the half century between 1910 and 1964, 60 slides were recorded in cuts along the canal and, although these slides were not analysed in rock mechanics terms, recent work by the US Corps of Engineers (Lutton et al (1979)) shows that these slides were predominantly controlled by structural discontinuities and that modern rock mechanics concepts are fully applicable to the analysis of these failures. In discussing the Panama Canal slides in his Presidential Address to the first international conference on Soil Mechanics and Foundation Engineering in 1936, Karl Terzaghi (Terzaghi (1936), Terzaghi and Voight (1979)) said 'The catastrophic descent of the slopes of the deepest cut of the Panama Canal issued a warning that we were overstepping the limits of our ability to predict the consequences of our actions ....'.

In 1920 Josef Stini started teaching 'Technical Geology' at the Vienna Technical University and before he died in 1958 he had published 333 papers and books (Müller (1979)). He founded the journal *Geologie und Bauwesen*, the forerunner of today's journal *Rock Mechanics*, and was probably the first to emphasise the importance of structural discontinuities on the engineering behaviour of rock masses.

Other notable scientists and engineers from a variety of disciplines did some interesting work on rock behaviour during the early part of this century. von Karman (1911), King (1912), Griggs (1936), Ide (1936), and Terzaghi (1945) all worked on the failure of rock materials. In 1921 Griffith proposed his theory of brittle material failure and, in 1931 Bucky started using a centrifuge to study the failure of mine models under simulated gravity loading.

None of these persons would have classified themselves as rock mechanics engineers - the title had not been invented at that time - but all of them made significant contributions to the fundamental basis of the subject as we know it today. I have made no attempt to provide an exhaustive list of papers related to rock mechanics which were published before 1960 but the references given above will show that important developments in the subject were taking place well before that date.

Figure 1.1a: The Vajont dam during impounding of the reservoir. In the middle distance, in the centre of the picture, is Mount Toc with the unstable slope visible as a white scar on the mountain side above the waterline.

Figure 1.1b: During the filling of the Vajont reservoir the toe of the slope on Mount Toc was submerged and this precipitated a slide. The mound of debris from the slide is visible in the central part of the photograph. The very rapid descent of the slide material displaced the water in the reservoir causing a 100 m high wave to overtop the dam wall. The dam itself, visible in the foreground, was largely undamaged.

Figure 1.1c: The town of Longarone, located downstream of the Vajont dam, before the Mount Toc failure in October 1963.

Figure 1.1d: The remains of the town of Longarone after the flood caused by the overtopping of the Vajont dam as a result of the Mount Toc failure. More than 2000 persons were killed in this flood.

The early 1960s were very important in the general development of rock mechanics world-wide because a number of catastrophic failures occurred which clearly demonstrated that, in rock as well as in soil, 'we were over-stepping the limits of our ability to predict the consequences of our actions' (Terzaghi and Voight (1979)).

In December 1959 the foundation of the Malpasset concrete arch dam in France failed and the resulting flood killed about 450 people. In October 1963 about 2500 people in the Italian town of Longarone were killed as a result of a landslide generated wave which overtopped the Vajont dam. These two disasters had a major impact on rock mechanics in civil engineering and a large number of papers were written on the possible causes of the failures (Jaeger (1972)).

In 1960 a coal mine at Coalbrook in South Africa collapsed with the loss of 432 lives. This event was responsible for the initiation of an intensive research programme which resulted in major advances in the methods used for designing coal pillars (Salamon and Munro (1967)).

The formal development of rock mechanics as an engineering discipline in its own right dates from this period in the early 1960s and I will attempt to review these developments in the following chapters of these notes. I consider myself extremely fortunate to have been intimately involved in the subject since 1958. I have also been fortunate to have been in positions which required extensive travel and which have brought me into personal contact with most of the persons with whom the development of modern rock mechanics is associated.

1.2 Rockbursts and elastic theory

Rockbursts are explosive failures of rock which occur when very high stress concentrations are induced around underground openings. The problem is particularly acute in deep level mining in hard brittle rock. Figure 1.2 shows the damage resulting from a rockburst in an underground mine. The deep level gold mines in the Witwatersrand area in South Africa, the Kolar gold mines in India, the nickel mines centred on Sudbury in Canada, the mines in the Coeur d'Alene area in Idaho in the USA and the gold mines in the Kalgoorlie area in Australia, are amongst the mines which have suffered from rockburst problems.

As early as 1935 the deep level nickel mines near Sudbury were experiencing rockburst problems and a report on these problems was prepared by Morrison in 1942 . Morrison also worked on rockburst problems in the Kolar gold fields in India and describes some of these problems in his book, *A Philosophy of Ground Control* (1976).

Early work on rockbursts in South African gold mines was reported by Gane et al (1946) and a summary of rockburst research up to 1966 was presented by Cook et al (1966). Work on the seismic location of rockbursts by Cook (1963) resulted in a significant improvement of our understanding of the mechanics of rockbursting and laid the foundations for the microseismic monitoring systems which are now common in mines with rockburst problems.

A characteristic of almost all rockbursts is that they occur in highly stressed, brittle rock. Consequently, the analysis of stresses induced around underground mining excavations, a key in the generation of rockbursts, can be dealt with by means of the

theory of elasticity. Much of the early work in rock mechanics applied to mining was focused on the problem of rockbursts and this work is dominated by theoretical solutions which assume isotropic elastic rock and which make no provision for the role of structural discontinuities. In the first edition of Jaeger and Cook's book *Fundamentals of Rock Mechanics* (1969), mention of structural discontinuities occurs on about a dozen of the 500 pages of the book. This comment does not imply criticism of this outstanding book but it illustrates the dominance of elastic theory in the approach to rock mechanics associated with deep-level mining problems. Books by Coates (1966) and by Obert and Duvall (1967) reflect the same emphasis on elastic theory.

This emphasis on the use of elastic theory for the study of rock mechanics problems was particularly strong in the English speaking world and it had both advantages and disadvantages. The disadvantage was that it ignored the critical role of structural features. The advantage was that the tremendous concentration of effort on this approach resulted in advances which may not have occurred if the approach had been more general.

Many mines and large civil engineering projects have benefited from this early work in the application of elastic theory and most of the modern underground excavation design methods have their origins in this work.

Figure 1.2: The results of a rockburst in an underground mine in brittle rock subjected to very high stresses.

Figure 1.3: A wedge failure controlled by intersecting structural features
in the rock mass forming the bench of an open pit mine.

1.3   Discontinuous rock masses

Stini was one of the pioneers of rock mechanics in Europe and he emphasised the
importance of structural discontinuities in controlling the behaviour of rock masses
(Müller (1979)). Stini was involved in a wide range of near-surface civil engineering

works and it is not surprising that his emphasis was on the role of discontinuities since this was obviously the dominant problem in all his work. Similarly, the text book by Talobre (1957), reflecting the French approach to rock mechanics, recognised the role of structure to a much greater extent than did the texts of Jaeger and Cook, Coates and Obert and Duvall.

A major impetus was given to this work by the Malpasset dam failure and the Vajont disaster mentioned earlier. The outstanding work by Londe and his co-workers in France (Londe (1965)), Londe et al (1969,1970)) and by Wittke (1965) and John (1968) in Germany laid the foundation for the three-dimensional structural analyses which we have available today. Figure 1.3 shows a wedge failure controlled by two intersecting structural features in the bench of an open pit mine.

1.4 Engineering rock mechanics

Civil and mining engineers have been building structures on or in rock for centuries and the principles of engineering in rock have been understood for a long time. Rock mechanics is merely a formal expression of some of these principles and it is only during the past few decades that the theory and practice in this subject have come together in the discipline which we know today as rock mechanics. A particularly important event in the development of the subject was the merging of elastic theory, which dominated the English language literature on the subject, with the discontinuum approach of the Europeans. The gradual recognition that rock could act both as an elastic material and a discontinuous mass resulted in a much more mature approach to the subject than had previously been the case. At the same time, the subject borrowed techniques for dealing with soft rocks and clays from soil mechanics and recognised the importance of viscoelastic and rheological behaviour in materials such as salt and potash.

I should point out that significant work on rock mechanics was being carried out in countries such as Russia, Japan and China during the 25 years covered by this review but,due to language differences, this work was almost unknown in the English language and European rock mechanics centres and almost none of it was incorporated into the literature produced by these centres.

1.5 Geological data collection

The corner-stone of any practical rock mechanics analysis is the geological data base upon which the definition of rock types, structural discontinuities and material properties is based. Even the most sophisticated analysis can become a meaningless exercise if the geological information upon which it is based is inadequate or inaccurate.

Methods for the collection of geological data have not changed a great deal over the past 25 years and there is still no acceptable substitute for the field mapping and core logging. There have been some advances in the equipment used for such logging and a typical example is the electronic compass illustrated in Figure 1.4. The emergence of geological engineering or engineering geology as recognised university degree courses has been an important step in the development of rock mechanics. These courses train geologists to be specialists in the recognition and interpretation of geological information which is significant in engineering design. These geological engineers, following in the

tradition started by Stini in the 1920s, play an increasingly important role in modern rock engineering.

Once the geological data have been collected, computer processing of this data can be of great assistance in plotting the information and in the interpretation of statistically significant trends. Figure 1.5 illustrates a plot of contoured pole concentrations and corresponding great circles produced by the program DIPS[1] developed at the University of Toronto.

Surface and down-hole geophysical tools and devices such as borehole cameras have been available for several years and their reliability and usefulness has gradually improved as electronic components and manufacturing techniques have been improved. However, current capital and operating costs of these tools are high and these factors, together with uncertainties associated with the interpretation of the information obtained from them, have tended to restrict their use in rock engineering. It is probable that the use of these tools will become more widespread in years to come as further developments occur.

1.6 Laboratory testing of rock

There has always been a tendency to equate rock mechanics with laboratory testing of rock specimens and hence laboratory testing has played a disproportionately large role in the subject. This does not imply that laboratory testing is not important but I would suggest that only about 10 to 20 percent of a well balanced rock mechanics program should be allocated to laboratory testing.

Laboratory testing techniques have been borrowed from civil and mechanical engineering and have remained largely unaltered for the past 25 years. An exception has been the development of servo-controlled stiff testing machines which permit the determination of the complete stress-strain curve for rocks. This information is important in the design of underground excavations since the properties of the failed rock surrounding the excavations have a significant influence upon the stability of the excavations.

1.7 Rock mass classification

A major deficiency of laboratory testing of rock specimens is that the specimens are limited in size and therefore represent a very small and highly selective sample of the rock mass from which they were removed. In a typical engineering project, the samples tested in the laboratory represent only a very small fraction of one percent of the volume of the rock mass. In addition, since only those specimens which survive the collection and preparation process are tested, the results of these tests represent a highly biased sample. How then can these results be used to estimate the properties of the in situ rock mass ?

In an attempt to provide guidance on the properties of rock masses upon which the selection of tunnel support systems can be based, a number of rock mass classification systems have been developed.

---

[1] Available from Rocscience Inc., 31 Balsam Ave., Toronto, Ontario, Canada M4E 3B5 tel: 1-416-698-8217

fax: 1-416-698-0908   email: software@rocscience.com
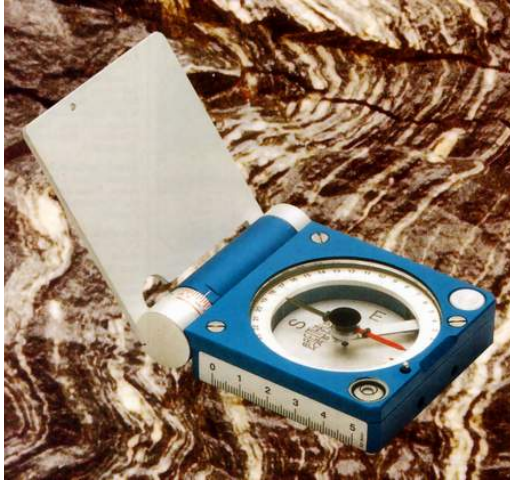
Gekom - Small Stratum Compass

Cocla – Geological Stratum compass

Tectronic 4000 – Geological data collector

Figure 1.4: Geological compasses manufactured by F.W. Breihapt & Sohn, P.O. Box 10 05 69, D-3500 Kassel. W. Germany.
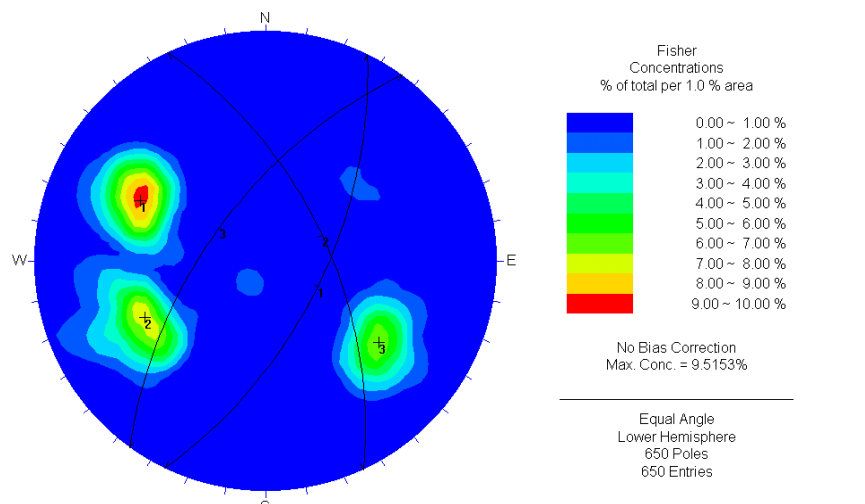
Figure 1.5: Plot of structural features using the program DIPS.

Typical of these classifications are those published by Bieniawski (1973, 1974) and by Barton, Lien and Lunde (1974). These classifications include information on the strength of the intact rock material, the spacing, number and surface properties of the structural discontinuities as well as allowances for the influence of subsurface groundwater, in situ stresses and the orientation and inclination of dominant discontinuities. Figure 1.6 reproduces a chart, published by Barton (1989), which can be used for selecting different types of support for underground excavations on the basis of the rock mass classification published by Barton, Lien and Lunde (1974).

These rock mass classification systems have proved to be very useful practical engineering tools, not only because they provide a starting point for the design of tunnel support but also because they force users to examine the properties of the rock mass in a very systematic manner. The engineering judgements which can be made as a result of the familiarity and understanding gained from this systematic study are probably as useful as any of the calculations associated with the classification systems.
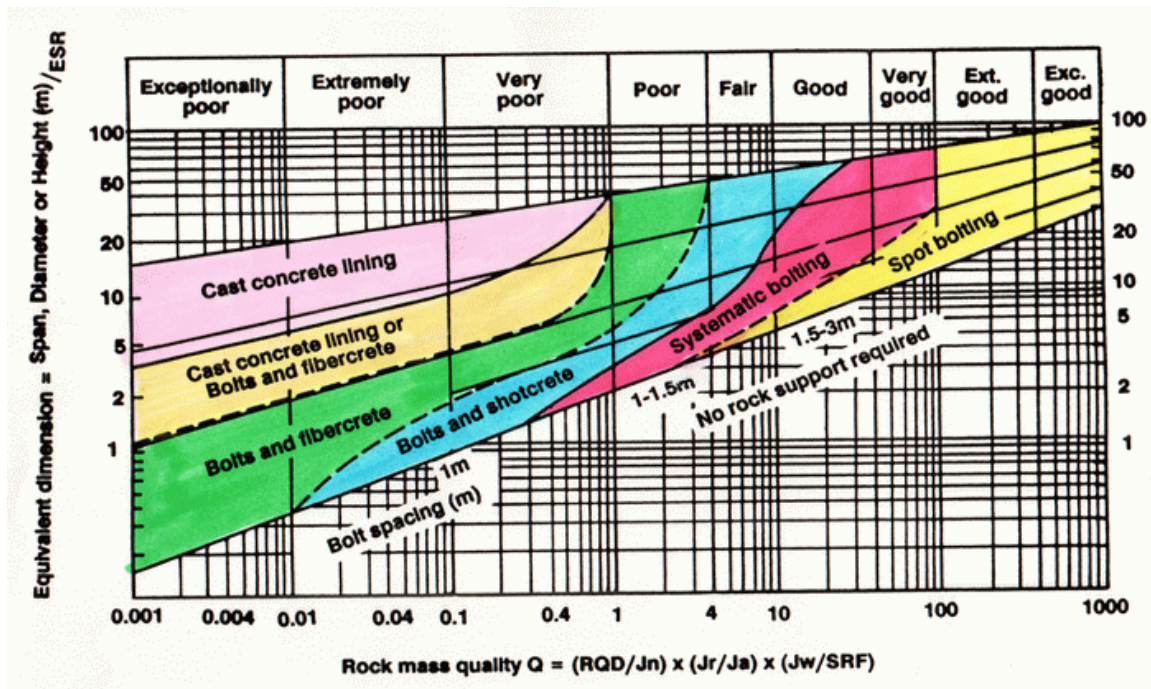
Figure 1.6: Chart for preliminary selection of support for underground excavations on the basis of the Tunnelling Quality Index Q published by Barton, Lien and Lunde (1974). The Excavation Support Ratio ESR depends upon the application for which the underground excavation has been designed. After Barton (1989).

1.8 Rock mass strength

One of the major problems confronting designers of engineering structures in rock is that of estimating the strength of the rock mass. This rock mass is usually made up of an interlocking matrix of discrete blocks. These blocks may have been weathered to varying degrees and the contact surfaces between the blocks may vary from clean and fresh to clay covered and slickensided.

Determination of the strength of an in situ rock mass by laboratory type testing is generally not practical. Hence this strength must be estimated from geological observations and from test results on individual rock pieces or rock surfaces which have been removed from the rock mass. This question has been discussed extensively by Hoek and Brown (1980) who used the results of theoretical (Hoek (1968)) and model studies (Brown (1970), Ladanyi and Archambault (1970)) and the limited amount of available strength data, to develop an empirical failure criterion for jointed rock masses. Hoek (1983) also proposed that the rock mass classification systems, described in the previous section of this paper, can be used for estimating the rock mass constants required for this empirical failure criterion. Practical application of this failure criterion in a number of engineering projects has shown that these estimates are reasonably good for disturbed rock masses but that, in tightly interlocked undisturbed rock masses such as those which may be encountered in tunnelling, the estimated strength values are too low. Further work is required to improve the Hoek-Brown and other failure criteria for jointed rock masses and some ideas on this topic are discussed in a later chapter in these notes.

1.9 In situ stress measurements

The stability of deep underground excavations depends upon the strength of the rock mass surrounding the excavations and upon the stresses induced in this rock. These induced stresses are a function of the shape of the excavations and the in situ stresses which existed before the creation of the excavations. The magnitudes of pre-existing in situ stresses have been found to vary widely, depending upon the geological history of the rock mass in which they are measured (Hoek and Brown (1980)). Theoretical predictions of these stresses are considered to be unreliable and, hence, measurement of the actual in situ stresses is necessary for major underground excavation design. A phenomenon which is frequently observed in massive rock subjected to high in situ stresses is 'core disking', illustrated in Figure 1.7.

During early site investigations, when no underground access is available, the only practical method for measuring in situ stresses is hydrofracturing (Haimson (1978)) in which the hydraulic pressure required to open existing cracks is used to estimate in situ stress levels. Once underground access is available, overcoring techniques for in situ stress measurement (Leeman and Hayes (1966), Worotnicki and Walton (1976)) can be used and, provided that sufficient care is taken in executing the measurements, the results are usually adequate for design purposes. One of the instruments used for in situ stress measurement is illustrated in Figure 1.8.

Figure 1.7: Disking of a 150 mm core of granite as a result of high in situ stresses.
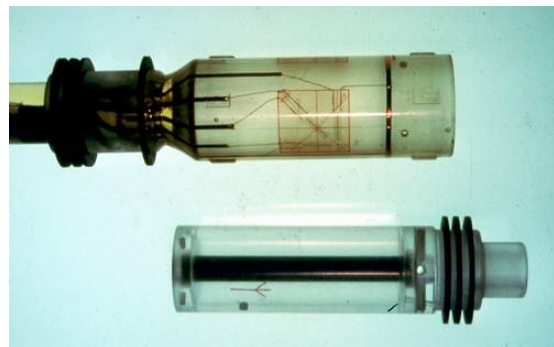
Figure 1.8: A cell for measuring the in situ triaxial stress field in a rock mass, developed in Australia (Worotnicki and Walton 1976).

1.10 Groundwater problems

The presence of large volumes of groundwater is an operational problem in tunnelling but water pressures are generally not too serious a problem in underground excavation engineering (Hoek (1982)). Exceptions are pressure tunnels associated with hydroelectric projects. In these cases, inadequate confining stresses due to insufficient depth of burial of the tunnel can cause serious problems in the tunnel and in the adjacent slopes. The steel linings for these tunnels can cost several thousand dollars per metre and are frequently a critical factor in the design of a hydroelectric project. The installation of a steel tunnel lining is illustrated in Figure 1.9.

Groundwater pressures are a major factor in all slope stability problems and an understanding of the role of subsurface groundwater is an essential requirement for any meaningful slope design (Hoek and Bray (1981), Brown (1982)).

Figure 1.9: Installation of steel lining in a pressure tunnel in a hydroelectric project.

While the actual distributions of water pressures in rock slopes are probably much more complex than the simple distributions normally assumed in slope stability analyses (Freeze and Cherry (1979)), sensitivity studies based upon these simple assumptions are generally adequate for the design of drainage systems (Masur and Kaufman (1962)). Monitoring of groundwater pressures by means of piezometers (Brown (1982)) is the most reliable means of establishing the input parameters for these groundwater models and for checking upon the effectiveness of drainage measures

In the case of dams, forces generated by the water acting on the upstream face of the dam and water pressures generated in the foundations are critical in the assessment of the stability of the dam. Estimates of the water pressure distribution in the foundations and of the influence of grout and drainage curtains upon this distribution have to be made with care since they have a significant impact upon the overall dam and foundation design (Soos (1979)).

The major advances which have been made in the groundwater field during the past decade have been in the understanding of the transport of pollutants by groundwater. Because of the urgency associated with nuclear and toxic waste disposal in industrialised countries, there has been a concentration of research effort in this field and advances have been impressive. The results of this research do not have a direct impact on conventional geotechnical engineering but there have been many indirect benefits from the development of instrumentation and computer software which can be applied to both waste disposal and geotechnical problems.

1.11 Rock reinforcement

Safety during construction and long term stability are factors which have to be considered by the designers of excavations in rock. It is not unusual for these requirements to lead to a need for the installation of some form of rock support. Fortunately, practical developments in this field have been significant during the past 25 years and today's rock engineer has a wide choice of support systems (Hoek and Brown (1980), Hoek (1982), Farmer and Shelton (1980)).

In tunnelling, there is still an important role for steel sets and concrete lining in dealing with very poor ground but, in slightly better ground, the use of combinations of rockbolts and shotcrete has become very common. The use of long untensioned grouted cables in underground mining (Clifford (1974), Fuller (1983), Hunt and Askew (1977), Brady and Brown (1985)) has been a particularly important innovation which has resulted in significant improvements in safety and mining costs in massive ore bodies. The lessons learned from these mining systems have been applied with considerable success in civil engineering and the use of untensioned dowels, installed as close as possible to the advancing face, has many advantages in high speed tunnel construction. The use of untensioned grouted cables or reinforcing bars has also proved to be a very effective and economical technique in rock slope stabilisation. This reinforcement is installed progressively as the slope is benched downward and it is very effective in knitting the rock mass together and preventing the initiation of ravelling.

The design of rock support systems tends to be based upon empirical rules generated from experience (Lang (1961), Endersbee and Hofto (1963), Cording, Hendron and Deere (1971)) and currently available analytical models are not very reliable. Some interesting theoretical models, which provide a very clear understanding of the mechanics

of rock support in tunnels, have been developed in recent years (Rabcewicz (1969), Daeman (1977), Brown et al (1983), Brown and Bray (1982)). These models have to be used with caution when designing actual tunnel support since they are based upon very simple assumptions and rock conditions underground may vary from these assumptions. With the development of powerful numerical models such as that described by Lorig and Brady (1984), more realistic and reliable support designs will eventually become possible but it will be several years before these models can be used as design tools.

1.12 Excavation methods in rock

As pointed out earlier, the strength of jointed rock masses is very much dependent upon the interlocking between individual rock pieces. This interlocking is easily destroyed and careless blasting during excavation is one of the most common causes of underground excavation instability. The following quotation is taken from a paper by Holmberg and Persson (1980):

The innocent rock mass is often blamed for insufficient stability that is actually the result of rough and careless blasting. Where no precautions have been taken to avoid blasting damage, no knowledge of the real stability of the undisturbed rock can be gained from looking at the remaining rock wall. What one sees are the sad remains of what could have been a perfectly safe and stable rock face.

Techniques for controlling blast damage in rock are well-known (Svanholm et al (1977), Langefors and Kihlstrom (1963), Hagan (1980)) but it is sometimes difficult to persuade owners and contractors that the application of these techniques is worthwhile. Experience in projects in which carefully controlled blasting has been used generally shows that the amount of support can be reduced significantly and that the overall cost of excavation and support is lower than in the case of poorly blasted excavations (Hoek (1982)). Examples of poor and good quality blasting in tunnels are illustrated in Figures 1.10 and 1.11.

Machine excavation is a technique which causes very little disturbance to the rock surrounding an underground excavation. A wide range of tunnelling machines have been developed over the past 25 years and these machines are now capable of working in almost all rock types (Robbins (1976), McFeat-Smith (1982)). Further development of these machines can be expected and it is probable that machine excavation will play a much more important role in future tunnelling than it does today.

1.13 Analytical tools

Analytical models have always played an important role in rock mechanics. The earliest models date back to closed form solutions such as that for calculating the stresses surrounding a circular hole in a stressed plate published by Kirsch in 1898. The development of the computer in the early 1960s made possible the use of iterative numerical techniques such as finite element (Clough (1960)), boundary element (Crouch and Starfield (1983)), discrete element (Cundall (1971)) and combinations of these methods (von Kimmelmann et al (1984), Lorig and Brady (1984)). These have become almost universal tools in rock mechanics.

Figure 1.10: An example of poor blasting in a tunnel.

Figure 1.11: An example of good blasting in a tunnel.

The computer has also made it much more convenient to use powerful limit equilibrium methods (Sarma (1979), Brown and Ferguson (1979), Shi and Goodman (1981), Warburton (1981)) and probabilistic approaches (McMahon (1971), Morriss and Stoter (1983), Priest and Brown (1982), Read and Lye (1983)) for rock mechanics studies.

The recent advent of the micro-computer and the rapid developments which have taken place in inexpensive hardware have brought us close to the era of a computer on every professional's desk. The power of these machines is transforming our approach to rock mechanics analysis since it is now possible to perform a large number of sensitivity or probabilistic studies in a fraction of the time which was required for a single analysis a few years ago. Given the inherently inhomogeneous nature of rock masses, such sensitivity studies enable us to explore the influence of variations in the value of each input parameter and to base our engineering judgements upon the rate of change in the calculated value rather than on a single answer.

1.14 Conclusions

Over the past 25 years, rock mechanics has developed into a mature subject which is built on a solid foundation of geology and engineering mechanics. Individuals drawn from many different disciplines have contributed to this subject and have developed a wide range of practical tools and techniques. There is still a great deal of room for development, innovation and improvement in almost every aspect of the subject and it is a field which will continue to provide exciting challenges for many years to come.

2

When is a rock engineering design acceptable

2.1   Introduction

When is a design in rock engineering acceptable? The aim of the following text[1] is to demonstrate that there are no simple universal rules for acceptability nor are there standard factors of safety which can be used to guarantee that a rock structure will be safe and that it will perform adequately. Each design is unique and the acceptability of the structure has to be considered in terms of the particular set of circumstances, rock types, design loads and end uses for which it is intended. The responsibility of the geotechnical engineer is to find a safe and economical solution which is compatible with all the constraints which apply to the project. Such a solution should be based upon engineering judgement guided by practical and theoretical studies such as stability or deformation analyses, if and when these analyses are applicable.

Tables 1 to 4 summarise some of the typical problems, critical parameters, analysis methods and acceptability criteria which apply to a number of different rock engineering structures. These examples have been drawn from my own consulting experience and I make no claims that this is a complete list nor do I expect readers to agree with all of the items which I have included under the various headings. The purpose of presenting these tables is to demonstrate the diversity of problems and criteria which have to be considered and to emphasise the dangers of attempting to use standard factors of safety or other acceptability criteria.

In order to amplify some of the items included in Tables 1 to 4, several case histories will be discussed in terms of the factors which were considered and the acceptability criteria which were used.

2.2   Landslides in reservoirs

The presence of unstable slopes in reservoirs is a major concern for the designers of dams for hydroelectric and irrigation projects. The Vajont failure in 1963 alerted the engineering community of the danger of underestimating the potential for the mobilisation of existing landslides as a result of submergence of the slide toe during impounding of the reservoir.

---

[1]Based upon the text of the Müller lecture presented at the 7th Congress of the International Society for Rock Mechanics held in Aachen, Germany, in September 1991.

Table 1 : Typical problems, critical parameters, methods of analysis and acceptability criteria for slopes.
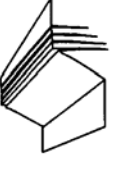
STRUCTURE	TYPICAL PROBLEMS	CRITICAL PARAMETERS	ANALYSIS METHODS	ACCEPTABILITY CRITERIA
Landslides.	Complex failure along a circular or near circular failure surface involving sliding on faults and other structural features as well as failure of intact materials.	• Presence of regional faults. • Shear strength of materials along failure surface. • Groundwater distribution in slope, particularly in response to rainfall or to submergence of slope toe. • Potential earthquake loading.	Limit equilibrium methods which allow for non-circular failure surfaces can be used to estimate changes in factor of safety as a result of drainage or slope profile changes. Numerical methods such as finite element or discrete element analysis can be used to investigate failure mechanisms and history of slope displacement.	Absolute value of factor of safety has little meaning but rate of change of factor of safety can be used to judge effectiveness of remedial measures. Long term monitoring of surface and subsurface displacements in slope is the only practical means of evaluating slope behaviour and effectiveness of remedial action.
Soil or heavily jointed rock slopes.	Circular failure along a spoon-shaped surface through soil or heavily jointed rock masses.	• Height and angle of slope face. • Shear strength of materials along failure surface. • Groundwater distribution in slope. • Potential surcharge or earthquake loading.	Two-dimensional limit equilibrium methods which include automatic searching for the critical failure surface are used for parametric studies of factor of safety. Probability analyses, three-dimensional limit equilibrium analyses or numerical stress analyses are occasionally used to investigate unusual slope problems.	Factor of safety > 1.3 for "temporary" slopes with minimal risk of damage. Factor of safety > 1.5 for "permanent" slopes with significant risk of damage. Where displacements are critical, numerical analyses of slope deformation may be required and higher factors of safety will generally apply in these cases.
Jointed rock slopes.	Planar or wedge sliding on one structural feature or along the line of intersection of two structural features.	• Slope height, angle and orientation. • Dip and strike of structural features. • Groundwater distribution in slope. • Potential earthquake loading. • Sequence of excavation and support installation.	Limit equilibrium analyses which determine three-dimensional sliding modes are used for parametric studies on factor of safety. Failure probability analyses, based upon distribution of structural orientations and shear strengths, are useful for some applications.	Factor of safety > 1.3 for "temporary" slopes with minimal risk of damage. Factor of safety > 1.5 for "permanent" slopes with significant risk of damage. Probability of failure of 10 to 15% may be acceptable for open pit mine slopes where cost of clean up is less than cost of stabilization.
Vertically jointed rock slopes.	Toppling of columns separated from the rock mass by steeply dipping structural features which are parallel or nearly parallel to the slope face.	• Slope height, angle and orientation. • Dip and strike of structural features. • Groundwater distribution in slope. • Potential earthquake loading.	Crude limit equilibrium analyses of simplified block models are useful for estimating potential for toppling and sliding. Discrete element models of simplified slope geometry can be used for exploring toppling failure mechanisms.	No generally acceptable criterion for toppling failure is available although potential for toppling is usually obvious. Monitoring of slope displacements is the only practical means of determining slope behaviour and effectiveness of remedial measures.
Loose boulders on rock slopes.	Sliding, rolling, falling and bouncing of loose rocks and boulders on the slope.	• Geometry of slope. • Presence of loose boulders. • Coefficients of restitution of materials forming slope. • Presence of structures to arrest falling and bouncing rocks.	Calculation of trajectories of falling or bouncing rocks based upon velocity changes at each impact is generally adequate. Monte Carlo analyses of many trajectories based upon variation of slope geometry and surface properties give useful information on distribution of fallen rocks.	Location of fallen rock or distribution of a large number of fallen rocks will give an indication of the magnitude of the potential rockfall problem and of the effectiveness of remedial measures such as draped mesh, catch fences and ditches at the toe of the slope.

Table 2 : Typical problems, critical parameters, methods of analysis and acceptability criteria for dams and foundations.
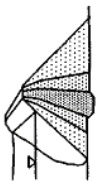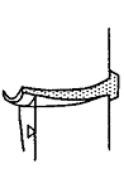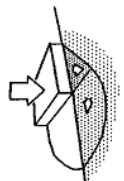
STRUCTURE	TYPICAL PROBLEMS	CRITICAL PARAMETERS	ANALYSIS METHODS	ACCEPTABILITY CRITERIA
Zoned fill dams.	Circular or near-circular failure of dam, particularly during rapid drawdown. Foundation failure on weak seams. Piping and erosion of core.	• Presence of weak or permeable zones in foundation. • Shear strength, durability, gradation and placement of dam construction materials, particularly filters. • Effectiveness of grout curtain and drainage system. • Stability of reservoir slopes.	Seepage analyses are required to determine water pressure and velocity distribution through dam and abutments. Limit equilibrium methods should be used for parametric studies of stability. Numerical methods can be used to investigate dynamic response of dam during earthquakes.	Safety factor >1.5 for full pool with steady state seepage; >1.3 for end of construction with no reservoir loading and undissipated foundation porewater pressures; >1.2 for probable maximum flood with steady state seepage and >1.0 for full pool with steady state seepage and maximum credible horizontal psuedo-static seismic loading.
Gravity dams.	Shear failure of interface between concrete and rock or of foundation rock. Tension crack formation at heel of dam. Leakage through foundations or abutments.	• Presence of weak or permeable zones in rock mass. • Shear strength of interface between concrete and rock. • Shear strength of rock mass. • Effectiveness of grout curtain and drainage system. • Stability of reservoir slopes.	Parametric studies using limit equilibrium methods should be used to investigate sliding on the interface between concrete and rock and sliding on weak seams in the foundation. A large number of trial failure surfaces are required unless a non-circular failure analysis with automatic detection of critical failure surfaces is available.	Safety factor against foundation failure should exceed 1.5 for normal full pool operating conditions provided that conservative shear strength values are used ($c' \approx 0$). Safety factor > 1.3 for probable maximum flood (PMF). Safety factor > 1 for extreme loading - maximum credible earthquake and PMF.
Arch dams.	Shear failure in foundation or abutments. Cracking of arch due to differential settlements of foundation. Leakage through foundations or abutments.	• Presence of weak, deformable or permeable zones in rock mass. • Orientation, inclination and shear strength of structural features. • Effectiveness of grout curtain and drainage system. • Stability of reservoir slopes.	Limit equilibrium methods are used for parametric studies of three-dimensional sliding modes in the foundation and abutments, including the influence of water pressures and reinforcement. Three-dimensional numerical analyses are required to determine stresses and displacements in the concrete arch.	Safety factor against foundation failure >1.5 for normal full pool operating conditions and >1.3 for probable maximum flood conditions provided that conservative shear strength values are used ($c' \approx 0$). Stresses and deformations in concrete arch should be within allowable working levels defined in concrete specifications.
Foundations on rock slopes.	Slope failure resulting from excessive foundation loading. Differential settlement due to anisotropic deformation properties of foundation rocks.	• Orientation, inclination and shear strength of structural features in rock mass forming foundation. • Presence of inclined layers with significantly different deformation properties. • Groundwater distribution in slope.	Limit equilibrium analyses of potential planar or wedge failures in the foundation or in adjacent slopes are used for parametric studies of factor of safety. Numerical analyses can be used to determine foundation deformation, particularly for anisotropic rock masses.	Factor of safety against sliding of any potential foundation wedges or blocks should exceed 1.5 for normal operating conditions. Differential settlement should be within limits specified by structural engineers.
Foundations on soft rock or soil.	Bearing capacity failure resulting from shear failure of soils or weak rocks underlying foundation slab.	• Shear strength of soil or jointed rock materials. • Groundwater distribution in soil or rock foundation. • Foundation loading conditions and potential for earthquake loading.	Limit equilibrium analyses using inclined slices and non-circular failure surfaces are used for parametric studies of factor of safety. Numerical analyses may be required to determine deformations, particularly for anisotropic foundation materials.	Bearing capacity failure should not be permitted for normal loading conditions. Differential settlement should be within limits specified by structural engineers.

Table 3 : Typical problems, critical parameters, methods of analysis and acceptability criteria for underground civil engineering excavations.

STRUCTURE	TYPICAL PROBLEMS	CRITICAL PARAMETERS	ANALYSIS METHODS	ACCEPTABILITY CRITERIA
Pressure tunnels in hydro-power projects.	Excessive leakage from unlined or concrete lined tunnels. Rupture or buckling of steel lining due to rock deformation or external pressure.	• Ratio of maximum hydraulic pressure in tunnel to minimum principal stress in the surrounding rock. • Length of steel lining and effectiveness of grouting. • Groundwater levels in the rock mass.	Determination of minimum cover depths along pressure tunnel route from accurate topographic maps. Stress analyses of sections along and across tunnel axis. Comparison between minimum principal stresses and maximum dynamic hydraulic pressure to determine steel lining lengths.	Steel lining is required where the minimum principal stress in the rock is less than 1.3 times the maximum static head for typical hydroelectric operations or 1.15 for operations with very low dynamic pressures. Hydraulic pressure testing in boreholes at the calculated ends of the steel lining is essential to check the design assumptions.
Soft rock tunnels.	Rock failure where strength is exceeded by induced stresses. Swelling, squeezing or excessive closure if support is inadequate.	• Strength of rock mass and of individual structural features. • Swelling potential, particularly of sedimentary rocks. • Excavation method and sequence. • Capacity and installation sequence of support systems.	Stress analyses using numerical methods to determine extent of failure zones and probable displacements in the rock mass. Rock-support interaction analyses using closed-form or numerical methods to determine capacity and installation sequence for support and to estimate displacements in the rock mass.	Capacity of installed support should be sufficient to stabilize the rock mass and to limit closure to an acceptable level. Tunnelling machines and internal structures must be designed for closure of the tunnel as a result of swelling or time-dependent deformation. Monitoring of deformations is an important aspect of construction control.
Shallow tunnels in jointed rock.	Gravity driven falling or sliding wedges or blocks defined by intersecting structural features. Unravelling of inadequately supported surface material.	• Orientation, inclination and shear strength of structural features in the rock mass. • Shape and orientation of excavation. • Quality of drilling and blasting during excavation. • Capacity and installation sequence of support systems.	Spherical projection techniques or analytical methods are used for the determination and visualization of all potential wedges in the rock mass surrounding the tunnel. Limit equilibrium analyses of critical wedges are used for parametric studies on the mode of failure, factor of safety and support requirements.	Factor of safety, including the effects of reinforcement, should exceed 1.5 for sliding and 2.0 for falling wedges and blocks. Support installation sequence is critical and wedges or blocks should be identified and supported before they are fully exposed by excavation. Minimum deformation. Displacement monitoring is of little value.
Large caverns in jointed rock.	Gravity driven falling or sliding wedges or tensile and shear failure of rock mass, depending upon spacing of structural features and magnitude of in situ stresses.	• Shape and orientation of cavern in relation to orientation, inclination and shear strength of structural features in the rock mass. • In situ stresses in the rock mass. • Excavation and support sequence and quality of drilling and blasting.	Spherical projection techniques or analytical methods are used for the determination and visualization of all potential wedges in the rock mass. Stresses and displacements induced by each stage of cavern excavation are determined by numerical analyses and are used to estimate support requirements for the cavern roof and walls.	An acceptable design is achieved when numerical models indicate that the extent of failure has been controlled by installed support, that the support is not overstressed and that the displacements in the rock mass stabilize. Monitoring of displacements is essential to confirm design predictions.
Underground nuclear waste disposal.	Stress and/or thermally induced spalling of the rock surrounding the excavations resulting in increased permeability and higher probability of radioactive leakage.	• Orientation, inclination, permeability and shear strength of structural features in the rock mass. • In situ and thermal stresses in the rock surrounding the excavations. • Groundwater distribution in the rock mass.	Numerical analyses are used to calculate stresses and displacements induced by excavation and by thermal loading from waste canisters. Groundwater flow patterns and velocities, particularly through blast damaged zones, fissures in the rock and shaft seals are calculated using numerical methods.	An acceptable design requires extremely low rates of groundwater movement through the waste canister containment area in order to limit transport of radioactive material. Shafts, tunnels and canister holes must remain stable for approximately 50 years to permit retrieval of waste if necessary.

Table 4 : Typical problems, critical parameters, methods of analysis and acceptability criteria for underground hard rock mining excavations.
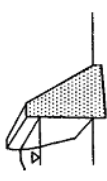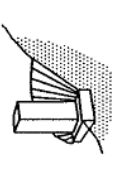
STRUCTURE	TYPICAL PROBLEMS	CRITICAL PARAMETERS	ANALYSIS METHODS	ACCEPTABILITY CRITERIA
Pillars.	Progressive spalling and slabbing of the rock mass leading to eventual pillar collapse or rockbursting.	• Strength of the rock mass forming the pillars. • Presence of unfavourably oriented structural features. • Pillar geometry, particularly width to height ratio. • Overall mine geometry including extraction ratio.	For horizontally bedded deposits, pillar strength from empirical relationships based upon width to height ratios and average pillar stress based on tributary area calculations are compared to give a factor of safety. For more complex mining geometry, numerical analyses including progressive pillar failure may be required.	Factor of safety for simple pillar layouts in horizontally bedded deposits should exceed 1.6 for "permanent" pillars. In cases where progressive failure of complex pillar layouts is modelled, individual pillar failures can be tolerated provided that they do not initiate "domino" failure of adjacent pillars.
Crown pillars.	Caving of surface crown pillars for which the ratio of pillar depth to stope span is inadequate. Rockbursting or gradual spalling of overstressed internal crown pillars.	• Strength of the rock mass forming the pillars. • Depth of weathering and presence of steeply dipping structural features in the case of surface crown pillars. • In situ stress levels and geometry of internal crown pillars.	Rock mass classification and limit equilibrium analyses can give useful guidance on surface crown pillar dimensions for different rock masses. Numerical analyses, including discrete element studies, can give approximate stress levels and indications of zones of potential failure.	Surface crown pillar depth to span ratio should be large enough to ensure very low probability of failure. Internal crown pillars may require extensive support to ensure stability during mining of adjacent stopes. Careful planning of mining sequence may be necessary to avoid high stress levels and rockburst problems.
Cut and fill stopes.	Falls of structurally defined wedges and blocks from stope backs and hanging walls. Stress induced failures and rockbursting in high stress environments.	• Orientation, inclination and shear strength of structural features in the rock mass. • In situ stresses in the rock mass. • Shape and orientation of stope. • Quality, placement and drainage of fill.	Numerical analyses of stresses and displacements for each excavation stage will give some indication of potential problems. Some of the more sophisticated numerical models will permit inclusion of the support provided by fill or the reinforcement of the rock by means of grouted cables.	Local instability should be controlled by the installation of rockbolts or grouted cables to improve safety and to minimize dilution. Overall stability is controlled by the geometry and excavation sequence of the stopes and the quality and sequence of filling. Acceptable mining conditions are achieved when all the ore is recovered safely.
Non-entry stopes.	Ore dilution resulting from rockfalls from stope back and walls. Rockbursting or progressive failure induced by high stresses in pillars between stopes.	• Quality and strength of the rock. • In situ and induced stresses in the rock surrounding the excavations. • Quality of drilling and blasting in excavation of the stope.	Some empirical rules, based on rock mass classification, are available for estimating safe stope dimensions. Numerical analyses of stope layout and mining sequence, using three-dimensional analyses for complex orebody shapes, will provide indications of potential problems and estimates of support requirements.	A design of this type can be considered acceptable when safe and low cost recovery of a large proportion of the orebody has been achieved. Rockfalls in shafts and haulages are an unacceptable safety hazard and pattern support may be required. In high stress environments, local destressing may be used to reduce rockbursting.
Drawpoints and orepasses.	Local rock mass failure resulting from abrasion and wear of poorly supported drawpoints or orepasses. In extreme cases this may lead to loss of stopes or orepasses.	• Quality and strength of the rock. • In situ and induced stresses and stress changes in the rock surrounding the excavations. • Selection and installation sequence of support.	Limit equilibrium or numerical analyses are not particularly useful since the processes of wear and abrasion are not included in these models. Empirical designs based upon previous experience or trial and error methods are generally used.	The shape of the opening should be maintained for the design life of the drawpoint or orepass. Loss of control can result in serious dilution of the ore or abandonment of the excavation. Wear resistant flexible reinforcement such as grouted cables, installed during excavation of the opening, may be successful in controlling instability.

During the construction of the Mica and Revelstoke dams on the Columbia River in British Columbia, Canada, several potential slides were investigated. Two of these, the Downie Slide, a 1.4 billion cubic metre ancient rock slide, and Dutchman's Ridge, a 115 million cubic metre potential rock slide, were given special attention because of the serious consequences which could have resulted from failure of these slides (Imrie (1983), Lewis and Moore (1989), Imrie, Moore and Enegren (1992)).

The Downie Slide and Dutchman's Ridge are located in steep, narrow, V-shaped sections of the Columbia River valley which has been subjected to several episodes of glaciation. The bedrock at these sites consists mainly of Pre-Cambrian para-gneisses and schists within or on the fringe of the Shuswap Metamorphic Complex. In both cases, the potential slide planes, determined by diamond drilling and slope displacement monitoring, are relatively flat-lying outward-dipping tectonic faults or shears which daylight in the base of the river valley.

Based on thorough investigation and monitoring programs, British Columbia Hydro and Power Authority (BC Hydro) decided that remedial measures had to be taken to improve the stability of both the Downie Slide and Dutchman's Ridge. These remedial measures consisted of drainage adits extending within and/or behind the failure surfaces and supplemented by drainholes drilled from chambers excavated along the adits. Work on the Downie Slide was carried out in the period 1977 to 1982 (which included a 3 year observation period) and work on Dutchman's Ridge was carried out from 1986 to 1988.
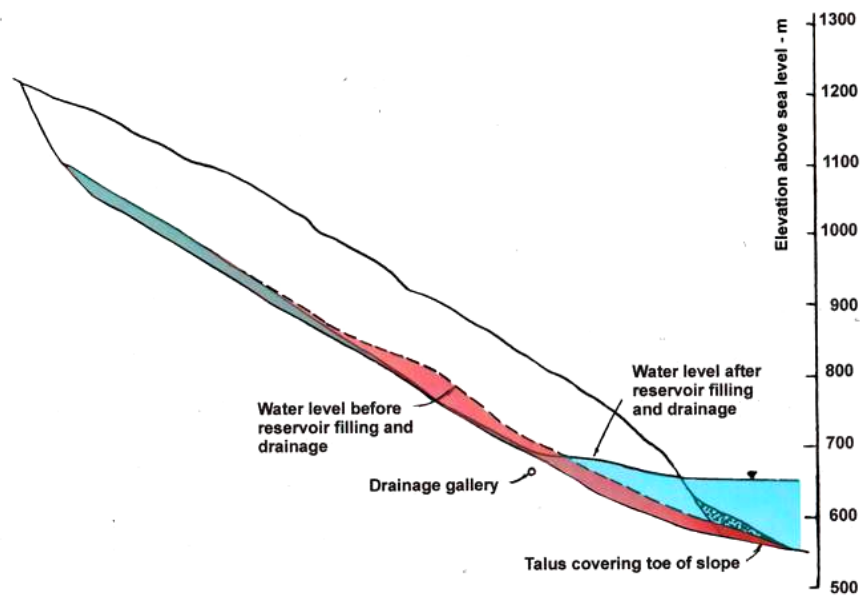
Figure 2.1 : Section through Dutchman's Ridge showing potential slide
surface and water levels before and after drainage.

A section through Dutchman's Ridge is given in Figure 2.1 and this shows the water levels in the slope before reservoir filling and after reservoir filling and the construction of the drainage system. Figure 2.2 shows contours of reduction in water levels as a result of the installation of the drainage system which consisted of 872 m of adit and 12,000 m of drainhole drilling. Note that the drawdown area on the right hand side of the potential slide was achieved by long boreholes from the end of the drainage adit branch.

KINBASKET LAKE
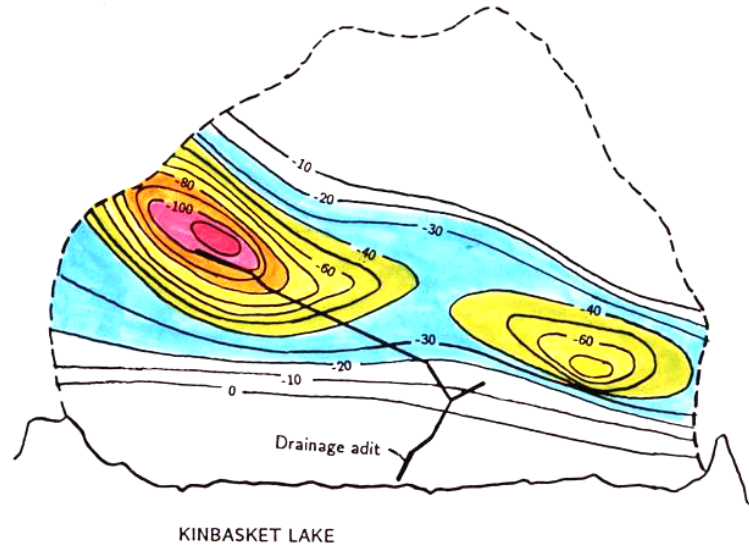
Figure 2.2 : Contours of water level reduction (in metres) as a result of the implementation of drainage in Dutchman's Ridge.

   Comparative studies of the stability of the slope section shown in Figure 2.1, based upon a factor of safety of 1.00 for the slope after reservoir filling but before implementation of the drainage system, gave a factor of safety of 1.06 for the drained slope. This 6% improvement in factor of safety may not seem very significant to the designer of small scale rock and soil slopes but it was considered acceptable in this case for a number of reasons:

1. The factor of safety of 1.00 calculated for the undrained slope is based upon a 'back-analysis' of observed slope behaviour. Provided that the same method of analysis and shear strength parameters are used for the stability analysis of the same slope with different groundwater conditions, the ratio of the factors of safety is a very reliable indicator of the change in slope stability, even if the absolute values of the factor of safety are not accurate. Consequently, the degree of uncertainty, which has to be allowed for in slope designs where no back-analyses have been performed, can be eliminated and a lower factor of safety accepted.

2. The groundwater levels in the slope were reduced by drainage to lower than the pre-reservoir conditions and the stability of the slope is at least as good if not better then these pre-reservoir conditions. This particular slope is considered to have withstood several significant earthquakes during the 10,000 years since the last episode of glaciation which is responsible for the present valley shape.

3. Possibly the most significant indicator of an improvement in stability, for both the Downie Slide and Dutchman's Ridge, has been a significant reduction in the rate of down-slope movement which has been monitored for the past 25 years. In the case of the Downie Slide, this movement has practically ceased. At Dutchman's Ridge, the movements are significantly slower and it is anticipated that they will stabilize when the drainage system has been in operation for a few more years.

2.3   Deformation of rock slopes

In a slope in which the rock is jointed but where there are no significant discontinuities dipping out of the slope which could cause sliding, deformation and failure of the slope is controlled by a complex process of block rotation, tilting and sliding. In an extreme case, where the rock mass consists of near vertical joints separating columns of massive rock, toppling movement and failure may occur.

Figure 2.3 is a section through part of the power tunnel for the Wahleach hydroelectric project in British Columbia, Canada. A break in the steel lining in this power tunnel occurred in January 1989 and it is thought this break was caused by a slow down-slope gravitational movement caused by block rotations within a near-surface zone of loosened jointed rock.
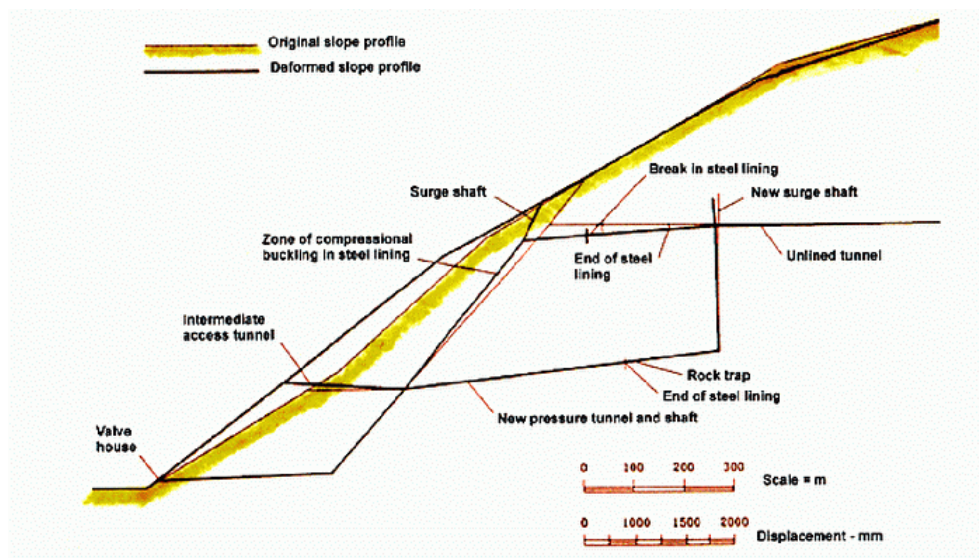
Figure 2.3 : Cross-section through a section of the Wahleach power tunnel showing the original tunnel alignment and the location of the replacement conduit. The dashed line is the approximate location of a gradational boundary between loosened, fractured and weathered rock and more intact rock. Down-slope movement currently being monitored is well above this boundary.

The Wahleach project is located 120 km east of Vancouver and power is generated from 620 m of head between Wahleach Lake and a surface powerhouse located adjacent to the Fraser River. Water flows through a 3500 m long three metre diameter unlined upper tunnel, a rock trap, a 600 m two metre diameter concrete encased steel lined shaft inclined at 48° to the horizontal, a 300 m long lower tunnel and a 485 m long surface penstock to the powerhouse.

The tunnels were excavated mainly in granodiorite which varies from highly fractured and moderately weathered in the upper portions of the slope to moderately fractured and fresh in both the lower portions of the slope and below the highly fractured mass. Two main joint sets occur in the rock mass, one set striking parallel to the slope and the other perpendicular to it. Both dip very steeply. Average joint spacings range from 0.5 to 1 m.

A few joints occur sub-parallel to the ground surface and these joints are most well developed in the ground surface adjacent to the inclined shaft. Thorough investigations failed to reveal any significant shear zones or faults oriented in a direction conducive to sliding.

The toe of the slope is buried beneath colluvial and fan deposits from two creeks which have incised the Fraser Valley slope to form the prominence in which the inclined shaft was excavated. This prominence is crossed by several linear troughs which trend along the ground surface contours and are evidence of previous down-slope movement of the prominence. Mature trees growing in these troughs indicate a history of movement of at least several hundred years (Moore, Imrie and Baker (1991)).

The water conduit operated without incident between the initial filling in 1952 and May 1981 when leakage was first noted from the upper access adit located near the intersection of the inclined shaft and the upper tunnel (see Figure 2.3). This leakage stopped when two drain pipes embedded in the concrete backfill beneath the steel lining were plugged at their upstream ends. Large holes had been eroded in these drainage pipes where they were not encased in concrete and it was concluded that this corrosion was responsible for the leakage. This conclusion appeared to be valid until 25 January, 1989 when a much larger water flow occurred.

Investigations in the dewatered tunnel revealed a 150 mm wide circumferential tension crack in the steel lining of the upper tunnel, about 55 m from its intersection with the inclined shaft. In addition, eight compressional buckle zones were found in the upper portion of the inclined shaft. Subsequent investigations revealed that approximately 20 million cubic metres of rock are involved in down-slope creep which, during 1989-90, amounted to several centimetres per year and which appears to be ongoing. This down-slope creep appears to be related to a process of block rotation rather than to any deep seated sliding as was the case at both the Downie Slide and Dutchman's Ridge.

While discrete element models may give some indication of the overall mechanics of this type of slope deformation, there is no way in which a factor of safety, equivalent to that for sliding failure, can be calculated. Consequently, in deciding upon the remedial measures to be implemented, other factors have to be taken into consideration.

After thorough study by the BC Hydro and their consultants, it was decided to construct a replacement conduit consisting of an unlined shaft and tunnel section and a steel lined section where the rock cover is insufficient to contain the internal pressure in the tunnel. This replacement conduit, illustrated in Figure 2.3, will remove the steel lined portions of the system from zones in which large displacements are likely to occur in the future. This in turn will minimise the risk of a rupture of the steel lining which would inject high pressure water into the slope. It was agreed that such high pressure water leakage could be a cause for instability of the overall slope. Further studies are being undertaken to determine whether additional drainage is required in order to provide further safeguards.

Careful measurements of the displacements in the inclined shaft, the length of the steel lining cans as compared with the original specified lengths and the opening of the tensile crack in the upper portion of the steel lined tunnel, provided an overall picture of the displacements in the rock mass. These observed displacements were compared with displacement patterns computed by means of a number of numerical studies using both

continuum and discrete element models and the results of these studies were used in deciding upon the location of the replacement conduit.

In addition to the construction of this replacement conduit to re-route the water away from the upper and potentially unstable part of the slope, a comprehensive displacement and water pressure monitoring system has been installed and is being monitored by BC Hydro (Baker (1991), Tatchell (1991)).

2.4   Structural failures in rock masses

In slopes, foundations and shallow underground excavations in hard rock, failure is frequently controlled by the presence of discontinuities such as faults, shear zones, bedding planes and joints. The intersection of these structural features can release blocks or wedges which can fall or slide from the surface of the excavation. Failure of the intact rock is seldom a problem in these cases where deformation and failure are caused by sliding along individual discontinuity surfaces or along lines of intersection of surfaces. Separation of planes and rotation of blocks and wedges can also play a role in the deformation and failure process.

An analysis of the stability of these excavations depends primarily upon a correct interpretation of the structural geological conditions in the rock mass followed by a study of the blocks and wedges which can be released by the creation of the excavation. Identification and visualisation of these blocks and wedges is by far the most important part of this analysis. Analysis of the stability of the blocks and wedges, and of the reinforcing forces required to stabilize them, is a relatively simple process once this identification has been carried out.

The Río Grande Pumped Storage Project is located in the Province of Córdoba in the Republic of Argentina. Four reversible pump-turbines operating at an average head of 170 m give the project a total installed capacity of 750 MW. These turbines are installed in a 25 m span, 50 m high, 105 m long cavern at an average depth of 160 m .

The rock in which the underground excavations are situated is a massive tonalitic gneiss of excellent quality (Amos et al (1981)). The gneiss has an average uniaxial compressive strength of 140 MPa. The maximum principal stress, determined by overcoring tests, is 9.4 MPa and is almost horizontal and oriented approximately normal to the cavern axis. In massive rocks, this 15:1 ratio of uniaxial strength to maximum principal stress is unlikely to result in any significant failure in the rock and this was confirmed by numerical stress analyses (Moretto (1982), Sarra Pistone and del Río (1982)). The principal type of instability which had to be dealt with in the underground excavations was that of potentially unstable blocks and wedges defined by intersecting structural features (Hammett and Hoek, (1981)).   In one section of the cavern, the axis of which is oriented in the direction 158-338, four joint sets were mapped and were found to have the following dip/dip direction values:

Table 5. Dip and dip direction values for joints in one location in the Río Grande cavern

N.	Dip	Dip dir.	Comments
1	50	131	infrequently occuring joints
2	85	264	shear joint set
3	70	226	shear joint set
4	50	345	tension joint set
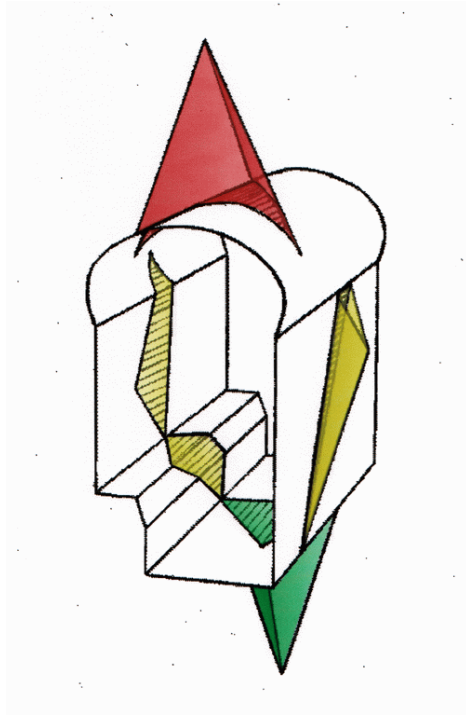
Figure 2.4 : Perspective view of Río Grande power cavern showing potentially unstable wedges in the roof, sidewalls, bench and floor.

Figure 2.4 is a perspective view of the Río Grande power cavern showing typical wedges which can be formed in the roof, sidewalls, bench and floor by joint sets 2, 3 and 4. These figures represent the maximum possible sizes of wedges which can be formed and, during construction, the sizes of the wedges were scaled down in accordance with average joint trace lengths measured in the excavation faces. In Figure 2.4 it is evident that the roof and the two sidewall wedges were potentially unstable and that they needed to be stabilised. This stabilisation was achieved by the placement of tensioned and grouted rockbolts which were installed at each stage of the cavern excavation. Decisions on the number, length and capacity of the rockbolts were made by on-site geotechnical staff using limit equilibrium calculations based upon the volume of the wedges defined by the measured trace lengths. For those wedges which involved sliding on one plane or along the line of intersection of two planes, rockbolts were installed across these planes to bring the sliding factor of safety of the wedge up to 1.5. For wedges which were free to fall from the roof, a factor of safety of 2 was used. This factor was calculated as the ratio of the total capacity of the bolts to the weight of the wedge and was intended to account for uncertainties associated with the bolt installation.

The floor wedge was of no significance while the wedges in the bench at the base of the upstream wall were stabilised by dowels placed in grout-filled vertical holes before excavation of the lower benches.

Early recognition of the potential instability problems, identification and visualization of the wedges which could be released and the installation of support at each stage of excavation, before the wedge bases were fully exposed, resulted in a very effective stabilisation program. Apart from a minimal amount of mesh and shotcrete applied to areas of intense jointing, no other support was used in the power cavern which has operated without any signs of instability since its completion in 1982.

2.5   Excavations in weak rock

In contrast to the structurally controlled failures in strong rock discussed in the previous section, there are many cases where tunnels and caverns are excavated in rock masses which are weak as a result of intense jointing or because the rock material itself has a low strength. Rocks such as shales, mudstones, siltstones, phyllites and tuffs are typical weak rocks in which even moderate in situ stresses are likely to induce failure in the rock surrounding underground excavations.

   Progressive failure of this type, which can occur in the rock surrounding an underground excavation in a weak rock mass, is a difficult analytical problem and there are no simple numerical models nor factor of safety calculations which can be used to define acceptable limits to this failure process. Judgement on the adequacy of a support design has to be based upon an evaluation of a number of factors such as the magnitude and distribution of deformations in the rock and the stresses induced in support elements such as grouted cables, steel sets or concrete linings. This design process is illustrated by means of an example.

   The Mingtan pumped storage project is located in the central region of the island of Taiwan and utilizes the 400 m head difference between the Sun Moon Lake and the Shuili River to generate up to 1600 MW at times of peak demand. The power cavern is 22 m wide, 46 m high and 158 m long and a parallel transformer hall is 13 m wide, 20 m high and 17 m long. The caverns are 45 m apart and are located at a depth of 30 m below surface in the steep left bank of the Shuili river (Liu, Cheng and Chang (1988)).

   The rock mass consists of weathered, interbedded sandstones, siltstones and shales dipping at about 35° to the horizontal. The Rock Mass Ratings (RMR) (Bieniawski (1974)) and Tunnelling Quality Index Q (Barton, Lien and Lunde (1974)) and approximate shear strength values for the various components of the rock mass are given in Table 6 below.

Table 6. Rock mass classifications and approximate friction angles ϕ and cohesive strengths c for the rock mass in which the Mingtan power cavern is excavated

Rock type	RMR	Q	ϕ' degrees	c' MPa
Jointed sandstone	63-75	12-39	50	1.0
Bedded sandstone	56-60	7-31	45	0.8
Fautle or shears	10-33	0.1-1.1	30-40	0.15-0.3

Weak beds of siltstone, up to 2 m thick, appear to have caused a concentration of shear movements during tectonic activity so that fault zones have developed parallel to the bedding. The common feature observed for all these faults is the presence of continuous clay filling with a thickness varying from a few mm to 200 mm. The cavern axis is intentionally oriented at right angles to the strike of these faults.

   The measured in situ stresses in the rock mass surrounding the cavern are approximately

   Maximum principal stress (horizontal) $\sigma_{max} = 10.9$ MPa

   Minimum principal stress (vertical) $\sigma_{min} = 7.5$ MPa

The Maximum principal stress is parallel to bedding and normal to the cavern axis.
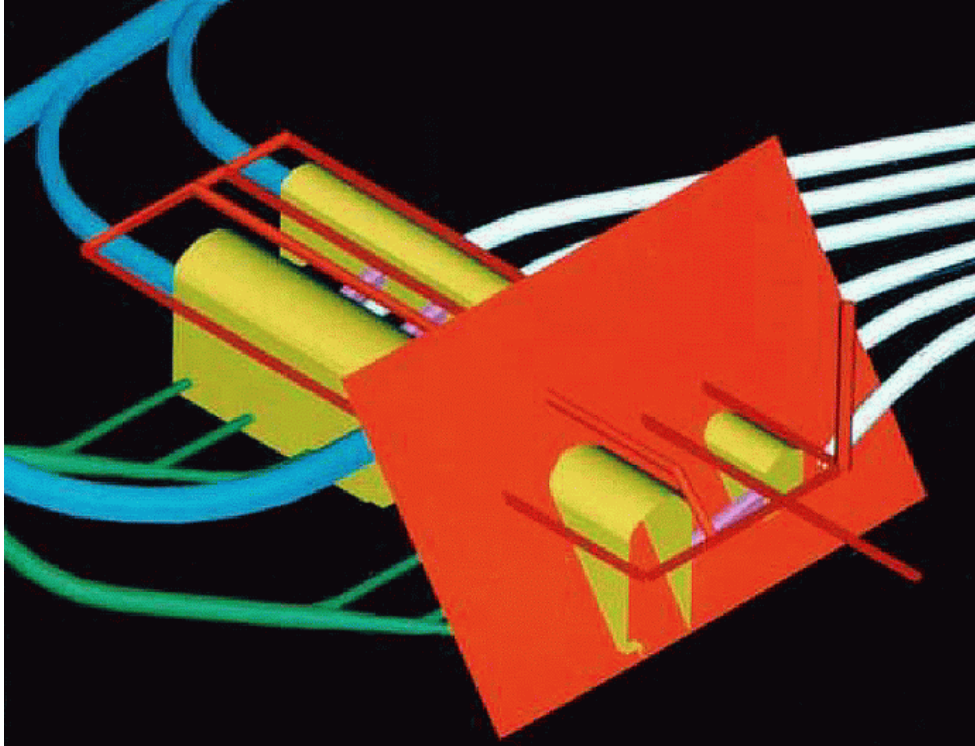
Figure 2.5: Orientation of the underground excavations in relation to the faults in the bedded sandstone surrounding the power cavern and transformer hall of the Mingtan Project. The red plane indicates the dip and strike of the faults.

Bedding faults of significant thickness which were intersected in the roof of the cavern were treated by using high pressure water jets to remove the clay and then filling the cavities with non shrink cementitious mortar (Cheng (1987), Moy and Hoek (1989)). This was followed by the installation of 50 tonne capacity untensioned grouted cables from a drainage gallery 10 m above the cavern roof in order to create a pre-reinforced rock mass above the cavern. All of this work was carried out from construction adits before the main contract for the cavern excavation commenced.

The initial design of the reinforcing cables was based upon experience and precedent practice. Figures 2.6 and 2.7 give the lengths of rockbolts and cables in the roof and sidewalls of some typical large powerhouse caverns in weak rock masses. Plotted on the same graphs are empirical relationships suggested by Barton (1989) for bolt and cable lengths for underground powerhouses.

During benching down in the cavern, 112 tonne capacity tensioned and grouted cables were installed on a 3 m x 3 m grid in the sidewalls. The final layout of the cables in the rock surrounding the power cavern and the transformer hall is illustrated in Figure 2.8. Five metre long grouted rockbolts were installed as required at the centre of the squares formed by the cable face plates A 50 mm layer of steel fibre reinforced microsilica shotcrete was applied within 5 to 10 m of the face. This shotcrete was later built up to a thickness of 150 mm on the roof and upper sidewalls and 50 mm on the lower sidewalls where it would eventually be incorporated into the concrete foundations.
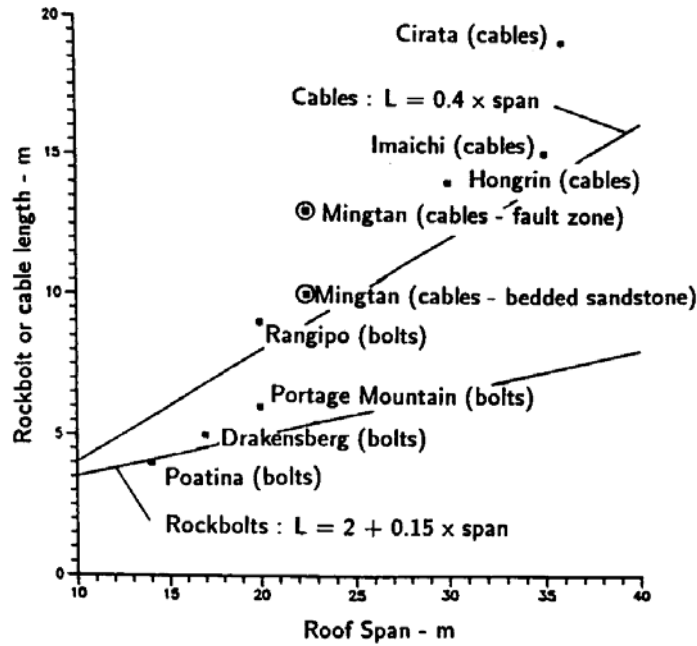
Figure 2.6 : Lengths of rockbolts and cables used for roof support in some large caverns in weak rock. Equations defining trend lines were suggested by Barton (1989).
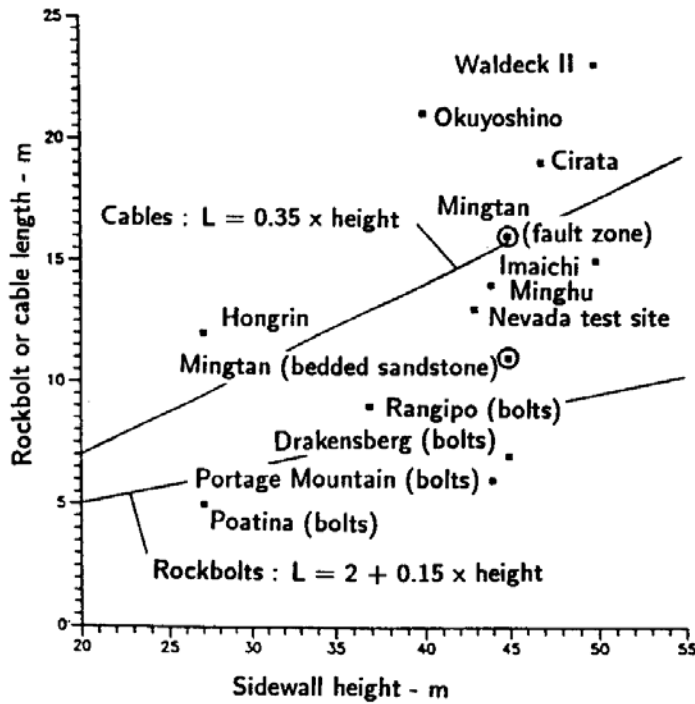
Figure 2.7 : Lengths of rockbolts and cables used for sidewall support in some large caverns in weak rock. Equations defining trend lines were suggested by Barton (1989).

A key element in the decision making process on the adequacy of the support system was a monitoring and analysis process which involved the following steps :

1. Displacements in the rock surrounding the excavations monitored by means of convergence arrays and extensometers, some of which had been installed from construction galleries before excavation of the caverns commenced.

2. Numerical modelling of each excavation stage using non-linear multiple-material models. The material properties used in the models of the early excavation stages were adjusted to obtain the best match between predicted and measured displacements.

3. Prediction of displacements and support loads during future excavation stages and adjustment of support capacity, installation and pre-tensioning to control displacements and cable loads.

4. Measurement of displacements and cable loads (using load cells on selected cables which had been de-bonded) and comparison between measured and predicted displacements and cable loads.

5. Installation of additional cables or adjustment of cable loads to control unusual displacements or support loads.

The aim of this program was to maintain as uniform a displacement pattern around the excavations as possible and to keep the loads on the cables at less than 45% of their yield load. The intermediate rockbolts and the shotcrete were not accounted for in the numerical modelling since it was assumed that their role was confined to supporting the rock immediately adjacent to the excavations and that the overall stability was controlled by the 10 to 15 m long grouted cables.

Figure 2.8 shows the combination of materials used in analysing one section of the cavern, assuming that the bedding faults could be represented by horizontal layers in the two-dimensional model. In order to match the measured and predicted displacements in the rock mass, it was found that a 2.5 m thick zone of softened and weakened material had to be wrapped around the excavations to account for blast damaged material (achieving good blasting results was difficult in this interbedded rock).

In Figure 2.9, the predicted and measured displacements along six extensometers installed in the power cavern sidewalls are compared. The overall agreement is considered to be acceptable. Maximum sidewall displacements were of the order of 100 mm at the mid-height of the upstream wall, adjacent to one of the major faults. Elsewhere, displacements were of the order to 25 to 46 mm.

Figure 2.10 shows the results of monitoring at seven stations along the axis of the power cavern. Before excavation of the cavern commenced, extensometers were installed at each of these stations from a drainage gallery above the roof arch and from construction galleries as shown in the upper part of Figure 2.10. In addition, load cells were installed on cables adjacent to some of the extensometers.

Rapid responses were recorded in all extensometers and load cells as the top heading passed underneath them. Further responses occurred as the haunches of the cavern arch were excavated and as the first bench was removed. As can be seen from the plots, after this rapid response to the initial excavation stages, the displacements and cable loads became stable and showed very little tendency to increase with time. The difference in the magnitudes of the displacements and cable loads at different stations can be related to the proximity of the monitoring instruments to faults in the rock above the cavern arch.

The rapid load acceptance and the modest loading of the cables together with the control of the displacements in the rock mass were the goals of the support design. Measurements obtained from the extensometers and cable load cells indicate that these goals have been met.
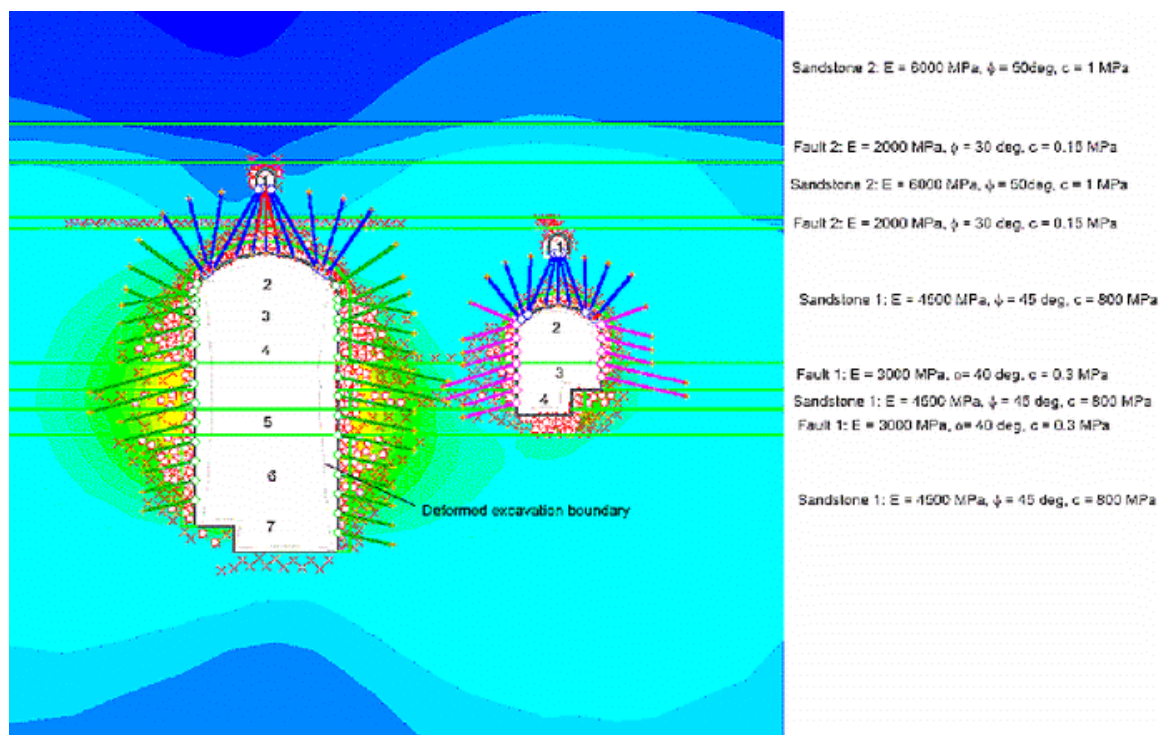
Figure 2.8: Displacement contours obtained from a two-dimensional finite element analysis of the seven excavation stages of the Mingtan power and transformer caverns. The layout of the cables used to support the rock surrounding the caverns and the location and properties of the rock units are indicated in the figure. Shear failure in the rock mass is indicated by the × symbols while tensile failure of shown by the o symbols. Note that almost all of the failures are within the envelope defined by the ends of the cables. Different types of cables are shown in different colours and failure of the cables (under the powerhouse drainage gallery) is shown in red. The deformed cavern boundaries are indicated and these indicate a uniform distribution of the deformations around the cavern. The maximum sidewall displacement for the in situ stresses and material properties used in this analysis is 90 mm.
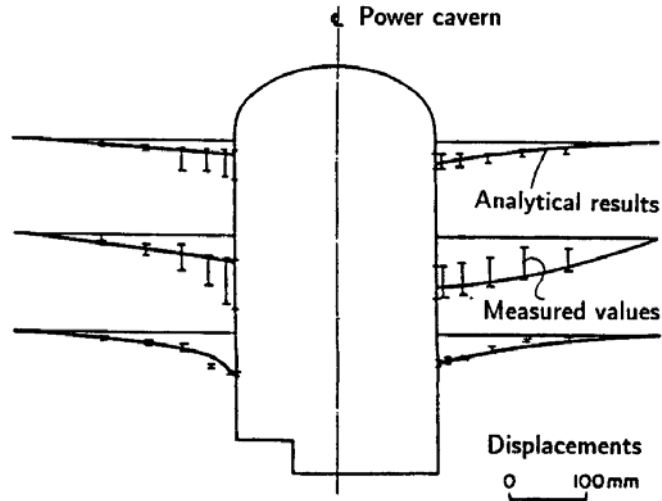
Figure 2.9: Comparison between calculated and measured displacements along six extensometers installed in the sidewalls of the Mingtan power cavern.
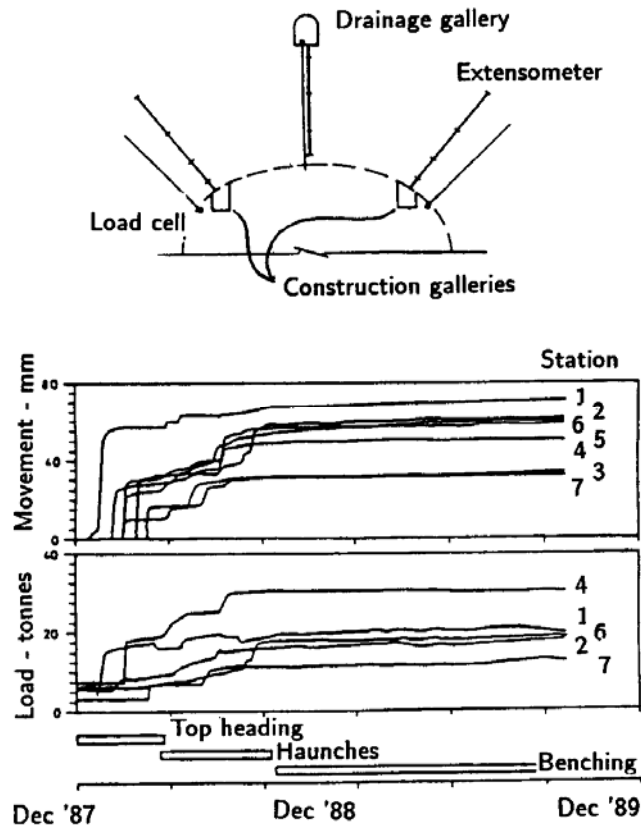
Figure 2.10 : Surface displacements and cable loads measured at seven stations along the power cavern axis.

2.6   Factor of safety

The four case histories, discussed in previous sections, have been presented to demonstrate that a variety of criteria have to be considered in deciding upon the adequacy of a rock structure to perform its design objectives. This is true for any design in rock since the performance of each structure will be uniquely dependent upon the particular set of rock conditions, design loads and intended end use.

In one group of structures, traditional designs have been based upon a `factor of safety' against sliding. These structures, which include gravity and fill dams as well as rock and soil slopes, all involve the potential for sliding along well defined failure surfaces. The factor of safety is defined as the factor by which the shear strength parameters may be reduced in order to bring the slope (or dam foundation) into a state of limiting equilibrium (Morgenstern (1991)). The numerical value of the factor of safety chosen for a particular design depends upon the level of confidence which the designer has in the shear strength parameters, the groundwater pressures, the location of the critical failure surface and the magnitude of the external driving forces acting upon the structure.
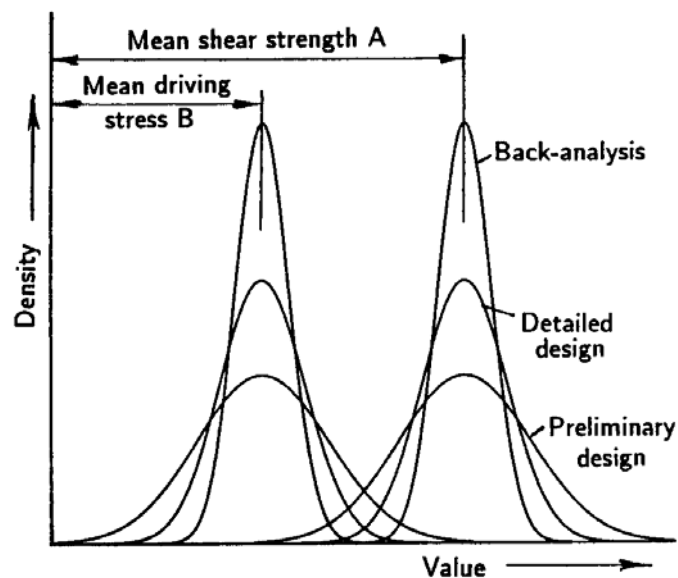
Figure 2.11 : Hypothetical distribution curves representing the degree of uncertainty associated with information on driving stresses and shear strengths at different stages in the design of a structure such as a dam foundation.

Figure 2.11 illustrates a set of hypothetical distribution curves representing the degree of uncertainty associated with available information on shear strength parameters and disturbing stresses for different stages in the design of a rock or soil structure. The factor of safety is defined as A/B where A is the mean of the distribution of shear strength values and B is the mean of the distribution of driving stresses. For the purpose of this discussion, the same factor of safety has been assumed for all three cases illustrated.

During preliminary design studies, the amount of information available is usually very limited. Estimates of the shear strength of the rock or soil are generally based upon the

judgement of an experienced engineer or geologist which may be supplemented, in some cases, by estimates based upon rock mass classifications or simple index tests. Similarly, the disturbing forces are not known with very much certainty since the location of the critical failure surface will not have been well defined and the magnitude of externally applied loads may not have been established. In the case of dam design, the magnitude of the probable maximum flood, which is usually based upon probabilistic analysis, frequently remains ill defined until very late in the design process.

For this case, the range of both available shear strength and disturbing stresses, which have to be considered, is large. If too low a factor of safety is used, there may be a significant probability of failure, represented by the section where the distribution curves overlap in Figure 2.11. In order to minimise this failure probability, a high value for the factor of safety is sometimes used. For example, in the 1977 edition of the US Bureau of Reclamation Engineering Monograph on Design Criteria for Concrete Arch and Gravity Dams, a factor of safety of 3.0 is recommended for normal loading conditions when 'only limited information is available on the strength parameters'. This value can be reduced to 2.0 when the strength parameters are 'determined by testing of core samples from a field investigation program or by past experience'.

During detailed design studies, the amount of information available is usually significantly greater than in the preliminary design stage discussed above. A comprehensive program of site investigations and laboratory or in situ shear strength tests will normally have been carried out and the external loads acting on the structure will have been better defined. In addition, studies of the groundwater flow and pressure distributions in the rock mass, together with modifications of these distributions by grouting and drainage, will usually have been carried out. Consequently, the ranges of shear strength and driving stress values, which have to be considered in the design, are smaller and the distribution curves are more tightly constrained.

The case histories of the Downie Slide and Dutchman's Ridge, discussed earlier, are good examples of designs based upon back-analyses. In both of these cases, very extensive site investigations and displacement monitoring had established the location of the critical failure surfaces with a high degree of certainty. Careful monitoring of the groundwater in the slopes (256 piezometer measuring points were installed in Dutchman's Ridge) had defined the water pressures in the slopes and their fluctuations over several years. Some shear testing on fault material recovered from cores was carried out but, more importantly, the mobilized shear strength along the potential failure surfaces was calculated by back-analysis, assuming a factor of safety of 1.00 for existing conditions.

Figure 2.11 illustrates the hypothetical distribution curves for the range of values for shear strength and driving stresses for the case of a structure in which an existing failure has been carefully back-analyzed. Depending upon the degree of care which has been taken with this back-analysis, these curves will be very tightly constrained and a low factor of safety can be used for the design of the remedial works.

This discussion illustrates the point that different factors of safety may be appropriate for different stages in the design of a rock structure. This difference is primarily dependent upon the level of confidence which the designer has in the values of shear strength to be included in the analysis. Hence, a critical question which arises in all of these cases is the determination or estimation of the shear strength along the potential

sliding surface. In a paper on the strength of rockfill materials, Marachi, Chan and Seed (1972) summarize this problem as follows: `No stability analysis, regardless of how intricate and theoretically exact it may be, can be useful for design if an incorrect estimation of the shearing strength of the construction material has been made'.

Except in simple cases involving homogeneous soils or planar continuous weak seams, determination of the shear strength along potential sliding surfaces is a notoriously difficult problem. This is particularly true of the determination of the cohesive component, *c'*, of the commonly used Mohr-Coulomb failure criterion. Laboratory test specimens tend to be too small to give representative results while in situ tests are difficult and expensive and, unless carried out with very great care, are liable to give unreliable results.

Table 7: Factors of safety for different loading conditions in the design of earth and rockfill dams.

Loading condition	S.F.	Remarks
End of construction porewater pressures in the dam and undissipated porewater pressures in the foundation. No reservoir loading.	1.3	
Reservoir at full supply level with steady state seepage in the dam and undissipated end-of-construction porewater pressures in the foundation.	1.3	Possibly the most critical (even if rare) condition.
Reservoir at full supply level with steady state seepage.	1.5	Critical to design.
Reservoir at probable maximum flood level with steady state seepage conditions.	1.2	
Rapid reservoir drawdown from full supply level to minimum supply level	1.3	Not significant in design. Failures very rare and, if they occur, usually shallow.

For failure surfaces which involve sliding on rough or undulating rock surfaces such as joints or bedding planes, the methodology proposed by Barton (1976) is appropriate for estimating the overall shear strength of the potential sliding surface. This involves adding a measured or estimated roughness component to the basic frictional strength which can be determined on sawn and polished laboratory shear test specimens.

For heavily jointed rock masses in which there are no dominant weakness zones such as faults or shear zones, a crude estimate of the shear strength of the rock mass can be obtained by means of the use of rock mass classification systems as proposed by Hoek and Brown (1988).

In all cases, a greater reliance can be placed upon the frictional component, ϕ, of the Mohr-Coulomb shear strength equation and extreme care has to be taken in the estimation of the cohesive strength, *c'*. Where no reliable estimates of this value are available from carefully conducted shear tests or from back-analysis of existing failures,

it is prudent to assume a cohesive strength of zero for any stability analysis involving structures such as dam foundations.

In the design of fill and gravity dams there is a tendency to move away from the high factors of safety of 2 or 3 which have been used in the past, provided that care is taken in choosing sensible conservative shear strength parameters, particularly for continuous weak seams in the foundations. An example of the range of factors of safety which can be used in the design of earth or rockfill dams is given in Table 7.

2.7   Probabilistic analyses

The uncertainty associated with the properties of geotechnical materials and the great care which has to be taken in selecting appropriate values for analyses has prompted several authors to suggest that the traditional deterministic methods of slope stability analyses should be replaced by probabilistic methods (Priest and Brown (1983), McMahon (1975), Vanmarcke (1980), Morriss and Stoter (1983), Read and Lye (1983)).

One branch of rock mechanics in which probabilistic analyses have been accepted for many years is that of the design of open pit mine slopes. This is because open pit planners are familiar with the concepts of risk analysis applied to ore grade and metal price fluctuations. Probabilistic methods are used in estimating the economic viability of various options in developing an open pit mine and so it is a small step to incorporate the probability of a geotechnical failure into the overall risk assessment of the mine. The mine planner has the choice of reducing the probability of failure by the installation of reinforcement, reducing the angle of the slope or accepting that failure will occur and providing for extra equipment which may be needed to clean up the failure. Since the mine is usually owned and operated by a single company and access to the mine benches is restricted to trained personnel, accepting a risk of failure and dealing with the consequences on a routine basis is a viable option.

On the other hand, the emotional impact of suggesting to the public that there is a finite risk of failure attached to a dam design is such that it is difficult to suggest the replacement of the standard factor of safety design approach with one which explicitly states a probability of failure or a coefficient of reliability. The current perception is that the factor of safety is more meaningful than the probability of failure. Even if this were not so, there is still the problem of deciding what probability of failure is acceptable for a rock structure to which the general public has access.

In spite of these difficulties, there does appear to be a slow but steady trend in society to accept the concepts of risk analysis more readily than has been the case in the past. The geotechnical community has an obligation to take note of these developments and to encourage the teaching and practical use of probabilistic as well as deterministic techniques with the aim of removing the cloak of mystery which surrounds the use of these methods.

Fortunately, there is a compromise solution which is a form of risk analysis used intuitively by most experienced engineers. This is a parametric analysis in which a wide range of possibilities are considered in a conventional deterministic analysis in order to gain a 'feel' for the sensitivity of the design. Hence, the factor of safety for a slope would be calculated for both fully drained and fully saturated groundwater conditions, for a range of friction angles and cohesive strengths covering the full spectrum which could be

anticipated for the geological conditions existing on the site, for external forces ranging from zero to the maximum possible for that slope. The availability of user-friendly microcomputer software for most forms of limit equilibrium analysis means that these parametric studies can be carried out quickly and easily for most designs.

3

Rock mass classification

3.1 Introduction

During the feasibility and preliminary design stages of a project, when very little detailed information on the rock mass and its stress and hydrologic characteristics is available, the use of a rock mass classification scheme can be of considerable benefit. At its simplest, this may involve using the classification scheme as a check-list to ensure that all relevant information has been considered. At the other end of the spectrum, one or more rock mass classification schemes can be used to build up a picture of the composition and characteristics of a rock mass to provide initial estimates of support requirements, and to provide estimates of the strength and deformation properties of the rock mass.

It is important to understand that the use of a rock mass classification scheme does not (and cannot) replace some of the more elaborate design procedures. However, the use of these design procedures requires access to relatively detailed information on in situ stresses, rock mass properties and planned excavation sequence, none of which may be available at an early stage in the project. As this information becomes available, the use of the rock mass classification schemes should be updated and used in conjunction with site specific analyses.

3.2 Engineering rock mass classification

Rock mass classification schemes have been developing for over 100 years since Ritter (1879) attempted to formalise an empirical approach to tunnel design, in particular for determining support requirements. While the classification schemes are appropriate for their original application, especially if used within the bounds of the case histories from which they were developed, considerable caution must be exercised in applying rock mass classifications to other rock engineering problems.

Summaries of some important classification systems are presented in this chapter, and although every attempt has been made to present all of the pertinent data from the original texts, there are numerous notes and comments which cannot be included. The interested reader should make every effort to read the cited references for a full appreciation of the use, applicability and limitations of each system.

Most of the multi-parameter classification schemes (Wickham et al (1972) Bieniawski (1973, 1989) and Barton et al (1974)) were developed from civil engineering case histories in which all of the components of the engineering geological character of the rock mass were included. In underground hard rock mining, however, especially at deep

levels, rock mass weathering and the influence of water usually are not significant and may be ignored. Different classification systems place different emphases on the various parameters, and it is recommended that at least two methods be used at any site during the early stages of a project.

3.2.1   Terzaghi's rock mass classification

The earliest reference to the use of rock mass classification for the design of tunnel support is in a paper by Terzaghi (1946) in which the rock loads, carried by steel sets, are estimated on the basis of a descriptive classification. While no useful purpose would be served by including details of Terzaghi's classification in this discussion on the design of support, it is interesting to examine the rock mass descriptions included in his original paper, because he draws attention to those characteristics that dominate rock mass behaviour, particularly in situations where gravity constitutes the dominant driving force. The clear and concise definitions and the practical comments included in these descriptions are good examples of the type of engineering geology information, which is most useful for engineering design.

Terzaghi's descriptions (quoted directly from his paper) are:

- *Intact* rock contains neither joints nor hair cracks. Hence, if it breaks, it breaks across sound rock. On account of the injury to the rock due to blasting, spalls may drop off the roof several hours or days after blasting. This is known as a *spalling* condition. Hard, intact rock may also be encountered in the *popping* condition involving the spontaneous and violent detachment of rock slabs from the sides or roof.

- *Stratified* rock consists of individual strata with little or no resistance against separation along the boundaries between the strata. The strata may or may not be weakened by transverse joints. In such rock the spalling condition is quite common.

- *Moderately jointed* rock contains joints and hair cracks, but the blocks between joints are locally grown together or so intimately interlocked that vertical walls do not require lateral support. In rocks of this type, both spalling and popping conditions may be encountered.

- *Blocky and seamy* rock consists of chemically intact or almost intact rock fragments which are entirely separated from each other and imperfectly interlocked. In such rock, vertical walls may require lateral support.

- *Crushed* but chemically intact rock has the character of crusher run. If most or all of the fragments are as small as fine sand grains and no recementation has taken place, crushed rock below the water table exhibits the properties of a water-bearing sand.

- *Squeezing* rock slowly advances into the tunnel without perceptible volume increase. A prerequisite for squeeze is a high percentage of microscopic and sub-microscopic particles of micaceous minerals or clay minerals with a low swelling capacity.

- *Swelling* rock advances into the tunnel chiefly on account of expansion. The capacity to swell seems to be limited to those rocks that contain clay minerals such as montmorillonite, with a high swelling capacity.

3.2.2   Classifications involving stand-up time

Lauffer (1958) proposed that the stand-up time for an unsupported span is related to the quality of the rock mass in which the span is excavated. In a tunnel, the unsupported span is defined as the span of the tunnel or the distance between the face and the nearest support, if this is greater than the tunnel span. Lauffer's original classification has since been modified by a number of authors, notably Pacher et al (1974), and now forms part of the general tunnelling approach known as the New Austrian Tunnelling Method.

The significance of the stand-up time concept is that an increase in the span of the tunnel leads to a significant reduction in the time available for the installation of support. For example, a small pilot tunnel may be successfully constructed with minimal support, while a larger span tunnel in the same rock mass may not be stable without the immediate installation of substantial support.

The New Austrian Tunnelling Method includes a number of techniques for safe tunnelling in rock conditions in which the stand-up time is limited before failure occurs. These techniques include the use of smaller headings and benching or the use of multiple drifts to form a reinforced ring inside which the bulk of the tunnel can be excavated. These techniques are applicable in soft rocks such as shales, phyllites and mudstones in which the squeezing and swelling problems, described by Terzaghi (see previous section), are likely to occur. The techniques are also applicable when tunnelling in excessively broken rock, but great care should be taken in attempting to apply these techniques to excavations in hard rocks in which different failure mechanisms occur.

In designing support for hard rock excavations it is prudent to assume that the stability of the rock mass surrounding the excavation is not time-dependent. Hence, if a structurally defined wedge is exposed in the roof of an excavation, it will fall as soon as the rock supporting it is removed. This can occur at the time of the blast or during the subsequent scaling operation. If it is required to keep such a wedge in place, or to enhance the margin of safety, it is essential that the support be installed as early as possible, preferably before the rock supporting the full wedge is removed. On the other hand, in a highly stressed rock, failure will generally be induced by some change in the stress field surrounding the excavation. The failure may occur gradually and manifest itself as spalling or slabbing or it may occur suddenly in the form of a rock burst. In either case, the support design must take into account the change in the stress field rather than the 'stand-up' time of the excavation.

3.2.3   Rock quality designation index (RQD)

The Rock Quality Designation index (*RQD*) was developed by Deere (Deere et al 1967) to provide a quantitative estimate of rock mass quality from drill core logs. *RQD* is defined as the percentage of intact core pieces longer than 100 mm (4 inches) in the total length of core. The core should be at least NW size (54.7 mm or 2.15 inches in diameter) and should be drilled with a double-tube core barrel. The correct procedures for measurement of the length of core pieces and the calculation of *RQD* are summarised in Figure 4.1.
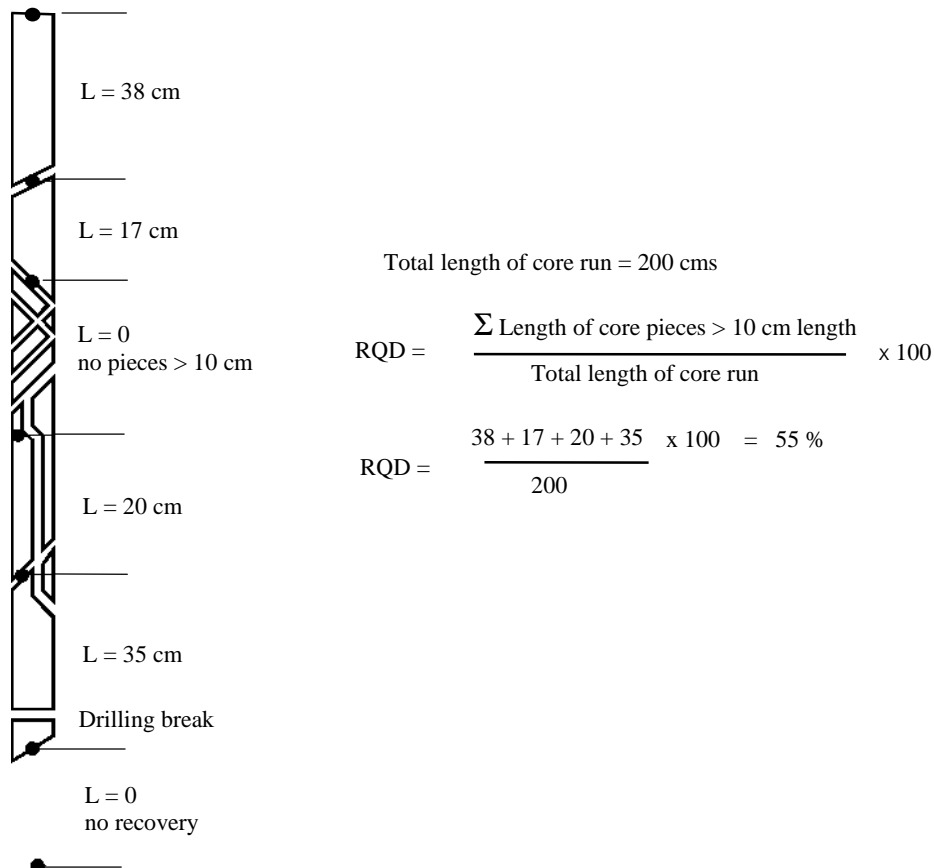
Figure 4.1: Procedure for measurement and calculation of *RQD* (After Deere, 1989).

Palmström (1982) suggested that, when no core is available but discontinuity traces are visible in surface exposures or exploration adits, the *RQD* may be estimated from the number of discontinuities per unit volume. The suggested relationship for clay-free rock masses is:

$$RQD = 115 - 3.3 J_v \qquad (4.1)$$

where J_v is the sum of the number of joints per unit length for all joint (discontinuity) sets known as the volumetric joint count.

RQD is a directionally dependent parameter and its value may change significantly, depending upon the borehole orientation. The use of the volumetric joint count can be quite useful in reducing this directional dependence.

RQD is intended to represent the rock mass quality in situ. When using diamond drill core, care must be taken to ensure that fractures, which have been caused by handling or the drilling process, are identified and ignored when determining the value of *RQD*. When using Palmström's relationship for exposure mapping, blast induced fractures should not be included when estimating J_v.

Deere's *RQD* has been widely used, particularly in North America, for the past 25 years. Cording and Deere (1972), Merritt (1972) and Deere and Deere (1988) have attempted to relate *RQD* to Terzaghi's rock load factors and to rockbolt requirements in

tunnels. In the context of this discussion, the most important use of *RQD* is as a component of the *RMR* and *Q* rock mass classifications covered later in this chapter.

3.2.4 Rock Structure Rating (RSR)

Wickham et al (1972) described a quantitative method for describing the quality of a rock mass and for selecting appropriate support on the basis of their Rock Structure Rating (*RSR*) classification. Most of the case histories, used in the development of this system, were for relatively small tunnels supported by means of steel sets, although historically this system was the first to make reference to shotcrete support. In spite of this limitation, it is worth examining the *RSR* system in some detail since it demonstrates the logic involved in developing a quasi-quantitative rock mass classification system.

The significance of the *RSR* system, in the context of this discussion, is that it introduced the concept of rating each of the components listed below to arrive at a numerical value of $RSR = A + B + C$.

1. *Parameter A, Geology:* General appraisal of geological structure on the basis of:
   a. Rock type origin (igneous, metamorphic, sedimentary).
   b. Rock hardness (hard, medium, soft, decomposed).
   c. Geologic structure (massive, slightly faulted/folded, moderately faulted/folded, intensely faulted/folded).

2. *Parameter B, Geometry*: Effect of discontinuity pattern with respect to the direction of the tunnel drive on the basis of:
   a. Joint spacing.
   b. Joint orientation (strike and dip).
   c. Direction of tunnel drive.

3. *Parameter C*: Effect of groundwater inflow and joint condition on the basis of:
   a. Overall rock mass quality on the basis of A and B combined.
   b. Joint condition (good, fair, poor).
   c. Amount of water inflow (in gallons per minute per 1000 feet of tunnel).
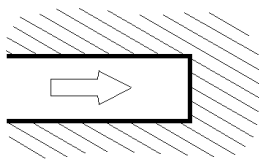
Drive with dip
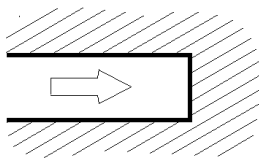
Drive against dip

Note that the *RSR* classification used Imperial units and that these units have been retained in this discussion.

Three tables from Wickham et al's 1972 paper are reproduced in Tables 4.1, 4.2 and 4.3. These tables can be used to evaluate the rating of each of these parameters to arrive at the *RSR* value (maximum *RSR* = 100).

For example, a hard metamorphic rock which is slightly folded or faulted has a rating of *A* = 22 (from Table 4.1). The rock mass is moderately jointed, with joints striking perpendicular to the tunnel axis which is being driven east-west, and dipping at between 20° and 50°. Table 4.2 gives the rating for *B* = 24 for driving with dip (defined in the margin sketch).

The value of $A + B = 46$ and this means that, for joints of fair condition (slightly weathered and altered) and a moderate water inflow of between 200 and 1,000 gallons per minute, Table 4.3 gives the rating for $C = 16$. Hence, the final value of the rock structure rating $RSR = A + B + C = 62$.

A typical set of prediction curves for a 24 foot diameter tunnel are given in Figure 4.2 which shows that, for the RSR value of 62 derived above, the predicted support would be 2 inches of shotcrete and 1 inch diameter rockbolts spaced at 5 foot centres. As indicated in the figure, steel sets would be spaced at more than 7 feet apart and would not be considered a practical solution for the support of this tunnel.

For the same size tunnel in a rock mass with $RSR = 30$, the support could be provided by 8 WF 31 steel sets (8 inch deep wide flange I section weighing 31 lb per foot) spaced 3 feet apart, or by 5 inches of shotcrete and 1 inch diameter rockbolts spaced at 2.5 feet centres. In this case it is probable that the steel set solution would be cheaper and more effective than the use of rockbolts and shotcrete.

Although the RSR classification system is not widely used today, Wickham et al's work played a significant role in the development of the classification schemes discussed in the remaining sections of this chapter.
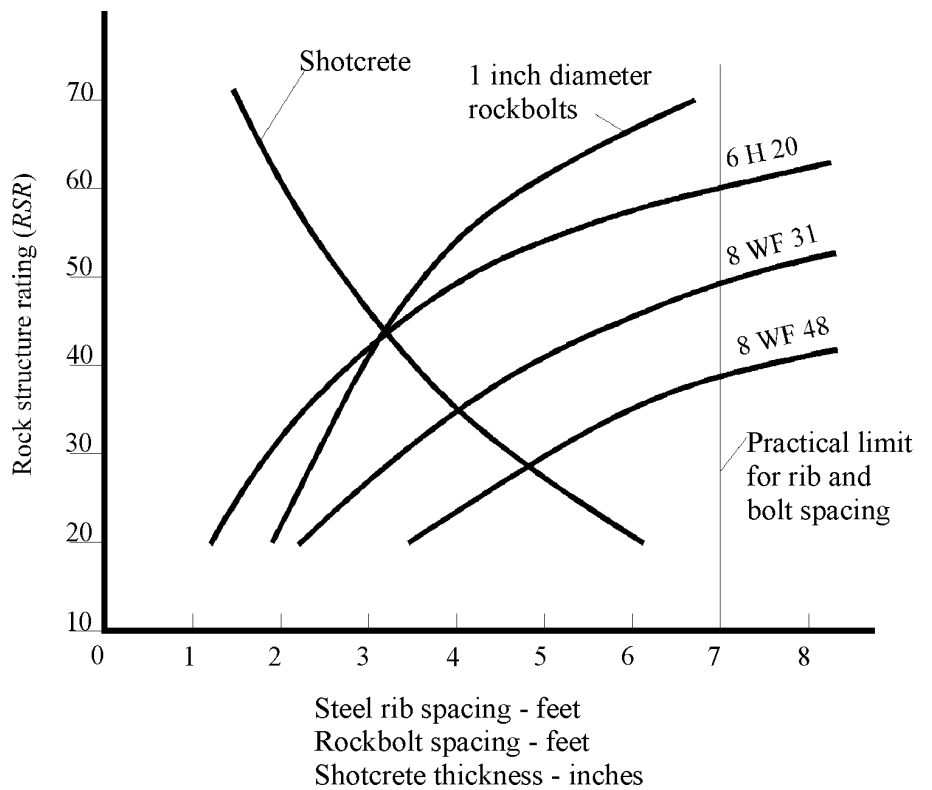
Figure 4.2: *RSR* support estimates for a 24 ft. (7.3 m) diameter circular tunnel. Note that rockbolts and shotcrete are generally used together. (After Wickham et al 1972).

Table 4.1: Rock Structure Rating: Parameter *A*: General area geology

| | Basic Rock Type | | | | | Geological Structure | | |
	Hard	Medium	Soft	Decomposed				
Igneous	1	2	3	4		Slightly	Moderately	Intensively
Metamorphic	1	2	3	4		Folded or	Folded or	Folded or
Sedimentary	2	3	4	4	Massive	Faulted	Faulted	Faulted
Type 1					30	22	15	9
Type 2					27	20	13	8
Type 3					24	18	12	7
Type 4					19	15	10	6

Table 4.2: Rock Structure Rating: Parameter *B*: Joint pattern, direction of drive

	Strike ⊥ to Axis					Strike ǁ to Axis		
	Direction of Drive					Direction of Drive		
	Both	With Dip		Against Dip		Either direction		
	Dip of Prominent Joints [a]					Dip of Prominent Joints		
Average joint spacing	Flat	Dipping	Vertical	Dipping	Vertical	Flat	Dipping	Vertical
1. Very closely jointed, < 2 in	9	11	13	10	12	9	9	7
2. Closely jointed, 2-6 in	13	16	19	15	17	14	14	11
3. Moderately jointed, 6-12 in	23	24	28	19	22	23	23	19
4. Moderate to blocky, 1-2 ft	30	32	36	25	28	30	28	24
5. Blocky to massive, 2-4 ft	36	38	40	33	35	36	24	28
6. Massive, > 4 ft	40	43	45	37	40	40	38	34

Table 4.3: Rock Structure Rating: Parameter *C*: Groundwater, joint condition

	Sum of Parameters *A* + *B*					
	13 - 44			45 - 75		
Anticipated water inflow	Joint Condition [b]					
gpm/1000 ft of tunnel	Good	Fair	Poor	Good	Fair	Poor
None	22	18	12	25	22	18
Slight, < 200 gpm	19	15	9	23	19	14
Moderate, 200-1000 gpm	15	22	7	21	16	12
Heavy, > 1000 gp	10	8	6	18	14	10

[a] Dip: flat: 0-20°; dipping: 20-50°; and vertical: 50-90°

[b] Joint condition: good = tight or cemented; fair = slightly weathered or altered; poor = severely weathered, altered or open

3.3   Geomechanics Classification

Bieniawski (1976) published the details of a rock mass classification called the Geomechanics Classification or the Rock Mass Rating (*RMR*) system. Over the years, this system has been successively refined as more case records have been examined and the reader should be aware that Bieniawski has made significant changes in the ratings assigned to different parameters. The discussion which follows is based upon the 1989 version of the classification (Bieniawski, 1989). Both this version and the 1976 version will be used in Chapter 8 which deals with estimating the strength of rock masses. The following six parameters are used to classify a rock mass using the *RMR* system:

1. Uniaxial compressive strength of rock material.
2. Rock Quality Designation (*RQD*).
3. Spacing of discontinuities.
4. Condition of discontinuities.
5. Groundwater conditions.
6. Orientation of discontinuities.

In applying this classification system, the rock mass is divided into a number of structural regions and each region is classified separately. The boundaries of the structural regions usually coincide with a major structural feature such as a fault or with a change in rock type. In some cases, significant changes in discontinuity spacing or characteristics, within the same rock type, may necessitate the division of the rock mass into a number of small structural regions.

The Rock Mass Rating system is presented in Table 4.4, giving the ratings for each of the six parameters listed above. These ratings are summed to give a value of *RMR*. The following example illustrates the use of these tables to arrive at an *RMR* value.

A tunnel is to be driven through a slightly weathered granite with a dominant joint set dipping at 60° against the direction of the drive. Index testing and logging of diamond drilled core give typical Point-load strength index values of 8 MPa and average *RQD* values of 70%. The slightly rough and slightly weathered joints with a separation of < 1 mm, are spaced at 300 mm. Tunnelling conditions are anticipated to be wet.

The *RMR* value is determined as follows :

Table	Item	Value	Rating
4.4: A.1	Point load index	8 MPa	12
4.4: A.2	*RQD*	70%	13
4.4: A.3	Spacing of discontinuities	300 mm	10
4.4: E.4	Condition of discontinuities	Note 1	22
4.4: A.5	Groundwater	Wet	7
4.4: B	Adjustment for joint orientation	Note 2	-5
		Total	59

Note 1. For slightly rough and altered discontinuity surfaces with a separation of < 1 mm, Table 4.4.A.4 gives a rating of 25. When more detailed information is available, Table 4.4.E can be used to obtain a more refined rating. Hence, in this case, the rating is the sum of: 4 (1-3 m discontinuity length), 4 (separation 0.1-1.0 mm), 3 (slightly rough), 6 (no infilling) and 5 (slightly weathered) = 22.

Note 2. Table 4.4.F gives a description of 'Fair' for the conditions assumed where the tunnel is to be driven against the dip of a set of joints dipping at 60°. Using this description for 'Tunnels and Mines' in Table 4.4.B gives an adjustment rating of -5.

Bieniawski (1989) published a set of guidelines for the selection of support in tunnels in rock for which the value of *RMR* has been determined. These guidelines are reproduced in Table 4.5. Note that these guidelines have been published for a 10 m span horseshoe shaped tunnel, constructed using drill and blast methods, in a rock mass subjected to a vertical stress < 25 MPa (equivalent to a depth below surface of <900 m).

For the case considered earlier, with *RMR* = 59, Table 4.5 suggests that a tunnel could be excavated by top heading and bench, with a 1.5 to 3 m advance in the top heading. Support should be installed after each blast and the support should be placed at a maximum distance of 10 m from the face. Systematic rock bolting, using 4 m long 20 mm diameter fully grouted bolts spaced at 1.5 to 2 m in the crown and walls, is recommended. Wire mesh, with 50 to 100 mm of shotcrete for the crown and 30 mm of shotcrete for the walls, is recommended.

The value of *RMR* of 59 indicates that the rock mass is on the boundary between the 'Fair rock' and 'Good rock' categories. In the initial stages of design and construction, it is advisable to utilise the support suggested for fair rock. If the construction is progressing well with no stability problems, and the support is performing very well, then it should be possible to gradually reduce the support requirements to those indicated for a good rock mass. In addition, if the excavation is required to be stable for a short amount of time, then it is advisable to try the less expensive and extensive support suggested for good rock. However, if the rock mass surrounding the excavation is expected to undergo large mining induced stress changes, then more substantial support appropriate for fair rock should be installed. This example indicates that a great deal of judgement is needed in the application of rock mass classification to support design.

It should be noted that Table 4.5 has not had a major revision since 1973. In many mining and civil engineering applications, steel fibre reinforced shotcrete may be considered in place of wire mesh and shotcrete.

3.4 Modifications to *RMR* for mining

Bieniawski's Rock Mass Rating (*RMR*) system was originally based upon case histories drawn from civil engineering. Consequently, the mining industry tended to regard the classification as somewhat conservative and several modifications have been proposed in order to make the classification more relevant to mining applications. A comprehensive summary of these modifications was compiled by Bieniawski (1989).

Laubscher (1977, 1984), Laubscher and Taylor (1976) and Laubscher and Page (1990) have described a Modified Rock Mass Rating system for mining. This *MRMR* system takes the basic *RMR* value, as defined by Bieniawski, and adjusts it to account for in situ and induced stresses, stress changes and the effects of blasting and weathering. A set of support recommendations is associated with the resulting *MRMR* value. In using Laubscher's *MRMR* system it should be borne in mind that many of the case histories upon which it is based are derived from caving operations. Originally, block caving in asbestos mines in Africa formed the basis for the modifications but, subsequently, other case histories from around the world have been added to the database.

Table 4.4: Rock Mass Rating System (After Bieniawski 1989).

A. CLASSIFICATION PARAMETERS AND THEIR RATINGS							
	Parameter		Range of values				
1	Strength of intact rock material	Point-load strength index	>10 MPa	4 - 10 MPa	2 - 4 MPa	1 - 2 MPa	For this low range - uniaxial compressive test is preferred	
		Uniaxial comp. strength	>250 MPa	100 - 250 MPa	50 - 100 MPa	25 - 50 MPa	5 - 25 MPa / 1 - 5 MPa / < 1 MPa	
	Rating		15	12	7	4	2 / 1 / 0	
2	Drill core Quality RQD		90% - 100%	75% - 90%	50% - 75%	25% - 50%	< 25%	
	Rating		20	17	13	8	3	
3	Spacing of discontinuities		> 2 m	0.6 - 2 . m	200 - 600 mm	60 - 200 mm	< 60 mm	
	Rating		20	15	10	8	5	
4	Condition of discontinuities (See E)		Very rough surfaces Not continuous No separation Unweathered wall rock	Slightly rough surfaces Separation < 1 mm Slightly weathered walls	Slightly rough surfaces Separation < 1 mm Highly weathered walls	Slickensided surfaces or Gouge < 5 mm thick or Separation 1-5 mm Continuous	Soft gouge >5 mm thick or Separation > 5 mm Continuous	
	Rating		30	25	20	10	0	
5	Ground water	Inflow per 10 m tunnel length (l/m)	None	< 10	10 - 25	25 - 125	> 125	
		(Joint water press)/ (Major principal σ)	0	< 0.1	0.1, - 0.2	0.2 - 0.5	> 0.5	
		General conditions	Completely dry	Damp	Wet	Dripping	Flowing	
	Rating		15	10	7	4	0	

B. RATING ADJUSTMENT FOR DISCONTINUITY ORIENTATIONS (See F)						
Strike and dip orientations		Very favourable	Favourable	Fair	Unfavourable	Very Unfavourable
Ratings	Tunnels & mines	0	-2	-5	-10	-12
	Foundations	0	-2	-7	-15	-25
	Slopes	0	-5	-25	-50	

C. ROCK MASS CLASSES DETERMINED FROM TOTAL RATINGS					
Rating	100 ← 81	80 ← 61	60 ← 41	40 ← 21	< 21
Class number	I	II	III	IV	V
Description	Very good rock	Good rock	Fair rock	Poor rock	Very poor rock

D. MEANING OF ROCK CLASSES					
Class number	I	II	III	IV	V
Average stand-up time	20 yrs for 15 m span	1 year for 10 m span	1 week for 5 m span	10 hrs for 2.5 m span	30 min for 1 m span
Cohesion of rock mass (kPa)	> 400	300 - 400	200 - 300	100 - 200	< 100
Friction angle of rock mass (deg)	> 45	35 - 45	25 - 35	15 - 25	< 15

E. GUIDELINES FOR CLASSIFICATION OF DISCONTINUITY conditions					
Discontinuity length (persistence) Rating	< 1 m 6	1 - 3 m 4	3 - 10 m 2	10 - 20 m 1	> 20 m 0
Separation (aperture) Rating	None 6	< 0.1 mm 5	0.1 - 1.0 mm 4	1 - 5 mm 1	> 5 mm 0
Roughness Rating	Very rough 6	Rough 5	Slightly rough 3	Smooth 1	Slickensided 0
Infilling (gouge) Rating	None 6	Hard filling < 5 mm 4	Hard filling > 5 mm 2	Soft filling < 5 mm 2	Soft filling > 5 mm 0
Weathering Ratings	Unweathered 6	Slightly weathered 5	Moderately weathered 3	Highly weathered 1	Decomposed 0

F. EFFECT OF DISCONTINUITY STRIKE AND DIP ORIENTATION IN TUNNELLING**			
Strike perpendicular to tunnel axis		Strike parallel to tunnel axis	
Drive with dip - Dip 45 - 90°	Drive with dip - Dip 20 - 45°	Dip 45 - 90°	Dip 20 - 45°
Very favourable	Favourable	Very unfavourable	Fair
Drive against dip - Dip 45-90°	Drive against dip - Dip 20-45°	Dip 0-20 - Irrespective of strike°	
Fair	Unfavourable	Fair	

* Some conditions are mutually exclusive . For example, if infilling is present, the roughness of the surface will be overshadowed by the influence of the gouge. In such cases use A.4 directly.
** Modified after Wickham et al (1972).

Table 4.5: Guidelines for excavation and support of 10 m span rock tunnels in accordance with the *RMR* system (After Bieniawski 1989).

Rock mass class	Excavation	Rock bolts (20 mm diameter, fully grouted)	Shotcrete	Steel sets
I - Very good rock *RMR*: 81-100	Full face, 3 m advance.	Generally no support required except spot bolting.		
II - Good rock *RMR*: 61-80	Full face , 1-1.5 m advance. Complete support 20 m from face.	Locally, bolts in crown 3 m long, spaced 2.5 m with occasional wire mesh.	50 mm in crown where required.	None.
III - Fair rock *RMR*: 41-60	Top heading and bench 1.5-3 m advance in top heading. Commence support after each blast. Complete support 10 m from face.	Systematic bolts 4 m long, spaced 1.5 - 2 m in crown and walls with wire mesh in crown.	50-100 mm in crown and 30 mm in sides.	None.
IV - Poor rock *RMR*: 21-40	Top heading and bench 1.0-1.5 m advance in top heading. Install support concurrently with excavation, 10 m from face.	Systematic bolts 4-5 m long, spaced 1-1.5 m in crown and walls with wire mesh.	100-150 mm in crown and 100 mm in sides.	Light to medium ribs spaced 1.5 m where required.
V – Very poor rock *RMR*: < 20	Multiple drifts 0.5-1.5 m advance in top heading. Install support concurrently with excavation. Shotcrete as soon as possible after blasting.	Systematic bolts 5-6 m long, spaced 1-1.5 m in crown and walls with wire mesh. Bolt invert.	150-200 mm in crown, 150 mm in sides, and 50 mm on face.	Medium to heavy ribs spaced 0.75 m with steel lagging and forepoling if required. Close invert.

Cummings et al (1982) and Kendorski et al (1983) have also modified Bieniawski's *RMR* classification to produce the *MBR* (modified basic *RMR*) system for mining. This system was developed for block caving operations in the USA. It involves the use of different ratings for the original parameters used to determine the value of *RMR* and the subsequent adjustment of the resulting *MBR* value to allow for blast damage, induced stresses, structural features, distance from the cave front and size of the caving block. Support recommendations are presented for isolated or development drifts as well as for the final support of intersections and drifts.

3.5 Rock Tunnelling Quality Index, Q

On the basis of an evaluation of a large number of case histories of underground excavations, Barton et al (1974) of the Norwegian Geotechnical Institute proposed a Tunnelling Quality Index (Q) for the determination of rock mass characteristics and tunnel support requirements. The numerical value of the index Q varies on a logarithmic scale from 0.001 to a maximum of 1,000 and is defined by:

$$Q = \frac{RQD}{J_n} \times \frac{J_r}{J_a} \times \frac{J_w}{SRF} \tag{4.2}$$

where

RQD is the Rock Quality Designation
J_n is the joint set number
J_r is the joint roughness number
J_a is the joint alteration number
J_w is the joint water reduction factor
SRF is the stress reduction factor

In explaining the meaning of the parameters used to determine the value of Q, Barton et al (1974) offer the following comments:

The first quotient (RQD/J_n), representing the structure of the rock mass, is a crude measure of the block or particle size, with the two extreme values (100/0.5 and 10/20) differing by a factor of 400. If the quotient is interpreted in units of centimetres, the extreme 'particle sizes' of 200 to 0.5 cm are seen to be crude but fairly realistic approximations. Probably the largest blocks should be several times this size and the smallest fragments less than half the size. (Clay particles are of course excluded).

The second quotient (J_r/J_a) represents the roughness and frictional characteristics of the joint walls or filling materials. This quotient is weighted in favour of rough, unaltered joints in direct contact. It is to be expected that such surfaces will be close to peak strength, that they will dilate strongly when sheared, and they will therefore be especially favourable to tunnel stability.

When rock joints have thin clay mineral coatings and fillings, the strength is reduced significantly. Nevertheless, rock wall contact after small shear displacements have occurred may be a very important factor for preserving the excavation from ultimate failure.

Where no rock wall contact exists, the conditions are extremely unfavourable to tunnel stability. The 'friction angles' (given in Table 4.6) are a little below the residual strength values for most clays, and are possibly down-graded by the fact that these clay bands or fillings may tend to consolidate during shear, at least if normal consolidation or if softening and swelling has occurred. The swelling pressure of montmorillonite may also be a factor here.

The third quotient (J_w/SRF) consists of two stress parameters. *SRF* is a measure of: 1) loosening load in the case of an excavation through shear zones and clay bearing rock, 2) rock stress in competent rock, and 3) squeezing loads in plastic

incompetent rocks. It can be regarded as a total stress parameter. The parameter J_w is a measure of water pressure, which has an adverse effect on the shear strength of joints due to a reduction in effective normal stress. Water may, in addition, cause softening and possible out-wash in the case of clay-filled joints. It has proved impossible to combine these two parameters in terms of inter-block effective stress, because paradoxically a high value of effective normal stress may sometimes signify less stable conditions than a low value, despite the higher shear strength. The quotient (J_w/SRF) is a complicated empirical factor describing the 'active stress'.

It appears that the rock tunnelling quality Q can now be considered to be a function of only three parameters which are crude measures of:

   1. Block size (RQD/J_n)
   2. Inter-block shear strength (J_r/J_a)
   3. Active stress (J_w/SRF)

Undoubtedly, there are several other parameters which could be added to improve the accuracy of the classification system. One of these would be the joint orientation. Although many case records include the necessary information on structural orientation in relation to excavation axis, it was not found to be the important general parameter that might be expected. Part of the reason for this may be that the orientations of many types of excavations can be, and normally are, adjusted to avoid the maximum effect of unfavourably oriented major joints. However, this choice is not available in the case of tunnels, and more than half the case records were in this category. The parameters J_n, J_r and J_a appear to play a more important role than orientation, because the number of joint sets determines the degree of freedom for block movement (if any), and the frictional and dilational characteristics can vary more than the down-dip gravitational component of unfavourably oriented joints. If joint orientations had been included the classification would have been less general, and its essential simplicity lost.

Table 4.6 gives the classification of individual parameters used to obtain the Tunnelling Quality Index Q for a rock mass. The use of this table is illustrated in the following example.

A 15 m span crusher chamber for an underground mine is to be excavated in a norite at a depth of 2,100 m below surface. The rock mass contains two sets of joints controlling stability. These joints are undulating, rough and unweathered with very minor surface staining. *RQD* values range from 85% to 95% and laboratory tests on core samples of intact rock give an average uniaxial compressive strength of 170 MPa. The principal stress directions are approximately vertical and horizontal and the magnitude of the horizontal principal stress is approximately 1.5 times that of the vertical principal stress. The rock mass is locally damp but there is no evidence of flowing water.

The numerical value of *RQD* is used directly in the calculation of Q and, for this rock mass, an average value of 90 will be used. Table 4.6.2 shows that, for two joint sets, the joint set number, $J_n = 4$. For rough or irregular joints which are undulating, Table 4.6.3

gives a joint roughness number of $J_r = 3$. Table 4.6.4 gives the joint alteration number, J_a = 1.0, for unaltered joint walls with surface staining only. Table 4.6.5 shows that, for an excavation with minor inflow, the joint water reduction factor, $J_w = 1.0$. For a depth below surface of 2,100 m the overburden stress will be approximately 57 MPa and, in this case, the major principal stress $\sigma_1 = 85$ MPa. Since the uniaxial compressive strength of the norite is approximately 170 MPa, this gives a ratio of $\sigma_c /\sigma_1 = 2$. Table 4.6.6 shows that, for competent rock with rock stress problems, this value of σ_c /σ_1 can be expected to produce heavy rock burst conditions and that the value of *SRF* should lie between 10 and 20. A value of *SRF* = 15 will be assumed for this calculation. Using these values gives:

$$Q = \frac{90}{4} \times \frac{3}{1} \times \frac{1}{15} = 4.5$$

In relating the value of the index Q to the stability and support requirements of underground excavations, Barton et al (1974) defined an additional parameter which they called the *Equivalent Dimension*, D_e, of the excavation. This dimension is obtained by dividing the span, diameter or wall height of the excavation by a quantity called the *Excavation Support Ratio*, *ESR*. Hence:

$$D_e = \frac{\text{Excavation span, diameter or height (m)}}{\text{Excavation Support Ratio } ESR}$$

The value of *ESR* is related to the intended use of the excavation and to the degree of security which is demanded of the support system installed to maintain the stability of the excavation. Barton et al (1974) suggest the following values:

Excavation category		*ESR*
A	Temporary mine openings.	3-5
B	Permanent mine openings, water tunnels for hydro power (excluding high pressure penstocks), pilot tunnels, drifts and headings for large excavations.	1.6
C	Storage rooms, water treatment plants, minor road and railway tunnels, surge chambers, access tunnels.	1.3
D	Power stations, major road and railway tunnels, civil defence chambers, portal intersections.	1.0
E	Underground nuclear power stations, railway stations, sports and public facilities, factories.	0.8

The crusher station discussed above falls into the category of permanent mine openings and is assigned an excavation support ratio *ESR* = 1.6. Hence, for an excavation span of 15 m, the equivalent dimension, $D_e = 15/1.6 = 9.4$.

The equivalent dimension, *De*, plotted against the value of *Q*, is used to define a number of support categories in a chart published in the original paper by Barton et al (1974). This chart has recently been updated by Grimstad and Barton (1993) to reflect the increasing use of steel fibre reinforced shotcrete in underground excavation support. Figure 4.3 is reproduced from this updated chart.

From Figure 4.3, a value of D_e of 9.4 and a value of *Q* of 4.5 places this crusher excavation in category (4) which requires a pattern of rockbolts (spaced at 2.3 m) and 40 to 50 mm of unreinforced shotcrete.

Because of the mild to heavy rock burst conditions which are anticipated, it may be prudent to destress the rock in the walls of this crusher chamber. This is achieved by using relatively heavy production blasting to excavate the chamber and omitting the smooth blasting usually used to trim the final walls of an excavation such as an underground powerhouse at shallower depth. Caution is recommended in the use of destress blasting and, for critical applications, it may be advisable to seek the advice of a blasting specialist before embarking on this course of action.

Løset (1992) suggests that, for rocks with $4 < Q < 30$, blasting damage will result in the creation of new 'joints' with a consequent local reduction in the value of *Q* for the rock surrounding the excavation. He suggests that this can be accounted for by reducing the *RQD* value for the blast damaged zone.

Assuming that the *RQD* value for the destressed rock around the crusher chamber drops to 50 %, the resulting value of $Q = 2.9$. From Figure 4.3, this value of *Q*, for an equivalent dimension, D_e of 9.4, places the excavation just inside category (5) which requires rockbolts, at approximately 2 m spacing, and a 50 mm thick layer of steel fibre reinforced shotcrete.

Barton et al (1980) provide additional information on rockbolt length, maximum unsupported spans and roof support pressures to supplement the support recommendations published in the original 1974 paper.

The length L of rockbolts can be estimated from the excavation width *B* and the Excavation Support Ratio *ESR*:

$$L = \frac{2 + 0.15B}{ESR} \tag{4.3}$$

The maximum unsupported span can be estimated from:

$$\text{Maximum span (unsupported)} = 2\ ESR\ Q^{0.4} \tag{4.4}$$

Based upon analyses of case records, Grimstad and Barton (1993) suggest that the relationship between the value of *Q* and the permanent roof support pressure P_{roof} is estimated from:

$$P_{\text{roof}} = \frac{2\ \sqrt{J_n}\ Q^{-\frac{1}{3}}}{3 J_r} \tag{4.5}$$

Table 4.6: Classification of individual parameters used in the Tunnelling Quality Index *Q* (After Barton et al 1974).

DESCRIPTION	VALUE	NOTES
1. ROCK QUALITY DESIGNATION	**RQD**	
A. Very poor	0 - 25	1. Where *RQD* is reported or measured as ≤ 10 (including 0),
B. Poor	25 - 50	a nominal value of 10 is used to evaluate *Q*.
C. Fair	50 - 75	
D. Good	75 - 90	2. *RQD* intervals of 5, i.e. 100, 95, 90 etc. are sufficiently
E. Excellent	90 - 100	accurate.
2. JOINT SET NUMBER	J_n	
A. Massive, no or few joints	0.5 - 1.0	
B. One joint set	2	
C. One joint set plus random	3	
D. Two joint sets	4	
E. Two joint sets plus random	6	
F. Three joint sets	9	1. For intersections use $(3.0 \times J_n)$
G. Three joint sets plus random	12	
H. Four or more joint sets, random,	15	2. For portals use $(2.0 \times J_n)$
heavily jointed, 'sugar cube', etc.		
J. Crushed rock, earthlike	20	
3. JOINT ROUGHNESS NUMBER	J_r	
a. Rock wall contact		
b. Rock wall contact before 10 cm shear		
A. Discontinuous joints	4	
B. Rough and irregular, undulating	3	
C. Smooth undulating	2	
D. Slickensided undulating	1.5	1. Add 1.0 if the mean spacing of the relevant joint set is
E. Rough or irregular, planar	1.5	greater than 3 m.
F. Smooth, planar	1.0	
G. Slickensided, planar	0.5	2. J_r = 0.5 can be used for planar, slickensided joints having
c. No rock wall contact when sheared		lineations, provided that the lineations are oriented for
H. Zones containing clay minerals thick	1.0	minimum strength.
enough to prevent rock wall contact	(nominal)	
J. Sandy, gravely or crushed zone thick	1.0	
enough to prevent rock wall contact	(nominal)	
4. JOINT ALTERATION NUMBER	J_a	*φr* degrees (approx.)
a. Rock wall contact		
A. Tightly healed, hard, non-softening,	0.75	1. Values of *φr*, the residual friction angle,
impermeable filling		are intended as an approximate guide
B. Unaltered joint walls, surface staining only	1.0	25 - 35 · to the mineralogical properties of the
C. Slightly altered joint walls, non-softening	2.0	25 - 30 · alteration products, if present.
mineral coatings, sandy particles, clay-free		
disintegrated rock, etc.		
D. Silty-, or sandy-clay coatings, small clay-	3.0	20 - 25
fraction (non-softening)		
E. Softening or low-friction clay mineral coatings,	4.0	8 - 16
i.e. kaolinite, mica. Also chlorite, talc, gypsum		
and graphite etc., and small quantities of swelling		
clays. (Discontinuous coatings, 1 - 2 mm or less)		

Table 4.6: (cont'd.) Classification of individual parameters used in the Tunnelling Quality Index Q (After Barton et al 1974).

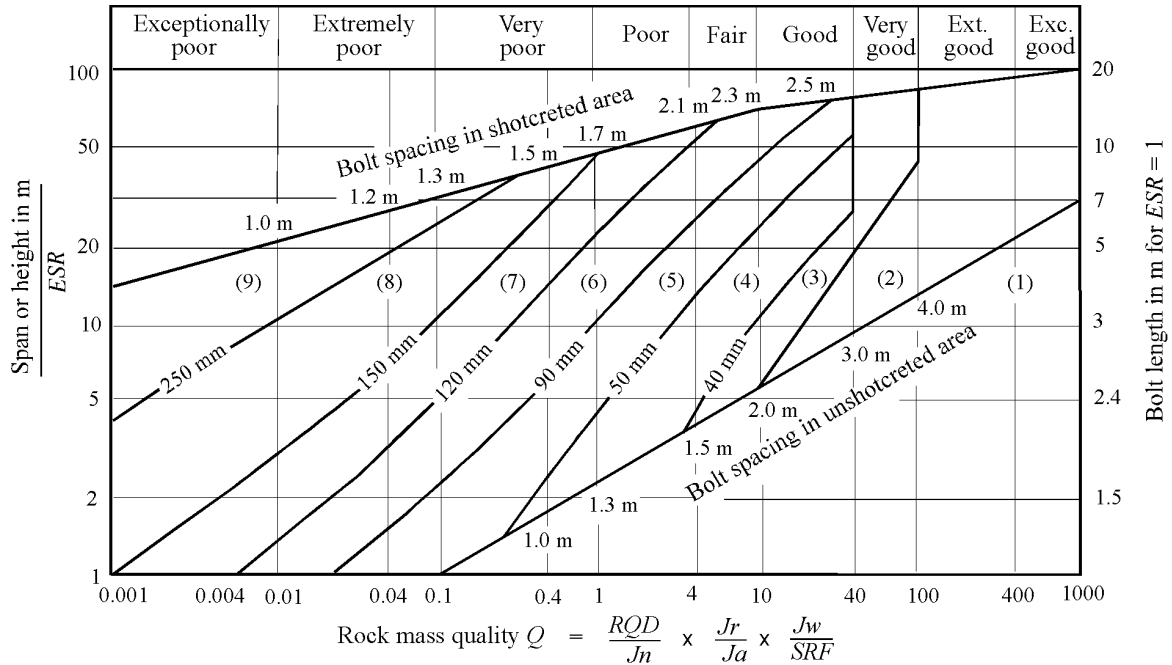| DESCRIPTION	VALUE	NOTES
4, JOINT ALTERATION NUMBER	J_a	ϕr degrees (approx.)
b. Rock wall contact before 10 cm shear		
F. Sandy particles, clay-free, disintegrating rock etc.	4.0	25 - 30
G. Strongly over-consolidated, non-softening clay mineral fillings (continuous < 5 mm thick)	6.0	16 - 24
H. Medium or low over-consolidation, softening clay mineral fillings (continuous < 5 mm thick)	8.0	12 - 16
J. Swelling clay fillings, i.e. montmorillonite, (continuous < 5 mm thick). Values of J_a depend on percent of swelling clay-size particles, and access to water.	8.0 - 12.0	6 - 12
c. No rock wall contact when sheared		
K. Zones or bands of disintegrated or crushed	6.0	
L. rock and clay (see G, H and J for clay	8.0	
M. conditions)	8.0 - 12.0	6 - 24
N. Zones or bands of silty- or sandy-clay, small clay fraction, non-softening	5.0	
O. Thick continuous zones or bands of clay	10.0 - 13.0	
P. & R. (see G.H and J for clay conditions)	6.0 - 24.0	
5. JOINT WATER REDUCTION	J_w	approx. water pressure (kgf/cm^2)
A. Dry excavation or minor inflow i.e. < 5 l/m locally	1.0	< 1.0
B. Medium inflow or pressure, occasional outwash of joint fillings	0.66	1.0 - 2.5
C. Large inflow or high pressure in competent rock with unfilled joints	0.5	2.5 - 10.0 1. Factors C to F are crude estimates; increase J_w if drainage installed.
D. Large inflow or high pressure	0.33	2.5 - 10.0
E. Exceptionally high inflow or pressure at blasting, decaying with time	0.2 - 0.1	> 10 2. Special problems caused by ice formation are not considered.
F. Exceptionally high inflow or pressure	0.1 - 0.05	> 10
6. STRESS REDUCTION FACTOR	*SRF*	
a. Weakness zones intersecting excavation, which may cause loosening of rock mass when tunnel is excavated		
A. Multiple occurrences of weakness zones containing clay or chemically disintegrated rock, very loose surrounding rock any depth)	10.0	1. Reduce these values of *SRF* by 25 - 50% but only if the relevant shear zones influence do not intersect the excavation
B. Single weakness zones containing clay, or chemically dis-tegrated rock (excavation depth < 50 m)	5.0	
C. Single weakness zones containing clay, or chemically dis-tegrated rock (excavation depth > 50 m)	2.5	
D. Multiple shear zones in competent rock (clay free), loose surrounding rock (any depth)	7.5	
E. Single shear zone in competent rock (clay free). (depth of excavation < 50 m)	5.0	
F. Single shear zone in competent rock (clay free). (depth of excavation > 50 m)	2.5	
G. Loose open joints, heavily jointed or 'sugar cube', (any depth)	5.0	

Table 4.6: (cont'd.) Classification of individual parameters in the Tunnelling Quality Index Q (After Barton et al 1974).

DESCRIPTION		VALUE		NOTES
6. STRESS REDUCTION FACTOR			*SRF*	
b. Competent rock, rock stress problems				
	σ_c/σ_1	$\sigma_t\sigma_1$		2. For strongly anisotropic virgin stress field
H. Low stress, near surface	> 200	> 13	2.5	(if measured): when $5 \leq \sigma_1/\sigma_3 \leq 10$, reduce σ_c
J. Medium stress	200 - 10	13 - 0.66	1.0	to $0.8\sigma_c$ and σ_t to $0.8\sigma_t$. When $\sigma_1/\sigma_3 > 10$,
K. High stress, very tight structure	10 - 5	0.66 - 0.33	0.5 - 2	reduce σ_c and σ_t to $0.6\sigma_c$ and $0.6\sigma_t$, where
(usually favourable to stability, may				σ_c = unconfined compressive strength, and
be unfavourable to wall stability)				σ_t = tensile strength (point load) and σ_1 and
L. Mild rockburst (massive rock)	5 - 2.5	0.33 - 0.16	5 - 10	σ_3 are the major and minor principal stresses.
M. Heavy rockburst (massive rock)	< 2.5	< 0.16	10 - 20	3. Few case records available where depth of
c. Squeezing rock, plastic flow of incompetent rock				crown below surface is less than span width.
under influence of high rock pressure				Suggest *SRF* increase from 2.5 to 5 for such
N. Mild squeezing rock pressure			5 - 10	cases (see H).
O. Heavy squeezing rock pressure			10 - 20	
d. Swelling rock, chemical swelling activity depending on presence of water				
P. Mild swelling rock pressure			5 - 10	
R. Heavy swelling rock pressure			10 - 15	

ADDITIONAL NOTES ON THE USE OF THESE TABLES

When making estimates of the rock mass Quality (Q), the following guidelines should be followed in addition to the notes listed in the tables:

1. When borehole core is unavailable, *RQD* can be estimated from the number of joints per unit volume, in which the number of joints per metre for each joint set are added. A simple relationship can be used to convert this number to *RQD* for the case of clay free rock masses: $RQD = 115 - 3.3 J_v$ (approx.), where J_v = total number of joints per m^3 ($0 < RQD < 100$ for $35 > J_v > 4.5$).

2. The parameter J_n representing the number of joint sets will often be affected by foliation, schistosity, slaty cleavage or bedding etc. If strongly developed, these parallel 'joints' should obviously be counted as a complete joint set. However, if there are few 'joints' visible, or if only occasional breaks in the core are due to these features, then it will be more appropriate to count them as 'random' joints when evaluating J_n.

3. The parameters J_r and J_a (representing shear strength) should be relevant to the weakest significant joint set or clay filled discontinuity in the given zone. However, if the joint set or discontinuity with the minimum value of J_r/J_a is favourably oriented for stability, then a second, less favourably oriented joint set or discontinuity may sometimes be more significant, and its higher value of J_r/J_a should be used when evaluating Q. The value of J_r/J_a should in fact relate to the surface most likely to allow failure to initiate.

4. When a rock mass contains clay, the factor *SRF* appropriate to loosening loads should be evaluated. In such cases the strength of the intact rock is of little interest. However, when jointing is minimal and clay is completely absent, the strength of the intact rock may become the weakest link, and the stability will then depend on the ratio rock-stress/rock-strength. A strongly anisotropic stress field is unfavourable for stability and is roughly accounted for as in note 2 in the table for stress reduction factor evaluation.

5. The compressive and tensile strengths (σ_c and σ_t) of the intact rock should be evaluated in the saturated condition if this is appropriate to the present and future in situ conditions. A very conservative estimate of the strength should be made for those rocks that deteriorate when exposed to moist or saturated conditions.

REINFORCEMENT CATEGORIES
1) Unsupported
2) Spot bolting
3) Systematic bolting
4) Systematic bolting with 40-100 mm
   unreinforced shotcrete

5) Fibre reinforced shotcrete, 50 - 90 mm, and bolting
6) Fibre reinforced shotcrete, 90 - 120 mm, and bolting
7) Fibre reinforced shotcrete, 120 - 150 mm, and bolting
8) Fibre reinforced shotcrete, > 150 mm, with reinforced
   ribs of shotcrete and bolting
9) Cast concrete lining

Figure 4.3: Estimated support categories based on the tunnelling quality index Q (After Grimstad and Barton 1993).

3.6 Using rock mass classification systems

The two most widely used rock mass classifications are Bieniawski's *RMR* (1976, 1989) and Barton et al's *Q* (1974). Both methods incorporate geological, geometric and design/engineering parameters in arriving at a quantitative value of their rock mass quality. The similarities between *RMR* and *Q* stem from the use of identical, or very similar, parameters in calculating the final rock mass quality rating. The differences between the systems lie in the different weightings given to similar parameters and in the use of distinct parameters in one or the other scheme
the other scheme.

RMR uses compressive strength directly while *Q* only considers strength as it relates to in situ stress in competent rock. Both schemes deal with the geology and geometry of the rock mass, but in slightly different ways. Both consider groundwater, and both include some component of rock material strength. Some estimate of orientation can be incorporated into *Q* using a guideline presented by Barton et al (1974): 'the parameters J_r and J_a should ... relate to the surface most likely to allow failure to initiate.' The greatest difference between the two systems is the lack of a stress parameter in the *RMR* system.
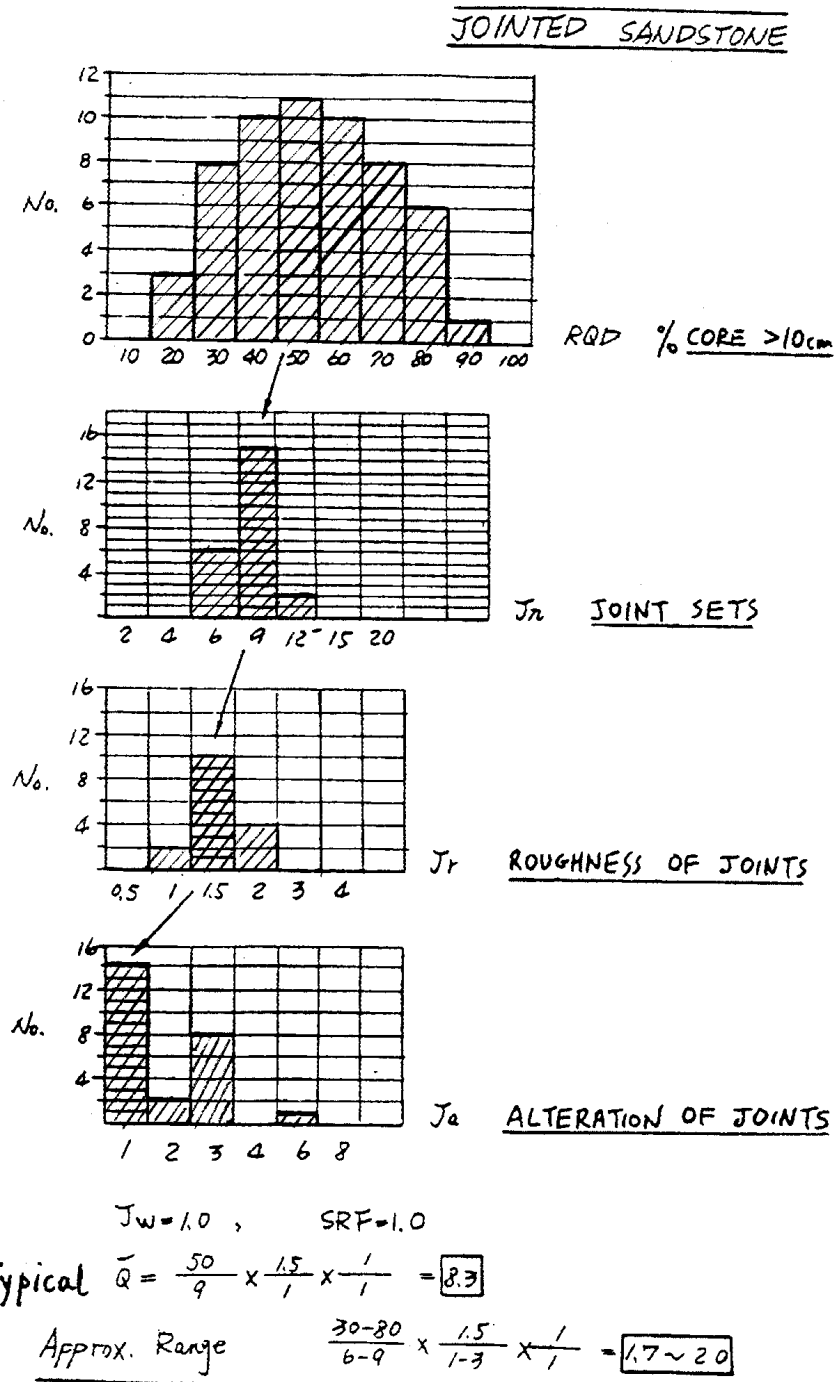
Figure 4.4: Histograms showing variations in RQD, J_n, J_r and J_a for a dry jointed sandstone under 'medium' stress conditions, reproduced from field notes prepared by Dr. N. Barton.

When using either of these methods, two approaches can be taken. One is to evaluate the rock mass specifically for the parameters included in the classification methods; the other is to accurately characterise the rock mass and then attribute parameter ratings at a later time. The latter method is recommended since it gives a full and complete description of the rock mass which can easily be translated into either classification index. If rating values alone had been recorded during mapping, it would be almost impossible to carry out verification studies.

In many cases, it is appropriate to give a range of values to each parameter in a rock mass classification and to evaluate the significance of the final result. An example of this approach is given in Figure 4.4 which is reproduced from field notes prepared by Dr. N. Barton on a project. In this particular case, the rock mass is dry and is subjected to 'medium' stress conditions (Table 4.6.6.K) and hence $J_w = 1.0$ and $SRF = 1.0$. Histograms showing the variations in RQD, J_n, J_r and J_a, along the exploration adit mapped, are presented in this figure. The average value of $Q = 8.9$ and the approximate range of Q is $1.7 < Q < 20$. The average value of Q can be used in choosing a basic support system while the range gives an indication of the possible adjustments which will be required to meet different conditions encountered during construction.

A further example of this approach is given in a paper by Barton et al (1992) concerned with the design of a 62 m span underground sports hall in jointed gneiss. Histograms of all the input parameters for the Q system are presented and analysed in order to determine the weighted average value of Q.

Carter (1992) has adopted a similar approach, but extended his analysis to include the derivation of a probability distribution function and the calculation of a probability of failure in a discussion on the stability of surface crown pillars in abandoned metal mines.

Throughout this chapter it has been suggested that the user of a rock mass classification scheme should check that the latest version is being used. An exception is the use of Bieniawski's *RMR* classification for rock mass strength estimates (discussed in Chapter 8) where the 1976 version as well as the 1989 version are used. It is also worth repeating that the use of two rock mass classification schemes is advisable.

4

Shear strength of discontinuities

4.1 Introduction

All rock masses contain discontinuities such as bedding planes, joints, shear zones and faults. At shallow depth, where stresses are low, failure of the intact rock material is minimal and the behaviour of the rock mass is controlled by sliding on the discontinuities. In order to analyse the stability of this system of individual rock blocks, it is necessary to understand the factors that control the shear strength of the discontinuities which separate the blocks. These questions are addressed in the discussion that follows.

4.2 Shear strength of planar surfaces

Suppose that a number of samples of a rock are obtained for shear testing. Each sample contains a through-going bedding plane that is cemented; in other words, a tensile force would have to be applied to the two halves of the specimen in order to separate them. The bedding plane is absolutely planar, having no surface irregularities or undulations. As illustrated in Figure 4.1, in a shear test each specimen is subjected to a stress σ_n normal to the bedding plane, and the shear stress τ, required to cause a displacement δ, is measured.

The shear stress will increase rapidly until the peak strength is reached. This corresponds to the sum of the strength of the cementing material bonding the two halves of the bedding plane together and the frictional resistance of the matching surfaces. As the displacement continues, the shear stress will fall to some residual value that will then remain constant, even for large shear displacements.

Plotting the peak and residual shear strengths for different normal stresses results in the two lines illustrated in Figure 4.1. For planar discontinuity surfaces the experimental points will generally fall along straight lines. The peak strength line has a slope of ϕ and an intercept of c on the shear strength axis. The residual strength line has a slope of ϕ_r.

The relationship between the peak shear strength τ_p and the normal stress σ_n can be represented by the Mohr-Coulomb equation:

$$\tau_p = c + \sigma_n \tan\phi \tag{4.1}$$

where c is the cohesive strength of the cemented surface and
        ϕ is the angle of friction.
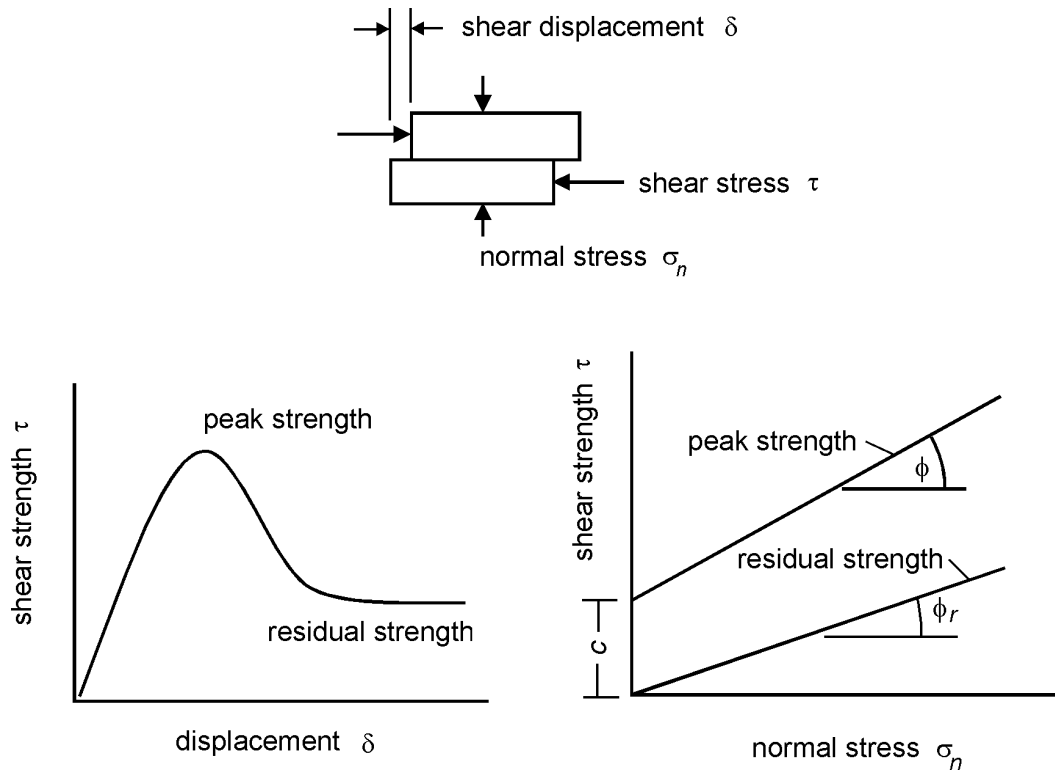
Figure 4.1: Shear testing of discontinuities

In the case of the residual strength, the cohesion c has dropped to zero and the relationship between ϕ_r and σ_n can be represented by:

$$\tau_r = \sigma_n \tan \phi_r \qquad (4.2)$$

where ϕ_r is the residual angle of friction.

This example has been discussed in order to illustrate the physical meaning of the term cohesion, a soil mechanics term, which has been adopted by the rock mechanics community. In shear tests on soils, the stress levels are generally an order of magnitude lower than those involved in rock testing and the cohesive strength of a soil is a result of the adhesion of the soil particles. In rock mechanics, true cohesion occurs when cemented surfaces are sheared. However, in many practical applications, the term cohesion is used for convenience and it refers to a mathematical quantity related to surface roughness, as discussed in a later section. Cohesion is simply the intercept on the τ axis at zero normal stress.

The basic friction angle ϕ_b is a quantity that is fundamental to the understanding of the shear strength of discontinuity surfaces. This is approximately equal to the residual friction angle ϕ_r but it is generally measured by testing sawn or ground rock surfaces. These tests, which can be carried out on surfaces as small as 50 mm × 50 mm, will produce a straight line plot defined by the equation :

$$\tau_r = \sigma_n \tan \phi_b \qquad (4.3)$$
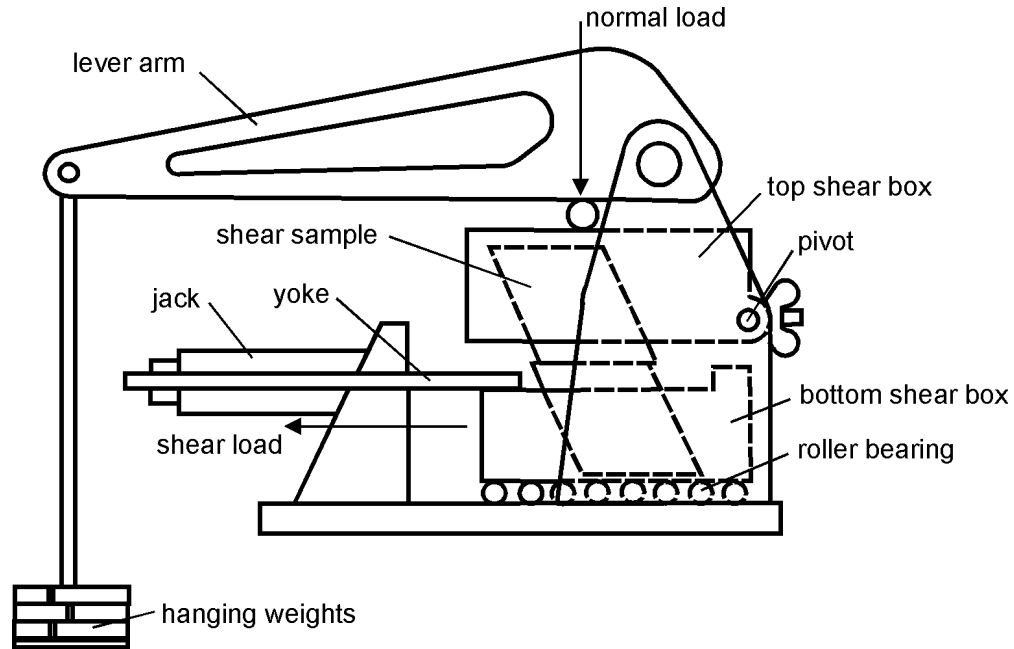
Figure 4.2: Diagrammatic section through shear machine used by Hencher and Richards (1982).
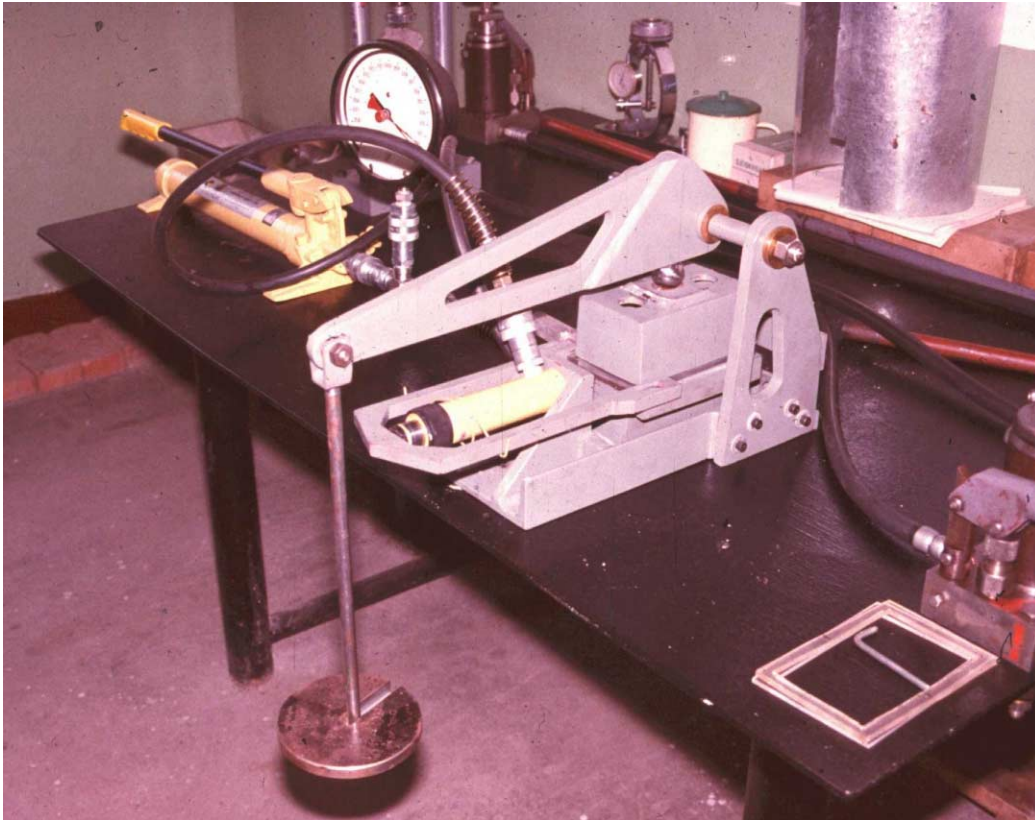
Figure 4.3: Shear machine of the type used by Hencher and Richards (1982) for measurement of the shear strength of sheet joints in Hong Kong granite.

A typical shear testing machine, which can be used to determine the basic friction angle ϕ_b is illustrated in Figures 4.2 and 4.3. This is a very simple machine and the use of a mechanical lever arm ensures that the normal load on the specimen remains constant throughout the test. This is an important practical consideration since it is difficult to maintain a constant normal load in hydraulically or pneumatically controlled systems and this makes it difficult to interpret test data.

Note that it is important that, in setting up the specimen, great care has to be taken to ensure that the shear surface is aligned accurately in order to avoid the need for an additional angle correction.

Most shear strength determinations today are carried out by determining the basic friction angle, as described above, and then making corrections for surface roughness as discussed in the following sections of this chapter. In the past there was more emphasis on testing full scale discontinuity surfaces, either in the laboratory or in the field. There are a significant number of papers in the literature of the 1960s and 1970s describing large and elaborate in situ shear tests, many of which were carried out to determine the shear strength of weak layers in dam foundations. However, the high cost of these tests together with the difficulty of interpreting the results has resulted in a decline in the use of these large scale tests and they are seldom seen today.

The author's opinion is that it makes both economical and practical sense to carry out a number of small scale laboratory shear tests, using equipment such as that illustrated in Figures 4.2 and 4.3, to determine the basic friction angle. The roughness component which is then added to this basic friction angle to give the effective friction angle is a number which is site specific and scale dependent and is best obtained by visual estimates in the field. Practical techniques for making these roughness angle estimates are described on the following pages.

4.3   Shear strength of rough surfaces

A natural discontinuity surface in hard rock is never as smooth as a sawn or ground surface of the type used for determining the basic friction angle. The undulations and asperities on a natural joint surface have a significant influence on its shear behaviour. Generally, this surface roughness increases the shear strength of the surface, and this strength increase is extremely important in terms of the stability of excavations in rock.

Patton (1966) demonstrated this influence by means of an experiment in which he carried out shear tests on 'saw-tooth' specimens such as the one illustrated in Figure 4.4. Shear displacement in these specimens occurs as a result of the surfaces moving up the inclined faces, causing dilation (an increase in volume) of the specimen.

The shear strength of Patton's saw-tooth specimens can be represented by:

$$\tau = \sigma_n \tan(\phi_b + i) \tag{4.4}$$

where ϕ_b is the basic friction angle of the surface and
i is the angle of the saw-tooth face.
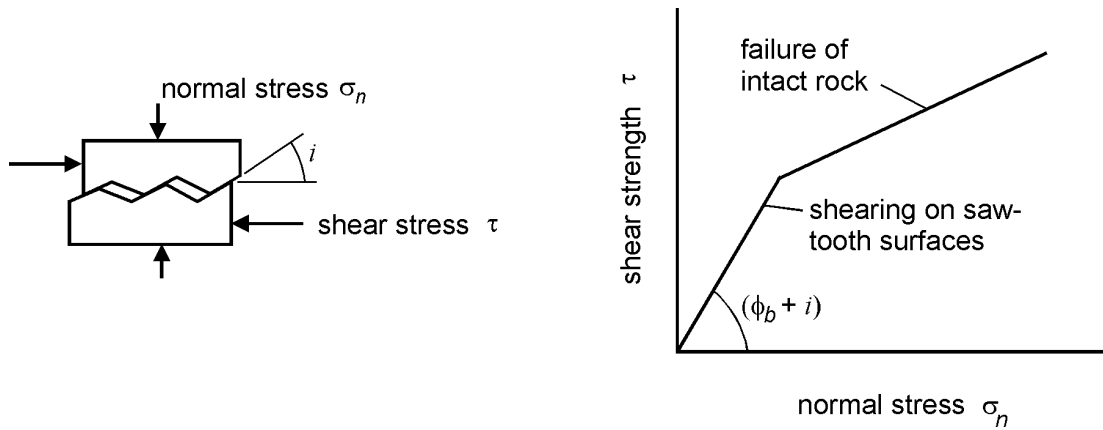
Figure 4.4: Patton's experiment on the shear strength of saw-tooth specimens.

4.4 Barton's estimate of shear strength

Equation (4.4) is valid at low normal stresses where shear displacement is due to sliding along the inclined surfaces. At higher normal stresses, the strength of the intact material will be exceeded and the teeth will tend to break off, resulting in a shear strength behaviour which is more closely related to the intact material strength than to the frictional characteristics of the surfaces.

While Patton's approach has the merit of being very simple, it does not reflect the reality that changes in shear strength with increasing normal stress are gradual rather than abrupt. Barton and his co-workers (1973, 1976, 1977, 1990) studied the behaviour of natural rock joints and have proposed that equation (4.4) can be re-written as:

$$\tau = \sigma_n \tan\left(\phi_b + JRC \log_{10}\left(\frac{JCS}{\sigma_n} \right) \right) \qquad (4.5)$$

where   JRC is the joint roughness coefficient and
        JCS is the joint wall compressive strength.

4.5 Field estimates of JRC

The joint roughness coefficient JRC is a number that can be estimated by comparing the appearance of a discontinuity surface with standard profiles published by Barton and others. One of the most useful of these profile sets was published by Barton and Choubey (1977) and is reproduced in Figure 4.2.

The appearance of the discontinuity surface is compared visually with the profiles shown and the JRC value corresponding to the profile which most closely matches that of the discontinuity surface is chosen. In the case of small scale laboratory specimens, the scale of the surface roughness will be approximately the same as that of the profiles illustrated. However, in the field the length of the surface of interest may be several metres or even tens of metres and the JRC value must be estimated for the full scale surface.
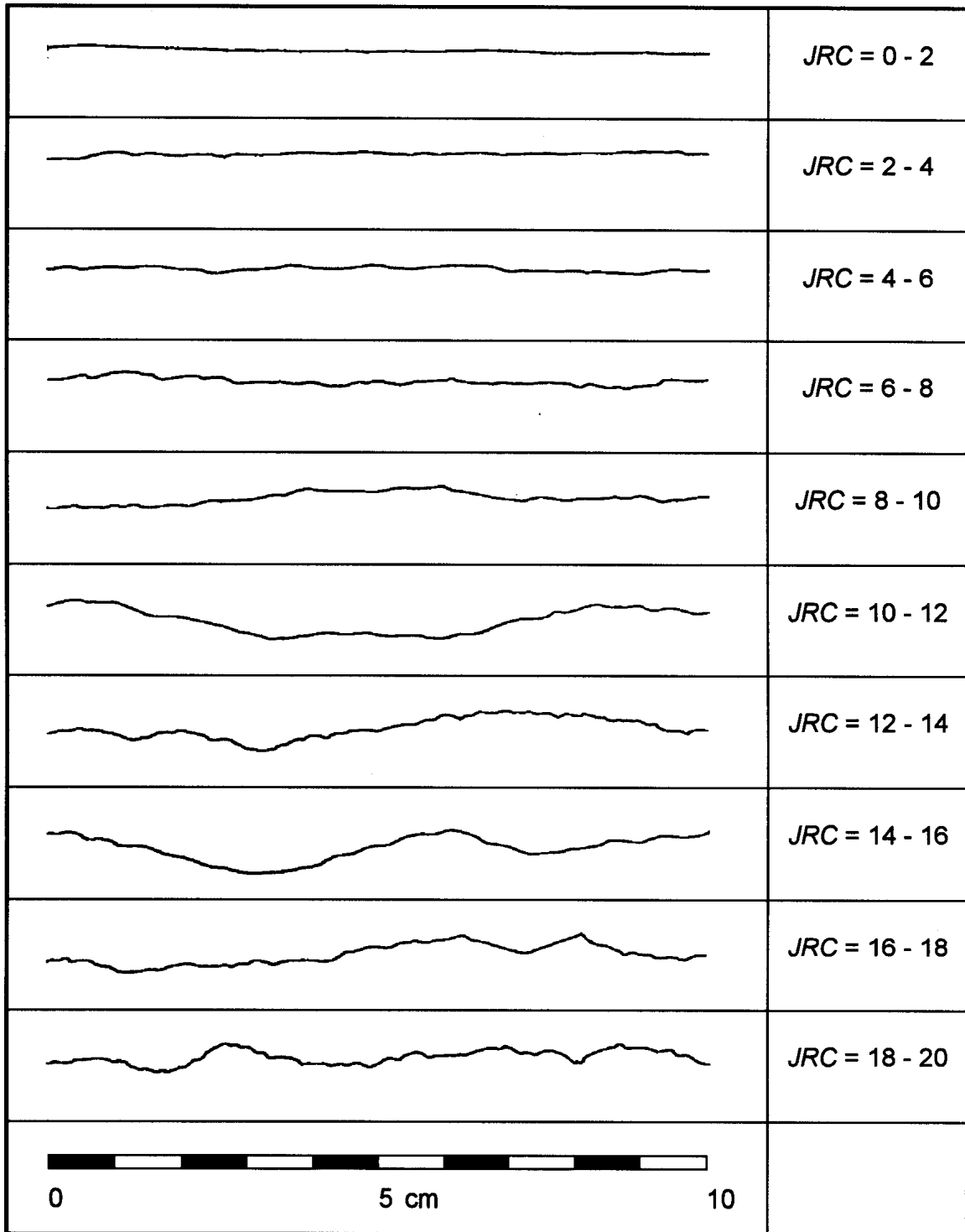
Figure 4.2: Roughness profiles and corresponding JRC values (After Barton and Choubey 1977).

Straight edge

Asperity amplitude - mm

Length of profile - m

Amplitude of asperities - mm

Joint Roughness Coefficient (JRC)

Length of profile - m
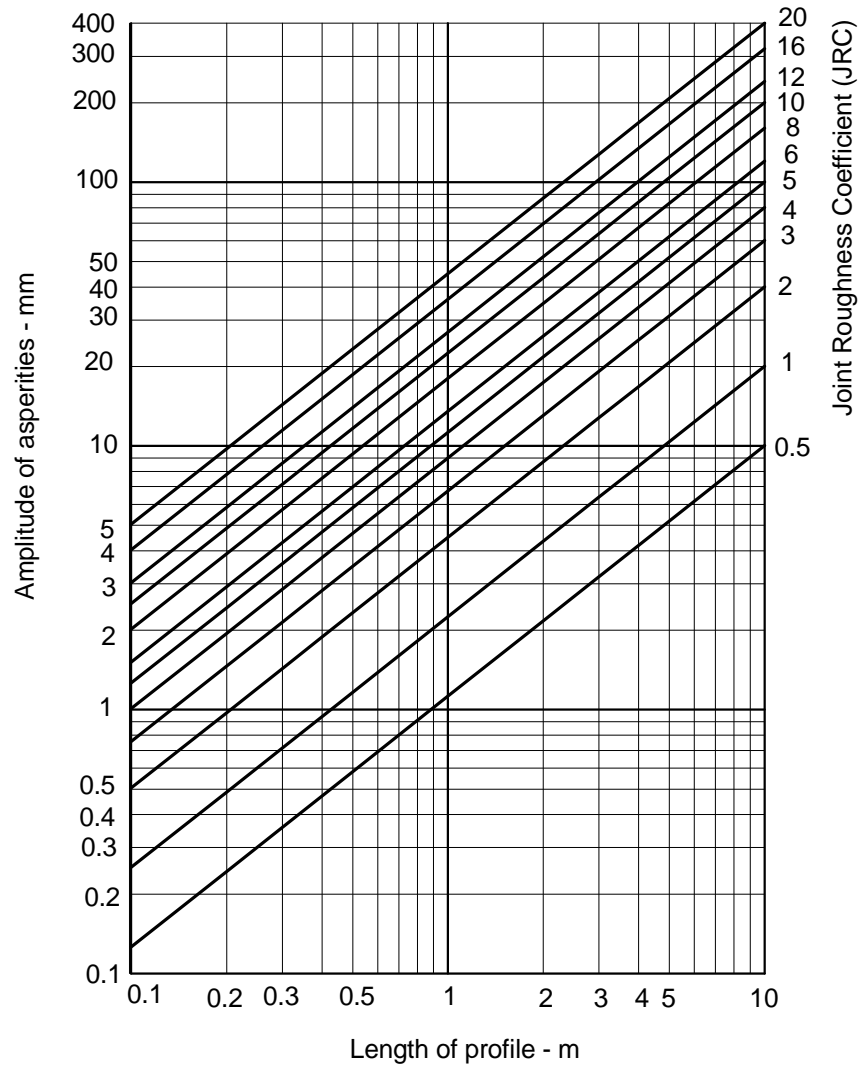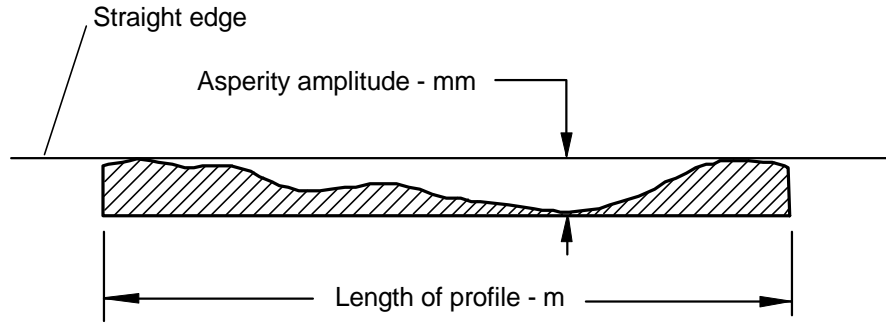
Figure 4.6: Alternative method for estimating *JRC* from measurements of surface roughness amplitude from a straight edge (Barton 1982).

4.6 Field estimates of JCS

Suggested methods for estimating the joint wall compressive strength were published by the ISRM (1978). The use of the Schmidt rebound hammer for estimating joint wall compressive strength was proposed by Deere and Miller (1966), as illustrated in Figure 4.7.
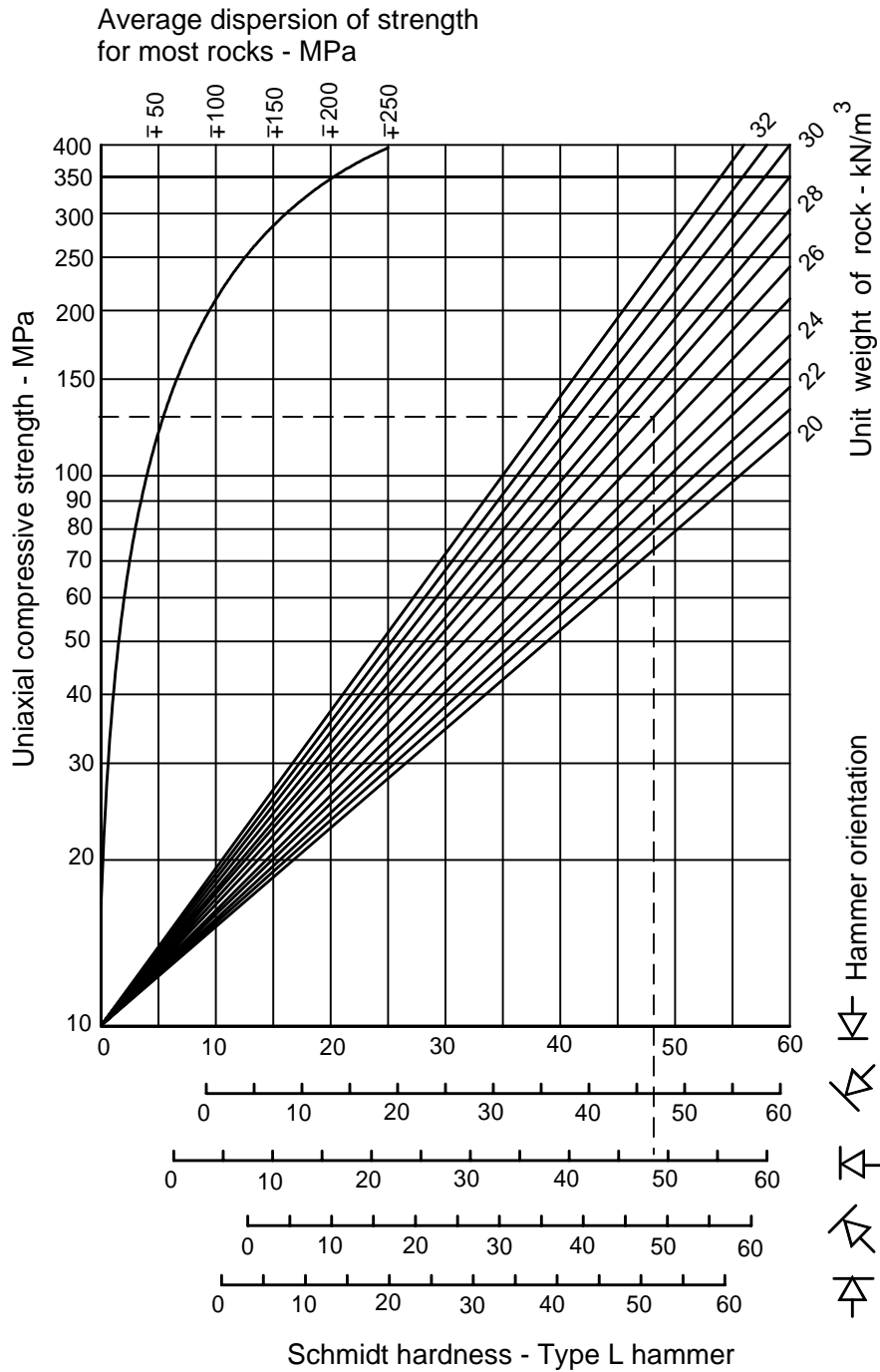
Figure 4.7: Estimate of joint wall compressive strength from Schmidt hardness.

4.7   Influence of scale on *JRC* and *JCS*

On the basis of extensive testing of joints, joint replicas, and a review of literature, Barton and Bandis (1982) proposed the scale corrections for JRC defined by the following relationship:

$$JRC_n = JRC_o \left(\frac{L_n}{L_o} \right)^{-0.02 JRC_o} \tag{4.6}$$

where JRC_o, and L_o (length) refer to 100 mm laboratory scale samples and JRC_n, and L_n refer to in situ block sizes.

Because of the greater possibility of weaknesses in a large surface, it is likely that the average joint wall compressive strength (JCS) decreases with increasing scale. Barton and Bandis (1982) proposed the scale corrections for JCS defined by the following relationship:

$$JCS_n = JCS_o \left(\frac{L_n}{L_o} \right)^{-0.03 JRC_o} \tag{4.7}$$

where JCS_o and L_o (length) refer to 100 mm laboratory scale samples and JCS_n and L_n refer to in situ block sizes.

4.8   Shear strength of filled discontinuities

The discussion presented in the previous sections has dealt with the shear strength of discontinuities in which rock wall contact occurs over the entire length of the surface under consideration. This shear strength can be reduced drastically when part or all of the surface is not in intimate contact, but covered by soft filling material such as clay gouge. For planar surfaces, such as bedding planes in sedimentary rock, a thin clay coating will result in a significant shear strength reduction. For a rough or undulating joint, the filling thickness has to be greater than the amplitude of the undulations before the shear strength is reduced to that of the filling material.

A comprehensive review of the shear strength of filled discontinuities was prepared by Barton (1974) and a summary of the shear strengths of typical discontinuity fillings, based on Barton's review, is given in Table 4.1.

Where a significant thickness of clay or gouge fillings occurs in rock masses and where the shear strength of the filled discontinuities is likely to play an important role in the stability of the rock mass, it is strongly recommended that samples of the filling be sent to a soil mechanics laboratory for testing.

Table 4.1: Shear strength of filled discontinuities and filling materials (After Barton 1974)

Rock	Description	Peak c' (MPa)	Peak $\phi°$	Residual c' (MPa)	Residual $\phi°$
Basalt	Clayey basaltic breccia, wide variation from clay to basalt content	0.24	42		
Bentonite	Bentonite seam in chalk	0.015	7.5		
	Thin layers	0.09-0.12	12-17		
	Triaxial tests	0.06-0.1	9-13		
Bentonitic shale	Triaxial tests	0-0.27	8.5-29		
	Direct shear tests			0.03	8.5
Clays	Over-consolidated, slips, joints and minor shears	0-0.18	12-18.5	0-0.003	10.5-16
Clay shale	Triaxial tests	0.06	32		
	Stratification surfaces			0	19-25
Coal measure rocks	Clay mylonite seams, 10 to 25 mm	0.012	16	0	11-11.5
Dolomite	Altered shale bed, ± 150 mm thick	0.04	14.5	0.02	17
Diorite, granodiorite and porphyry	Clay gouge (2% clay, PI = 17%)	0	26.5		
Granite	Clay filled faults	0-0.1	24-45		
	Sandy loam fault filling	0.05	40		
	Tectonic shear zone, schistose and broken granites, disintegrated rock and gouge	0.24	42		
Greywacke	1-2 mm clay in bedding planes			0	21
Limestone	6 mm clay layer			0	13
	10-20 mm clay fillings	0.1	13-14		
	<1 mm clay filling	0.05-0.2	17-21		
Limestone, marl and lignites	Interbedded lignite layers	0.08	38		
	Lignite/marl contact	0.1	10		
Limestone	Marlaceous joints, 20 mm thick	0	25	0	15-24
Lignite	Layer between lignite and clay	0.014-.03	15-17.5		
Montmorillonite Bentonite clay	80 mm seams of bentonite (mont-morillonite) clay in chalk	0.36 0.016-.02	14 7.5-11.5	0.08	11
Schists, quartzites and siliceous schists	100-15- mm thick clay filling	0.03-0.08	32		
	Stratification with thin clay	0.61-0.74	41		
	Stratification with thick clay	0.38	31		
Slates	Finely laminated and altered	0.05	33		
Quartz / kaolin / pyrolusite	Remoulded triaxial tests	0.042-.09	36-38		

4.9   Influence of water pressure

When water pressure is present in a rock mass, the surfaces of the discontinuities are forced apart and the normal stress σ_n is reduced. Under steady state conditions, where there is sufficient time for the water pressures in the rock mass to reach equilibrium, the reduced normal stress is defined by $\sigma_n' = (\sigma_n - u)$, where u is the water pressure. The reduced normal stress σ_n' is usually called the effective normal stress, and it can be used in place of the normal stress term σn in all of the equations presented in previous sections of this chapter.

4.10   Instantaneous cohesion and friction

Due to the historical development of the subject of rock mechanics, many of the analyses, used to calculate factors of safety against sliding, are expressed in terms of the Mohr-Coulomb cohesion (c) and friction angle (ϕ), defined in Equation 4.1. Since the 1970s it has been recognised that the relationship between shear strength and normal stress is more accurately represented by a non-linear relationship such as that proposed by Barton (1973). However, because this relationship (e.g. Equation 4.5) is not expressed in terms of c and ϕ, it is necessary to devise some means for estimating the equivalent cohesive strengths and angles of friction from relationships such as those proposed by Barton.

Figure 4.8 gives definitions of the *instantaneous cohesion c_i* and the *instantaneous friction* angle ϕ_i for a normal stress of σ_n. These quantities are given by the intercept and the inclination, respectively, of the tangent to the non-linear relationship between shear strength and normal stress. These quantities may be used for stability analyses in which the Mohr-Coulomb failure criterion (Equation 4.1) is applied, provided that the normal stress σ_n is reasonably close to the value used to define the tangent point.

In a typical practical application, a spreadsheet program can be used to solve Equation 4.5 and to calculate the instantaneous cohesion and friction values for a range of normal stress values. A portion of such a spreadsheet is illustrated in Figure 4.9.
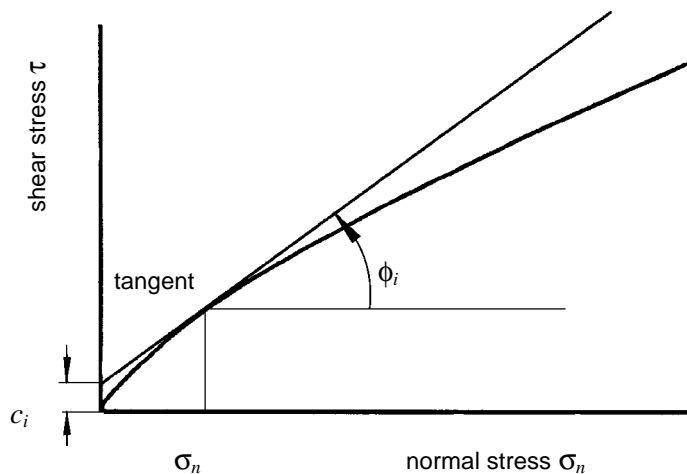
Figure 4.8: Definition of instantaneous cohesion c_i and instantaneous friction angle ϕ_i for a non-linear failure criterion.

Barton shear failure criterion

Input parameters:

Basic friction angle (PHIB) - degrees	29
Joint roughness coefficient (JRC)	16.9
Joint compressive strength (JCS)	96
Minimum normal stress (SIGNMIN)	0.360

Normal stress (SIGN) MPa	Shear strength (TAU) MPa	dTAU dSIGN (DTDS)	Friction angle (PHI) degrees	Cohesive strength (COH) MPa
0.360	0.989	1.652	58.82	0.394
0.720	1.538	1.423	54.91	0.513
1.440	2.476	1.213	50.49	0.730
2.880	4.073	1.030	45.85	1.107
5.759	6.779	0.872	41.07	1.760
11.518	11.344	0.733	36.22	2.907
23.036	18.973	0.609	31.33	4.953
46.073	31.533	0.496	26.40	8.666

Cell formulae:

SIGNMIN = 10^(LOG(JCS)-((70-PHIB)/JRC))

TAU = SIGN*TAN((PHIB+JRC*LOG(JCS/SIGN))*PI()/180)

DTDS = TAN((JRC*LOG(JCS/SIGN)+PHIB)*PI()/180)-(JRC/LN(10))
*(TAN((JRC*LOG(JCS/SIGN)+PHIB)*PI()/180)^2+1)*PI()/180

PHI = ATAN(DTDS)*180/PI()

COH = TAU-SIGN*DTDS

Figure 4.9 Printout of spreadsheet cells and formulae used to calculate shear strength, instantaneous friction angle and instantaneous cohesion for a range of normal stresses.

Note that equation 4.5 is not valid for $\sigma_n = 0$ and it ceases to have any practical meaning for $\phi_b + JRC \log_{10}(JCS/\sigma_n) > 70°$. This limit can be used to determine a minimum value for σ_n. An upper limit for σ_n is given by $\sigma_n = $ JCS.

In the spreadsheet shown in Figure 4.9, the instantaneous friction angle ϕ_i, for a normal stress of σ_n, has been calculated from the relationship

$$\phi_i = \arctan\left(\frac{\partial \tau}{\partial \sigma_n}\right) \tag{4.8}$$

$$\frac{\partial \tau}{\partial \sigma_n} = \tan\left(JRC\log_{10}\frac{JCS}{\sigma_n} + \phi_b \right) - \frac{\pi JRC}{180\ln 10}\left[\tan^2\left(JRC\log_{10}\frac{JCS}{\sigma_n} + \phi_b \right) + 1 \right] \quad (4.9)$$

The instantaneous cohesion c_i is calculated from:

$$c_i = \tau - \sigma_n \tan\phi_i \qquad (4.10)$$

In choosing the values of c_i and ϕ_i for use in a particular application, the average normal stress σ_n acting on the discontinuity planes should be estimated and used to determine the appropriate row in the spreadsheet. For many practical problems in the field, a single average value of σ_n will suffice but, where critical stability problems are being considered, this selection should be made for each important discontinuity surface.

5

Structurally controlled instability in tunnels

5.1   Introduction

In tunnels excavated in jointed rock masses at relatively shallow depth, the most common types of failure are those involving wedges falling from the roof or sliding out of the sidewalls of the openings. These wedges are formed by intersecting structural features, such as bedding planes and joints, which separate the rock mass into discrete but interlocked pieces. When a free face is created by the excavation of the opening, the restraint from the surrounding rock is removed. One or more of these wedges can fall or slide from the surface if the bounding planes are continuous or rock bridges along the discontinuities are broken.

Unless steps are taken to support these loose wedges, the stability of the back and walls of the opening may deteriorate rapidly. Each wedge, which is allowed to fall or slide, will cause a reduction in the restraint and the interlocking of the rock mass and this, in turn, will allow other wedges to fall. This failure process will continue until natural arching in the rock mass prevents further unravelling or until the opening is full of fallen material.

Falling wedge

Sliding wedge
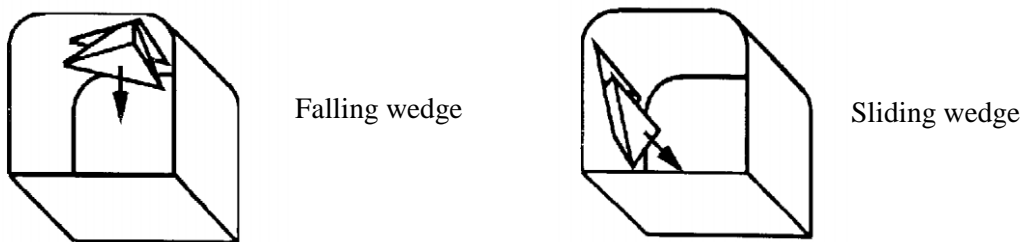
The steps which are required to deal with this problem are:

1.   Determination of average dip and dip direction of significant discontinuity sets.
2.   Identification of potential wedges which can slide or fall from the back or walls.
3.   Calculation of the factor of safety of these wedges, depending upon the mode of failure.
4.   Calculation of the amount of reinforcement required to bring the factor of safety of individual wedges up to an acceptable level.

5.2   Identification of potential wedges

The size and shape of potential wedges in the rock mass surrounding an opening depends upon the size, shape and orientation of the opening and also upon the orientation of the significant discontinuity sets. The three-dimensional geometry of the problem necessitates a set of relatively tedious calculations. While these can be performed by hand, it is far more efficient to utilise one of the computer programs which are available. One such program, called UNWEDGE[1], was developed specifically for use in underground hard rock mining and is utilised in the following discussion.

Consider a rock mass in which three strongly developed joint sets occur. The average dips and dip directions of these sets, shown as great circles in Figure 5.1, are as follows:

Joint set	dip°	dip direction°
J1	70 ± 5	036 ± 12
J2	85 ±8	144 ± 10
J3	55 ± 6	262 ± 15
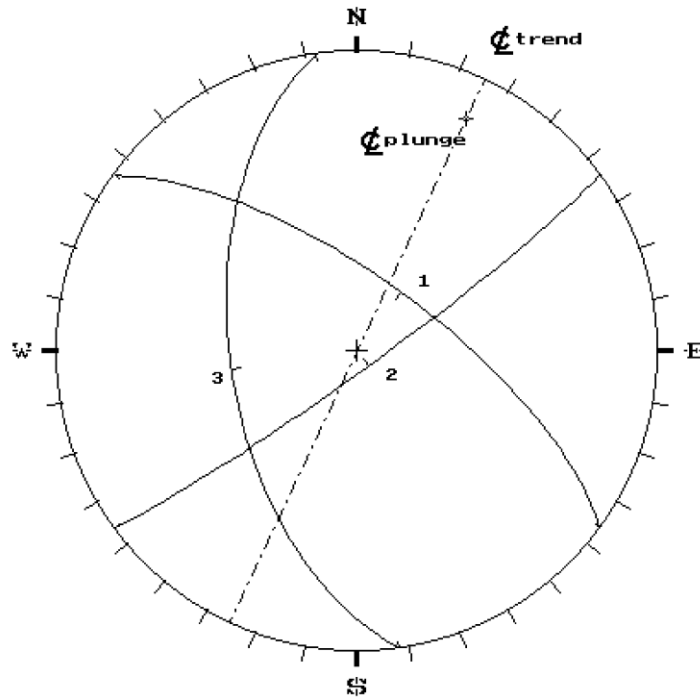
Figure 5.1: An equal area lower hemisphere plot of great circles representing the average dip and dip directions of three discontinuity sets in a rock mass. Also shown, as a chain dotted line, is the trend of the axis of a tunnel excavated in this rock mass. The tunnel plunge is marked with a cross.

It is assumed that all of these discontinuities are planar and continuous and that the shear strength of the surfaces can be represented by a friction angle $\phi = 30°$ and a cohesive strength of zero. These shear strength properties are very conservative estimates, but they provide a reasonable starting point for most analyses of this type. A more detailed discussion on the shear strength of discontinuities is given in Chapter 4.

A tunnel is to be excavated in this rock mass and the cross-section of the ramp is given in Figure 5.2. The axis of the tunnel is inclined at 15° to the horizontal or, to use the terminology associated with structural geology analysis, the tunnel axis *plunges* at 15°. In the portion of the tunnel under consideration in this example, the axis runs at 25° east of north or the *trend* of the axis is 025°.

The tunnel axis is shown as a chain dotted line in the stereonet in Figure 5.1. The trend of the axis is shown as 025°, measured clockwise from north. The plunge of the axis is 15° and this is shown as a cross on the chain dotted line representing the axis. The angle is measured inwards from the perimeter of the stereonet since this perimeter represents a horizontal reference plane.

The three structural discontinuity sets, represented by the great circles plotted in Figure 5.1, are entered into the program UNWEDGE, together with the cross-section of the tunnel and the plunge and trend of the tunnel axis. The program then determines the location and dimensions of the largest wedges which can be formed in the roof, floor and sidewalls of the excavation as shown in Figure 5.2.

The maximum number of simple tetrahedral wedges which can be formed by three discontinuities in the rock mass surrounding a circular tunnel is 6. In the case of a square or rectangular tunnel this number is reduced to 4. For the tunnel under consideration in this example, the arched roof allows an additional wedge to form, giving a total of five. However, this additional wedge is very small and is ignored in the analysis which follows.

Note that these wedges are the largest wedges which can be formed for the given geometrical conditions. The calculation used to determine these wedges assumes that the discontinuities are ubiquitous, in other words, they can occur anywhere in the rock mass. The joints, bedding planes and other structural features included in the analysis are also assumed to be planar and continuous. These conditions mean that the analysis will always find the largest possible wedges which can form. This result can generally be considered conservative since the size of wedges, formed in actual rock masses, will be limited by the persistence and the spacing of the structural features. The program UNWEDGE allows wedges to be scaled down to more realistic sizes if it is considered that maximum wedges are unlikely to form.

Details of the four wedges illustrated in Figure 5.2 are given in the following table:

Wedge	Weight - tonnes	Failure mode	Factor of Safety
Roof wedge	13	Falls	0
Side wedge 1	3.7	Slides on J1/J2	0.36
Side wedge 2	3.7	Slides on J3	0.52
Floor wedge	43	Stable	∞

6.7 m

7m

Tunnel section
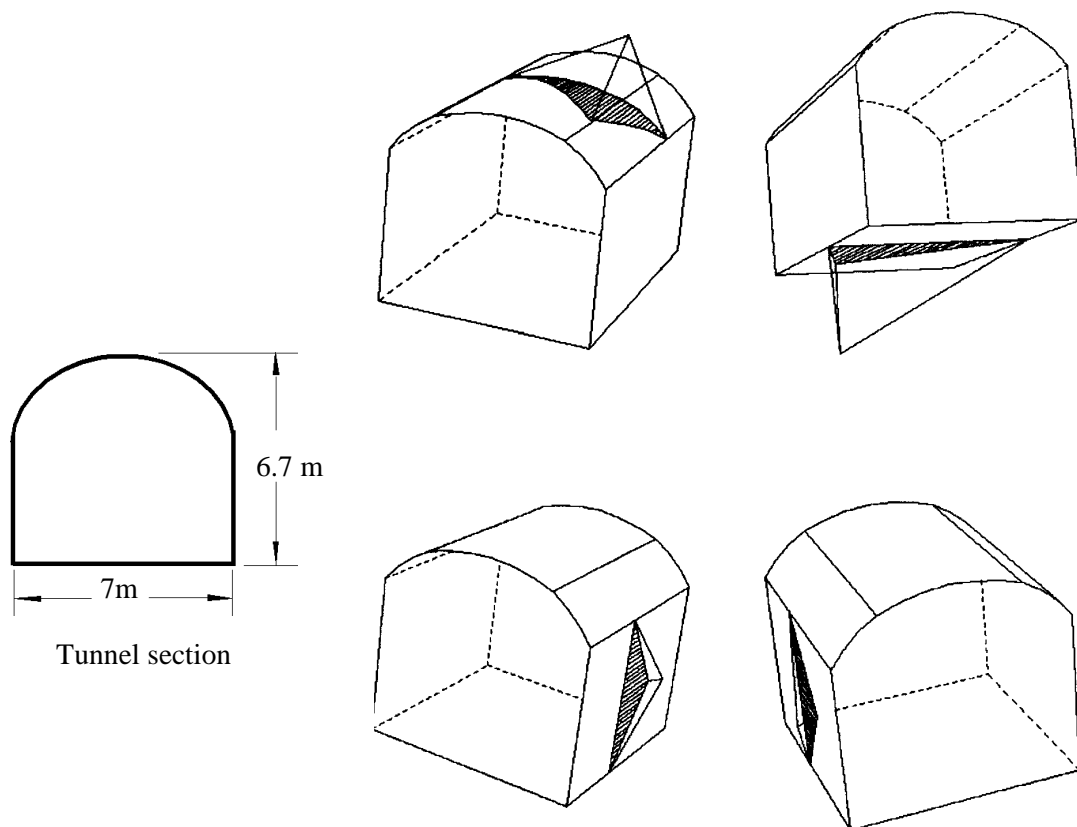
Figure 5.2: Wedges formed in the roof, floor and sidewalls of a ramp excavated in a jointed rock mass, in which the average dip and dip direction of three dominant structural features are defined by the great circles plotted in Figure 5.1.

The roof wedge will fall as a result of gravity loading and, because of its shape, there is no restraint from the three bounding discontinuities. This means that the factor of safety of the wedge, once it is released by excavation of the ramp opening, is zero. In some cases, sliding on one plane or along the line of intersection of two planes may occur in a roof wedge and this will result in a finite value for the factor of safety.

The two sidewall wedges are 'cousin' images of one another in that they are precisely the same shape but disposed differently in space. Consequently, the weights of these wedges are identical. The factors of safety are different since, as shown in the table, sliding occurs on different surfaces in the two cases.

The floor wedge is completely stable and requires no further consideration.

The program UNWEDGE is intended for use in situations where the in situ stresses are low and where their influence can be neglected without the introduction of significant errors. These are the conditions in which wedge failures are most prevalent in hard rock masses.

Where high in situ stress levels occur in blocky rock masses, the factors of safety predicted by the program UNWEDGE can be incorrect. In the case of tall thin wedges, the in situ stresses will tend to clamp the wedges in place and the calculated factor of safety will be too low. On the other hand, for shallow flat wedges, the calculated factor of safety may be too high since the high in situ stresses may force

the wedge out. For most practical tunnelling situations these errors are not significant and can be compensated for by an adjustment of the factor of safety. For research into failure mechanisms and for some site applications in which the influence of in situ stresses is critical, for example large caverns, a more sophisticated method of analysis may be required.

5.3   Support to control wedge failure

A characteristic feature of wedge failures in blocky rock is that very little movement occurs in the rock mass before failure of the wedge. In the case of a roof wedge that falls, failure can occur as soon as the base of the wedge is fully exposed by excavation of the opening. For sidewall wedges, sliding of a few millimetres along one plane or the line of intersection of two planes is generally sufficient to overcome the peak strength of these surfaces. This dictates that movement along the surfaces must be minimised. Consequently, the support system has to provide a 'stiff' response to movement. This means that mechanically anchored rockbolts need to be tensioned while fully grouted rockbolts or other continuously coupled devices can be left untensioned.
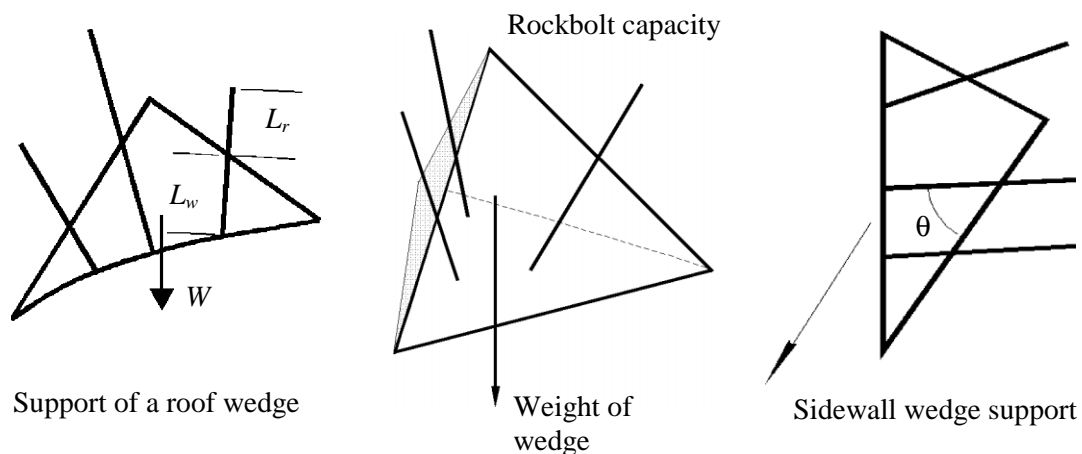
Figure 5.3: Rockbolt support mechanisms for wedges in the roof and sidewalls of tunnels

5.3.1 Rock bolting wedges

For roof wedges the total force, which should be applied by the reinforcement, should be sufficient to support the full dead weight of the wedge, plus an allowance for errors and poor quality installation. Hence, for the roof wedge illustrated in Figure 5.3, the total tension applied to the rock bolts or cables should be 1.3 to $1.5 \times W$, giving factors of safety of 1.3 to 1.5. The lower factor of safety would be acceptable in a temporary mine access opening, such as a drilling drive, while the higher factor of safety would be used in a more permanent access opening such as a highway tunnel.

When the wedge is clearly identifiable, some attempt should be made to distribute the support elements uniformly about the wedge centroid. This will prevent any rotations which can reduce the factor of safety.

In selecting the rock bolts or cable bolts to be used, attention must be paid to the length and location of these bolts. For grouted cable bolts, the length L_w through the wedge and the length L_r in the rock behind the wedge should both be sufficient to ensure that adequate anchorage is available, as shown in Figure 5.3. In the case of correctly grouted bolts or cables, these lengths should generally be about one metre. Where there is uncertainty about the quality of the grout, longer anchorage lengths should be used. When mechanically anchored bolts with face plates are used, the lengths should be sufficient to ensure that enough rock is available to distribute the loads from these attachments. These conditions are automatically checked in the program UNWEDGE.

In the case of sidewall wedges, the bolts or cables can be placed in such a way that the shear strength of the sliding surfaces is increased. As illustrated in Figure 5.3, this means that more bolts or cables are placed to cross the sliding planes than across the separation planes. Where possible, these bolts or cables should be inclined so that the angle θ is between 15° and 30° since this inclination will induce the highest shear resistance along the sliding surfaces.

The program UNWEDGE includes a number of options for designing support for underground excavations. These include: pattern bolting, from a selected drilling position or placed normal to the excavation surface; and spot bolting, in which the location and length of the bolts are decided by the user for each installation. Mechanically anchored bolts with face plates or fully grouted bolts or cables can be selected to provide support. In addition, a layer of shotcrete can be applied to the excavation surface.

Figure 5.4 shows the rock bolt designs for the roof wedge and one of the sidewall wedges for the tunnel excavation example discussed earlier. For the roof wedge, three 10 tonne capacity mechanically anchored rock bolts, each approximately 3 m long, produce a factor of safety of 1.63. The sidewall wedge, which only weighs 3.7 tonnes, requires only a single 10 tonne rock bolt for a factor of safety of 4.7. The position of the collar end of the bolt should be located for ease of drilling.
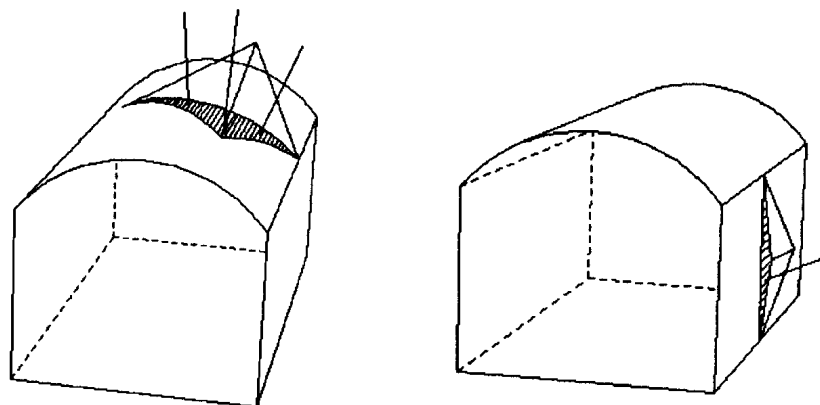
Figure 5.4: Rock bolting design for the roof wedge and one of the sidewall wedges in the tunnel example discussed earlier.

5.3.2 *Shotcrete support for wedges*

Shotcrete can be used for additional support of wedges in blocky ground, and can be very effective if applied correctly. This is because the base of a typical wedge has a large perimeter and hence, even for a relatively thin layer of shotcrete, a significant cross-sectional area of the material has to be punched through before the wedge can fail.

Consider the example illustrated in Figure 5.2. The base of the roof wedge (shown cross-hatched in the upper left hand diagram) has a perimeter of 16.4 m. A layer of shotcrete 50 mm thick will mean that a total cross-sectional area of 0.8 m^2 is available to provide support for the wedge. Assuming a relatively modest shear strength for the shotcrete layer of 2 MPa (200 tonnes/m^2) means that a wedge weighing 164 tonnes can be supported. In the case of the tunnel excavation discussed earlier, the wedge weighs 13 tonnes and hence a 50 mm thick layer of shotcrete would give a high ultimate factor of safety.

It is important to ensure that the shotcrete is well bonded to the rock surface in order to prevent a reduction in support capacity by peeling-off of the shotcrete layer. Good adhesion to the rock is achieved by washing the rock surface, using water only as feed to the shotcrete machine, before the shotcrete is applied.

The difficulty in using shotcrete for the support of wedges is that it has very little strength at the time of application and a period of several days is required before its full strength can be relied upon. Since wedges require immediate support, the use of shotcrete for short term stabilisation is clearly inappropriate. However, if a minimal number of rock bolts are placed to ensure that the short term stability of the rock mass is taken care of, a layer of shotcrete will provide additional long term security.

In very strong rock with large wedges, the use of shotcrete is wasteful since only that shotcrete covering the perimeter of the wedge is called upon to provide any resistance. The ideal application for shotcrete is in more closely jointed rock masses such as that illustrated in Figure 5.5. In such cases wedge failure would occur as a progressive process, starting with smaller wedges exposed at the excavation surface and gradually working its way back into the rock mass. In these circumstances, shotcrete provides very effective support and deserves to be much more widely used than is currently the case.
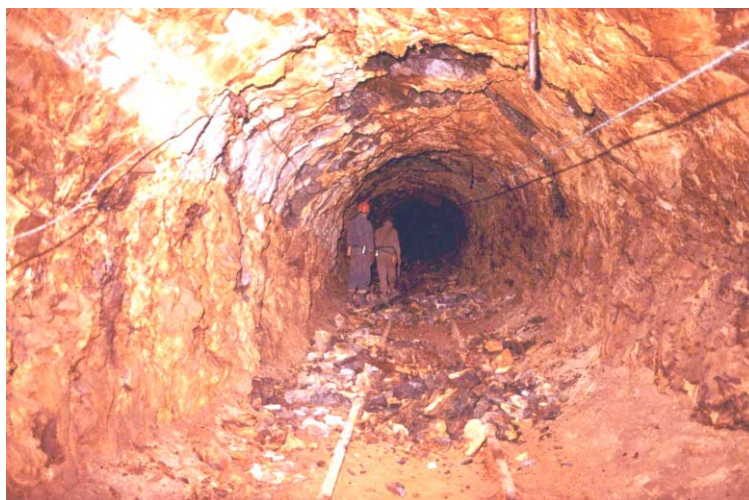
Figure 5.5: Ravelling of small wedges in a closely jointed rock mass. Shotcrete can provide effective support in such rock masses.

5.4   Consideration of excavation sequence

As has been emphasised several times in this chapter, wedges tend to fall or slide as soon as they are fully exposed in an excavated face. Consequently, they require immediate support in order to ensure stability. Placing this support is an important practical question to be addressed when working in blocky ground, which is prone to wedge failure.

When the structural geology of the rock mass is reasonably well understood the program UNWEDGE can be used to investigate potential wedge sizes and locations. A support pattern, which will secure these wedges, can then be designed and rockbolts can be installed as excavation progresses.

When dealing with larger excavations such as caverns, underground crusher chambers or shaft stations, the problem of sequential support installation is a little simpler, since these excavations are usually excavated in stages. Typically, in an underground crusher chamber, the excavation is started with a top heading which is then slashed out before the remainder of the cavern is excavated by benching.

The margin sketch shows a large opening excavated in four stages with rock bolts or cables installed at each stage to support wedges, which are progressively exposed in the roof and sidewalls of the excavation. The length, orientation and spacing of the bolts or cables are chosen to ensure that each wedge is adequately supported before it is fully exposed in the excavation surface.

When dealing with large excavations of this type, the structural geology of the surrounding rock mass will have been defined from core drilling or access adits and a reasonable projection of potential wedges will be available. These projections can be confirmed by additional mapping as each stage of the excavation is completed. The program UNWEDGE provides an effective tool for exploring the size and shape of potential wedges and the support required to stabilise them.

The margin sketch shows a situation in which the support design is based upon the largest possible wedges which can occur in the roof and

Top heading

Slash heading

First bench

Second bench
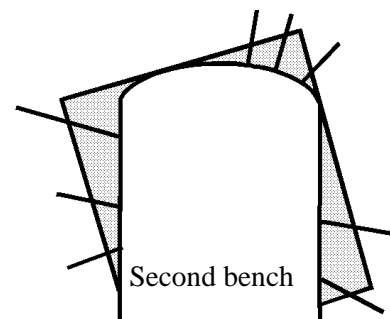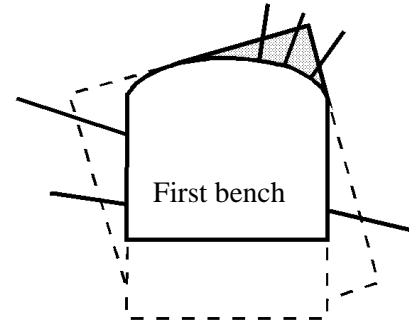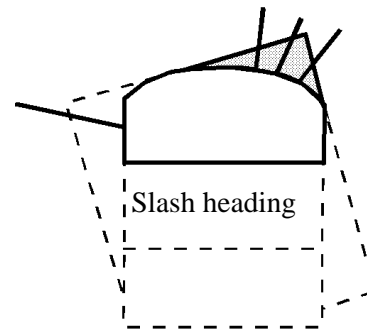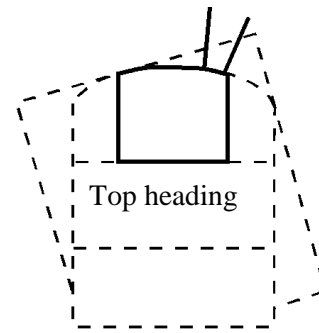
walls of the excavation. These wedges can sometimes form in rock masses with very persistent discontinuity surfaces such as bedding planes in layered sedimentary rocks. In many metamorphic or igneous rocks, the discontinuity surfaces are not continuous and the size of the wedges that can form is limited by the persistence of these surfaces.

The program UNWEDGE provides several options for sizing wedges. One of the most commonly measured lengths in structural mapping is the length of a joint trace on an excavation surface and one of the sizing options is based upon this trace length. The surface area of the base of the wedge, the volume of the wedge and the apex height of the wedge are all calculated by the program and all of these values can be edited by the user to set a scale for the wedge. This scaling option is very important when using the program interactively for designing support for large openings, where the maximum wedge sizes become obvious as the excavation progresses.

5.1   Application of probability theory

The program UNWEDGE has been designed for the analysis of a single wedge defined by three intersecting discontinuities. While this is adequate for many practical applications, it does not provide any facilities for selecting the three most critical joints in a large discontinuity population nor for analysing the number and location of wedges, which can form along the length of an opening such as a drive.

Early attempts have been made by a number of authors, including Tyler et al (1991) and Hatzor and Goodman (1992), to apply probability theory to these problems and some promising results have been obtained. The analyses developed thus far are not easy to use and cannot be considered as design tools. However, these studies have shown the way for future development of such tools and it is anticipated that powerful and user-friendly methods of probabilistic analysis will be available within a few years.

6

The Rio Grande project - Argentina

6.1   Introduction

The Rio Grande pumped storage project is located on the Rio Grande river near the town of Santa Rosa de Calamucita in the Province of Cordoba in Argentina. It has an installed capacity of 1000 MW and provides electrical storage facilities for the power grid and, in particular, for a nuclear power plant about 50 km away from Rio Grande.

The project is owned by Agua y Energia Electrica, the principal Argentinean electrical utility organisation. Preliminary feasibility studies were carried out by the owner and these were followed by detailed design studies by Studio G. Pietrangeli of Rome. The scheme was partly financed by Italy and some of the construction was done by Condote de Agua, an Italian contractor. Golder Associates were involved in the design and supervision of support installed to control the stability of most of the major underground excavations.

The main underground facilities are located in massive gneiss of very good quality. The upper reservoir is impounded behind a rockfill dam and water is fed directly from the intakes down twin penstocks which then bifurcate to feed into the four pump-turbines. These turbines, together with valves and the control equipment, are housed in a large underground cavern with a span of 25 m and a height of 44 m.

Draft tubes from the turbines feed into twin tunnels which, with a down-stream surge shaft, form the surge control system for this project. The twin tunnels join just downstream of the surge tank and discharge into a single tailrace tunnel with a span of 12 m and height of 18 m. This tailrace tunnel is about 6 km long and was constructed by a full- face drill-and-blast top heading, with a span of 12 m and height of 8m, followed by a 10 m benching operation. A view of the top heading is given in Figure 6.1.

6.2   Tailrace tunnel support

 Because of the excellent quality of the gneiss, most of the underground excavations did not require support and minimal provision for support was made in the contract documents. Assessment of underground stability and installation of support, where required, was done on a 'design-as-you-go' basis which proved to be very effective and economical. Recent reports from site, many years after the start of construction and commissioning of the plant, show that there have been no problems with rockfalls or underground instability.

Figure 6.1: The 12 m span 8 m high top heading for the tailrace tunnel was constructed by full-face drill-and-blast and, because of the excellent quality of the massive gneiss, was largely unsupported.
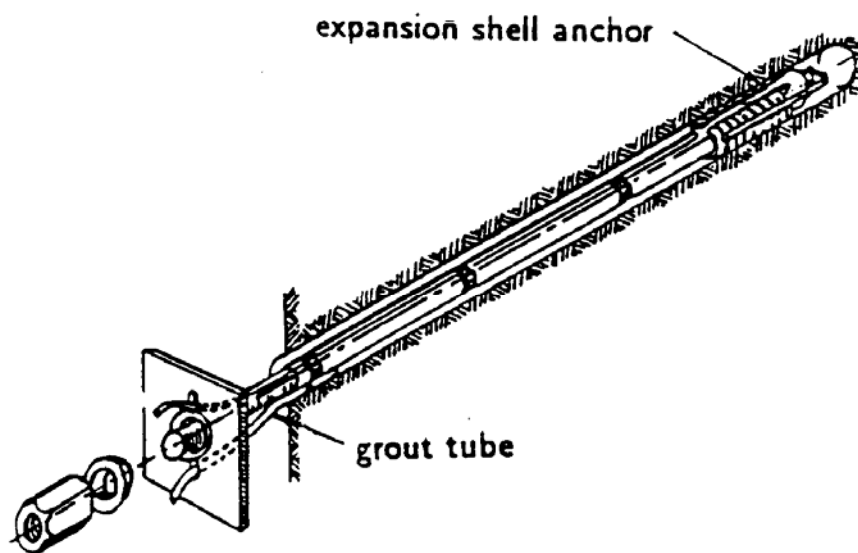
Figure 6.2: Mechanically anchored rockbolts of the type used on the Rio Grande project. These bolts were tensioned to 70% of their yield load upon installation and then, at a later stage, were re-tensioned and fully grouted.
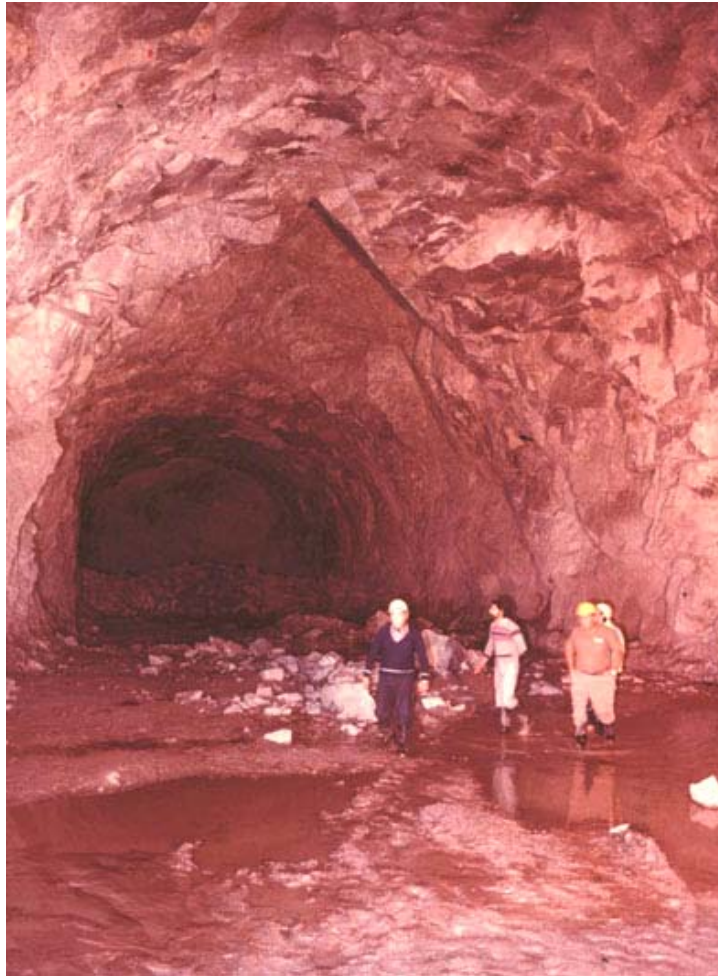
Figure 6.3: A wedge failure in the roof of the top heading of
the Rio Grande tailrace tunnel.

Decisions on support were made on the basis of inspection of the excavated faces by a resident team of geotechnical engineers. Where the appearance of the face indicated that a zone of heavily jointed rock, usually associated with faulting, was being entered, the top heading was reduced to a 6 m span by 8 m high pilot tunnel to limit the volume of unstable rock which could be released from the roof. This pilot tunnel was large enough to accommodate the seven-boom jumbo, as illustrated in Figure 6.4, but small enough to limit the size of roof falls to manageable proportions. Bolting from inside the pilot heading was used to pre-support the potentially unstable wedges and blocks in the roof.

In the case of the tailrace tunnel, which is itself a large excavation, the support comprised mechanically anchored and cement grouted rockbolts as illustrated in Figure 6.2, with mesh reinforced shotcrete where required. These bolts were generally installed to control the type of wedge failure illustrated in Figure 6.3. In the case of particularly large wedges, calculations of the factor of safety and support requirements were carried out on a programmable calculator, using an early version of the program UNWEDGE.

Figure 6.4: A 6 m wide heading driven ahead of the tunnel face to permit pre-reinforcement of potentially unstable wedges in the roof. The seven-boom jumbo is seen working in the heading.

6.3   Support for power cavern

A cross-section of the power cavern is given in Figure 6.5 and this figure includes the five main excavation stages for the cavern. Careful mapping of significant structural features in the roof and walls of the central access drive at the top of the cavern provided information for estimating potentially unstable blocks and wedges which could form in the roof of the cavern. Figure 6.6 illustrates a number of such wedges in one section of the cavern roof. At each stage of the cavern excavation, long rockbolts (up to 10 m length) were installed to stabilise wedges or blocks which had been determined as being potentially unstable.

Because gneiss has usually undergone some tectonic deformation during its geological history, projection of structural features from visible exposures tends to be an imprecise process. Consequently, the potentially unstable blocks and wedges had to be reassessed after each excavation step revealed new information. The structural plan illustrated in Figure 6.6 had to be modified many times during excavation and that shown is the final plan prepared after the full cavern roof had been exposed.

A general view of the cavern excavation is given in Figure 6.7. This photograph was taken when the bulk of the cavern had been completed and only a few benches in the bottom of the cavern remained to be excavated. The enlarged top of the cavern is to accommodate the overhanging crane that is supported on columns from the cavern floor. An alternative design for this cavern would have been to support the crane on concrete beams anchored to the walls as is commonly done in good quality rock.

Figure 6.5: Cavern profile and excavation stages.

Figure 6.6: A plan of the traces of geological features mapped in part of the cavern roof. The shaded areas represent potentially unstable wedges requiring reinforcement.
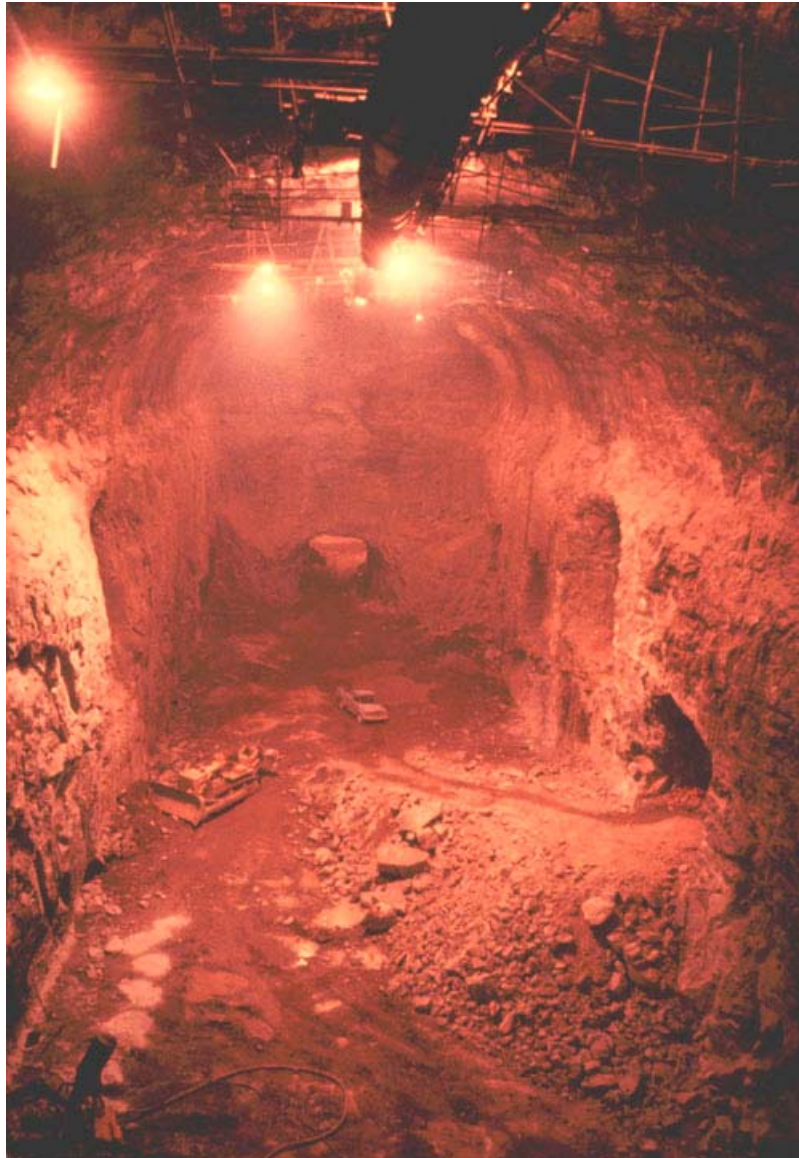
Figure 6.7: A view of the 25 m span Rio Grande power
cavern during excavation of the lower benches.

6.4 Discussion of support design and costs

Apart from rockbolts installed to control isolated structurally controlled blocks and
wedges in the roof and sidewalls and some areas of closely jointed rock which were
shotcreted, the cavern was unsupported. While this was successful for this particular
project, it is not the approach which should generally be used for a critical excavation
such as an underground powerhouse.

The damage resulting from even a small rockfall in such a cavern is out of all
proportion to the savings achieved by eliminating pattern rockbolting and full
shotcrete lining. Hence, in addition to the rockbolts installed to control structural
instability, as described earlier, I would recommend a normal pattern of 25 mm
diameter, 5 m long bolts (20% of the excavation span) on a 2.5 m grid. In addition, I
would recommend the placement of 50 mm of fibre-reinforced micro-silica shotcrete

over the entire roof and upper sidewalls of the cavern. Based on current north American costs, this additional support, involving approximately 600 rockbolts and about 300 m^3 of shotcrete, would have cost approximately US $200,000. In terms of the overall project cost and the increased long-term security in the cavern, this would normally be regarded as a good investment.

In contrast, consider the 6 km long tailrace tunnel in which the consequences of a small rockfall are minimal. Assume that a pattern of 4 m long bolts on a 2 m grid (say 10 bolts per section) and a 50 mm shotcrete thickness had been specified for the roof and upper sidewalls of the tailrace tunnel. This would involve 30,000 bolts and 5,400 m^3 of shotcrete at a total cost approaching US $5 million. This example illustrates the need to give careful consideration to the function and risks associated with each underground excavation before deciding upon the support system to be used.

6.5   Analysis using UNWEDGE program

UNWEDGE, described in the previous chapter, is a user-friendly micro-computer program which can be used to analyse the geometry and the stability of wedges defined by intersecting structural discontinuities in the rock mass surrounding an underground excavation. The analysis is based upon the assumption that the wedges, defined by three intersecting discontinuities, are subjected to gravitational loading only. In other words, the stress field in the rock mass surrounding the excavation is not taken into account. While this assumption leads to some inaccuracy in the analysis, it generally leads to a lower factor of safety than that which would occur if the in situ stresses were taken into account.

The application of the program UNWEDGE to the analysis of a potentially unstable wedge in the Rio Grande cavern is illustrated in the following discussion.

6.5.1 Input Data

The dips and dip directions of a number of planes (maximum 20) can be entered directly into the pop-up table which appears when the 'Input data' option is chosen or this information can be entered in the form of a DIPS file. Once the data has been read into the program, the great circles representing the discontinuities are displayed on the screen as illustrated in Figure 6.8 and the user is prompted to select the three joint planes to be included in the analysis. Once the information on these planes has been entered, the unit weight of the rock and the shear strengths of the joints are entered. Finally, the water pressure acting on the joint surface is entered. In most cases, the default water pressure of 0 will be chosen but the user may check the sensitivity of the wedge to pore water pressure by entering appropriate values.

In the case of the rock mass surrounding the Rio Grande Cavern, the dips and dip directions of the following four sets of joints are included in Figure 6.8:

> 1   50/131   infrequently occurring joints
> 2   88/225   shear joint set
> 3   85/264   shear joint set
> 4   50/345   tension joint set

Joints 2, 3 and 4 form the central wedge illustrated in Figure 6.6 and these joints have been included in the analysis which follows.
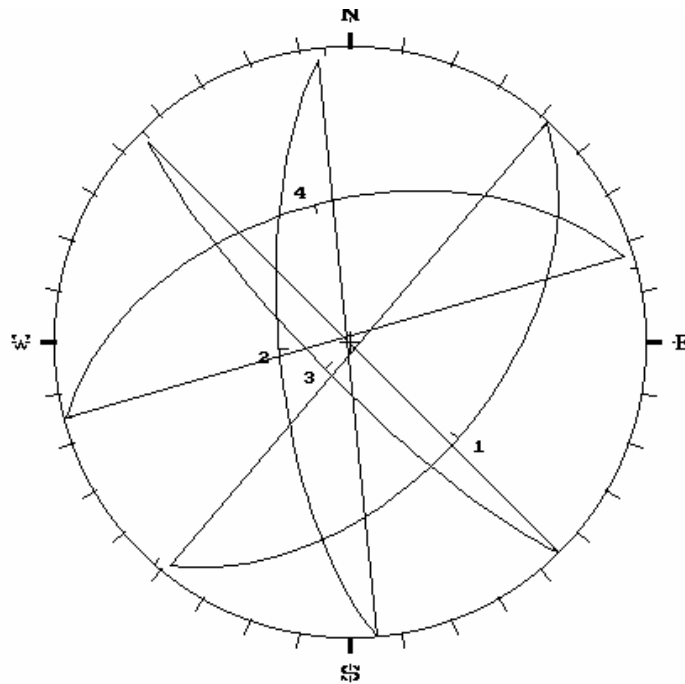
Figure 6.8: Great circles representing four joint sets which occur in the rock mass surrounding the Rio Grande cavern - imported as a DIPS file.

6.5.2 Input of excavation cross-section

In setting up this analysis, the co-ordinates shown in Figure 6.9 were used to define the cavern profile. These co-ordinates must be entered sequentially and must form a closed figure. The profile is formed from straight line and arc segments and a sufficient number of co-ordinates should be entered to ensure that a smooth profile is generated.

6.5.3 Determination of wedge geometry

Depending upon the shape of the cross-section, a maximum of six wedges can be formed with three intersecting joint planes. Selecting the 'View Wedges' option initiates the calculation which determines the shape and size of these wedges. The two wedges formed on the cavern end walls can be viewed by activating the 'View Ends' option.

Figure 6.10 shows the wedges formed in the case of the Rio Grande power cavern for the three joint planes 2, 3 and 4 defined in Figure 6.8. The right hand bar contains information on the weight of each of these wedges, the failure mode and the calculated factor of safety. Obviously, the most dangerous wedge in this situation is the wedge formed in the roof while the wedge formed in the floor is stable and need not be considered further in this analysis.
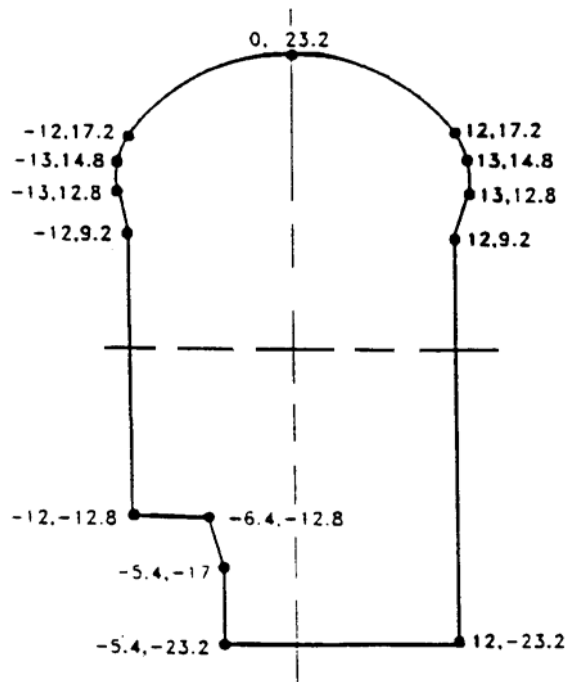
Figure 6.9: Co-ordinates used to define the profile of the cavern.
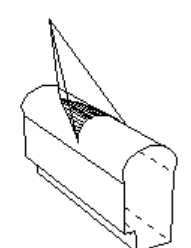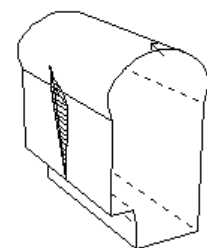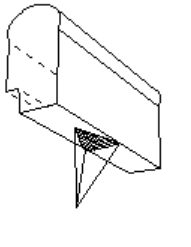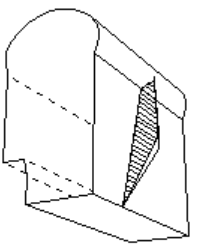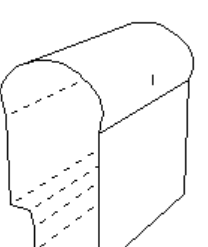
Figure 6.10: Perspective view of the wedges formed in the rock mass surrounding the Rio Grande power cavern.

6.5.4 Installation and analysis of rockbolts

The program UNWEDGE automatically determined the largest wedge which can occur in the rock mass adjacent to the excavation profile. In the case of the roof wedge, shown in Figure 6.10, the wedge extends over the full 25 m span of the cavern and weighs 11,610 tonnes. While, in exceptional circumstances, such wedges may occur, the limited extent of joints in many rock masses will restrict the size of the wedges to much smaller dimensions than those determined by UNWEDGE for the large excavations. As illustrated in Figure 6.6, the span of the central roof wedge (measured normal to the cavern axis) is about 5.5 m and the trace length of joint number 4 (50/345) is approximately 10 m.

When one of the wedges is selected for more detailed analysis a 'Size' option is displayed and this allows the user to define the size of the wedge in terms of the area of the face on the excavation surface, the volume of the wedge, the height of the apex of the wedge or the length of one of the joint traces. In this case a trace length of 10 m is entered for the joint defined by 50/345 and the resulting wedge is illustrated in Figure 6.11. This wedge weighs 255 tonnes and will require about seven 50 tonne capacity fully grouted cables to give a factor of safety of about 1.5 which is considered appropriate for a cavern of this type.
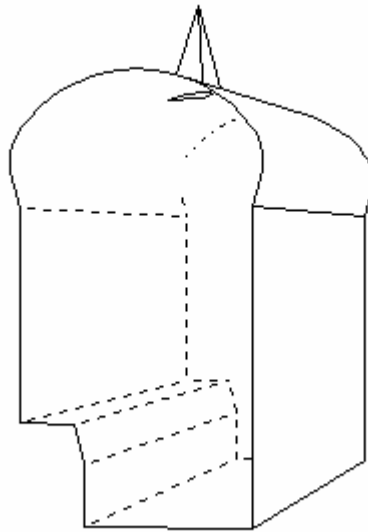
Figure 6.11: Perspective view of roof wedge in the Rig Grande cavern roof. The size of this wedge has been defined by setting the trace length of the 50/345 joint to 10 m.

UNWEDGE allows the user to add a layer of shotcrete and calculates the factor of safety increase as a result of such an addition. Since the shotcrete can only be added once the surface of the wedge is fully exposed it is not taken into account in calculating the support required to stabilise the wedge. The increase in safety factor which occurs after the shotcrete has set can be regarded as a long term bonus and it does allow the user to choose a slightly lower factor of safety for the immediate support of the wedge.

7

A slope stability problem in Hong Kong

7.1 Introduction

In the early 1970s a series of landslides occurred in Hong Kong as a result of exceptionally heavy rains. These slides caused some loss of life and a significant amount of property damage. Consequently, an extensive review was carried out on the stability of soil and rock slopes in the Territory.

During this review, a rock slope on Sau Mau Ping Road in Kowloon was identified as being potentially unstable. The stability of this particular slope was critical because it was located immediately across the road from two blocks of apartments, each housing approximately 5,000 people.

Figure 7.1 gives an general view down Sau Mau Ping Road, showing the steep rock slopes on the left and the apartment blocks on the right.

The concern was that a major rock slide could cross the road and damage the apartment blocks. In order to decide upon whether or not the residents of the two apartment blocks should be evacuated, the two questions which required an immediate response were :

1. What was the factor of safety of the slope under normal conditions and under conditions which could occur during an earthquake or during exceptionally heavy rains associated with a typhoon.

2. What factor of safety could be considered acceptable for long term conditions and what steps would be required in order to achieve this factor of safety.

7.2 Description of problem

The rock mass in which the slope adjacent to the Sau Mau Ping Road was cut is an unweathered granite with exfoliation or sheet joints similar to those illustrated in Figure 7.2. These joints are parallel to the surface of the granite and the spacing between successive joints increases with increasing distance into the rock mass. Undercutting of these sheet joints can cause a rock slide such as that illustrated in Figure 7.3.

During excavation of the original slopes for the Sau Mau Ping Road, a small rock slide was induced by blasting. The surface on which this failure occurred is illustrated in Figure 7.4. Blasting, such as that used in civil construction in an urban environment, does not impose very large loads on rock slopes and it can be assumed that the factor of safety of the slope was close to unity.

Figure 7.1: A view down Sau Mau Ping Road in Kowloon showing apartment blocks across the road from the steep rock slopes.

Figure 7.2: Sheet jointing in granite. These features, sometimes referred to as 'onion skin' joints, are the result of exfoliation processes during cooling of the granite.

Figure 7.3: A rock slide on a road caused by the undercutting of sheet joints in a granite slope. In hard rocks such as granite, failure can occur very suddenly if the factor of safety of the slope is close to 1. A rise in groundwater levels during a heavy storm or ice jacking in winter may be sufficient to induce failure.

Figure 7.4: The failure surface defined by a sheet joint surface on which a small slide occurred during blasting of the original cut slope for the Sau Mau Ping Road. The potentially unstable slope under consideration is visible in the back-ground.

The potentially unstable slope under consideration is visible in the background of this photograph. It is obvious from this photograph that the sheet joint surface continues under the potentially unstable slope. Hence, from the evidence of the small scale failure, it can be deduced that the factor of safety of the slope in question is not very high.

The geometry of the slope is illustrated in Figure 7.5 which shows a 60 m high slope with three 20 m high benches. The overall slope angle is 50° and the individual bench faces are inclined at 70° to the horizontal. An exfoliation joint surface dips at 35° and undercuts the slope as shown in the figure. The slope face strikes parallel to the underlying exfoliation surface and hence the slope can be analysed by means of a two-dimensional model.

Tension cracks are frequently observed behind the crest of slopes which have a factor of safety of less than about 1.2. These cracks are dangerous in that they allow water to enter the slope at a particularly critical location. Unfortunately, in the case of the Sau Mau Ping slope, recently cultivated market gardens located on the top of the slope made it impossible to determine whether or not such tension cracks were present and hence it was decided to carry out two sets of analyses - one with and one without tension cracks. These analyses were carried out for both the overall slope and for individual benches.
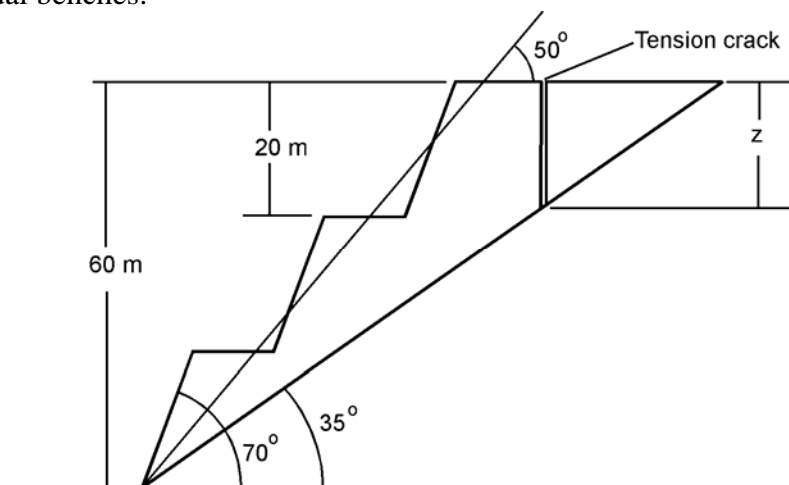
Figure 7.5: Geometry assumed for the two-dimensional analysis of the Sau Mau Ping Road slope.

7.3   Limit equilibrium models

At the time of this investigation, no rock mechanics facilities existed in Hong Kong and no diamond drilling or laboratory testing had ever been carried out on the granitic rocks in which this slope had been excavated. Consequently, the problem was tackled on the basis of a crude form of risk analysis, using simple analytical models to predict the response of the slope to a range of possible conditions. The two models are defined in Figure 7.6 and Figure 7.7.
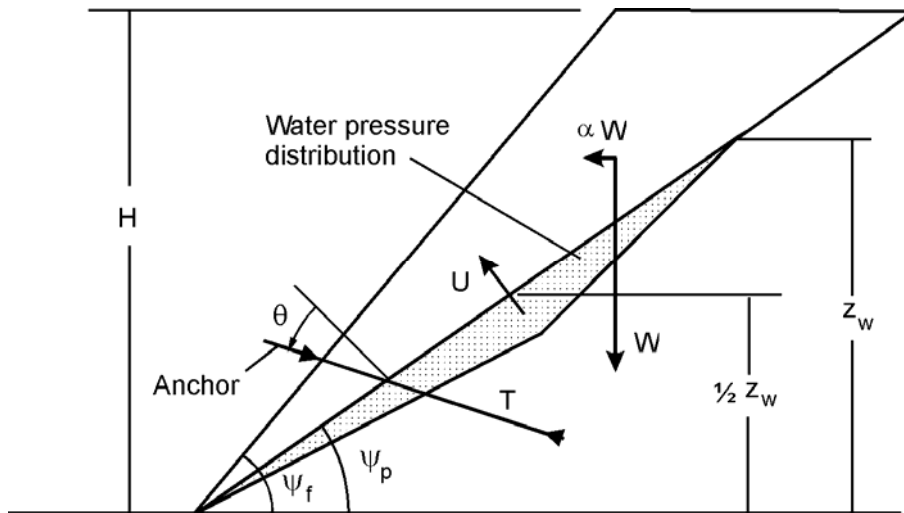
$$F = \frac{cA + \left(W(\cos \psi_p - \alpha \sin \psi_p) - U + T \cos \theta\right)\tan \phi}{W(\sin \psi_p + \alpha \cos \psi_p) - T \sin \theta} \tag{7.1}$$

where

$$A = \frac{H}{\sin \psi_p} \tag{7.2}$$

$$W = \frac{\gamma_r H^2}{2}(\cot \psi_p - \cot \psi_f) \tag{7.3}$$

$$U = \frac{\gamma_w H_w^2}{4 \sin \psi_p} \tag{7.4}$$

Figure 7.6: Factor of Safety calculation for a slope with no tension crack.
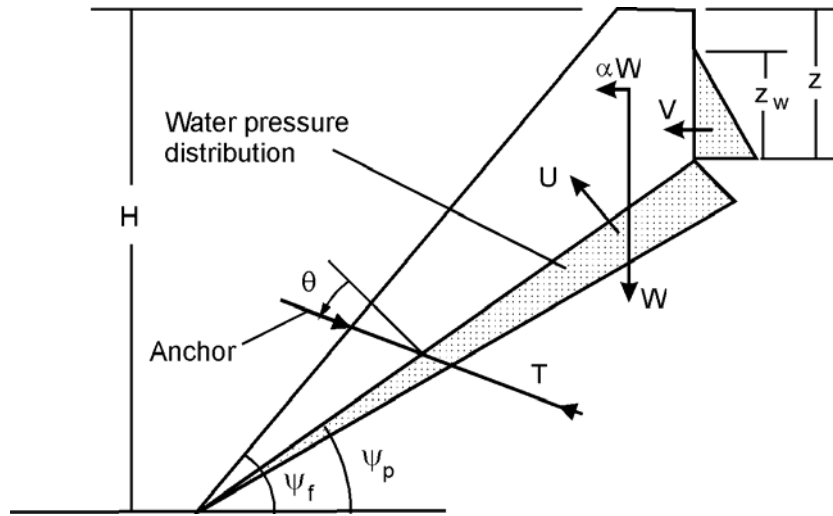
$$F = \frac{cA + \left(W(\cos \psi_p - \alpha \sin \psi_p) - U - V \sin \psi_p + T \cos \theta\right)\tan \phi}{W(\sin \psi_p + \alpha con\psi_p) + V \cos \psi_p - T \sin \theta} \tag{7.5}$$

where

$$z = H\left(1 - \sqrt{\cot \psi_f \, \tan \psi_p}\right) \tag{7.6}$$

$$A = \frac{H - z}{\sin \psi_p} \tag{7.7}$$

$$W = \frac{\gamma_r H^2}{2}\left(\left(1 - \left(\frac{z}{H}\right)^2\right)\cot \psi_p - \cot \psi_f\right) \tag{7.8}$$

$$U = \frac{\gamma_w z_w A}{2} \tag{7.9}$$

$$V = \frac{\gamma_w z_w^2}{2} \tag{7.10}$$

Figure 7.7: Factor of Safety calculation for a slope with a water-filled tension crack.

The Symbols and dimensions used in these models are as follows:

Symbol	Parameter	Dimensions
F	Factor of safety against sliding along sheet joint	Calculated
H	Height of the overall slope or of each bench	60 m or 20 m respectively
ψ_f	Angle of slope face, measured from horizontal	50°
ψ_p	Angle of failure surface, measured from horizontal	35°
z	Depth of tension crack	Calculated (m)
z_w	Depth of water in tension crack or on failure surface	Variable (m)
α	Horizontal earthquake acceleration	0.08 g (proportion of g)
γ_r	Unit weight of rock	0.027 MN/m^3
γ_w	Unit weight of water	0.01 MN/m^3
W	Weight of rock wedge resting on failure surface	Calculated (MN)
A	Base area of wedge	Calculated (m^2)
U	Uplift force due to water pressure on failure surface	Calculated (MN)
V	Horizontal force due to water in tension crack	Calculated (MN)
c	Cohesive strength along sliding surface	Variable (MN/m^2)
ϕ	Friction angle of sliding surface	Variable (degrees)
T	Force applied by anchor system (if present)	Specified (MN)
θ	Inclination of anchor, anti-clockwise from normal	Specified (degrees)

Note that this is a two-dimensional analysis and these dimensions refer to a 1 metre thick slice through the slope. It is also important to recognise that this analysis considers only force equilibrium and assumes that all forces pass through the centroid of the wedge. In other words, moment equilibrium is not considered in this analysis. While this is a simplification of the actual situation depicted in Figure 7.6 and Figure 7.7, the errors introduced are not considered to be significant, given the uncertainty of the other input data used in these analyses.

In Figure 7.7, the depth z of the tension crack is calculated by equation 7.6. This equation is obtained by minimising equation 7.5 with respect to the tension crack depth z (Hoek and Bray 1974). This minimisation is carried out for a dry slope and the accuracy of equation 7.6 decreases as the water depth in the tension crack increases. However, for the purposes of this analysis, the estimate given by equation 7.6 is considered acceptable.

7.4   Estimates of shear strength

One of the most critical steps in any limit equilibrium analysis is the determination or the estimation of the shear strength parameters (c and ϕ) for the surface along which it is anticipated that sliding will take place. In the case of this slope on Sau Mau Ping Road, no information on shear strength was available at the time of the initial studies and so estimates had to be made on the basis of published information for similar rocks.

Hoek and Bray (1974) published a plot, reproduced in Figure 7.8, of cohesive strengths and friction angles for rocks and soils, based upon the results of published

back analysis of slope failures. Superimposed on this plot is an elliptical zone which encompasses the estimated range of shear strength for sheet joints in unweathered granite. In choosing this range it was considered that the friction angle ϕ probably ranges from 30° for very smooth planar surfaces to 45° for rough or partly cemented surfaces. The cohesive strength c is more difficult to estimate and the range of 0.05 to 0.2 MPa was chosen on the basis of the results of back-analyses of slope failures, plotted in Figure 7.8.
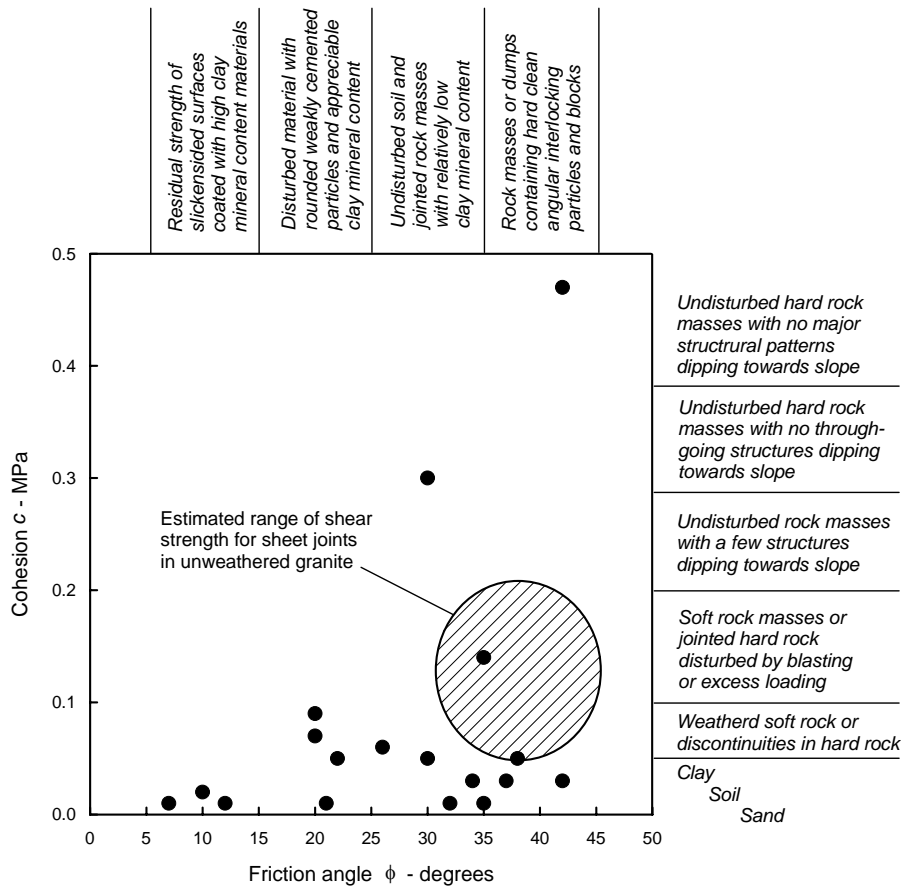
Figure 7.8: Relationship between friction angles and cohesive strengths mobilised at failure of slopes in various materials. The plotted points were obtained from published information from the back analysis of slope failures. (After Hoek and Bray 1974).

Some readers may be surprised that a cohesive strength has been assumed for joint surfaces which obviously have no tensile strength or 'stickiness' as would be found in a clayey soil. In fact, this assumed cohesive strength is defined by the intercept, on the shear strength axis, of a tangent to a curvilinear Mohr envelope. This curvature is the result of the interlocking of asperities on the matching surfaces of the joints and the increase in shear strength given by this interlocking plays a crucial role in the

stability of slopes such as that under consideration in this chapter. A full discussion on the shear strength of discontinuities in rock masses is given in Chapter 4.

7.5   Estimate of earthquake acceleration

Hong Kong is not considered a highly seismic region but relatively minor earthquakes are not unknown in the region. Consequently, it was felt that some allowance should be made for the possible influence of earthquake loading on the stability of the Sau Mau Ping slope.

The traditional method of incorporating the acceleration induced by earthquakes or large blasts in slope stability analyses is to add an outward force αW to the forces acting on the slope (see Figure 7.6 and Figure 7.7), where α is the acceleration as a proportion of g, the acceleration due to gravity. This 'pseudo-static' form of analysis is known to be very conservative but, in the case of the Sau Mau Ping slope, this conservatism was not considered to be out of place.

In discussion with local engineers and geologists, the consensus opinion was that the horizontal acceleration which could be induced by a 10 year return period earthquake in the region would be approximately 0.08 g. This value was used in all of the sensitivity analyses discussed in the following sections.

7.6   Analysis of mobilised shear strength

One method for assessing the stability of slopes is to calculate the shear strength that would be mobilised at failure and to compare this strength with the shear strength which is available along the failure surface. In the case of the Sau Mau Ping slope, this was done by substituting $F = 1$ in equations 7.1 and 7.5 and solving for the cohesive strength c and the friction angle ϕ. The results of this analysis are plotted in Figure 7.9. The estimated range of available shear strength (from Figure 7.8) is also shown on this plot.

Figure 7.9 shows that only two of the cases analysed result in conditions where the shear strength mobilised at failure falls within the estimated range of available shear strength. These two cases are designated 2 and 4 and they are for fully saturated slopes, with and without tension cracks.

7.7   Decision on short-term stability of the Sau Mau Ping slope

From the results of the sensitivity study described above it was concluded that instability of this particular slope could occur if the slope was fully saturated and subjected to earthquake loading. Typhoons occur several times every year in Hong Kong and the intensity of precipitation during these events is certainly sufficient to saturate the slopes. As discussed earlier, minor earthquakes do occur in the region but they are not very frequent. Consequently, the chance of simultaneous saturation and earthquake loading was considered to be small and it was concluded that there was no serious short-term threat of instability of the Sau Mau Ping slope.
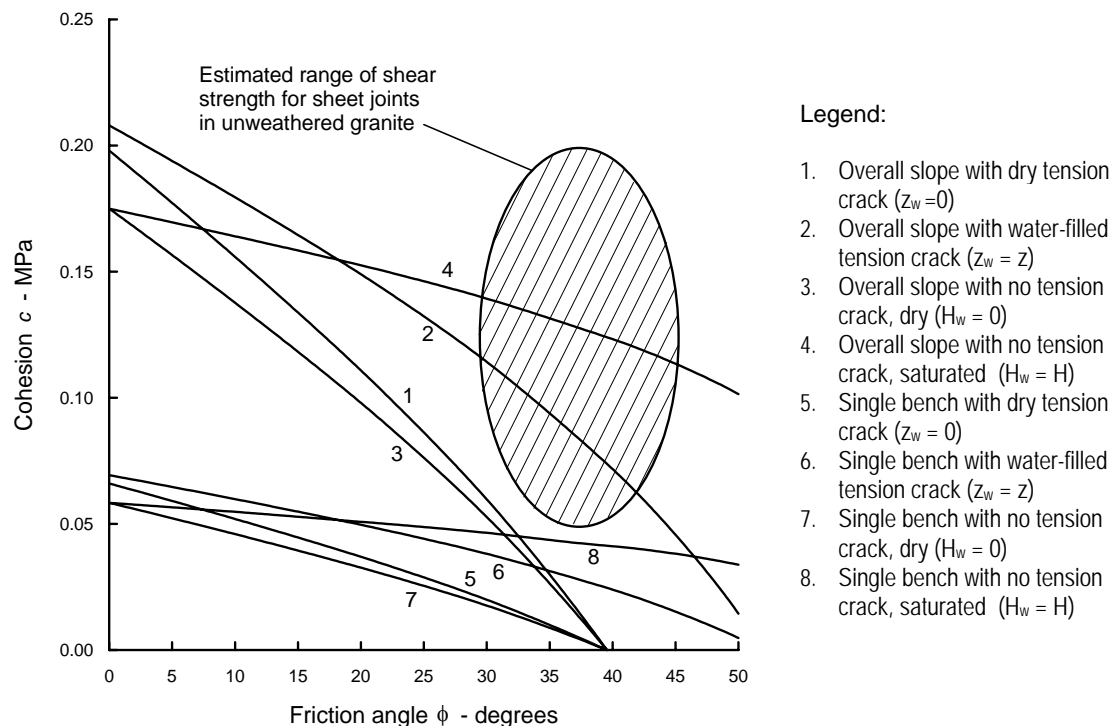
Figure 7.9: Comparison of the shear strength mobilised by failure under various conditions with the estimated shear strength available on sheet joints in unweathered granite.

In discussion with the highway authorities in Hong Kong, the following decisions were made:

1. No evacuation of the residents of the two apartment blocks, located across the street from the slope in question, would be carried out.
2. Horizontal drainage holes would be drilled into the slope face to penetrate the potential failure surface in an attempt to reduce uplift pressures in the slope.
3. Piezometers would be installed in holes drilled from the top of the slope. These piezometers would be measured regularly during periods of significant rainfall and the road would be closed to traffic if water levels rose to levels decided by the engineers responsible for the project.
4. An investigation would be carried out into the most effective remedial measures to stabilise the slope for the long-term.

Figure 7.10 shows the drilling of the horizontal drain holes into the slope face and Figure 7.11 shows the drilling of the vertical holes into which the piezometers were installed. These piezometers were monitored for the next few years, while preparations for the final stabilisation of the slope were made, and the road was closed to traffic on two occasions when water levels were considered to be dangerously high.

Figure 7.10: Drilling horizontal drain holes into the face of one of the benches of the Sau Mau Ping slope.

Figure 7.11: Drilling vertical diamond core holes into the Sau Mau Ping slope. These holes were used for geotechnical investigation purposes and also for the installation of piezometers in the rock mass.
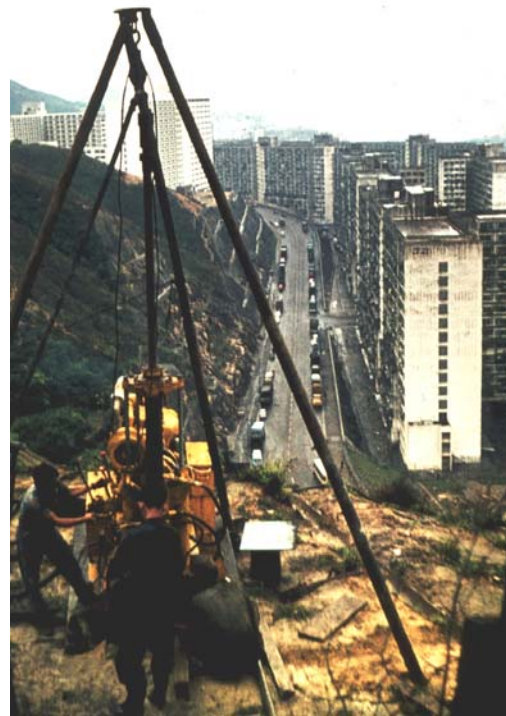
7.8   Evaluation of long-term remedial measures

While the short-term threat of instability was considered to be small, the longer-term stability of the slope was considered to be unacceptable and a study was carried out to evaluate various options for stabilising the slope. It was agreed that a factor of safety of 1.5 was required to meet long term requirements. The following alternatives were considered:

1. Reducing the height of the slope.
2. Reducing the angle of the slope face.
3. Drainage of the slope.
4. Reinforcement of the slope.

The limit equilibrium models defined in Figure 7.6 and Figure 7.7 were used for this evaluation and the results are plotted in Figure 7.12.

In calculating the factors of safety shown in this figure, the shear strength was maintained constant and was defined by $c = 0.10$ MPa and $\phi = 35°$. Similarly, an earthquake acceleration of $\alpha = 0.08$ *g* was used for all the analyses. The percentage change refers to the ratios of slope height, slope angle and water depth to the original dimensions defined in Figure 7.5.
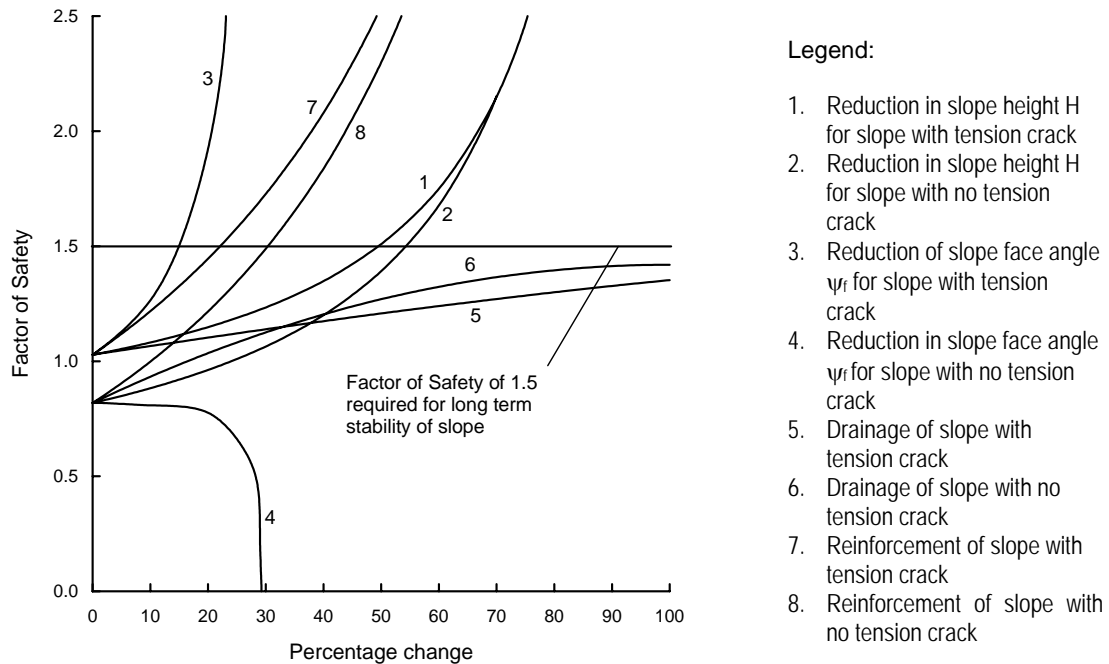
Figure 7.12: Evaluation of remedial options to increase the stability of the slope

In the case of the reinforcement options, the percentage change refers to the ratio of anchor force T to the weight of the wedges (24.8 MN for the slope with the tension crack and 28.6 MN for the slope with no tension crack). The anchor inclination was kept constant at $\theta = \phi = 35°$. This anchor inclination gives the minimum anchor load for a dry slope and it can be determined by minimising equations 7.1 or 7.5 with respect to θ.

The curves presented in Figure 7.12 show clearly that some remedial measures are much more effective than others and it is worth examining each of the options in turn.

- Curves 1 (slope with tension crack) and 2 (slope without tension crack) show that reduction of the slope height is not an effective solution to the problem. In order to achieve the required factor of safety of 1.5, the slope height would have to be reduced by 50%. If this solution were to be adopted, it would be more practical to excavate the entire slope since most of the volume of the rock to be excavated is contained in the upper half of the slope.

- Curve 3 (slope with tension crack) shows that reduction of the slope angle is a very effective remedial measure. The required factor of safety of 1.5 is achieved

for a reduction of less than 25% of the slope angle. In other words, a reduction of the overall slope face angle from 50° to 37.5° would achieve the desired result. This finding is generally true and a reduction in the face angle of a slope is usually an effective remedial step. In the case of slopes under construction, using a flatter slope is always one of the prime choices for achieving greater stability.

- Curve 4 (slope without tension crack) is an anomaly and demonstrates that calculations can sometimes produce nonsense. The reduction in factor of safety shown by this curve is a result of the reduction in the weight of the sliding block as the face angle is reduced. Since the water pressure on the sliding surface remains constant, the *effective stress* acting on the sliding surface decreases and hence the frictional component of the resisting forces decreases. When a very thin sliver of rock remains, the water pressure will float it off the slope. The problem with this analysis lies in the assumption that the block is completely impermeable and that the water remains trapped beneath the failure surface. In fact, the block would break up long before it floated and hence the water pressure acting on the failure plane would be dissipated.

- Curves 5 and 6 show that drainage is not a very effective option for either of the slope models considered. In neither case is a factor of safety of 1.5 achieved. This is something of a surprise since drainage is usually one of the most effective and economical remedial measures. The reasons for the poor performance of drainage in this case is due to the combination of the geometry of the slope and the shear strength of the failure surface.

- Curves 7 and 8 show that, for both slope models considered, slope reinforcement by means of rockbolts or cables can be an effective remedial measure. The anchor force required for a factor of safety of 1.5 would be about 100 tonnes per metre of slope length for the slope with no tension crack.

7.9   Final decision on long term remedial works

The two most attractive options for long term remedial works on this slope are reinforcement by means of cables or bolts or reduction of the slope face angle. The first option was finally rejected because of the high cost and because of the uncertainty about the long term corrosion resistance of reinforcement which could be placed in the slope. This latter concern may not have been justified but, considering the very poor quality of some of the construction in Hong Kong at the time of this study, it was decided that the risk was not worth taking.

The option finally chosen was to reduce the slope face angle down to 35° by excavating the entire block resting on the failure surface and hence removing the problem entirely. Since good quality aggregate is always required in Hong Kong it was decided to work this slope face as a quarry. It took several years to organise this activity and, during this time, the water levels in the slope were monitored by means of piezometers. Although the road was closed twice during this period, no major problems occurred and the slope was finally excavated back to the failure plane.

8

Factor of safety and probability of failure

8.1 Introduction

How does one assess the acceptability of an engineering design? Relying on judgement alone can lead to one of the two extremes illustrated in Figure 8.1. The first case is economically unacceptable while the example illustrated in the lower drawing violates all normal safety standards.
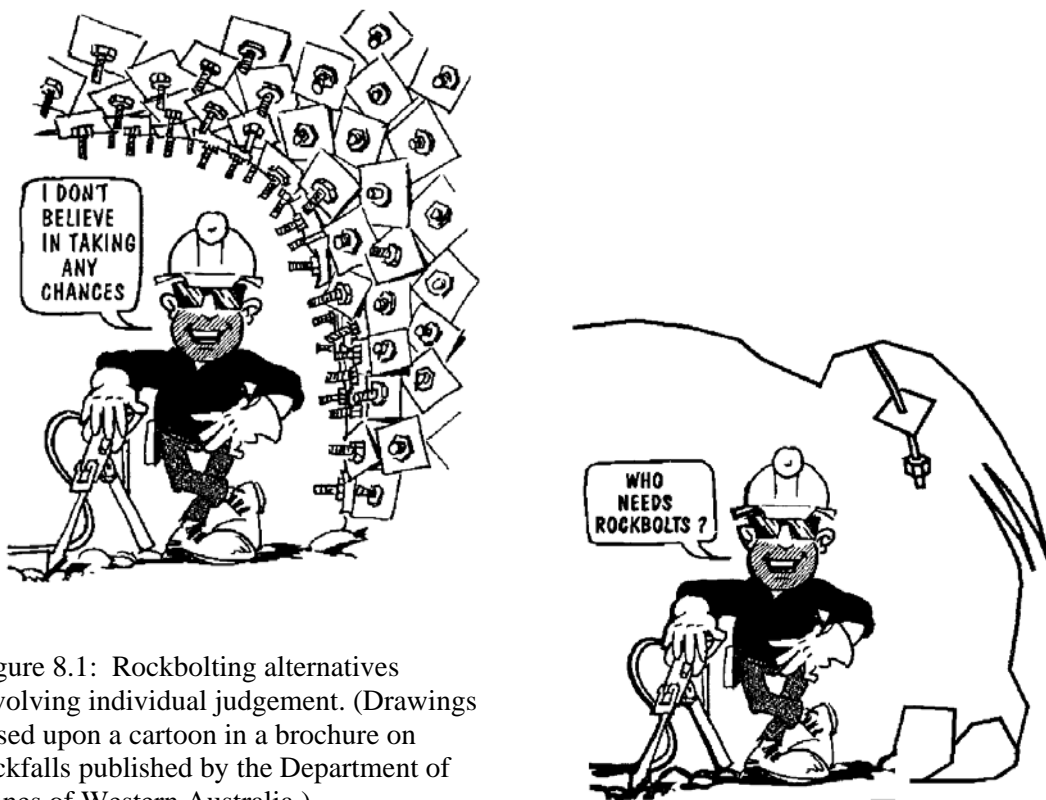
Figure 8.1: Rockbolting alternatives involving individual judgement. (Drawings based upon a cartoon in a brochure on rockfalls published by the Department of Mines of Western Australia.)

8.2   Sensitivity studies

The classical approach used in designing engineering structures is to consider the relationship between the capacity C (strength or resisting force) of the element and the demand D (stress or disturbing force). The Factor of Safety of the structure is defined as $F = C/D$ and failure is assumed to occur when F is less than 1.

Rather than base an engineering design decision on a single calculated factor of safety, an approach which is frequently used to give a more rational assessment of the risks associated with a particular design is to carry out a sensitivity study. This involves a series of calculations in which each significant parameter is varied systematically over its maximum credible range in order to determine its influence upon the factor of safety.

This approach was used in the analysis of the Sau Mau Ping slope in Hong Kong discussed in the previous chapter. It provided a useful means of exploring a range of possibilities and reaching practical decisions on some difficult problems. On the following pages this idea of sensitivity studies will be extended to the use of probability theory and it will be shown that, even with very limited field data, practical, useful information can be obtained from an analysis of probability of failure.

8.3   An introduction to probability theory

A complete discussion on probability theory exceeds the scope of these notes and the techniques discussed on the following pages are intended to introduce the reader to the subject and to give an indication of the power of these techniques in engineering decision making. A more detailed treatment of this subject will be found in a book by Harr (1987) entitled *Reliability-based design in civil engineering*. A paper on geotechnical applications of probability theory entitled 'Evaluating calculated risk in geotechnical engineering' was published by Whitman (1984) and is recommended reading for anyone with a serious interest in this subject. Pine (1992), Tyler et al (1991), Hatzor and Goodman (1993) and Carter (1992) have published papers on the application of probability theory to the analysis of problems encountered in underground mining and civil engineering.

Most geotechnical engineers regard the subject of probability theory with doubt and suspicion. At least part of the reason for this mistrust is associated with the language which has been adopted by those who specialise in the field of probability theory and risk assessment. The following definitions are given in an attempt to dispel some of the mystery which tends to surround this subject.

Random variables: Parameters such as the angle of friction of rock joints, the uniaxial compressive strength of rock specimens, the inclination and orientation of discontinuities in a rock mass and the measured in situ stresses in the rock surrounding an opening do not have a single fixed value but may assume any number of values. There is no way of predicting exactly what the value of one of these parameters will be at any given location. Hence these parameters are described as random variables.

Probability distribution: A probability density function (PDF) describes the relative likelihood that a random variable will assume a particular value. A typical probability density function is illustrated opposite. In this case the random variable is continuously distributed (i.e., it can take on all possible values). The area under the PDF is always unity.

$f_x(x)$

x_1 x
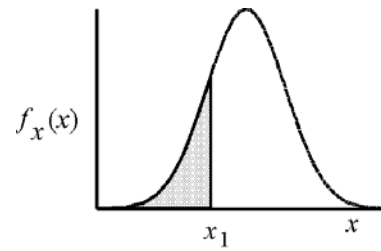
Probability density function (PDF)

An alternative way of presenting the same information is in the form of a cumulative distribution function (CDF), which gives the probability that the variable will have a value less than or equal to the selected value. The CDF is the integral of the corresponding probability density function, i.e., the ordinate at x1 on the cumulative distribution is the area under the probability density function to the left of x1. Note the fx(x) is used for the ordinate of a PDF while Fx(x) is used for a CDF.

1

$F_x(x)$

0

x_1 x
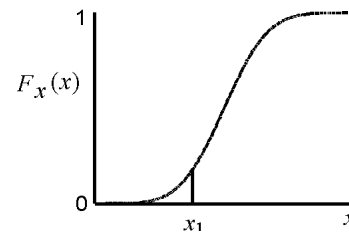
Cumulative distribution function (CDF)

One of the most common graphical representations of a probability distribution is a histogram in which the fraction of all observations falling within a specified interval is plotted as a bar above that interval.

Data analysis: For many applications it is not necessary to use all of the information contained in a distribution function and quantities summarised only by the dominant features of the distribution may be adequate.

The *sample mean* or *expected value* or *first moment* indicates the centre of gravity of a probability distribution. A typical application would be the analysis of a set of results $x_1, x_2,.........,x_n$ from uniaxial strength tests carried out in the laboratory. Assuming that there are n individual test values x_i, the mean $\bar{x}$ is given by:

$$\bar{x} = \frac{1}{n}\sum_{i=1}^{n} x_i \qquad (8.1)$$

The *sample variance* s^2 or the *second moment about the mean* of a distribution is defined as the mean of the square of the difference between the value of x_i and the mean value $\bar{x}$. Hence:

$$s^2 = \frac{1}{n-1}\sum_{i=1}^{n}(x_i - \bar{x})^2 \qquad 8.2)$$

Note that, theoretically, the denominator for calculation of variance of samples should be n, not (n - 1). However, for a finite number of samples, it can be shown that the correction factor $n/(n-1)$, known as Bessel's correction, gives a better estimate. For practical purposes the correction is only necessary when the sample size is less than 30.

The *standard deviation s* is given by the positive square root of the variance s^2. In the case of the commonly used normal distribution, about 68% of the test values will fall within an interval defined by the *mean ± one standard deviation* while approximately 95% of all the test results will fall within the range defined by the *mean ± two standard deviations*. A small standard deviation will indicate a tightly clustered data set while a large standard deviation will be found for a data set in which there is a large scatter about the mean.

The *coefficient of variation* (COV) is the ratio of the standard deviation to the mean, i.e. COV $= s/\overline{x}$. COV is dimensionless and it is a particularly useful measure of uncertainty. A small uncertainty would typically be represented by a COV = 0.05 while considerable uncertainty would be indicated by a COV = 0.25.

Normal distribution: The *normal* or *Gaussian* distribution is the most common type of probability distribution function and the distributions of many random variables conform to this distribution. It is generally used for probabilistic studies in geotechnical engineering unless there are good reasons for selecting a different distribution. Typically, variables which arise as a sum of a number of random effects, none of which dominate the total, are normally distributed.

The problem of defining a normal distribution is to estimate the values of the governing parameters which are the true mean (μ) and true standard deviation (σ). Generally, the best estimates for these values are given by the sample mean and standard deviation, determined from a number of tests or observations. Hence, from equations 8.1 and 8.2:

$$\mu = \overline{x} \tag{8.3}$$

$$\sigma = s \tag{8.4}$$

It is important to recognise that equations 8.3 and 8.4 give the most probable values of μ and σ and not necessarily the true values.

Obviously, it is desirable to include as many samples as possible in any set of observations but, in geotechnical engineering, there are serious practical and financial limitations to the amount of data which can be collected. Consequently, it is often necessary to make estimates on the basis of judgement, experience or from comparisons with results published by others. These difficulties are often used as an excuse for not using probabilistic tools in geotechnical engineering but, as will be shown later in this chapter, useful results can still be obtained from very limited data. Having estimated the mean μ and standard deviation σ, the probability density function for a normal distribution is defined by:

$$f_x(x) = \frac{\exp\left[-\frac{1}{2}\left(\frac{x-\mu}{\sigma}\right)^2\right]}{\sigma\sqrt{2\pi}} \tag{8.5}$$

for $-\infty \leq x \leq \infty$.

As will be seen later, this range of $-\infty \le x \le \infty$ can cause problems when a normal distribution is used as a basis for a Monte Carlo analysis in which the entire range of values is randomly sampled. This can give rise to a few very small numbers (sometimes negative) and very large numbers which, in certain analyses, can cause numerical instability. In order to overcome this problem the normal distribution is sometimes truncated so that only values falling within a specified range are considered valid.

There is no closed form solution for the cumulative distribution function (CDF) which must by found by numerical integration.

Other distributions: In addition to the commonly used normal distribution there are a number of alternative distributions which are used in probability analyses. Some of the most useful are:

- *Beta distributions* (Harr, 1987) are very versatile distributions which can be used to replace almost any of the common distributions and which do not suffer from the extreme value problems discussed above because the domain (range) is bounded by specified values.

- *Exponential distributions* are sometimes used to define events such as the occurrence of earthquakes or rockbursts or quantities such as the length of joints in a rock mass.

- *Lognormal distributions* are useful when considering processes such as the crushing of aggregates in which the final particle size results from a number of collisions of particles of many sizes moving in different directions with different velocities. Such multiplicative mechanisms tend to result in variables which are lognormally distributed as opposed to the normally distributed variables resulting from additive mechanisms.

- *Weibul distributions* are used to represent the lifetime of devices in reliability studies or the outcome of tests such as point load tests on rock core in which a few very high values may occur.

It is no longer necessary for the person starting out in the field of probability theory to know and understand the mathematics involved in all of these probability distributions since commercially available software programs can be used to carry out many of the computations automatically. Note that the author is not advocating the blind use of 'black-box' software and the reader should exercise extreme caution in using such software without trying to understand exactly what the software is doing. However there is no point in writing reports by hand if one is prepared to spend the time learning how to use a good word-processor correctly and the same applies to mathematical software.

One of the most useful software packages for probability analysis is a program called BestFit[1] which has a built-in library of 18 probability distributions and which

---

[1] BestFit for Windows and its companion program @RISK for Microsoft Excel of Lotus 1-2-3 (for Windows or Macintosh) are available from the Palisade Corporation, 31 Decker Road, Newfield, New York 14867, USA. Fax number 1 607 277 8001.

can be used to fit any one of these distributions to a given set of data or it can be allowed automatically to determine the ranking of the fit of all 18 distributions to the data set. The results from such an analysis can be entered directly into a companion program called @RISK which can be used for risk evaluations using the techniques described below.

Sampling techniques: Consider a problem in which the factor of safety depends upon a number of random variables such as the cohesive strength *c*, the angle of friction ϕ and the acceleration α due to earthquakes or large blasts. Assuming that the values of these variables are distributed about their means in a manner which can be described by one of the continuous distribution functions such as the normal distribution described earlier, the problem is how to use this information to determine the distribution of factor of safety values and the probability of failure.

The Monte Carlo method uses random or pseudo-random numbers to sample from probability distributions and, if sufficiently large numbers of samples are generated and used in a calculation such as that for a factor of safety, a distribution of values for the end product will be generated. The term 'Monte Carlo' is believed to have been introduced as a code word to describe this hit-and-miss technique used during secret work on the development of the atomic bomb during World War II (Harr 1987). Today, Monte Carlo techniques can be applied to a wide variety of problems involving random behaviour and a number of algorithms are available for generating random Monte Carlo samples from different types of input probability distributions. With highly optimised software programs such as @RISK, problems involving relatively large samples can be run efficiently on most desktop or portable computers.

The *Latin Hypercube* sampling technique (Imam et al (1980), Startzman and Watterbarger (1985)) is a relatively recent development which gives comparable results to the Monte Carlo technique but with fewer samples. The method is based upon stratified sampling with random selection within each stratum. Typically an analysis using 1000 samples obtained by the Latin Hypercube technique will produce comparable results to an analysis using 5000 samples obtained using the Monte Carlo method. Both techniques are incorporated in the program @RISK.

Note that both the Monte Carlo and the Latin Hypercube techniques require that the distribution of all the input variables should either be known or that they be assumed. When no information on the distribution is available it is usual to assume a normal or a truncated normal distribution.

The *Generalised Point Estimate Method*, developed by Rosenbleuth (1981) and discussed in detail by Harr (1987), can be used for rapid calculation of the mean and standard deviation of a quantity such as a factor of safety which depends upon random behaviour of input variables. Hoek (1989) discussed the application of this technique to the analysis of surface crown pillar stability while Pine (1992) has applied this technique to the analysis of slope stability and other mining problems.

To calculate a quantity such as a factor of safety, two point estimates are made at one standard deviation on either side of the mean ($\mu \pm \sigma$) from each distribution representing a random variable. The factor of safety is calculated for every possible combination of point estimates, producing 2^n solutions where *n* is the number of

random variables involved. The mean and the standard deviation of the factor of safety are then calculated from these 2^n solutions.

While this technique does not provide a full distribution of the output variable, as do the Monte Carlo and Latin Hypercube methods, it is very simple to use for problems with relatively few random variables and is useful when general trends are being investigated. When the probability distribution function for the output variable is known, for example, from previous Monte Carlo analyses, the mean and standard deviation values can be used to calculate the complete output distribution .

8.4 Probability of failure

In the case of the Sau Mau Ping slope problem the factor of safety of the overall slope with a tension crack is defined by:

1. Fixed dimensions:

Overall slope height	H	$= 60$ m
Overall slope angle	ψ_f	$= 50°$
Failure plane angle	ψ_p	$= 35°$
Unit weight of rock	γ_r	$= 2.6$ tonnes/m^3
Unit weight of water	γ_w	$= 1.0$ tonnes/m^3

2. Random variables — *Mean values*

Friction angle on joint surface	$\phi = 35°$
Cohesive strength of joint surface	$c = 10$ tonnes/m^2
Depth of tension crack	$z = 14$ m
Depth of water in tension crack	$z_w = z/2$
Ratio of horizontal earthquake to gravitational acceleration	$\alpha = 0.08$

Figure 8.2 illustrates the layout of a Microsoft Excel spreadsheet with plots of the probability distribution functions of the random input variables and of the calculated factor of safety. It is worth discussing each of the plots in detail to demonstrate the reasoning behind the choice of the probability distribution functions.

1. *Friction angle ϕ* - A truncated normal distribution has been assumed for this variable. The mean is assumed to be 35° which is the approximate centre of the assumed shear strength range illustrated in Figure 7.8. The standard deviation of 5° implies that about 68% of the friction angle values defined by the distribution will lie between 30° and 40°. The normal distribution is truncated by a minimum value of 15° and a maximum value of 60° which have been arbitrarily chosen as the extreme values represented by a smooth slickensided surface and a fresh, rough tension fracture.

Ananlysis of overall Sau Mau Ping Slope wiat a water-filled tension crack						
Fixed quantities				*Calculated Quantities*		
Overall slope height	H =	60	metres	zcalc =	14.01	metres
Overall slope angle	psif =	50	degrees	A =	80.19	sq.m
Failure plane angle	psip =	35	degrees	W =	2392.46	tonnes
Unit weight of rock	gammar =	2.6	t/cu.m	U =	360.19	tonnes
Unit weight of water	gammaw=	1	t/cu.m	V =	40.36	tonnes
Reinforcing force	T =	0	tonnes	Capacity =	1852.91	tonnes
Reinforcing angle	theta =	0	desgrees	Demand =	1513.02	tonnes
				Factor of Safety =	**1.22**	
Randon variables						
Quantity			Mean	std. dev.	Min.	Max.	Distr.
Friction angle	phi	35.00	5.00	15.00	60.00	35.00
Cohesive strength	coh	10.00	2.00	0.00	25.00	10.00
Tension crack depth	z	14.01	3.00	0.10	24.75	14.01
Depth of water	zw	14.01		0.10	24.75	8.98
Earthquake acc.	alpha	0.08		0.00	0.16	0.05
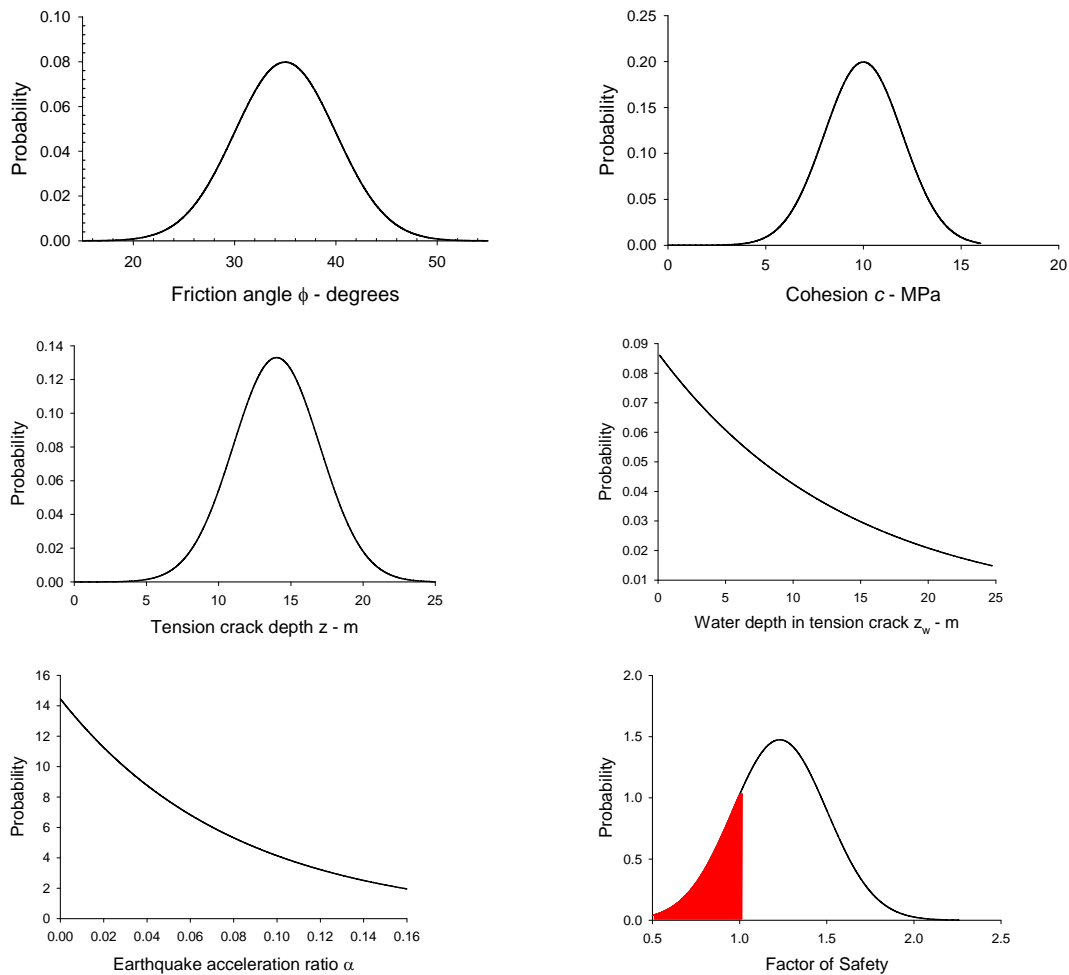
Figure 8.2: Spreadsheet for @RISK Latin Hypercube analysis of Sau Mau Ping slope with distributions of random input variables and the probability density function for the calculated factor of safety. The probability of failure, shown by the dark region for F<1, is approximately 21% for the assumed conditions.
.

2. *Cohesive strength c* - Again using the assumed range of shear strength values illustrated in Figure 7.8, a value of 10 tonnes/m^2 has been chosen as the mean cohesive strength and the standard deviation has been set at 2 tonnes/m^2 on the basis of this diagram. In order to allow for the wide range of possible cohesive strengths the minimum and maximum values used to truncate the normal distribution are 0 and 25 tonnes/m^2 respectively. Those with experience in the interpretation of laboratory shear strength test results may argue that the friction angle ϕ and the cohesive strength *c* are not independent variables as has been assumed in this analysis. This is because the cohesive strength generally drops as the friction angle rises and vice versa. The program @RISK allows the user to define variables as dependent but, for the sake of simplicity, the friction angle ϕ and the cohesive strength *c* have been kept independent for this analysis.

3. *Tension crack depth z* - Equation 7.6, defining the tension crack depth, has been derived by minimisation of equation 7.5. For the purposes of this analysis it has been assumed that this value of *z* (14 m for the assumed conditions) represents the mean tension crack depth. A truncated normal distribution is assumed to define the possible range of tension crack depths and the standard deviation has been arbitrarily chosen at 3 m. The minimum tension crack depth is zero but a value of 0.1 m has been chosen to avoid possible numerical problems. The maximum tension crack depth is given by $z = H(1 - \tan \phi_p / \tan \psi_f) = 24.75$ m which occurs when the vertical tension crack is located at the crest of the slope.

4. *Water depth z_w in tension crack* - The water which would fill the tension crack in this slope would come from direct surface run-off during heavy rains. In Hong Kong the heaviest rains occur during typhoons and it is likely that the tension crack would be completely filled during such events. The probability of occurrence of typhoons has been defined by a truncated exponential distribution where the mean water depth is assumed to be one half the tension crack depth. The maximum water depth cannot exceed the tension crack depth *z* and, as defined by the exponential distribution, this value would occur very rarely. The minimum water depth is zero during dry conditions and this is assumed to be a frequent occurrence. Note that the water depth z_w is defined in terms of the tension crack depth *z* which is itself a random variable. In calculating z_w the program @RISK first samples the truncated normal distribution defining *z* and then combines this value with the information obtained from sampling the truncated exponential distribution to calculate z_w.

5. *Ratio of horizontal earthquake acceleration to gravitational acceleration α* - The frequent occurrence of earthquakes of different magnitudes can be estimated by means of an exponential distribution which suggests that large earthquakes are very rare while small ones are very common. In the case of Hong Kong local wisdom suggested a 'design' horizontal acceleration of 0.08g. In other words, this level of acceleration could be anticipated at least once during the operating life of a civil engineering structure. A rough rule of thumb suggests that the 'maximum credible' acceleration is approximately twice the 'design' value. Based upon these very crude guidelines, the distribution of values of α used in these calculations

was defined by a truncated exponential distribution with a mean value of α = 0.08, a maximum of 0.16 and a minimum of 0.

Using the distributions shown in Figure 8.2, the program @RISK was used, with Latin Hypercube sampling to carry out 1,000 iterations on the factor of safety. The resulting probability distribution was not a smooth curve, indicating that an insufficient number of iterations had been performed for this combination of variables. A second analysis was carried out using 10,000 iterations and the resulting factor of safety distribution is plotted in the lower right hand corner of Figure 8.2. Note that this distribution closely resembles a normal distribution.

From the statistical tables produced by the program @RISK it was determined that the probability of failure for this slope is approximately 21%. This value is given by the ratio of the area under the distribution curve for F<1 (shown in red in Figure 8.2) divided by the total area under the distribution curve. This means that, for the combination of slope geometry, shear strength, water pressure and earthquake acceleration parameters assumed, 21 out of 100 similar slopes could be expected to fail at some time during the life of the slope. Alternatively, a length of 21 m could be expected to fail in every 1000 m of slope.

This is a reasonable risk of failure and it confirms the earlier conclusion, discussed in Chapter 7, that this slope was not adequately stable for a densely populated region such as Kowloon. Incidentally, a risk of this magnitude may be acceptable in an open pit mine, with limited access of trained miners, and even on a rural road. The decisions reached in Chapter 7 on the long term stabilisation measures for this slope are considered appropriate and the type of analysis described here could be used to evaluate the effectiveness of these remedial measures.

Note:

The author wishes to express his thanks to Dr Eugenio Casteli and Mr Damiano Giordano for bringing to his attention a number of errors in the original Monte Carlo analysis presented in Figure 8.2. These errors have been corrected in this revision on the notes.

9

Analysis of rockfall hazards

9.1   Introduction

Rockfalls are a major hazard in rock cuts for highways and railways in mountainous terrain. While rockfalls do not pose the same level of economic risk as large scale failures which can and do close major transportation routes for days at a time, the number of people killed by rockfalls tends to be of the same order as people killed by all other forms of rock slope instability. Badger and Lowell (1983) summarised the experience of the Washington State Department of Highways. They stated that 'A significant number of accidents and nearly a half dozen fatalities have occurred because of rockfalls in the last 30 years … [and] … 45 percent of all unstable slope problems are rock fall related'. Hungr and Evans (1989) note that, in Canada, there have been 13 rockfall deaths in the past 87 years. Almost all of these deaths have been on the mountain highways of British Columbia.

Figure 9.1: A rock slope on a mountain highway. Rockfalls are a major hazard on such highways.
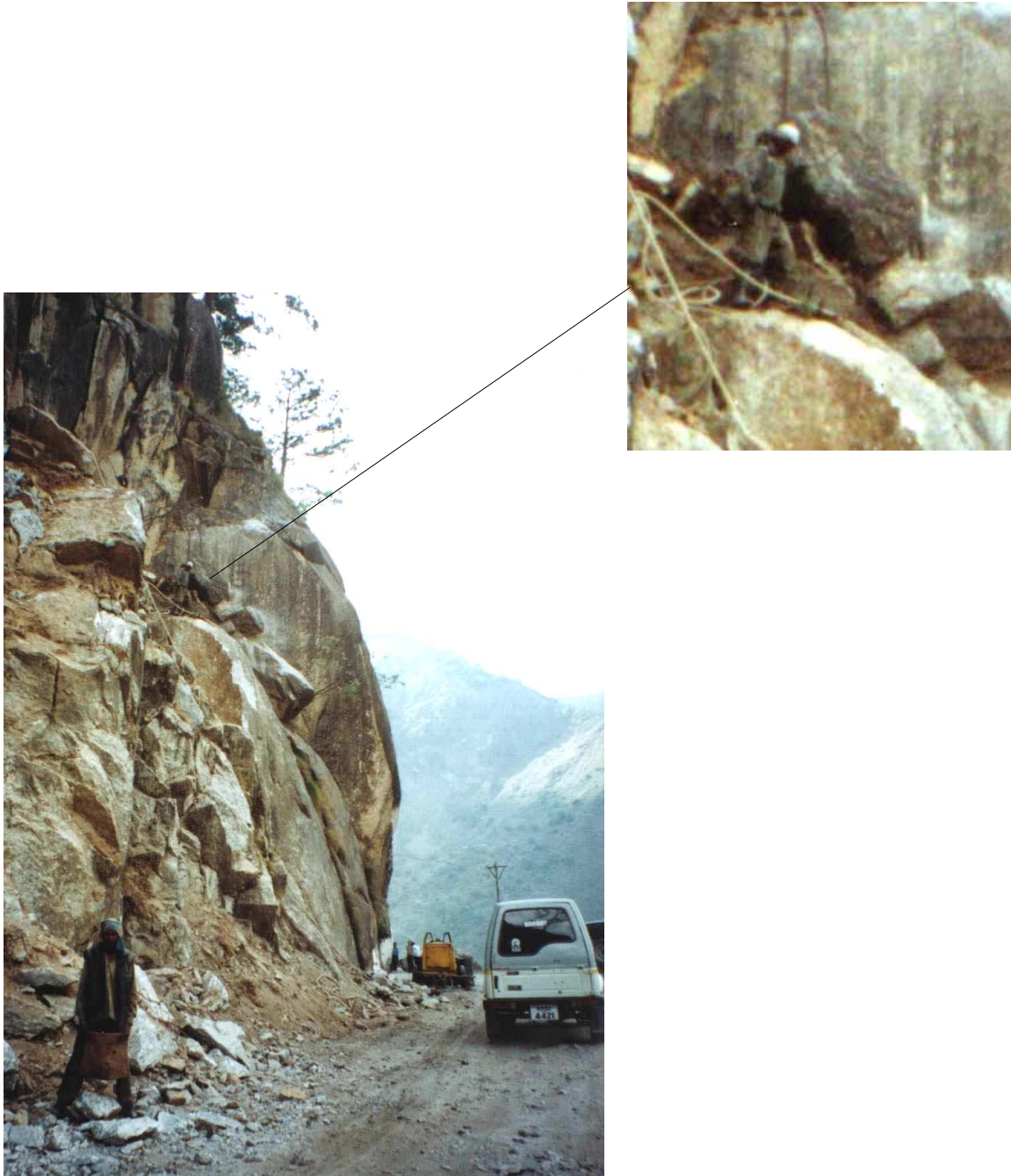
Figure 9.2: Construction on a active roadway, sometimes necessary when there is absolutely no alternative access, increases the rockfall hazard many times over that for slopes without construction or for situations in which the road can be closed during construction.

In some circumstances, where no alternative access is available, it becomes necessary to carry out construction activities on highway slopes while maintaining partial traffic flow. This increases the rockfall hazard many times and can only be considered acceptable if the road can be closed during the most hazardous construction activities.

9.2 Mechanics of rockfalls

Rockfalls are generally initiated by some climatic or biological event that causes a change in the forces acting on a rock. These events may include pore pressure increases due to rainfall infiltration, erosion of surrounding material during heavy rain storms, freeze-thaw processes in cold climates, chemical degradation or weathering of the rock, root growth or leverage by roots moving in high winds. In an active construction environment, the potential for mechanical initiation of a rockfall will probably be one or two orders of magnitude higher than the climatic and biological initiating events described above.

Once movement of a rock perched on the top of a slope has been initiated, the most important factor controlling its fall trajectory is the geometry of the slope. In particular, dip slope faces, such as those created by the sheet joints in granites, are important because they impart a horizontal component to the path taken by a rock after it bounces on the slope or rolls off the slope. The most dangerous of these surfaces act as 'ski-jumps' and impart a high horizontal velocity to the falling rock, causing it to bounce a long way out from the toe of the slope.

Clean faces of hard unweathered rock are the most dangerous because they do not retard the movement of the falling or rolling rock to any significant degree. On the other hand, surfaces covered in talus material, scree or gravel absorb a considerable amount of the energy of the falling rock and, in many cases, will stop it completely.

This retarding capacity of the surface material is expressed mathematically by a term called the *coefficient of restitution*. The value of this coefficient depends upon the nature of the materials that form the impact surface. Clean surfaces of hard rock have high coefficients of restitution while soil, gravel and completely decomposed granite have low coefficients of restitution. This is why gravel layers are placed on catch benches in order to prevent further bouncing of falling rocks.

Other factors such as the size and shape of the rock boulders, the coefficients of friction of the rock surfaces and whether or not the rock breaks into smaller pieces on impact are all of lesser significance than the slope geometry and the coefficients of restitution described above. Consequently, relative crude rockfall simulation models, such as the program written by Hoek (1986), are capable of producing reasonably accurate predictions of rockfall trajectories. Obviously more refined models will produce better results, provided that realistic input information is available. Some of the more recent rockfall models are those of Bozzolo et al (1988), Hungr and Evans (1988), Spang and Rautenstrauch (1988) and Azzoni et al (1995).

Most of these rockfall models include a Monte Carlo simulation technique to vary the parameters included in the analysis. This technique, named after the gambling casinos of Monte Carlo, is similar to the random process of throwing dice - one for each parameter being considered. A typical rockfall analysis is reproduced in Figure 9.3.
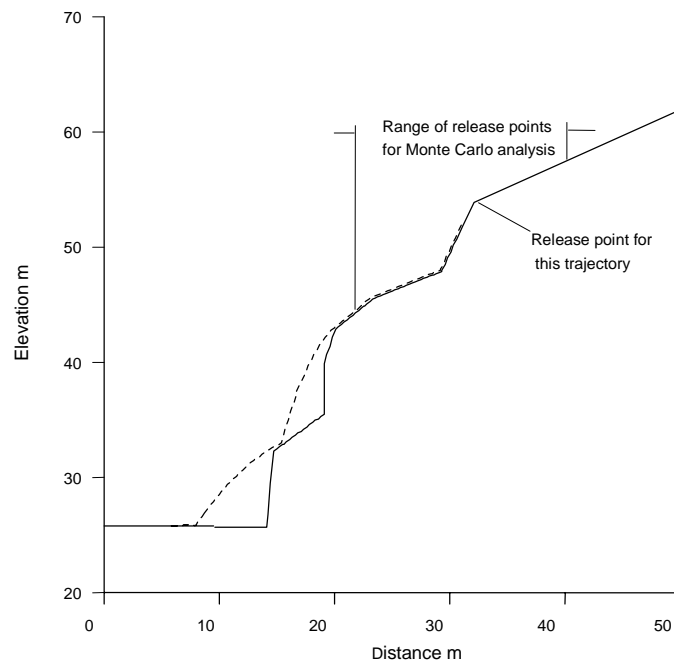
a) Typical trajectory for a 1000 kg boulder.
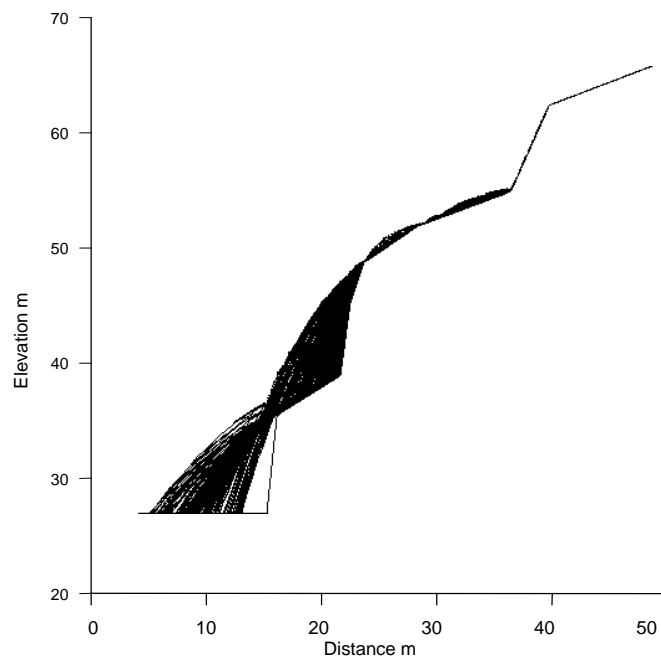
b) Trajectories for 1000 boulders weighing between 200 and 20,000
kg released within the range shown in a) above.

Figure 9.3: Typical example of a rockfall trajectory for a granite slope.

The analysis illustrated in Figure 9.3 was carried out using the program developed by Hungr[1]. The principal advantage of this program is that it includes a plasticity function which absorbs the impact energy of boulders, depending upon their size. This simulates the process in which large boulders will be damaged or will indent the impact surface while small boulders will bounce off the impact surface with little energy loss.

In the analysis reproduced in Figure 9.3b, the road surface was assigned a coefficient of restitution close to zero so that any bounce after the first impact was suppressed. The purpose of this study was to determine the spread of first impacts so that an effective catch ditch and barrier fence could be designed.

9.3   Possible measures which could be taken to reduce rockfall hazards

9.3.1   Identification of potential rockfall problems

It is either possible or practical to detect all potential rockfall hazards by any techniques currently in use in rock engineering.

In some cases, for example, when dealing with boulders on the top of slopes, the rockfall hazards are obvious. However, the most dangerous types of rock failure occur when a block is suddenly released from an apparently sound face by relatively small deformations in the surrounding rock mass. This can occur when the forces acting across discontinuity planes, which isolate a block from its neighbours, change as a result of water pressures in the discontinuities or a reduction of the shear strength of these planes because of long term deterioration due to weathering. This release of 'keyblocks' can sometimes precipitate rockfalls of significant size or, in extreme cases, large scale slope failures.

While it is not suggested that rock faces should not be carefully inspected for potential rockfall problems, it should not be assumed that all rockfall hazards will be detected by such inspections.

9.3.2   Reduction of energy levels associated with excavation

Traditional excavation methods for hard rock slopes involve the use of explosives. Even when very carefully planned controlled blasts are carried out, high intensity short duration forces act on the rock mass. Blocks and wedges which are at risk can be dislodged by these forces. Hence, an obvious method for reducing rockfall hazards is to eliminate excavation by blasting or by any other method, such as ripping, which imposes concentrated, short duration forces or vibrations on the rock mass.

Mechanical and hand excavation methods can used and, where massive rock has to be broken, chemical expanding rock breaking agents may be appropriate.

9.3.3   Physical restraint of rockfalls

If it is accepted that it is not possible to detect or to prevent all rockfalls, then methods for restraining those rockfalls, which do occur, must be considered. These methods are illustrated in Figure 9.4.

---

[1] Dynamic Analysis of Fragmental Rockfall, available from O. Hungr Geotechnical Research Inc., 4195 Almondel Road, West Vancouver, BC, Canada V7V 3L6.
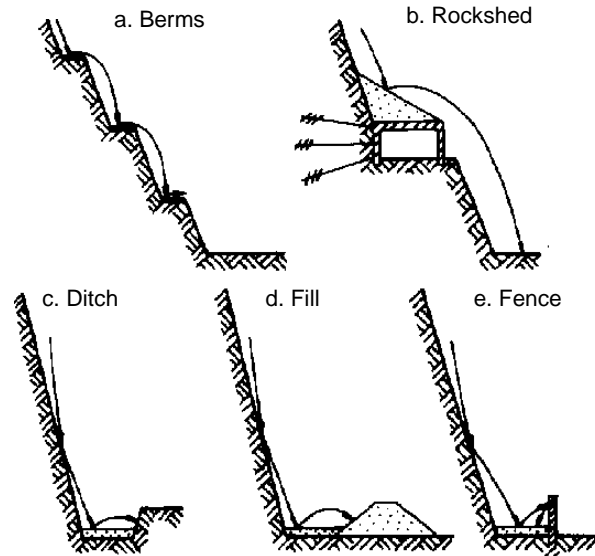
Figure 9.4: Possible measures to reduce the damage due to rockfalls. After Spang (1987).

Berms are a very effective means of catching rockfalls and are frequently used on permanent slopes. However, berms can only be excavated from the top downwards and they are of limited use in minimising the risk of rockfalls during construction.

Rocksheds or avalanche shelters are widely used on steep slopes above narrow railways or roadways. An effective shelter requires a steeply sloping roof covering a relatively narrow span. In the case of a wide multi-lane highway, it may not be possible to design a rockshed structure with sufficient strength to withstand large rockfalls.

Rock traps work well in catching rockfalls provided that there is sufficient room at the toe of the slope to accommodate these rock traps. In the case of very narrow roadways at the toe of steep slopes, there may not be sufficient room to accommodate rock traps. This restriction also applies to earth or rock fills and to gabion walls or massive concrete walls.

Catch fences or barrier fences in common use are estimated to have an energy absorption capacity of 100 kNm[2]. This is equivalent to a 250 kg rock moving at about 20 metres per second. More robust barrier fences, such as those used in the European Alps[3], have an energy absorbing capacity of up to 2500 kNm which means that they could stop a 6250 kg boulder moving at approximately 20 metres per second. Details of a typical high capacity net are illustrated in Figure 9.5.

Another restraint system which merits further consideration is the use of mesh draped over the face. This type of restraint is commonly used for permanent slopes and is illustrated in Figure 9.6. The mesh is draped over the rock face and attached at several locations along the slope. The purpose of the mesh is not to stop rockfalls but to trap the falling rock between the mesh and the rock face and so to reduce the horizontal velocity component which causes the rock to bounce out onto the roadway below.

---

[2] The kinetic energy of a falling body is given by 0.5 x mass x velocity[2].

[3] Wire mesh fence which incorporates cables and energy absorbing slipping joints is manufactured by Geobrugg Protective Systems, CH-8590 Romanshorn, Switzerland, Fax +41 71466 81 50.

a: Anchor grouted into rock
with cables attached.

b: Geobrugg ring net shown
restraining a boulder. These nets
can be designed with energy
absorbing capacities of up to
2500 kNm which is equivalent to
a 6 tonne boulder moving at 20 m
per second.

c: Geobrugg energy absorbing ring.
When subjected to impact loading
the ring deforms plastically and
absorbs the energy of the boulder.

Figure 9.5: Details of a rockfall net system manufactured by Geobrugg of Switzerland.
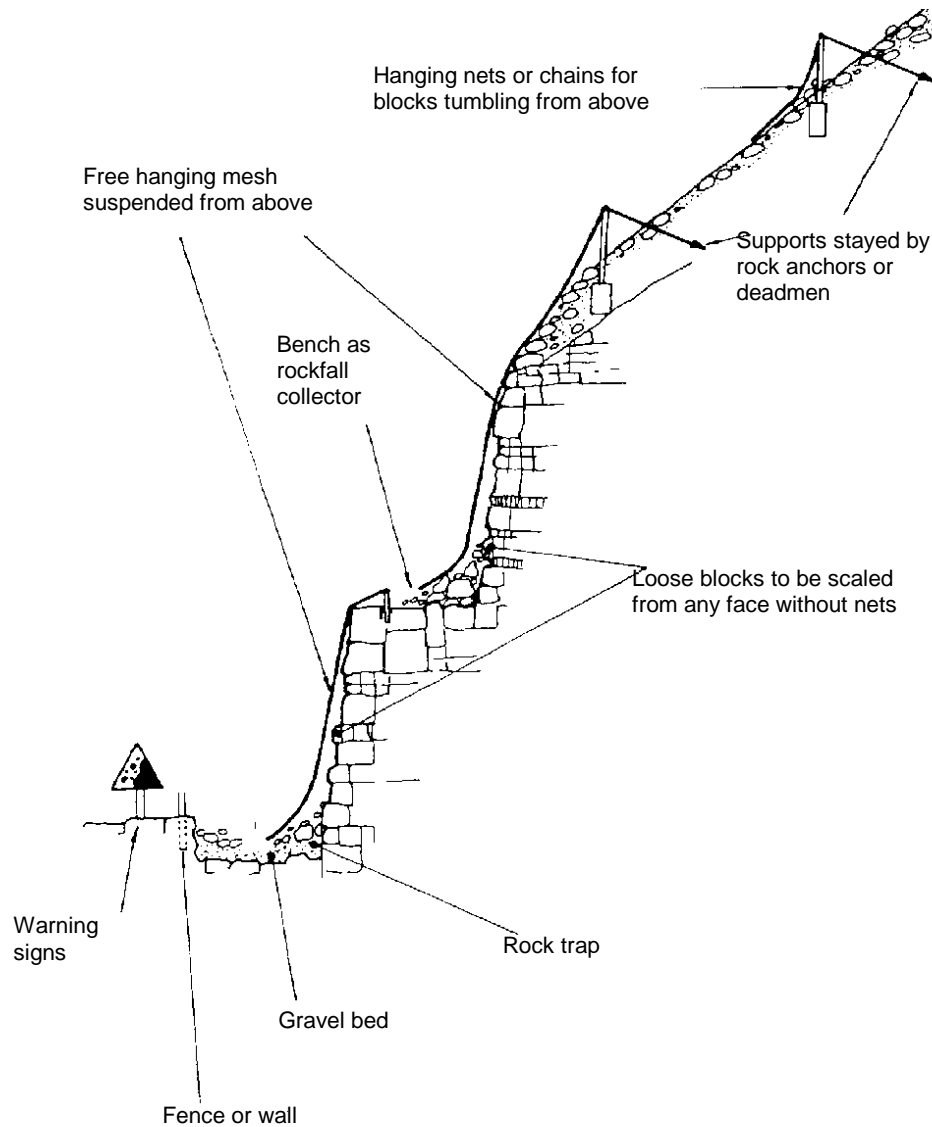
Figure 9.6: Rockfall control measures. After Fookes and Sweeney (1976).

Probably the most effective permanent rockfall protective system for most highways is the construction of a catch ditch at the toe of the slope. The base of this ditch should be covered by a layer of gravel to absorb the energy of falling rocks and a sturdy barrier fence should be placed between the ditch and the roadway. The location of the barrier fence can be estimated by means of a rockfall analysis such as that used to calculate the trajectories presented in Figure 9.3. The criterion for the minimum distance between the toe of the slope and the rock fence is that no rocks can be allowed to strike the fence before their kinetic energy has been diminished by the first impact on the gravel layer in the rock trap.

A simple design chart for ditch design, based upon work by Ritchie (1963), is reproduced in Figure 9.7.
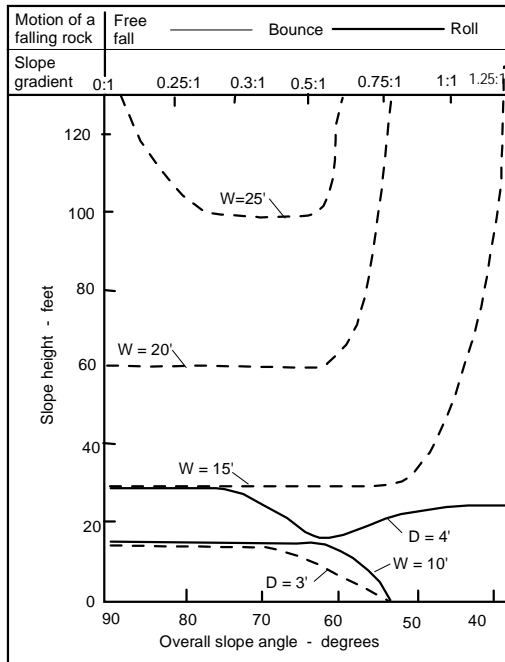
Ditch Design Chart
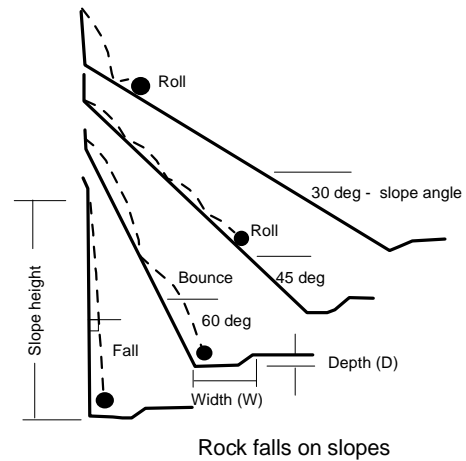
Rock falls on slopes

Figure 9.7: Rockfall ditch design chart based upon work by Ritchie (1963).

9.4 Rockfall Hazard Rating System

Highway and railway construction in mountainous regions presents a special challenge to geologists and geotechnical engineers. This is because the extended length of these projects makes it difficult to obtain sufficient information to permit stability assessments to be carried out for each of the slopes along the route. This means that, except for sections which are identified as particularly critical, most highway slopes tend to be designed on the basis of rather rudimentary geotechnical analyses. Those analyses which are carried out are almost always concerned with the overall stability of the slopes against major sliding or toppling failures which could jeopardise the operation of the highway or railway. It is very rare to find an analysis of rockfall hazards except in heavily populated regions in highly developed countries such as Switzerland.

In recognition of the seriousness of this problem and of the difficulty of carrying out detailed investigations and analyses on the hundreds of kilometres of mountain highway in the western United States and Canada, highway and railway departments have worked on classification schemes which can be carried out by visual inspection and simple calculations. The purpose of these classifications is to identify slopes which are particularly hazardous and which require urgent remedial work or further detailed study.

In terms of rockfall hazard assessment, one of the most widely accepted[4] is the Rockfall Hazard Rating System (RHRS) developed by the Oregon State Highway Division (Pierson et al. 1990). Table 9.1 gives a summary of the scores for different

---

[4] This system has been adopted by the States of Oregon, Washington, New Mexico and Idaho and, in slightly modified form, by California, Colorado and British Columbia.

categories included in the classification while Figure 9.8 shows a graph which can be used for more refined estimates of category scores. The curve shown in Figure 9.8 is calculated from the equation $y = 3^x$ where, in this case, $x = $ (Slope height- feet)/25. Similar curves for other category scores can be calculated from the following values of the exponent *x*.

Slope height	$x = $ slope height (feet) / 25
Average vehicle risk	$x = $ % time / 25
Sight distance	$x = (120 - $ % Decision sight distance) / 20
Roadway width	$x = (52 - $ Roadway width (feet)) / 8
Block size	$x = $ Block size (feet)
Volume	$x = $ Volume (cu.ft.) / 3
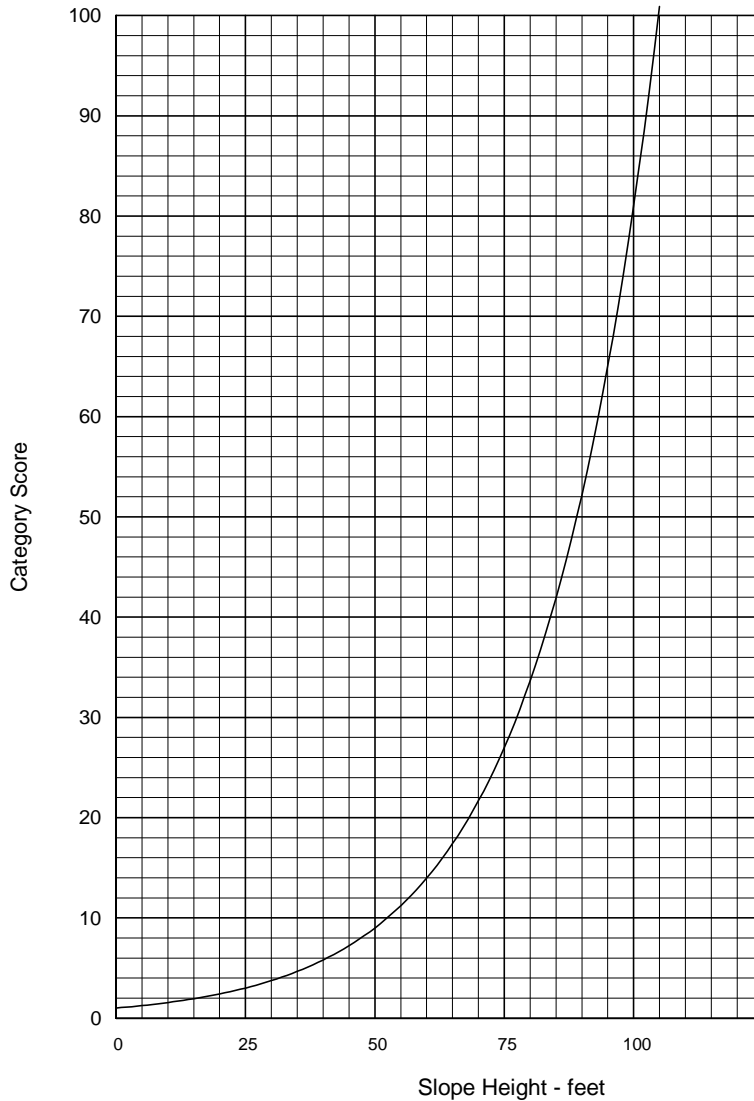
Figure 9.8: Category score graph for slope height.

Table 9.1: Rockfall Hazard Rating System.

CATEGORY			RATING CRITERIA AND SCORE			
			POINTS 3	POINTS 9	POINTS 27	POINTS 81
SLOPE HEIGHT			25 FT	50 FT	75 FT	100 FT
DITCH EFFECTIVENESS			Good catchment	Moderate catchment	Limited catchment	No catchment
AVERAGE VEHICLE RISK			25% of the time	50% of the time	75% of the time	100% of the time
PERCENT OF DECISION SIGHT DISTANCE			Adequate site distance, 100% of low design value	Moderate sight distance, 80% of low design value	Limited site distance, 60% of low design value	Very limited sight distance, 40% of low design value
ROADWAY WIDTH INCLUDING PAVED SHOULDERS			44 feet	36 feet	28 feet	20 feet
GEOLOGIC CHARACTER	CASE 1	STRUCTURAL CONDITION	Discontinuous joints, favorable orientation	Discontinuous joints, random orientation	Discontinuous joints, adverse orientation	Continuous joints, adverse orientation
		ROCK FRICTION	Rough, irregular	Undulating	Planar	Clay infilling or slickensided
	CASE 2	STRUCTURAL CONDITION	Few differential erosion features	Occasional erosion features	Many erosion features	Major erosion features
		DIFFERENCE IN EROSION RATES	Small difference	Moderate difference	Large difference	Extreme difference
BLOCK SIZE ———— QUANTITY OF ROCKFALL/EVENT			1 FT ———— 3 cubic yards	2 FT ———— 6 cubic yards	3 FT ———— 9 cubic yards	4 FT ———— 12 cubic yards
CLIMATE AND PRESENCE OF WATER ON SLOPE			Low to moderate precipitation; no freezing periods, no water on slope	Moderate precipitation or short freezing periods or intermittent water on slope	High precipitation or long freezing periods or continual water on slope	High precipitation and long freezing periods or continual water on slope and long freezing periods
ROCKFALL HISTORY			Few falls	Occasional falls	Many falls	Constant falls

9.4.1 Slope Height

This item represents the vertical height of the slope not the slope distance. Rocks on high slopes have more potential energy than rocks on lower slopes, thus they present a greater hazard and receive a higher rating. Measurement is to the highest point from which rockfall is expected. If rocks are coming from the natural slope above the cut, use the cut height plus the additional slope height (vertical distance). A good approximation of vertical slope height can be obtained using the relationships shown below.

TOTAL SLOPE HEIGHT $= \dfrac{(X)\,\sin\alpha\,\sin\beta}{\sin(\alpha-\beta)} + H.I$

where   X = distance between angle measurements
         H.I = height of the instrument.

Figure 9.9: Measurement of slope height.

9.4.2   Ditch Effectiveness

The effectiveness of a ditch is measured by its ability to prevent falling rock from reaching the roadway. In estimating the ditch effectiveness, the rater should consider several factors, such as: 1) slope height and angle; 2) ditch width, depth and shape; 3) anticipated block size and quantity of rockfall; 4) impact of slope irregularities (launching features) on falling rocks. It's especially important for the rater to evaluate the impact of slope irregularities because a launching feature can negate the benefits expected from a fallout area. The rater should first evaluate whether any of the irregularities, natural or man-made, on a slope will launch falling rocks onto the paved roadway. Then based on the number and size of the launching features estimate what portion of the falling rocks will be effected. Valuable information on ditch performance can be obtained from maintenance personnel. Rating points should be assigned as follows:

3 points	*Good Catchment*. All or nearly all of falling rocks are retained in the catch ditch.
9 points	*Moderate Catchment*. Falling rocks occasionally reach the roadway.
27 points	*Limited Catchment*. Falling rocks frequently reach the roadway.
81 points	*No Catchment*. No ditch or ditch is totally ineffective. All or nearly all falling rocks reach the roadway.

Reference should also be made to Figure 9.7 in evaluating ditch effectiveness.

9.4.3   Average Vehicle Risk (AVR)

This category measures the percentage of time that a vehicle will be present in the rockfall hazard zone. The percentage is obtained by using a formula (shown below) based on slope length, average daily traffic (ADT), and the posted speed limit at the site. A rating of 100% means that on average a car can be expected to be within the hazard section 100% of the time. Care should be taken to measure only the length of a slope where rockfall is a problem. Over estimated lengths will strongly skew the formula results. Where high ADT's or longer slope lengths exist values greater than 100% will result. When this occurs it means that at any particular time more than one car is present within the measured section. The formula used is:

$$\frac{\text{ADT (cars/hour)} \quad x \quad \text{Slope Length (miles)} \quad x \quad 100\%}{\text{Posted Speed Limit (miles per hour)}} = \text{AVR}$$

9.4.4   Percent of Decision Sight Distance

The decision sight distance (DSD) is used to determine the length of roadway in feet a driver must have to make a complex or instantaneous decision. The DSD is critical when obstacles on the road are difficult to perceive, or when unexpected or unusual manoeuvres are required. Sight distance is the shortest distance along a roadway that an object of specified height is continuously visible to the driver.

Throughout a rockfall section the sight distance can change appreciably. Horizontal and vertical highway curves along with obstructions such as rock outcrops and roadside vegetation can severely limit a driver's ability to notice a rock in the road. To determine where these impacts are most severe, first drive through the rockfall section from both directions. Decide which direction has the shortest line of sight. Both horizontal and vertical sight distances should be evaluated. Normally an object will be most obscured when it is located just beyond the sharpest part of a curve. Place a six-inch object in that position on the fogline or on the edge of pavement if there is no fogline. The rater then walks along the fogline (edge of pavement) in the opposite direction of traffic flow, measuring the distance it takes for the object to disappear when your eye height is 3.5 ft above the road surface. This is the measured sight distance. The decision sight distance can be determined by the table below. The distances listed represent the low design value. The posted speed limit through the rockfall section should be used.

Posted Speed Limit (mph)	Decision Sight Distance (ft)
30	450
40	600
50	750
60	1,000
70	1.100

These two values can be substituted into the formula below to calculate the 'Percent of Decision Sight Distance.'

$$\frac{\text{Actual Site Distance} \quad (\quad) \quad x \quad 100\%}{\text{Decision Site Distance} \quad (\quad)} = \underline{\qquad}\%$$

9.4.5   Roadway Width

This dimension is measured perpendicular to the highway centreline from edge of pavement to edge of pavement. This measurement represents the available manoeuvring room to avoid a rockfall. This measurement should be the minimum width when the roadway width is not consistent.

9.4.6   Geologic Character

The geologic conditions of the slope are evaluated with this category. Case 1 is for slopes where joints, bedding planes, or other discontinuities, are the dominant structural feature of a rock slope. Case 2 is for slopes where differential erosion or oversteepened slopes is the dominant condition that controls rockfall. The rater should use whichever case best fits the slope when doing the evaluation. If both situations are present, both are scored but only the worst case (highest score) is used in the rating.

Case 1

Structural Condition   Adverse joint orientation, as it is used here, involves considering such things as rock friction angle, joint filling, and hydrostatic head if water is present. Adverse joints are those that cause block, wedge or toppling failures. 'Continuous' refers to joints greater than 10 feet in length.

3 points	*Discontinuous Joints, Favourable Orientation* Jointed rock with no adversely oriented joints, bedding planes, etc.
9 points	*Discontinuous Joints, Random Orientation* Rock slopes with randomly oriented joints creating a three-dimensional pattern. This type of pattern is likely to have some scattered blocks with adversely oriented joints but no dominant adverse joint pattern is present.
27 points	*Discontinuous Joints, Adverse Orientation* Rock slope exhibits a prominent joint pattern, bedding plane, or other discontinuity, with an adverse orientation. These features have less than 10 feet of continuous length.
81 points	*Continuous Joints, Adverse Orientation* Rock slope exhibits a dominant joint pattern, bedding plane, or other discontinuity, with an adverse orientation and a length of greater than 10 feet.

Rock Friction   This parameter directly effects the potential for a block to move relative to another. Friction along a joint, bedding plane or other discontinuity is governed by the macro and micro roughness of a surface. Macro roughness is the degree of undulation of the joint. Micro roughness is the texture of the surface of the joint. In areas where joints contain highly weathered or hydrothermally altered products, where movement has occurred causing slickensides or fault gouge to form, where open joints dominate the slope, or where joints are water filled, the rockfall potential is greater. Noting the failure

angles from previous rockfalls on a slope can aid in estimating general rock friction along discontinuities.

3 points	*Rough, Irregular*	The surface of the joints are rough and the joint planes are irregular enough to cause interlocking. This macro and micro roughness provides an optimal friction situation.
9 points	*Undulating*	Also macro and micro rough but without the interlocking ability.
27 points	*Planar*	Macro smooth and micro rough joint surfaces. Surface contains no undulations. Friction is derived strictly from the roughness of the rock surface.
81 points	*Clay Infilling or Slickensided*	Low friction materials, such as clay and weathered rock, separate the rock surfaces negating any micro or macro roughness of the joint planes. These infilling materials have much lower friction angles than a rock on rock contact. Slickensided joints also have a very low friction angle and belong in this category.

Case 2

Structural Condition   This case is used for slopes where differential erosion or oversteepening is the dominant condition that leads to rockfall. Erosion features include oversteepened slopes, unsupported rock units or exposed resistant rocks on a slope that may eventually lead to a rockfall event. Rockfall is caused by a loss of support either locally or throughout the slope. Common slopes that are susceptible to this condition are: layered units containing easily weathered rock that erodes undermining more durable rock; talus slopes; highly variable units such as conglomerates, mudflows, etc. that weather causing resistant rocks and blocks to fall, and rock/soil slopes that weather allowing rocks to fall as the soil matrix material is eroded.

3 points	*Few Differential Erosion Features*	Minor differential erosion features that are not distributed throughout the slope.
9 points	*Occasional Erosion Features*	Minor differential erosion features that are widely distributed throughout the slope.
27 points	*Many Erosion Features*	Differential erosion features are large and numerous throughout the slope.
81 points	*Major Erosion Features*	Severe cases such as dangerous erosion-created overhangs; or significantly oversteepened soil/rock slopes or talus slopes.

Difference in Erosion Rates   The Rate of Erosion on a Case 2 slope directly relates to the potential for a future rockfall event. As erosion progresses, unsupported or oversteepened slope conditions develop. The impact of the common physical and chemical erosion processes as well as the effects of man's actions should be considered. The degree of hazard caused by erosion and thus the score given this category should reflect how quickly erosion is occurring; the size of rocks, blocks, or units being exposed; the frequency of rockfall events; and the amount of material released during an event.

3 points	*Small Difference* The difference in erosion rates is such that erosion features develop over many years. Slopes that are near equilibrium with their environment are covered by this category.
9 points	*Moderate Difference* The difference in erosion rates is such that erosion features develop over a few years.
27 points	*Large Difference* The difference in erosion rates is such that erosion features develop annually.
81 points	*Extreme Difference* The difference in erosion rates is such that erosion features develop rapidly

9.4.7   Block Size or Quantity of Rockfall Per Event

This measurement should be representative of whichever type of rockfall event is most likely to occur. If individual blocks are typical of the rockfall, the block size should be used for scoring. If a mass of blocks tends to be the dominant type of rockfall, the quantity per event should be used. This can be determined from the maintenance history or estimated from observed conditions when no history is available. This measurement will also be beneficial in determining remedial measures.

9.4.8   Climate and Presence of Water on Slope

Water and freeze/thaw cycles both contribute to the weathering and movement of rock materials. If water is known to flow continually or intermittently from the slope it is rated accordingly. Areas receiving less than 20 inches per year are 'low precipitation areas.' Areas receiving more than 50 inches per year are considered 'high precipitation areas.' The impact of freeze/thaw cycles can be interpreted from knowledge of the freezing conditions and its effects at the site.

   The rater should note that the 27-point category is for sites with long freezing periods or water problems such as high precipitation or continually flowing water. The 81-point category is reserved for sites that have both long freezing periods and one of the two extreme water conditions.

9.4.9   Rockfall History

This information is best obtained from the maintenance person responsible for the slope in question. It directly represents the known rockfall activity at the site. There may be no

history available at newly constructed sites or where poor documentation practices have been followed and a turnover of personnel has occurred. In these cases, the maintenance cost at a particular site may be the only information that reflects the rockfall activity at that site. This information is an important check on the potential for future rockfalls. If the score you give a section does not compare with the rockfall history, a review should be performed. As a better database of rockfall occurrences is developed, more accurate conclusions for the rockfall potential can be made.

> 3 points   *Few Falls* - Rockfalls have occurred several times according to historical information but it is not a persistent problem. If rockfall only occurs a few times a year or less, or only during severe storms this category should be used. This category is also used if no rockfall history data is available.
>
> 9 points   *Occasional Falls* - Rockfall occurs regularly. Rockfall can be expected several times per year and during most storms.
>
> 27 points   *Many Falls* - Typically rockfall occurs frequently during a certain season, such as the winter or spring wet period, or the winter freeze-thaw, etc. This category is for sites where frequent rockfalls occur during a certain season and is not a significant problem during the rest of the year. This category may also be used where severe rockfall events have occurred.
>
> 81 points   *Constant Falls* - Rockfalls occur frequently throughout the year. This category is also for sites where severe rockfall events are common.

In addition to scoring the above categories, the rating team should gather enough field information to recommend which rockfall remedial measure is best suited to the rockfall problem. Both total fixes and hazard reduction approaches should be considered. A preliminary cost estimate should be prepared.

9.5   Risk analysis of rockfalls on highways

The analysis of the risk of damage to vehicles or the death of vehicle occupants as a result of rockfalls on highways has not received very extensive coverage in the geotechnical literature. Papers which deal directly with the probability of a slope failure event and the resulting death, injury or damage have been published by Hunt (1984), Fell (1994), Morgan (1991), Morgan et al (1992) and Varnes (1984). Most of these papers deal with landslides rather than with rockfalls. An excellent study of risk analysis applied to rockfalls on highways is contained in an MSc thesis by Christopher M. Bunce (1994), submitted to the Department of Civil Engineering at the University of Alberta. This thesis reviews risk assessment methodology and then applies this methodology to a specific case in which a rockfall killed a passenger and injured the driver of a vehicle.

Figure 9.10: The Argillite Cut on Highway 99 in British Columbia, Canada.

9.5.1 RHRS rating for Argillite Cut

Bunce carried out a study using the Rockfall Hazard Rating System for the Argillite Cut in which the rockfall occurred. A summary of his ratings for the section in which the rockfall happened and for the entire cut is presented in Table 9.2. The ratings which he obtained were 394 for the rockfall section and 493 for the entire cut.

The RHRS system does not include recommendations on actions to be taken for different ratings. This is because decisions on remedial action for a specific slope depend upon many factors such as the budget allocation for highway work which cannot be taken into account in the ratings. However, in personal discussions with Mr Lawrence Pierson, the principal author of the RHRS, I was informed that in the State of Oregon, slopes with a rating of less than 300 are assigned a very low priority while slopes with a rating in excess of 500 are identified for urgent remedial action.

Table 9.2: RHRS ratings for Argillite Cut on Highway 99 in British Columbia (after Bunce, 1994).

	Section where rockfall occurred		Rating for entire cut	
Parameter	Value	Rating	Value	Rating
Slope height	36	100	35	100
Ditch effectiveness	Limited	27	Limited	27
Average vehicle risk	7	1	225	100
Sight distance	42	73	42	73
Roadway width	9.5	17	9.5	17
Geological structure	Very adverse	81	Adverse	60
Rock friction	Planar	27	Planar	27
Block size	0.3 m	3	1 m	35
Climate and water	High precip.	27	High precip.	27
Rockfall history	Many falls	40	Many falls	27
Total score		394		493

9.5.2 Risk analysis for Argillite Cut

Bunce (1994) presented a number of approaches for the estimation of the annual probability of a fatality occurring as a result of a rockfall in the Argillite Cut. Some of these approaches are relatively sophisticated and I have to question whether this level of sophistication is consistent with the quality of the input information which is available on highway projects.

One approach which I consider to be compatible with the rockfall problem and with quality of input information available is the event tree analysis. This technique is best explained by means of the practical example of the analysis for the Argillite Cut, shown in Figure 9.10. I have modified the event tree presented by Bunce (1994) to make it simpler to follow.

In the event tree analysis, a probability of occurrence is assigned to each event in a sequence which could lead to a rockfall fatality. For example, in Figure 9.11, it is assumed that it rains 33% of the time, that rockfalls occur on 5% of rainy days, that vehicles are impacted by 2% of these rockfalls, that 50% of these impacts are significant, i.e. they would result in at least one fatality. Hence, the annual probability of fatality resulting from a vehicle being hit by a rockfall triggered by rain is given by $(0.333 * 0.05 * 0.02 * 0.5) = 1.67*10^{-4}$.

Initiating event (annual)	Rockfall	Vehicle beneath failure	Impact significant	Annual probability of occurrence	Potential number of fatalities	Annual probability of occurrence
rain 33%	no 95%			0.317	nil	
	yes 5%	no 98%		$1.63*10^{-2}$	nil	
		yes 2%	no 50%	$1.67*10^{-4}$	nil	
			yes 50%	$1.67*10^{-4}$	one 50%	$8.33*10^{-5}$
					two 33%	$5.56*10^{-5}$
					3 or more 17%	$2.78*10^{-5}$

Annual probability of a single fatality	$= (8.33+ 5.56 + 2.78) * 10^{-5}$	$= 1.67 * 10^{-4}$
Annual probability of two fatalities	$= (5.56+ 2.78) * 10^{-5}$	$= 8.34 * 10^{-5}$
Annual probability of three or more fatalities	$= 2.78 * 10^{-5}$	$= 2.78 * 10^{-5}$

Figure 9.11: Event tree analysis of rockfalls in the Argillite Cut in British Columbia. (After Bunce, 1994)

The event tree has been extended to consider the annual probability of occurrence of one, two and three or more fatalities in a single accident. These probabilities are shown in the final column of Figure 9.11. Since there would be at least one fatality in any of these accidents, the total probability of occurrence of a single fatality is $(8.33 + 5.56 + 2.78)*10^{-5} = 1.7 * 10^{-4}$, as calculated above. The total probability of at least two fatalities

is $(5.56 + 2.78) * 10^{-5} = 8.34 * 10^{-5}$ while the probability of three or more fatalities remains at $2.78 * 10^{-5}$ as shown in Figure 9.11.

Suppose that it is required to carry out construction work on the slopes of the Argillite cut and that, because this is an important access road to an international ski resort area, it is required to maintain traffic flow during this construction. It is assumed that the construction work lasts for 6 months (50% of a year) and that rockfalls are initiated 20% of the working time, i.e. on 36 days. All other factors in the event tree remain the same as those assumed in Figure 9.11. The results of this analysis are presented in Figure 9.12 which shows that there is an almost ten fold increase in the risk of fatalities from rockfalls as a result of the ongoing construction activities. (Note that this is a hypothetical example only and that no such construction activities are planned on this highway).

Initiating event (annual)	Rockfall	Vehicle beneath failure	Impact significant	Annual probability of occurrence	Potential number of fatalities	Annual probability of occurrence
construction 50%	no 80%			0.40	nil	
	yes 20%	No 98%		$9.80*10^{-2}$	nil	
		Yes 2%	no 50%	$1.00*10^{-3}$	nil	
			yes 50%	$1.00*10^{-3}$	one 50%	$5.00*10^{-4}$
					two 33%	$3.30*10^{-4}$
					3 or more 17%	$1.70*10^{-4}$

Annual probability of a single fatality	$= (5.00+3.30+1.70) * 10^{-4}$	$= 1.00 * 10^{-3}$
Annual probability of two fatalities	$= (3.30+1.70) * 10^{-4}$	$= 5.00 * 10^{-4}$
Annual probability of three or more fatalities	$= 1.70 * 10^{-4}$	$= 1.70 * 10^{-4}$

Figure 9.12: Event tree for a hypothetical example in which construction activities on the Argillite Cut are carried out for a period of six months while the highway is kept open.

9.6   Comparison between assessed risk and acceptable risk

The estimated annual probabilities of fatalities from rockfalls, discussed in the previous sections, have little meaning unless they are compared with acceptable risk guidelines used on other major civil engineering construction projects.

One of the earliest attempts to develop an acceptable risk criterion was published by Whitman (1984). This paper was very speculative and was published in order to provide a basis for discussion on this important topic. In the ten years since this paper was published a great deal of work has been done to refine the concepts of acceptable risk and there are now more reliable acceptability criteria than those suggested by Whitman.

Figure 9.13, based on a graph published by Nielsen, Hartford and MacDonald (1994), summarises published and proposed guidelines for tolerable risk. The line marked 'Proposed BC Hydro Societal Risk' is particularly interesting since this defines an annual probability of occurrence of fatalities due to dam failures as 0.001 lives per year or 1

fatality per 1000 years. A great deal of effort has gone into defining this line and I consider it to be directly applicable to rock slopes on highways which, like dams, must be classed as major civil engineering structures for which the risks to the public must be reduced to acceptable levels.
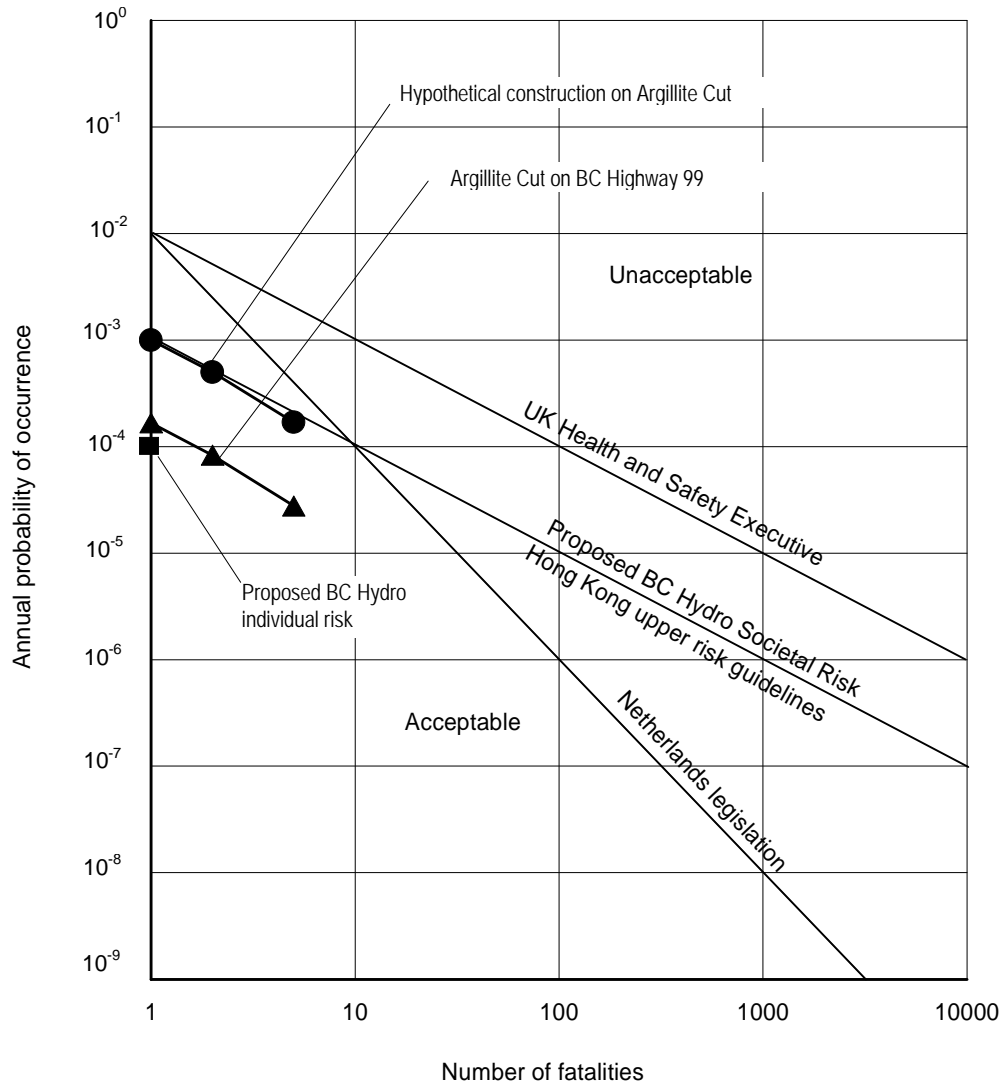
Figure 9.13: Comparison between risks of fatalities due to rockfalls with published and proposed acceptable risk criteria.

Another point to be noted in Figure 9.13 is that marked 'Proposed BC Hydro Individual risk'. This annual probability of fatalities of 10^{-4} (1 in 10,000) is based upon the concept that the risk to an individual from a dam failure should not exceed the individual 'natural death' risk run by the safest population group (10 to 14 year old children). Consensus is also developing that the annual probability of fatality of 10^{-4} defines the boundary between voluntary (restricted access to site personnel) and involuntary (general public access) risk (Nielsen, Hartford and MacDonald, 1994).

On Figure 9.13, I have plotted the estimated annual probabilities of fatalities from rockfalls on the Argillite Cut on BC Highway 99, with and without construction. These plots show that the estimated risk for these slopes, without construction, is significantly lower than the 0.001 lives per year line. The estimated risk for the Argillite Cut slopes during active construction is approximately ten times higher and is marginally higher than the 0.001 lives per year criterion. Given the fact that courts tend to be unsympathetic to engineers who knowingly put the public at risk, it would be unwise to proceed with construction while attempting to keep the traffic flowing. A more prudent course of action would be to close the highway during periods of active construction on the slopes, even if this meant having to deal with the anger of frustrated motorists.

9.7   Conclusions

The Rockfall Hazard Rating System and the Event Tree risk assessments, discussed on the previous pages, are very crude tools which can only be regarded as semi-quantitative. However, the trends indicated by these tools together with common sense engineering judgement, give a reasonable assessment of the relative hazards due to rockfalls from cut slopes adjacent to highways and railways.

10

In situ and induced stresses

10.1 Introduction

Rock at depth is subjected to stresses resulting from the weight of the overlying strata and from locked in stresses of tectonic origin. When an opening is excavated in this rock, the stress field is locally disrupted and a new set of stresses are induced in the rock surrounding the opening. A knowledge of the magnitudes and directions of these in situ and induced stresses is an essential component of underground excavation design since, in many cases, the strength of the rock is exceeded and the resulting instability can have serious consequences on the behaviour of the excavations.

This chapter deals with the question of in situ stresses and also with the stress changes that are induced when tunnels or caverns are excavated in stressed rock. Problems, associated with failure of the rock around underground openings and with the design of support for these openings, will be dealt with in later chapters.

The presentation, which follows, is intended to cover only those topics which are essential for the reader to know about when dealing with the analysis of stress induced instability and the design of support to stabilise the rock under these conditions.

10.2 In situ stresses

Consider an element of rock at a depth of 1,000 m below the surface. The weight of the vertical column of rock resting on this element is the product of the depth and the unit weight of the overlying rock mass (typically about 2.7 tonnes/m^3 or 0.027 MN/m^3). Hence the vertical stress on the element is 2,700 tonnes/m^2 or 27 MPa. This stress is estimated from the simple relationship:

$$\sigma_v = \gamma\, z \tag{10.1}$$

where σ_v is the vertical stress

   γ is the unit weight of the overlying rock and
   z is the depth below surface.

Measurements of vertical stress at various mining and civil engineering sites around the world confirm that this relationship is valid although, as illustrated in Figure 10.1, there is a significant amount of scatter in the measurements.

Vertical stress, σ_v (MPa)
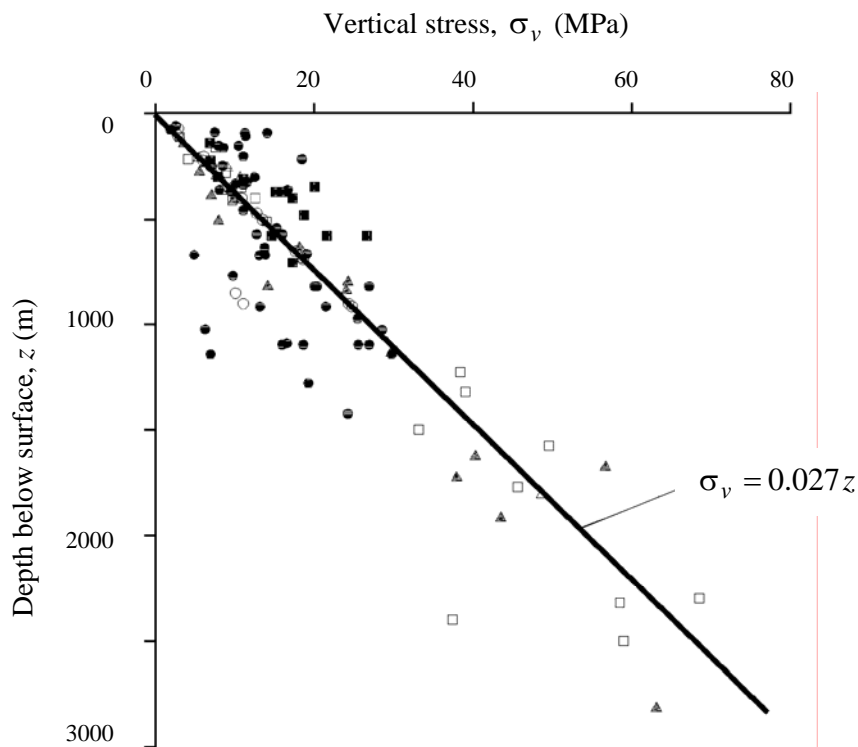
Figure 10.1: Vertical stress measurements from mininig and civil engineering projects around the world. (Afret Hoek and Brown 1978).

The horizontal stresses acting on an element of rock at a depth z below the surface are much more difficult to estimate than the vertical stresses. Normally, the ratio of the average horizontal stress to the vertical stress is denoted by the letter k such that:

$$\sigma_h = k\sigma_v = k\,\gamma\,z \tag{10.2}$$

Terzaghi and Richart (1952) suggested that, for a gravitationally loaded rock mass in which no lateral strain was permitted during formation of the overlying strata, the value of k is independent of depth and is given by $k = \nu/(1-\nu)$, where ν is the Poisson's ratio of the rock mass. This relationship was widely used in the early days of rock mechanics but, as discussed below, it proved to be inaccurate and is seldom used today.

Measurements of horizontal stresses at civil and mining sites around the world show that the ratio k tends to be high at shallow depth and that it decreases at depth (Brown and Hoek, 1978, Herget, 1988). In order to understand the reason for these horizontal stress variations it is necessary to consider the problem on a much larger scale than that of a single site.

Sheorey (1994) developed an elasto-static thermal stress model of the earth. This model considers curvature of the crust and variation of elastic constants, density and thermal expansion coefficients through the crust and mantle. A detailed discussion on Sheorey's model is beyond the scope of this chapter, but he did provide a simplified

equation which can be used for estimating the horizontal to vertical stress ratio k. This equation is:

$$k = 0.25 + 7E_h \left(0.001 + \frac{1}{z} \right) \tag{10.3}$$

where z (m) is the depth below surface and E_h (GPa) is the average deformation modulus of the upper part of the earth's crust measured in a horizontal direction. This direction of measurement is important particularly in layered sedimentary rocks, in which the deformation modulus may be significantly different in different directions.

A plot of this equation is given in Figure 10.2 for a range of deformation moduli. The curves relating k with depth below surface z are similar to those published by Brown and Hoek (1978), Herget (1988) and others for measured in situ stresses. Hence equation 7.3 is considered to provide a reasonable basis for estimating the value of k.

As pointed out by Sheorey, his work does not explain the occurrence of measured vertical stresses that are higher than the calculated overburden pressure, the presence of very high horizontal stresses at some locations or why the two horizontal stresses are seldom equal. These differences are probably due to local topographic and geological features that cannot be taken into account in a large scale model such as that proposed by Sheorey.
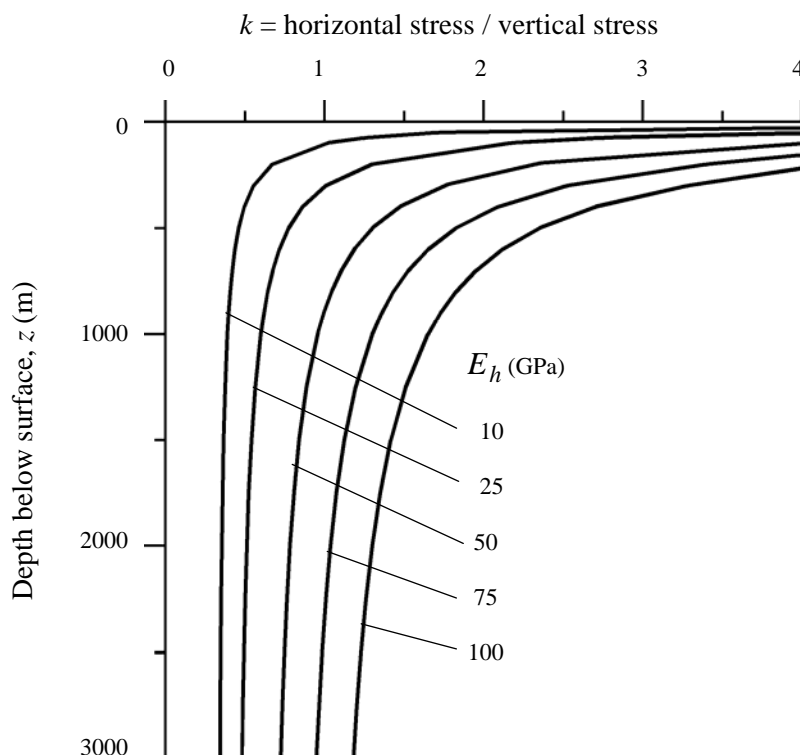
Figure 10.2: Ratio of horizontal to vertical stress for different deformation moduli based upon Sheorey's equation. (After Sheorey 1994).

Where sensitivity studies have shown that the in situ stresses are likely to have a significant influence on the behaviour of underground openings, it is recommended that the in situ stresses should be measured. Suggestions for setting up a stress measuring programme are discussed later in this chapter.

10.3 The World stress map

The World Stress Map project, completed in July 1992, involved over 30 scientists from 18 countries and was carried out under the auspices of the International Lithosphere Project (Zoback, 1992). The aim of the project was to compile a global database of contemporary tectonic stress data. Currently over 7,300 stress orientation entries are included in a digital database. Of these approximately 4,400 observations are considered reliable tectonic stress indicators, recording horizontal stress orientations to within $< \pm 25°$.

The data included in the World Stress Map are derived mainly from geological observations on earthquake focal mechanisms, volcanic alignments and fault slip interpretations. Less than 5% of the data is based upon hydraulic fracturing or overcoring measurements of the type commonly used in mining and civil engineering projects.

Figure 10.3 is a version of the World Stress Map in which the orientations of maximum horizontal stress σ_{hmax} are plotted on a base of average topography. Major tectonic plate boundaries are shown as heavy lines on this map. Figure 10.4 is a generalised version of the World Stress Map which shows mean stress directions based on averages of clusters of data shown in Figure 10.3.

The stress symbols in Figure 10.4 are defined as follows:

- A single set of thick inward pointing arrows indicates $\sigma_{h\max}$ orientations in a thrust faulting stress regime ($\sigma_{h\max} > \sigma_{h\min} > \sigma_v$).

- A single set of outward pointing arrows indicates $\sigma_{h\min}$ orientations in a normal faulting stress regime ($\sigma_v > \sigma_{h\max} > \sigma_{h\min}$).

- Thick inward pointing arrows, indicating $\sigma_{h\max}$, together with thin outward pointing arrows, indicating $\sigma_{h\min}$, are located in strike-slip faulting stress regimes ($\sigma_{h\max} > \sigma_v > \sigma_{h\min}$).

In discussing hydraulic fracturing and overcoring stress measurements, Zoback (1992) has the following comments:

> 'Detailed hydraulic fracturing testing in a number of boreholes beginning very close to surface (10-20 m depth) has revealed marked changes in stress orientations and relative magnitudes with depth in the upper few hundred metres, possibly related to effects of nearby topography or a high degree of near surface fracturing.
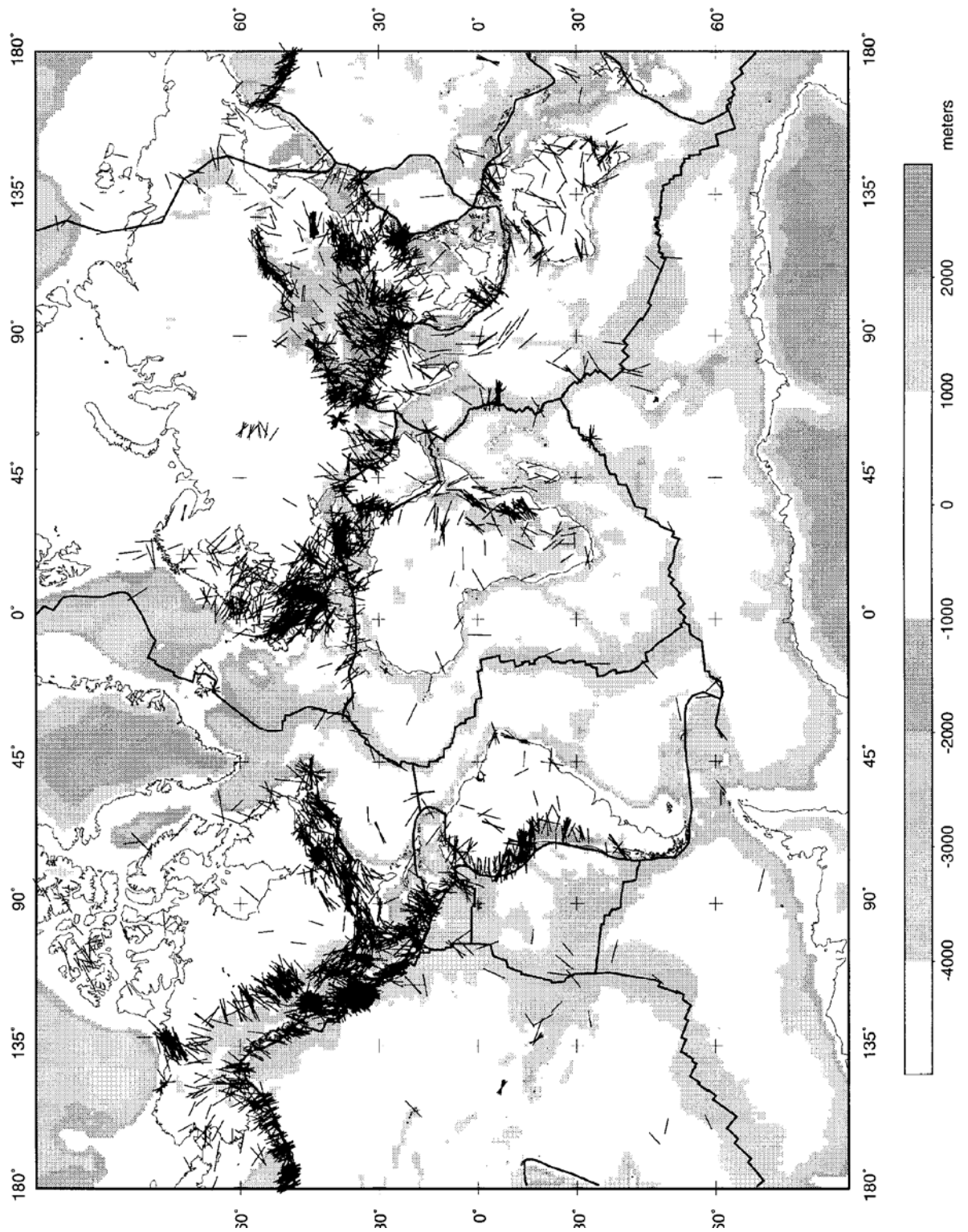
Figure 10.3: World stress map giving maximum horizontal stress orientations on a base of average topography (indicated by the shading defined in the vertical bar on the right hand side of the picture). Map provided by Dr. M.L Zoback from a paper by Zoback (1992).
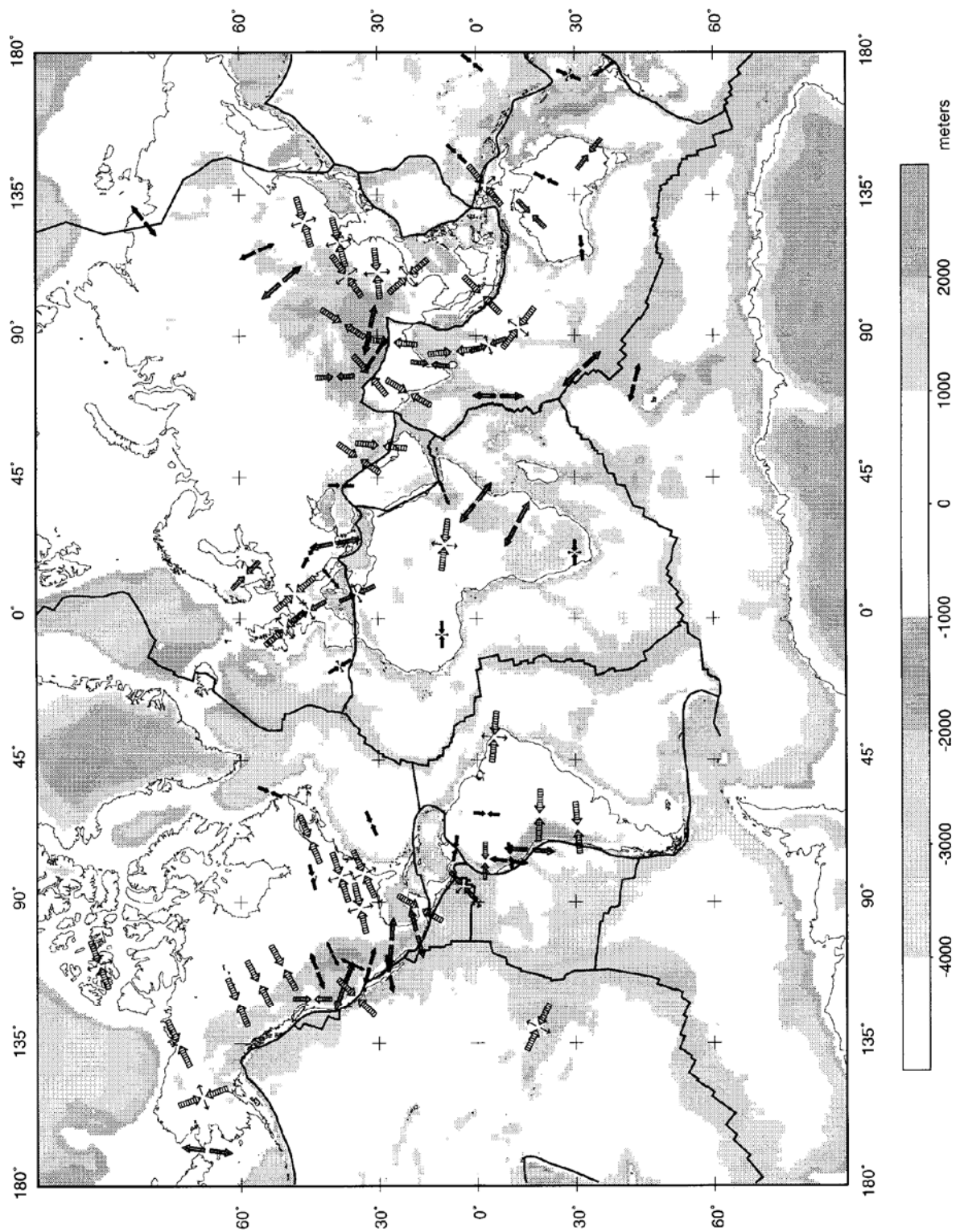
Figure 10.4: Generalised stress map showing mean directions based on average clusters of data shown in Figure 7.3. The meaning of the symbols is described in the text. Map provided by Dr M.L. Zoback from a paper by Zoback (1992).

Included in the category of 'overcoring' stress measurements are a variety of stress or strain relief measurement techniques. These techniques involve a three-dimensional measurement of the strain relief in a body of rock when isolated from the surrounding rock volume; the three-dimensional stress tensor can subsequently be calculated with a knowledge of the complete compliance tensor of the rock. There are two primary drawbacks with this technique which restricts its usefulness as a tectonic stress indicator: measurements must be made near a free surface, and strain relief is determined over very small areas (a few square millimetres to square centimetres). Furthermore, near surface measurements (by far the most common) have been shown to be subject to effects of local topography, rock anisotropy, and natural fracturing (Engelder and Sbar, 1984). In addition, many of these measurements have been made for specific engineering applications (e.g. dam site evaluation, mining work), places where topography, fracturing or nearby excavations could strongly perturb the regional stress field.'

Obviously, from a global or even a regional scale, the type of engineering stress measurements carried out in a mine or on a civil engineering site are not regarded as very reliable. Conversely, the World Stress Map versions presented in Figures 10.3 and 10.4 can only be used to give first order estimates of the stress directions which are likely to be encountered on a specific site. Since both stress directions and stress magnitudes are critically important in the design of underground excavations, it follows that a stress measuring programme is essential in any major underground mining or civil engineering project.

10.4 Developing a stress measuring programme

Consider the example of a tunnel to be driven a depth of 1,000 m below surface in a hard rock environment. The depth of the tunnel is such that it is probable that in situ and induced stresses will be an important consideration in the design of the excavation. Typical steps that could be followed in the analysis of this problem are:

a. During preliminary design, the information presented in equations 10.1, 10.2 and 10.3 can be used to obtain a first rough estimate of the vertical and average horizontal stress in the vicinity of the tunnel. For a depth of 1,000 m, these equations give the vertical stress $\sigma_v =$ 27 MPa , the ratio $k = 1.3$ (for $E_h = 75$ GPa) and hence the average horizontal stress $\sigma_h =$ 35.1 MPa. A preliminary analysis of the stresses induced around the proposed tunnel (as described later in this chapter) shows that these induced stresses are likely to exceed the strength of the rock and that the question of stress measurement must be considered in more detail. Note that for many openings in strong rock at shallow depth, stress problems may not be significant and the analysis need not proceed any further.
b. For this particular case, stress problems are considered to be important. A typical next step would be to search the literature in an effort to determine whether the results of in situ stress measurement programmes are available for mines or civil engineering projects within a radius of say 50 km of the site. With luck, a few stress measurement results will be available for the region in which the tunnel is located and these results can be used to refine the analysis discussed above.
c. Assuming that the results of the analysis of induced stresses in the rock surrounding the proposed tunnel indicate that significant zones of rock failure are likely to develop, and that support costs are likely to be high, it is probably

justifiable to set up a stress measurement project on the site. These measurements can be carried out in deep boreholes from the surface, using hydraulic fracturing techniques, or from underground access using overcoring methods. The choice of the method and the number of measurements to be carried out depends upon the urgency of the problem, the availability of underground access and the costs involved in the project. Note that very few project organisations have access to the equipment required to carry out a stress measurement project and, rather than purchase this equipment, it may be worth bringing in an organisation which has the equipment and which specialises in such measurements.

Where regional tectonic features such as major faults are likely to be encountered the in situ stresses in the vicinity of the feature may be rotated with respect to the regional stress field. The stresses may be significantly different in magnitude from the values estimated from the general trends described earlier. These differences can be very important in the design of the openings and in the selection of support and, where it is suspected that this is likely to be the case, in situ stress measurements become an essential component of the overall design process.

10.5 Analysis of induced stresses

When an underground opening is excavated into a stressed rock mass, the stresses in the vicinity of the new opening are re-distributed. Consider the example of the stresses induced in the rock surrounding a horizontal circular tunnel as illustrated in Figure 10.5, showing a vertical slice normal to the tunnel axis.

Before the tunnel is excavated, the in situ stresses σ_v, σ_{h1} and σ_{h2} are uniformly distributed in the slice of rock under consideration. After removal of the rock from within the tunnel, the stresses in the immediate vicinity of the tunnel are changed and new stresses are induced. Three principal stresses σ_1, σ_2 and σ_3 acting on a typical element of rock are shown in Figure 10.5.

The convention used in rock mechanics is that *compressive* stresses are always *positive* and the three principal stresses are numbered such that σ_1 is the largest and σ_3 is the smallest (algebraically) of the three.

The three principal stresses are mutually perpendicular, but they may be inclined to the direction of the applied in situ stress. This is evident in Figure 10.6, which shows the directions of the stresses in the rock surrounding a horizontal tunnel subjected to a horizontal in situ stress σ_{h1} equal to three times the vertical in situ stress σ_v. The longer bars in this figure represent the directions of the maximum principal stress σ_1, while the shorter bars give the directions of the minimum principal stress σ_3 at each element considered. In this particular case, σ_2 is coaxial with the in situ stress σ_{h2}, but the other principal stresses σ_1 and σ_3 are inclined to σ_{h1} and σ_v.
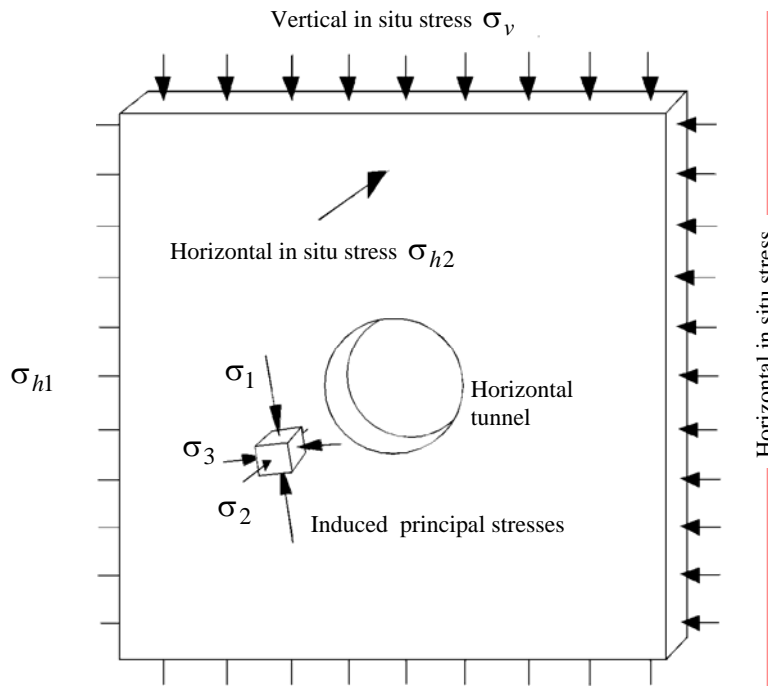
Figure 10.5: Illustration of principal stresses induced in an element of rock close to a horizontal tunnel subjected to a vertical in situ stress σ_v, a horizontal in situ stress σ_{h1} in a plane normal to the tunnel axis and a horizontal in situ stress σ_{h2} parallel to the tunnel axis.
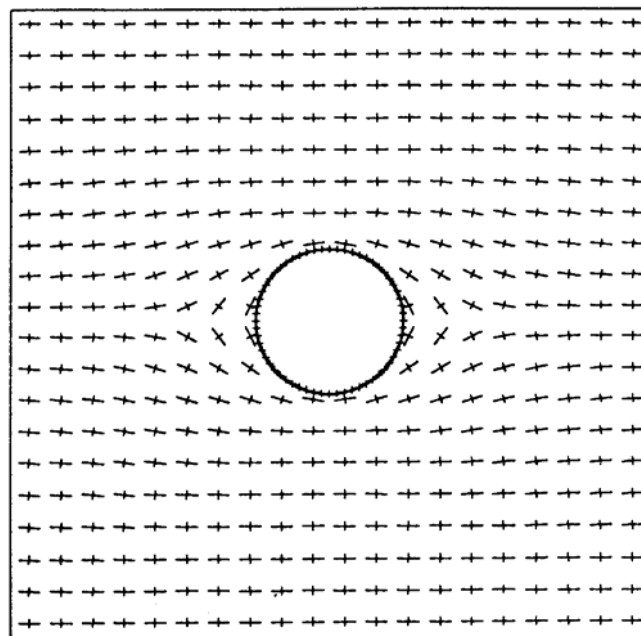
Figure 10.6: Principal stress directions in the rock surrounding a horizontal tunnel subjected to a horizontal in situ stress σ_{h1} equal to $3\sigma_v$, where σ_v is the vertical in situ stress.
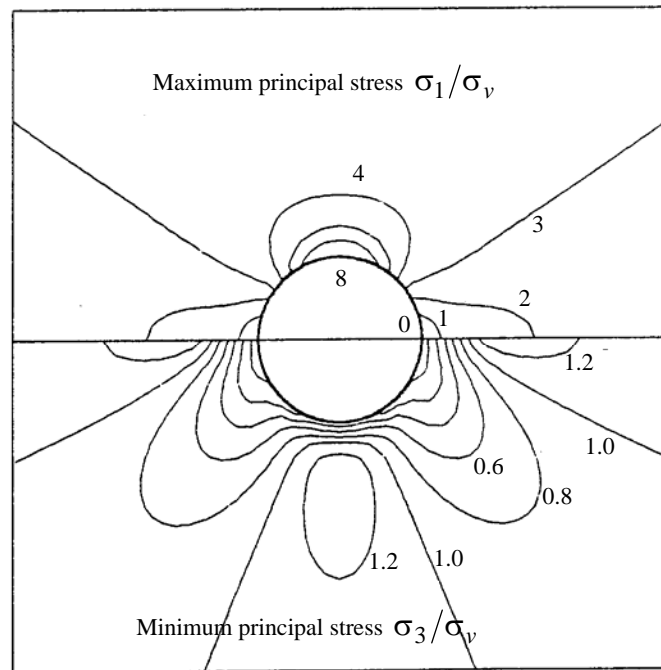
Figure 10.7: Contours of maximum and minimum principal stress magnitudes in the rock surrounding a horizontal tunnel, subjected to a vertical in situ stress of σ_v and a horizontal in situ stress of $3\sigma_v$.

Contours of the magnitudes of the maximum principal stress σ_1 and the minimum principal stress σ_3 are given in Figure 10.7. This figure shows that the redistribution of stresses is concentrated in the rock close to the tunnel and that, at a distance of say three times the radius from the centre of the hole, the disturbance to the in situ stress field is negligible.

An analytical solution for the stress distribution in a stressed elastic plate containing a circular hole was published by Kirsch (1898) and this formed the basis for many early studies of rock behaviour around tunnels and shafts.

Following along the path pioneered by Kirsch, researchers such as Love (1927), Muskhelishvili (1953) and Savin (1961) published solutions for excavations of various shapes in elastic plates. A useful summary of these solutions and their application in rock mechanics was published by Brown in an introduction to a volume entitled *Analytical and Computational Methods in Engineering Rock Mechanics* (1987).

Closed form solutions still possess great value for conceptual understanding of behaviour and for the testing and calibration of numerical models. For design purposes, however, these models are restricted to very simple geometries and material models. They are of limited practical value. Fortunately, with the development of computers, many powerful programs which provide numerical solutions to these problems are now readily available. A brief review of some of these numerical solutions is given below.

10.6 Numerical methods of stress analysis

Most underground excavations are irregular in shape and are frequently grouped close to other excavations. These groups of excavations can form a set of complex three-dimensional shapes. In addition, because of the presence of geological features such as faults and intrusions, the rock properties are seldom uniform within the rock volume of interest. Consequently, the closed form solutions described earlier are of limited value in calculating the stresses, displacements and failure of the rock mass surrounding underground excavations. Fortunately a number of computer-based numerical methods have been developed over the past few decades and these methods provide the means for obtaining approximate solutions to these problems.

Numerical methods for the analysis of stress driven problems in rock mechanics can be divided into two classes:

- *Boundary methods*, in which only the boundary of the excavation is divided into elements and the interior of the rock mass is represented mathematically as an infinite continuum.

- *Domain methods*, in which the interior of the rock mass is divided into geometrically simple elements each with assumed properties. The collective behaviour and interaction of these simplified elements model the more complex overall behaviour of the rock mass. *Finite element* and *finite difference* methods are domain techniques which treat the rock mass as a continuum. The *distinct element* method is also a domain method which models each individual block of rock as a unique element.

These two classes of analysis can be combined in the form of *hybrid models* in order to maximise the advantages and minimise the disadvantages of each method.

It is possible to make some general observations about the two types of approaches discussed above. In domain methods, a significant amount of effort is required to create the mesh that is used to divide the rock mass into elements. In the case of complex models, such as those containing multiple openings, meshing can become extremely difficult. The availability of highly optimised mesh-generators in many models makes this task much simpler than was the case when the mesh had to be created manually. In contrast, boundary methods require only that the excavation boundary be discretized and the surrounding rock mass is treated as an infinite continuum. Since fewer elements are required in the boundary method, the demand on computer memory and on the skill and experience of the user is reduced.

In the case of domain methods, the outer boundaries of the model must be placed sufficiently far away from the excavations in order that errors, arising from the interaction between these outer boundaries and the excavations, are reduced to an acceptable minimum. On the other hand, since boundary methods treat the rock mass as an infinite continuum, the far field conditions need only be specified as stresses acting on the entire rock mass and no outer boundaries are required. The main strength of boundary methods lies in the simplicity achieved by representing the rock mass as a continuum of infinite extent. It is this representation, however, that makes it difficult to incorporate variable material properties and the modelling of rock-support interaction. While techniques have been developed to allow some boundary element

modelling of variable rock properties, these types of problems are more conveniently modelled by domain methods.

Before selecting the appropriate modelling technique for particular types of problems, it is necessary to understand the basic components of each technique.

10.6.1   Boundary Element Method

The boundary element method derives its name from the fact that only the boundaries of the problem geometry are divided into elements. In other words, only the excavation surfaces, the free surface for shallow problems, joint surfaces where joints are considered explicitly and material interfaces for multi-material problems are divided into elements. In fact, several types of boundary element models are collectively referred to as 'the boundary element method'. These models may be grouped as follows:

1. Indirect (Fictitious Stress) method, so named because the first step in the solution is to find a set of fictitious stresses that satisfy prescribed boundary conditions. These stresses are then used in the calculation of actual stresses and displacements in the rock mass.

2. Direct method, so named because the displacements are solved directly for the specified boundary conditions.

3. Displacement Discontinuity method, so named because it represents the result of an elongated slit in an elastic continuum being pulled apart.

The differences between the first two methods are not apparent to the program user. The direct method has certain advantages in terms of program development, as will be discussed later in the section on Hybrid approaches.

The fact that a boundary element model extends 'to infinity' can also be a disadvantage. For example, a heterogeneous rock mass consists of regions of finite, not infinite, extent. Special techniques must be used to handle these situations. Joints are modelled explicitly in the boundary element method using the displacement discontinuity approach, but this can result in a considerable increase in computational effort. Numerical convergence is often found to be a problem for models incorporating many joints. For these reasons, problems, requiring explicit consideration of several joints and/or sophisticated modelling of joint constitutive behaviour, are often better handled by one of the domain methods such as finite elements.

A widely-used application of displacement discontinuity boundary elements is in the modelling of tabular ore bodies. Here, the entire ore seam is represented as a 'discontinuity' which is initially filled with ore. Mining is simulated by reduction of the ore stiffness to zero in those areas where mining has occurred, and the resulting stress redistribution to the surrounding pillars may be examined (Salamon, 1974, von Kimmelmann et al., 1984).

Further details on boundary element methods can be found in the book *Boundary element methods in solid mechanics* by Crouch and Starfield (1983).

10.6.2 *Finite element and finite difference methods*

In practice, the finite element method is usually indistinguishable from the finite difference method; thus, they will be treated here as one and the same. For the boundary element method, it was seen that conditions on a surface could be related to the state at *all* points throughout the remaining rock, even to infinity. In comparison, the finite element method relates the conditions at a few points within the rock (nodal points) to the state within a finite closed region formed by these points (the element). The physical problem is modelled numerically by dividing the entire problem region into elements.

The finite element method is well suited to solving problems involving heterogeneous or non-linear material properties, since each element explicitly models the response of its contained material. However, finite elements are not well suited to modelling infinite boundaries, such as occur in underground excavation problems. One technique for handling infinite boundaries is to discretize beyond the zone of influence of the excavation and to apply appropriate boundary conditions to the outer edges. Another approach has been to develop elements for which one edge extends to infinity i.e. so-called 'infinity' finite elements. In practice, efficient pre- and post-processors allow the user to perform parametric analyses and assess the influence of approximated far-field boundary conditions. The time required for this process is negligible compared to the total analysis time.

Joints can be represented explicitly using specific 'joint elements'. Different techniques have been proposed for handling such elements, but no single technique has found universal favour. Joint interfaces may be modelled, using quite general constitutive relations, though possibly at increased computational expense depending on the solution technique.

Once the model has been divided into elements, material properties have been assigned and loads have been prescribed, some technique must be used to redistribute any unbalanced loads and thus determine the solution to the new equilibrium state. Available solution techniques can be broadly divided into two classes - implicit and explicit. Implicit techniques assemble systems of linear equations that are then solved using standard matrix reduction techniques. Any material non-linearity is accounted for by modifying stiffness coefficients (secant approach) and/or by adjusting prescribed variables (initial stress or initial strain approach). These changes are made in an iterative manner such that all constitutive and equilibrium equations are satisfied for the given load state.

The response of a non-linear system generally depends upon the sequence of loading. Thus it is necessary that the load path modelled be representative of the actual load path experienced by the body. This is achieved by breaking the total applied load into load increments, each increment being sufficiently small, that solution convergence for the increment is achieved after only a few iterations. However, as the system being modelled becomes increasingly non-linear and the load increment represents an ever smaller portion of the total load, the incremental solution technique becomes similar to modelling the quasi-dynamic behaviour of the body, as it responds to gradual application of the total load.

In order to overcome this, a 'dynamic relaxation' solution technique was proposed (Otter et al., 1966) and first applied to geomechanics modelling by Cundall (1971). In this technique no matrices are formed. Rather, the solution proceeds explicitly -

unbalanced forces, acting at a material integration point, result in acceleration of the mass associated with the point; applying Newton's law of motion expressed as a difference equation yields incremental displacements; applying the appropriate constitutive relation produces the new set of forces, and so on marching in time, for each material integration point in the model. This solution technique has the advantage that both geometric and material non-linearities are accommodated, with relatively little additional computational effort as compared to a corresponding linear analysis, and computational expense increases only linearly with the number of elements used. A further practical advantage lies in the fact that numerical divergence usually results in the model predicting obviously anomalous physical behaviour. Thus, even relatively inexperienced users may recognise numerical divergence.

Most commercially available finite element packages use implicit (i.e. matrix) solution techniques. For linear problems and problems of moderate non-linearity, implicit techniques tend to perform faster than explicit solution techniques. However, as the degree of non-linearity of the system increases, imposed loads must be applied in smaller increments which implies a greater number of matrix re-formations and reductions, and hence increased computational expense. Therefore, highly non-linear problems are best handled by packages using an explicit solution technique.

10.6.3   Distinct Element Method

In ground conditions conventionally described as blocky (i.e. where the spacing of the joints is of the same order of magnitude as the excavation dimensions), intersecting joints form wedges of rock that may be regarded as rigid bodies. That is, these individual pieces of rock may be free to rotate and translate, and the deformation, that takes place at block contacts, may be significantly greater than the deformation of the intact rock, so that individual wedges may be considered rigid. For such conditions it is usually necessary to model many joints explicitly. However, the behaviour of such systems is so highly non-linear, that even a jointed finite element code, employing an explicit solution technique, may perform relatively inefficiently.

An alternative modelling approach is to develop data structures that represent the blocky nature of the system being analysed. Each block is considered a unique free body that may interact at contact locations with surrounding blocks. Contacts may be represented by the overlaps of adjacent blocks, thereby avoiding the necessity of unique joint elements. This has the added advantage that arbitrarily large relative displacements at the contact may occur, a situation not generally tractable in finite element codes.

Due to the high degree of non-linearity of the systems being modelled, explicit solution techniques are favoured for distinct element codes. As is the case for finite element codes employing explicit solution techniques, this permits very general constitutive modelling of joint behaviour with little increase in computational effort and results in computation time being only linearly dependent on the number of elements used. The use of explicit solution techniques places fewer demands on the skills and experience than the use of codes employing implicit solution techniques.

Although the distinct element method has been used most extensively in academic environments to date, it is finding its way into the offices of consultants, planners and designers. Further experience in the application of this powerful modelling tool to practical design situations and subsequent documentation of these case histories is

required, so that an understanding may be developed of where, when and how the distinct element method is best applied.

10.6.4   Hybrid approaches

The objective of a hybrid method is to combine the above methods in order to eliminate undesirable characteristics while retaining as many advantages as possible. For example, in modelling an underground excavation, most non-linearity will occur close to the excavation boundary, while the rock mass at some distance will behave in an elastic fashion. Thus, the near-field rock mass might be modelled, using a distinct element or finite element method, which is then linked at its outer limits to a boundary element model, so that the far-field boundary conditions are modelled exactly. In such an approach, the direct boundary element technique is favoured as it results in increased programming and solution efficiency.

Lorig and Brady (1984) used a hybrid model consisting of a discrete element model for the near field and a boundary element model for the far field in a rock mass surrounding a circular tunnel.

10.6.5   Two-dimensional and three-dimensional models

A two-dimensional model, such as that illustrated in Figure 10.5, can be used for the analysis of stresses and displacements in the rock surrounding a tunnel, shaft or borehole, where the length of the opening is much larger than its cross-sectional dimensions. The stresses and displacements in a plane, normal to the axis of the opening, are not influenced by the ends of the opening, provided that these ends are far enough away.

On the other hand, as an underground powerhouse of crusher chamber has a much more equi-dimensional shape and the effect of the end walls cannot be neglected. In this case, it is much more appropriate to carry out a three-dimensional analysis of the stresses and displacements in the surrounding rock mass. Unfortunately, this switch from two to three dimensions is not as simple as it sounds and there are relatively few good three-dimensional numerical models, which are suitable for routine stress analysis work in a typical mining environment.

EXAMINE3D[1] is a three-dimensional boundary element programs that provide a starting point for an analysis of a problem in which the three-dimensional geometry of the openings is important. Such three-dimensional analyses provide clear indications of stress concentrations and of the influence of three-dimensional geometry. In many cases, it is possible to simplify the problem to two-dimensions by considering the stresses on critical sections identified in the three-dimensional model.

More sophisticated three-dimensional finite element models such as VISAGE[2] are available, but are not particularly easy to use at the present time. In addition, definition of the input parameters and interpretation of the results of these models would stretch the capabilities of all but the most experienced modellers. It is probably best to leave this type of modelling in the hands of these specialists.

---

[1]Available from Available from Rocscience Inc., 31 Balsam Avenue, Toronto, Ontario, Canada M4E 3B5, Fax 1 416 698 0908, Phone 1 416 698 8217, Email: software@rocscience.com, Internet http://www.rocscience.com.
[2]Available from Vector International Processing Systems Ltd., Suites B05 and B06, Surrey House, 34 Eden Street, Kingston on Thames, KT1 1ER, England. Fax 44 81 541 4550, Phone 44 81 549 3444.

It is recommended that, where the problem being considered is obviously three-dimensional, a preliminary elastic analysis be carried out by means of one of the three-dimensional boundary element programs. The results can then be used to decide whether further three-dimensional analyses are required or whether appropriate two-dimensional sections can be modelled using a program such as PHASE^2, described in the following section.

10.6.6   Stress analysis using the program PHASE^2

In order to meet the requirements of modelling the post-failure behaviour of rock masses and the interaction of these rocks with support, a two-dimensional finite element model called PHASE^2 [3] was developed by the Rock Engineering Group in the Department of Civil Engineering at the University of Toronto. This program is very powerful but user-friendly and it will generally meet the needs of most underground excavation design projects. More sophisticated analyses such as those involving thremal stresses, fluid flow or dynamic loading will require the use of more powerful software such as the program FLAC[4].

The capability of the program PHASE^2 is best demonstrated by a practical example such as that presented below.

10.7   Practical example of two-dimensional stress analysis

The details included in this example, based upon an actual case, are as follows:

A spillway tunnel for an embankment dam is to be constructed in a poor quality sandstone. The excavated diameter of the tunnel is about 13 m and the cover over the roof is 8 m. The tunnel is to have a 1.3 m thick un-reinforced concrete lining and, after placement of this lining, a 28 m high portion of the rockfill dam will be constructed over the tunnel.

The questions to be addressed are:

1. What support is required in order to excavate the tunnel safely under the very shallow cover?
2. Is the proposed top heading and bench excavation sequence, using drill and blast methods, appropriate for this tunnel?
3. How will the concrete lining respond to the loading imposed by the placement of 28 m of rockfill over the tunnel?

In order to answer these questions a series of two-dimensional finite element analyses were carried using the program PHASE^2. The first of these analyses examined the stability and support requirements for the top heading excavation. The final analysis included the entire excavation and support sequence and the placement of the rockfill over the tunnel. The complete finite element model is illustrated in Figure 10.8. An enlarged view of the excavation and the final support system is given in Figure 10.9.

---

[3]Available from Rocscience Inc., 31 Balsam Avenue, Toronto, Ontario, Canada M4E 3B5, Fax 1 416 698 0908, Phone 1 416 698 8217, Email: software@rocscience.com, Internet http://www.rocscience.com.
[4] Available from ITASCA Consulting Group Inc., Thresher Square East, 708 South Third Street, Suite 310, Minneapolis, Minnesota 55415, USA, Fax 1 612 371 4717
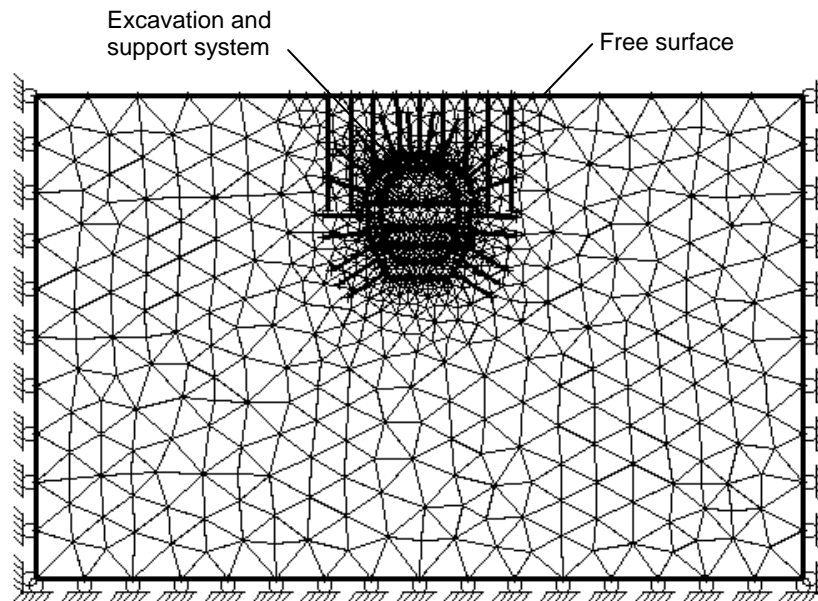
Figure 10.8: Finite element model showing mesh geometry and boundary conditions. The final support system used for this case is also shown and will be discussed in the text which follows.
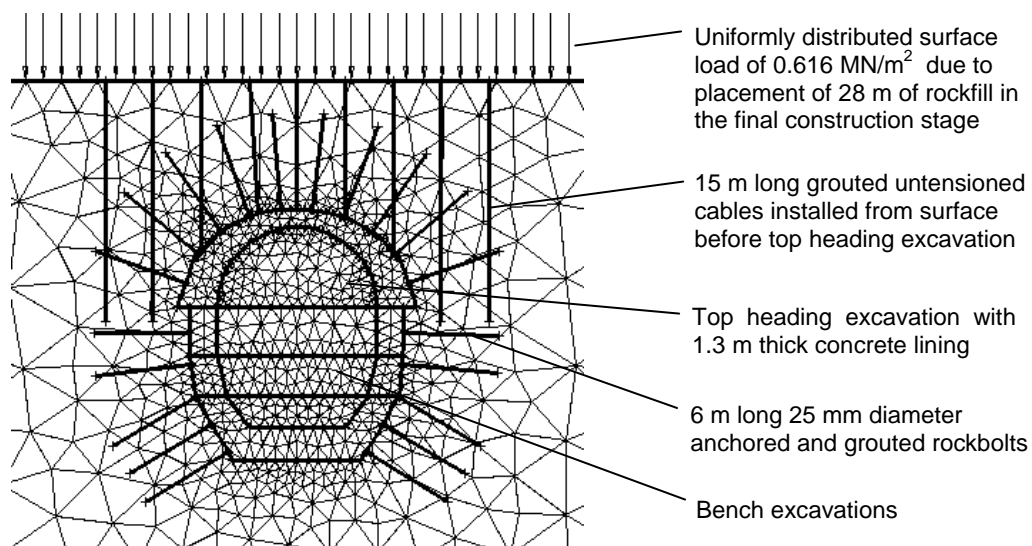
Figure 10.9: Details of the finite element mesh , excavation sequence, support system and external load for the complete model.

The rock mass is a poor quality sandstone that, being close to surface, is heavily jointed. The mechanical properties[5] assumed for this rock mass are a cohesive strength $c = 0.04$ MPa, a friction angle $\phi = 40°$ and a modulus of deformation $E = 1334$ MPa. No in situ stress measurements are available but, because of the location of the tunnel in the valley side, it has been assumed that the horizontal stress normal to the tunnel axis has been reduced by stress relief. The model is loaded by gravity and a ratio of horizontal to vertical stress of 0.5 is assumed.

10.7.1 Analysis of top heading stability

A simplified version of the model illustrated in Figures 10.8 and 10.9 was used to analyse the stability and support requirements for the top heading. This model did excluded the concrete lining and the bench excavations.

The first model was used to examine the conditions for a full-face excavation of the top heading without any support. This is always a useful starting point in any tunnel support design study since it gives the designer a clear picture of the magnitude of the problems that have to be dealt with.

The model was loaded in two stages. The first stage involved the model without any excavations and this was created by assigning the material within the excavation boundary the properties of the surrounding rock mass. This first stage is carried out in order to allow the model to consolidate under gravitational loading It is required in order to create a reference against which subsequent displacements in the model can be measured.

The results of the analysis are illustrated in Figure 10.10, that shows the extent of yield in the rock mass surrounding the top heading, and Figure 10.11 that shows the induced displacements around the tunnel.

The large amount of yield in the rock mass overlying the top heading suggests that this excavation will be unstable without support. This view is supported by the displacements shown in Figure 10.11.
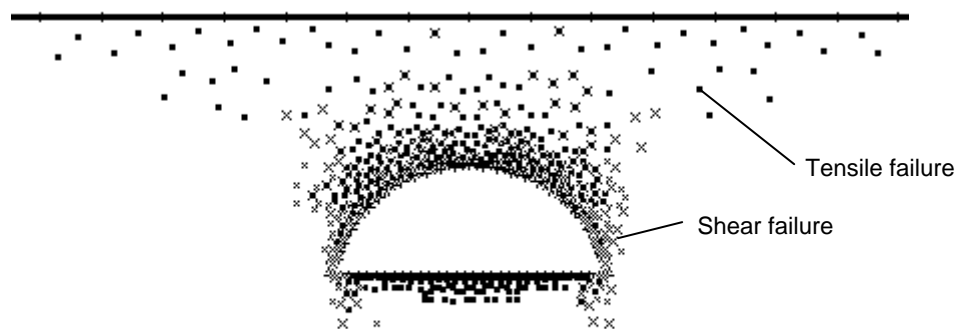
Figure 10.10: Yield in the rock mass surrounding the top heading excavation with no support installed.

---

[5] A full discussion on methods for estimating rock mass properties is given in Chapter 11.
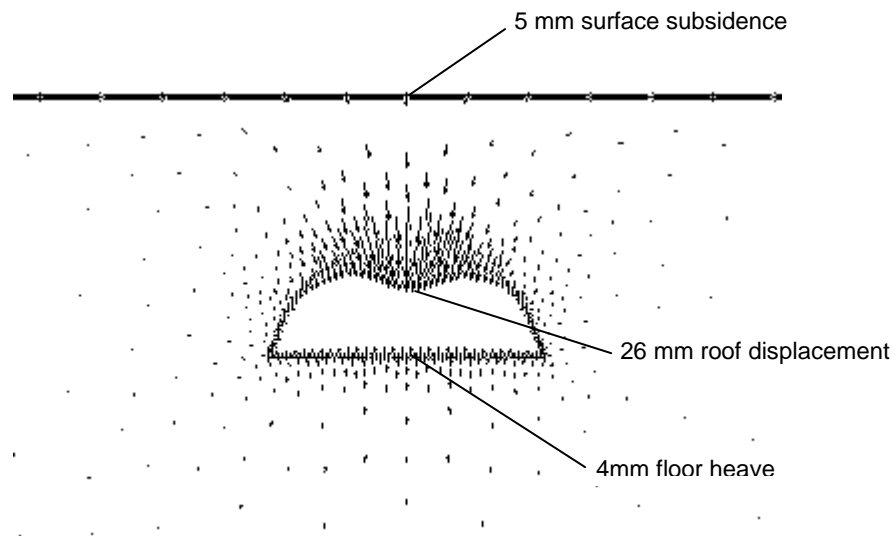
Figure 10.11: Displacements induced in the rock mass by the excavation of an unsupported top heading.

The reader may be surprised that the displacement in the roof of the tunnel is only 26 mm when the extent of the yield zone suggests complete collapse of the roof. It has to be remembered that PHASE^2 is a small strain finite element model and that it cannot accommodate the very large strains associated with the complete collapse of a tunnel. In examining Figure 10.11 it is more important to look at the shape of the overall displacement profile than the magnitude of the displacements. A rock mass will not tolerate the differential displacements illustrated and progressive ravelling leading to ultimate collapse would almost certainly result from the excavation of an unsupported top heading.

A general rule of thumb used by experienced tunnellers is that an underground excavation will not be self-supporting unless the cover over the tunnel exceeds 1½ times the span of the opening. This is a typical situation that occurs when excavating tunnel portals and there are several options available for dealing with the problem.

One of these options is to use a shotcrete lining to stabilise the rock mass above the tunnel. A finite element analysis of this option shows that a 50 mm thick layer of fully hardened shotcrete (uniaxial compressive strength of 30 MPa) is sufficient to stabilise the tunnel. The problem is how to get a fully hardened layer of shotcrete into an advancing tunnel heading. A second problem is whether the workers would have sufficient confidence in such a solution to work in the tunnel.

One project on which this solution was used was the construction of an 8 m span diversion tunnel for a dam. The rock mass was a very weakly cemented limestone that could be excavated by hand but which had sufficient strength that it was marginally self-supporting. The Scandinavian contractor on the project had used shotcrete for many years and the very experienced tunnellers had complete confidence in working under a cover of shotcrete. The tunnel was not on the critical path of the project and so construction could proceed at a sufficiently slow pace to allow the shotcrete to set before the next advance. A layer of un-reinforced shotcrete

was the sole support used in this tunnel, with occasional steel sets embedded in the shotcrete where ground conditions were particularly difficult.

In the case of the top heading in sandstone under consideration here, the shotcrete solution was rejected because, in spite of the finite element analysis, the designers did not have sufficient confidence in the ability of the shotcrete layer to support the large span of blocky sandstone. In addition, the contractor on this dam project did not have a great deal of experience in using shotcrete in tunnels and it was unlikely that the workers would have been prepared to operate under a cover of shotcrete only.

Another alternative that is commonly used in excavating tunnel portals is to use steel sets to stabilise the initial portion of the tunnel under low cover. This solution works well in the case of small tunnels but, in this case, a 13 m span tunnel would require very heavy sets. An additional disadvantage in this case is that the installation of sets would permit too much deformation in the rock mass. This is because the steel sets are a passive support system and they only carry a load when the rock mass has deformed onto the sets. Since this tunnel is in the foundation of a dam, excessive deformation is clearly not acceptable because of the additional leakage paths which would be created through the rock mass.

The solution finally adopted was 'borrowed' from the mining industry where un-tensioned fully grouted dowels are frequently used to pre-support the rock mass above underground excavations. In this case, a pattern 3 m x 3 m pattern of 15 m long 60 ton capacity cables were installed from the ground surface before excavation of the top heading was commenced. When these cables were exposed in the excavation, face plates were attached and the excess cable length was cut off. In addition a 2 m x 2 m pattern of 6 m long mechanically anchored rockbolts were installed radially from the roof of the top heading.

The results of an analysis of this support system are illustrated in Figures 10.12 and 10.13 which show the extent of the yield zone and the deformations in the rock mass above the top heading.
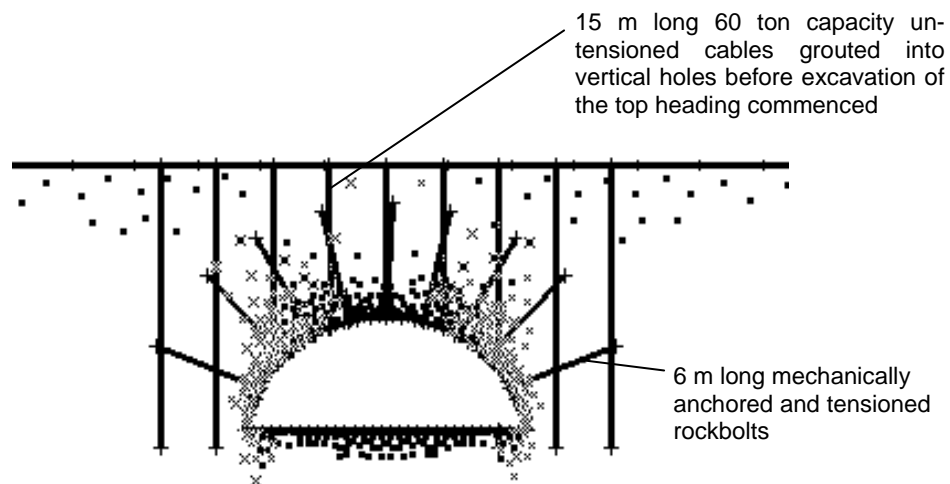
Figure 10.12: Yield zone in the rock mass surrounding the top heading supported by meand of pre-placed grouted cabled and mechanically anchored and tensioned rockbolts.
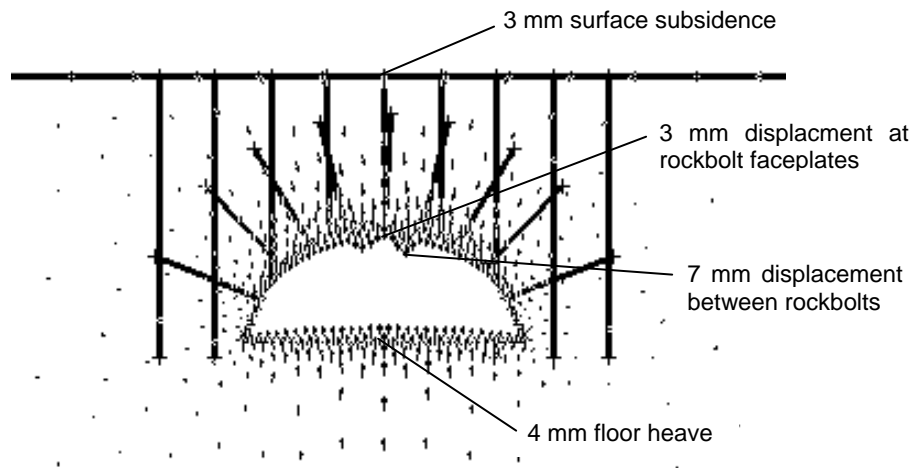
Figure 10.13: Displacements in the rock mass supported by means of pre-placed grouted cables and tensioned rockbolts.

Comparing Figures 10.10 and 10.12 shows that that the extet of the yield zone is only reduced by a small amount by the installation of the support system. This is not surprising since some deformation of the rock mass is required in order to mobilise the supporting loads in the untensioned cables. This deformation occurs as a reullt of failure of the rock mass.

Figure 10.13 shows that the displacements in the roof of the top heading have been reduced substantially as a result of the placement of the support. However, a small problem remains and that is the excessive displacement of the rock between the rockbolt faceplates which are spaced on a 2 m x 2 m grid. Unless this displacement is controlled it can lead to progressive ravelling of the rock mass.

Only a small surface pressure is required to control this ravelling and this could be achieved by means of a layer of mesh or shotcrete of by the installation of light steel sets. In this case the latter soltion was adopted because of the sense of security which these gave for the workers in the tunnel. The appearance of the supported top heading is illustrated in Figure 10.14.

Figure 11.14: Top heading supported by cables and rock-bolts and light steel sets.

10.7.2   *Analysis of complete excavation*

Having successfully excavated the top heading of this spillway tunnel, as discussed in the previous section, the next question was how the excavation would behave during benching down and how the concrete lining would tolerate the additional loads imposed by the placement of 28 m of compacted rock fill.

The complete model, illustrated in Figure 10.9, was used for this investigation and it was found that there were no problems with the excavation of the benches. Figures 10.15 and 10.16 illustrate the yield zone and the displacements of the rock mass surrounding the complete excavation supported by means of cables and rockbolts and, for the purposes of this study, a thin shotcrete lining.
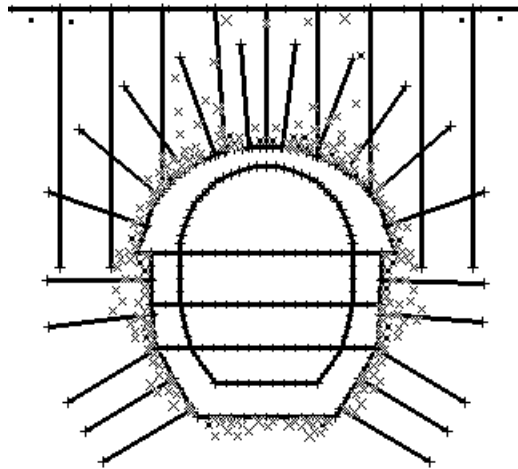
Figure 10.15: Extent of yield in the rock mass surrounding the complete spillway tunnel excavation before placement of the concrete lining.
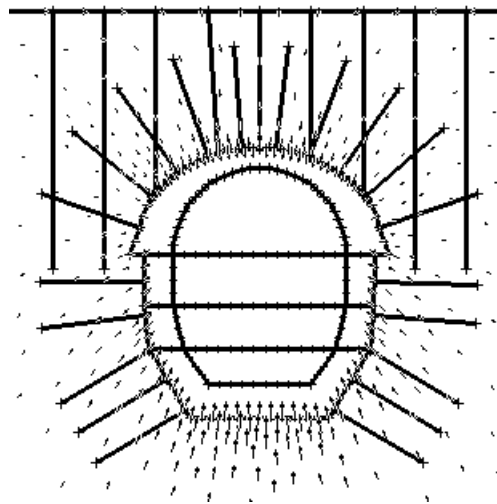
Figure 10.16: Displacements in the rock mass surrounding the complete spillway tunnel excavation. The maximum displacements in the centre of the roof and the centre of the floor are both 5 mm.

The self-weight of the concrete lining induces displacements in the rock mass and these are increased by the imposition of the surface load due to the placement of 28 m of compacted rockfill above the tunnel. The induced displacements are illustrated in Figures 10.17 amd 10.18.
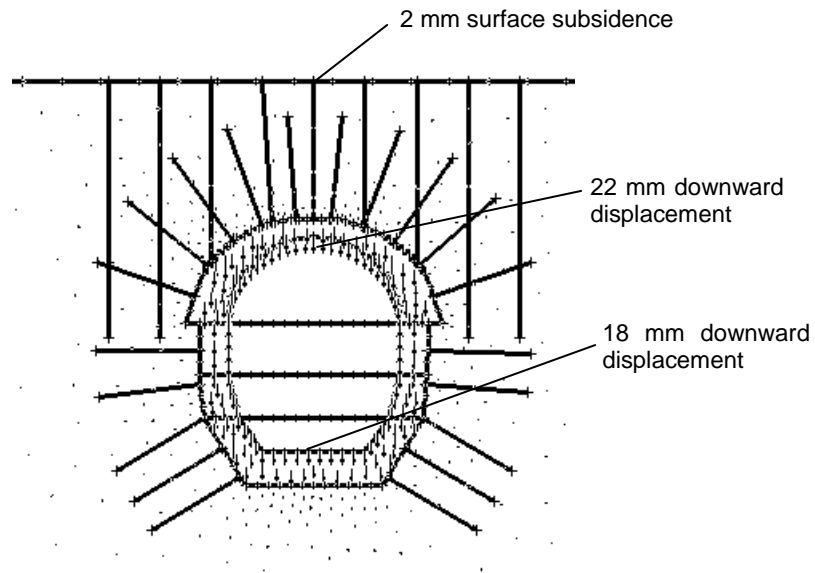
Figure 10.17: Displacements induced as a result of the self-weight of the concrete lining.
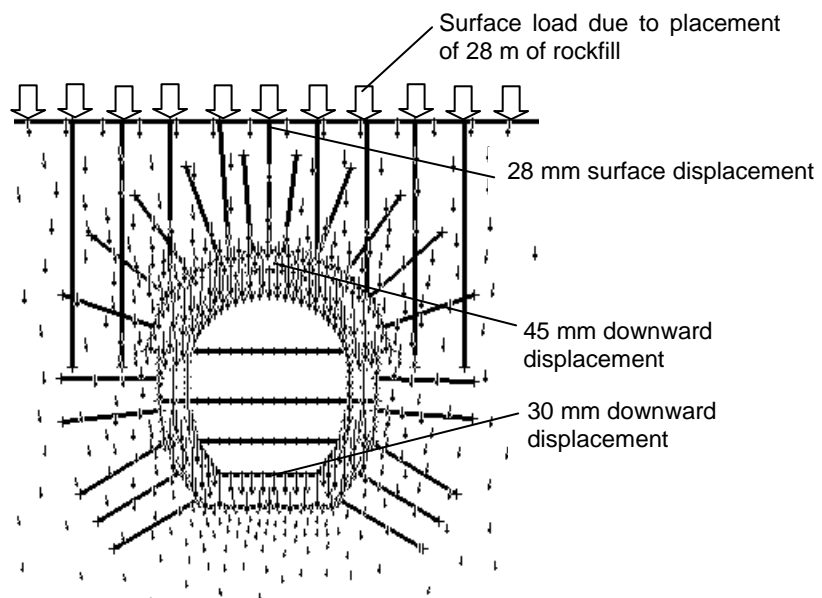
Figure 10.18: Displacements induced as a result of the placement of 28 m of rockfill above the completed tunnel.

Figures 10.17 and 10.18 show that significant displacements are induced as a result of the casting of the concrete lining and the subsequent placement of the rockfill above the tunnel. No failure of the concrete lining was shown by this analysis, in spite of the assumption of a very weak concrete (10 MPa uniaxial compressive strength). The only problem that could be anticipated from the placement of the rockfill was the possibility of bending of the entire length of the concrete lining and the formation of tensile cracks normal to the tunnel axis. It was therefore recommended that the concrete lining be carefully inspected for such cracks after the completion of the rockfill. Repair of such cracks by dental concrete and grouting would not be a major problem but, in any case, it proved not to be necessary.

10.7.3   Conclusion

The analysis presented on the preceding pages is intended to demonstrate how a numerical analysis should be used as a tool to aid designers. In all cases, practical issues take precedence and the results of the analysis should only be used to guide the practical decisions and to clarify matters of doubt or uncertainty. Given the assumptions that have to be made in the construction for an analysis of this type, it would be very unwise for the designer to place too much credence in the results of the analysis and to allow all his or her decisions to be driven by these results.

A discussion of the results with an experienced tunnel contractor will soon dispel any misconceptions that the tunnel designer will have acquired as the results of such a theoretical analysis and such a discussion is an essential part of any practical design process.

11

Rock mass properties

11.1 Introduction

Reliable estimates of the strength and deformation characteristics of rock masses are required for almost any form of analysis used for the design of slopes, foundations and underground excavations. Hoek and Brown (1980a, 1980b) proposed a method for obtaining estimates of the strength of jointed rock masses, based upon an assessment of the interlocking of rock blocks and the condition of the surfaces between these blocks. This method was modified over the years in order to meet the needs of users who were applying it to problems that were not considered when the original criterion was developed (Hoek 1983, Hoek and Brown 1988). The application of the method to very poor quality rock masses required further changes (Hoek, Wood and Shah 1992) and, eventually, the development of a new classification called the Geological Strength Index (Hoek, Kaiser and Bawden 1995, Hoek 1995, Hoek and Brown 1997). A review of the development of the criterion and of the equations proposed at various stages in this development is given in Hoek and Brown (1997).

This chapter presents the Hoek-Brown criterion in a form that has been found practical in the field and that appears to provide the most reliable set of results for use as input for methods of analysis in current use in rock engineering.

11.2 Generalised Hoek-Brown criterion

The Generalised Hoek-Brown failure criterion for jointed rock masses is defined by:

$$\sigma_1' = \sigma_3' + \sigma_{ci}\left(m_b \frac{\sigma_3'}{\sigma_{ci}} + s \right)^a \tag{11.1}$$

where σ_1' and σ_3' are the maximum and minimum effective stresses at failure,

m_b is the value of the Hoek-Brown constant m for the rock mass,

s and a are constants which depend upon the rock mass characteristics, and

σ_{ci} is the uniaxial compressive strength of the intact rock pieces.

The Mohr envelope, relating normal and shear stresses, can be determined by the method proposed by Hoek and Brown (1980a). In this approach, equation 11.1 is used to generate a series of triaxial test values, simulating full scale field tests, and a

statistical curve fitting process is used to derive an equivalent Mohr envelope defined by the equation:

$$\tau = A\sigma_{ci}\left(\frac{\sigma_n' - \sigma_{tm}}{\sigma_{ci}}\right)^B \tag{11.2}$$

where *A* and *B* are material constants

σ_n' is the normal effective stress, and

σ_{tm} is the 'tensile' strength of the rock mass.

This 'tensile' strength, which reflects the interlocking of the rock particles when they are not free to dilate, is given by:

$$\sigma_{tm} = \frac{\sigma_{ci}}{2}\left(m_b - \sqrt{m_b^2 + 4s}\right) \tag{11.3}$$

In order to use the Hoek-Brown criterion for estimating the strength and deformability of jointed rock masses, three 'properties' of the rock mass have to be estimated. These are

1. the uniaxial compressive strength σ_{ci} of the intact rock pieces,
2. the value of the Hoek-Brown constant m_i for these intact rock pieces, and
3. the value of the Geological Strength Index *GSI* for the rock mass.

11.3   Intact rock properties

For the intact rock pieces that make up the rock mass equation 11.1 simplifies to:

$$\sigma_1' = \sigma_3' + \sigma_{ci}\left(m_i\frac{\sigma_3'}{\sigma_{ci}} + 1\right)^{0.5} \tag{11.4}$$

The relationship between the principal stresses at failure for a given rock is defined by two constants, the uniaxial compressive strength σ_{ci} and a constant m_i. Wherever possible the values of these constants should be determined by statistical analysis of the results of a set of triaxial tests on carefully prepared core samples.

Note that the range of minor principal stress (σ_3') values over which these tests are carried out is critical in determining reliable values for the two constants. In deriving the original values of σ_{ci} and m_i, Hoek and Brown (1980a) used a range of $0 < \sigma_3'$ $< 0.5\sigma_{ci}$ and, in order to be consistent, it is essential that the same range be used in any laboratory triaxial tests on intact rock specimens. At least five data points should be included in the analysis.

One type of triaxial cell that can be used for these tests is illustrated in Figure 11.1. This cell, described by Hoek and Franklin (1968), does not require draining between tests and is convenient for the rapid testing or a large number of specimens. More sophisticated cells are available for research purposes but the results obtained from

the cell illustrated in Figure 11.1 are adequate for the rock strength estimates required for estimating σ_{ci} and m_i. This cell has the additional advantage that it can be used in the field when testing materials such as coals, shales and phyllites that are extremely difficult to preserve during transportation and normal specimen preparation for laboratory testing.
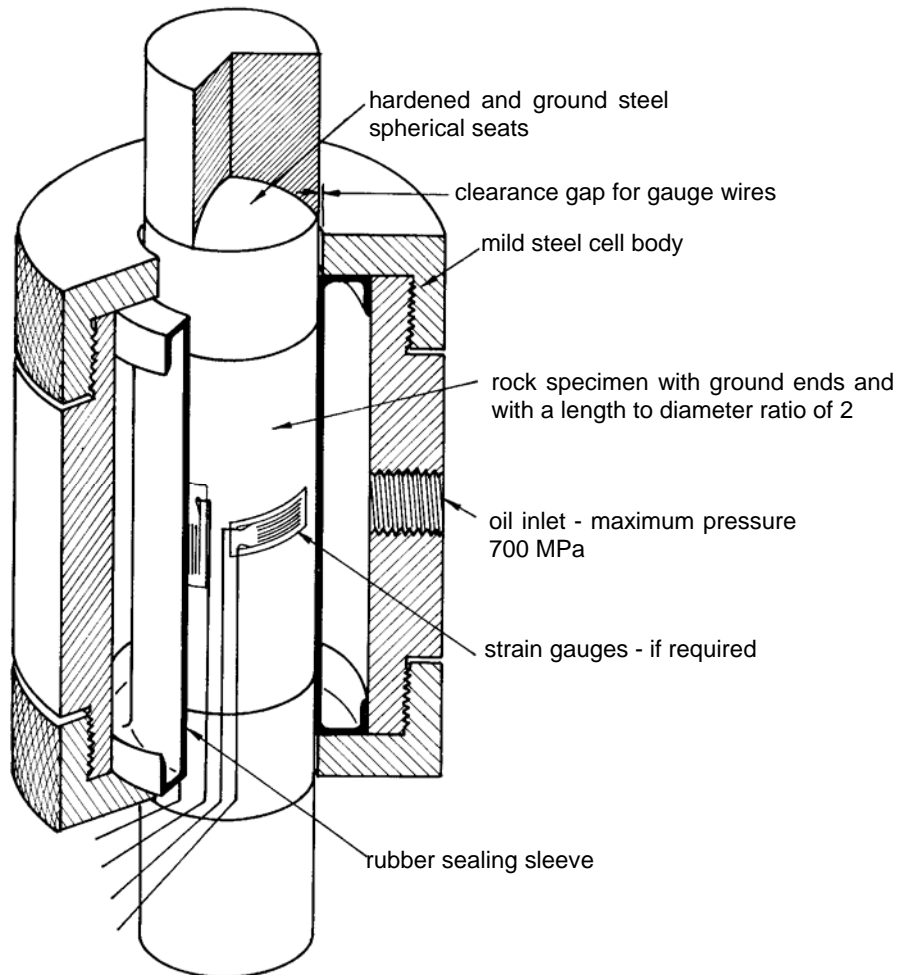
Figure 11.1:   Cut-away view of a triaxial cell for testing rock specimens.

Laboratory tests should be carried out at moisture contents as close as possible to those which occur in the field. Many rocks show a significant strength decrease with increasing moisture content and tests on samples, which have been left to dry in a core shed for several months, can give a misleading impression of the intact rock strength.

   Once the five or more triaxial test results have been obtained, they can be analysed to determine the uniaxial compressive strength σ_{ci} and the Hoek-Brown constant m_i as described by Hoek and Brown (1980a). In this analysis, equation 11.1 is re-written in the form:

$$y = m\sigma_{ci}x + s\sigma_{ci} \tag{11.5}$$

where $x = \sigma_3^{'}$ and $y = (\sigma_1^{'} - \sigma_3^{'})^2$

For *n* specimens the uniaxial compressive strength σ_{ci}, the constant m_i and the coefficient of determination r^2 are calculated from:

$$\sigma_{ci}^2 = \frac{\sum y}{n} - \left[\frac{\sum xy - (\sum x \sum y/n)}{\sum x^2 - ((\sum x)^2/n)} \right] \frac{\sum x}{n} \tag{11.6}$$

$$m_i = \frac{1}{\sigma_{ci}} \left[\frac{\sum xy - (\sum x \sum y/n)}{\sum x^2 - ((\sum x)^2/n)} \right] \tag{11.7}$$

$$r^2 = \frac{\left[\sum xy - (\sum x \sum y/n)\right]^2}{[\sum x^2 - (\sum x)^2/n][\sum y^2 - (\sum y)^2/n]} \tag{11.8}$$

A spreadsheet for the analysis of triaxial test data is given in Table 11.1. Note that high quality triaxial test data will usually give a coefficient of determination r^2 of greater than 0.9.

When laboratory tests are not possible, Table 11.2 and Table 11.3 can be used to obtain estimates of σ_{ci} and m_i.

Short-term laboratory tests on very hard brittle rocks tend to overestimate the in situ rock mass strength. Laboratory tests and field studies on excellent quality Lac du Bonnet granite, reported by Martin and Chandler (1994), show that the in situ strength of this rock is only about 70% of that measured in the laboratory. This appears to be due to damage resulting from micro-cracking of the rock which initiates and develops critical intensities at lower stress levels in the field than in laboratory tests carried out at higher loading rates on smaller specimens. Hence, when analysing the results of laboratory tests on these types of rocks to estimate the values of σ_{ci} and m_i, it is prudent to reduce the values of the major effective principal stress at failure to 70% of the measured values.

Anisotropic and foliated rocks such as slates, schists and phyllites, the behaviour of which is dominated by closely spaced planes of weakness, cleavage or schistosity, present particular difficulties in the determination of the uniaxial compressive strengths.

Salcedo (1983) has reported the results of a set of directional uniaxial compressive tests on a graphitic phyllite from Venezuela. These results are summarised in Figure 11.2. It will be noted that the uniaxial compressive strength of this material varies by a factor of about 5, depending upon the direction of loading. Evidence of the behaviour of this graphitic phyllite in the field suggests that the rock mass properties are dependent upon the strength parallel to schistosity rather than that normal to it.

Table 11.1: Spreadsheet for the calculation of σ_{ci} and m_i from triaxial test data

---

Triaxial test data

x		y	xy	xsq	ysq
sig3	sig1				
0	38.3	1466.89	0.0	0.0	2151766
5	72.4	4542.76	22713.8	25.0	20636668
7.5	80.5	5329.00	39967.5	56.3	28398241
15	115.6	10120.36	151805.4	225.0	102421687
20	134.3	13064.49	261289.8	400.0	170680899
47.5	441.1	34523.50	475776.5	706.3	324289261
sumx		sumy	sumxy	sumxsq	sumysq

Calculation results

Number of tests	n =	5
Uniaxial strength	sigci =	37.4
Hoek-Brown constant	mi =	15.50
Hoek-Brown constant	s =	1.00
Coefficient of determination	r2 =	0.997

Cell formulae

y = (sig1-sig3)^2
sigci = SQRT(sumy/n - (sumxy-sumx*sumy/n)/(sumxsq-(sumx^2)/n)*sumx/n)
mi = (1/sigci)*((sumxy-sumx*sumy/n)/(sumxsq-(sumx^2)/n))
r2 = ((sumxy-(sumx*sumy/n))^2)/((sumxsq-(sumx^2)/n)*(sumysq-(sumy^2)/n))
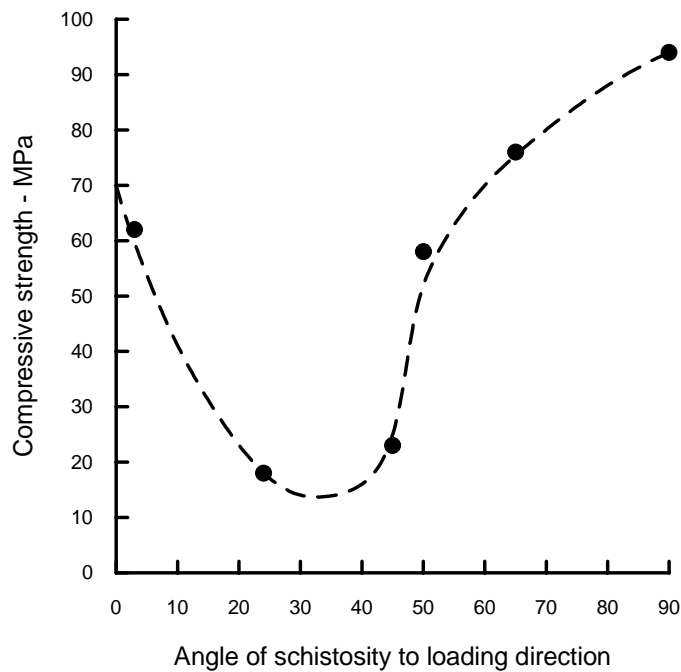
Figure 11.2: Influence of loading direction on the strength of graphitic phyllite tested by Salcedo (1983).

Table 11.2: Field estimates of uniaxial compressive strength.

Grade*	Term	Uniaxial Comp. Strength (MPa)	Point Load Index (MPa)	Field estimate of strength	Examples
R6	Extremely Strong	> 250	>10	Specimen can only be chipped with a geological hammer	Fresh basalt, chert, diabase, gneiss, granite, quartzite
R5	Very strong	100 - 250	4 - 10	Specimen requires many blows of a geological hammer to fracture it	Amphibolite, sandstone, basalt, gabbro, gneiss, granodiorite, limestone, marble, rhyolite, tuff
R4	Strong	50 - 100	2 - 4	Specimen requires more than one blow of a geological hammer to fracture it	Limestone, marble, phyllite, sandstone, schist, shale
R3	Medium strong	25 - 50	1 - 2	Cannot be scraped or peeled with a pocket knife, specimen can be fractured with a single blow from a geological hammer	Claystone, coal, concrete, schist, shale, siltstone
R2	Weak	5 - 25	**	Can be peeled with a pocket knife with difficulty, shallow indentation made by firm blow with point of a geological hammer	Chalk, rocksalt, potash
R1	Very weak	1 - 5	**	Crumbles under firm blows with point of a geological hammer, can be peeled by a pocket knife	Highly weathered or altered rock
R0	Extremely weak	0.25 - 1	**	Indented by thumbnail	Stiff fault gouge

* Grade according to Brown (1981).
** Point load tests on rocks with a uniaxial compressive strength below 25 MPa are likely to yield highly ambiguous results.

Table 11.3: Values of the constant m_i for intact rock, by rock group. Note that values in parenthesis are estimates.

Rock type	Class	Group	Texture			
			Coarse	Medium	Fine	Very fine
SEDIMENTARY	Clastic		Conglomerate (22)	Sandstone 19	Siltstone 9	Claystone 4
			——— Greywacke ——— (18)			
	Non-Clastic	Organic	——— Chalk ——— 7			
			——— Coal ——— (8-21)			
		Carbonate	Breccia (20)	Sparitic Limestone (10)	Micritic Limestone 8	
		Chemical		Gypstone 16	Anhydrite 13	
METAMORPHIC	Non Foliated		Marble 9	Hornfels (19)	Quartzite 24	
	Slightly foliated		Migmatite (30)	Amphibolite 25 - 31	Mylonites (6)	
	Foliated*		Gneiss 33	Schists 4 - 8	Phyllites (10)	Slate 9
IGNEOUS	Light		Granite 33		Rhyolite (16)	Obsidian (19)
			Granodiorite (30)		Dacite (17)	
	Dark		Diorite (28)		Andesite 19	
			Gabbro 27	Dolerite (19)	Basalt (17)	
			Norite 22			
	Extrusive pyroclastic type		Agglomerate (20)	Breccia (18)	Tuff (15)	

* These values are for intact rock specimens tested normal to bedding or foliation. The value of m_i will be significantly different if failure occurs along a weakness plane.

In deciding upon the value of σ_{ci} for foliated rocks, a decision has to be made on whether to use the highest or the lowest uniaxial compressive strength obtained from

results such as those given in Figure 11.1. Mineral composition, grain size, grade of metamorphism and tectonic history all play a role in determining the characteristics of the rock mass. The author cannot offer any precise guidance on the choice of σ_{ci} but suggest that the maximum value should be used for hard, well interlocked rock masses such as good quality slates. The lowest uniaxial compressive strength should be used for tectonically disturbed, poor quality rock masses such as the graphitic phyllite tested by Salcedo (1983).

Unlike other rocks, coal is organic in origin and therefore has unique constituents and properties. Unless these properties are recognised and allowed for in characterising the coal, the results of any tests will exhibit a large amount of scatter. Medhurst, Brown and Trueman (1995) have shown that, by taking into account the 'brightness' which reflects the composition and the cleating of the coal, it is possible to differentiate between the mechanical characteristics of different coals.

11.4 Influence of sample size

The influence of sample size upon rock strength has been widely discussed in geotechnical literature and it is generally assumed that there is a significant reduction in strength with increasing sample size. Based upon an analysis of published data, Hoek and Brown (1980a) have suggested that the uniaxial compressive strength σ_{cd} of a rock specimen with a diameter of d mm is related to the uniaxial compressive strength σ_{c50} of a 50 mm diameter sample by the following relationship:

$$\sigma_{cd} = \sigma_{c50}\left(\frac{50}{d}\right)^{0.18}$$

(11.9)

This relationship, together with the data upon which it was based, is illustrated in Figure 11.3.

The author suggests that the reduction in strength is due to the greater opportunity for failure through and around grains, the 'building blocks' of the intact rock, as more and more of these grains are included in the test sample. Eventually, when a sufficiently large number of grains are included in the sample, the strength reaches a constant value.

Medhurst and Brown (1996) have reported the results of laboratory triaxial tests on samples of 61, 101, 146 and 300 mm diameter samples of a highly cleated mid-brightness coal from the Moura mine in Australia. The results of these tests are summarised in Table 11.4 and Figure 11.4.

The results obtained by Medhurst and Brown show a significant decrease in strength with increasing sample size. This is attributed to the effects of cleat spacing. For this coal, the persistent cleats are spaced at 0.3 to 1.0 m while non-persistent cleats within vitrain bands and individual lithotypes define blocks of 1 cm or less. This cleating results in a 'critical' sample size of about 1 m above which the strength remains constant.

It is reasonable to extend this argument further and to suggest that, when dealing with large scale rock masses, the strength will reach a constant value when the size of individual rock pieces is sufficiently small in relation to the overall size of the

structure being considered. This suggestion is embodied in Figure 11.5 which shows the transition from an isotropic intact rock specimen, through a highly anisotropic rock mass in which failure is controlled by one or two discontinuities, to an isotropic heavily jointed rock mass.
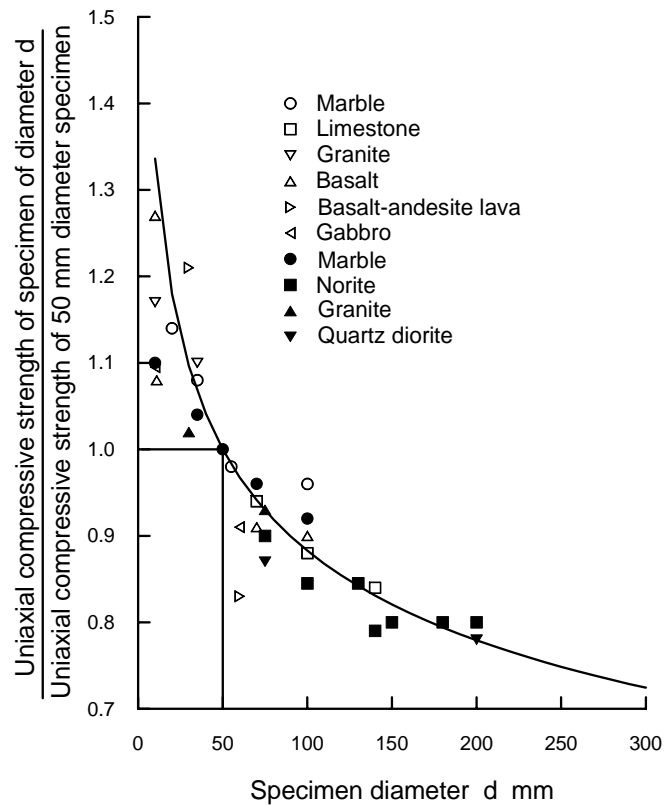
Figure 11.3 Influence of specimen size on the strength of intact rock. After Hoek and Brown (1980a).

Table11.4 Peak strength of Moura DU coal in terms of the parameters contained in equation (11.1) based upon a value of $\sigma_{ci} = 32.7$ MPa.

Dia.(mm)	m_b	s	a
61	19.4	1.0	0.5
101	13.3	0.555	0.5
146	10.0	0.236	0.5
300	5.7	0.184	0.6
mass	2.6	0.052	0.65
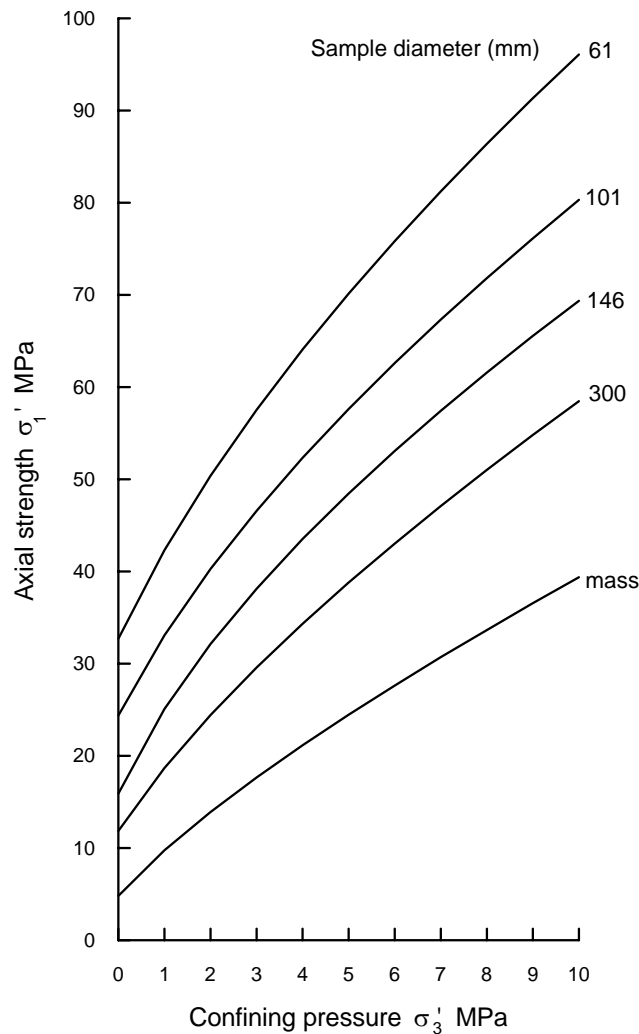
Figure 11.4 Peak strength for Australian Moura coal.
After Medhurst and Brown (1996).

The Hoek-Brown failure criterion, which assumes isotropic rock and rock mass behaviour, should only be applied to those rock masses in which there are a sufficient number of closely spaced discontinuities, with similar surface characteristics, that isotropic behaviour involving failure on discontinuities can be assumed. When the structure being analysed is large and the block size small in comparison, the rock mass can be treated as a Hoek-Brown material.

   Where the block size is of the same order as that of the structure being analysed or when one of the discontinuity sets is significantly weaker than the others, the Hoek-Brown criterion should not be used. In these cases, the stability of the structure should be analysed by considering failure mechanisms involving the sliding or rotation of blocks and wedges defined by intersecting structural features.
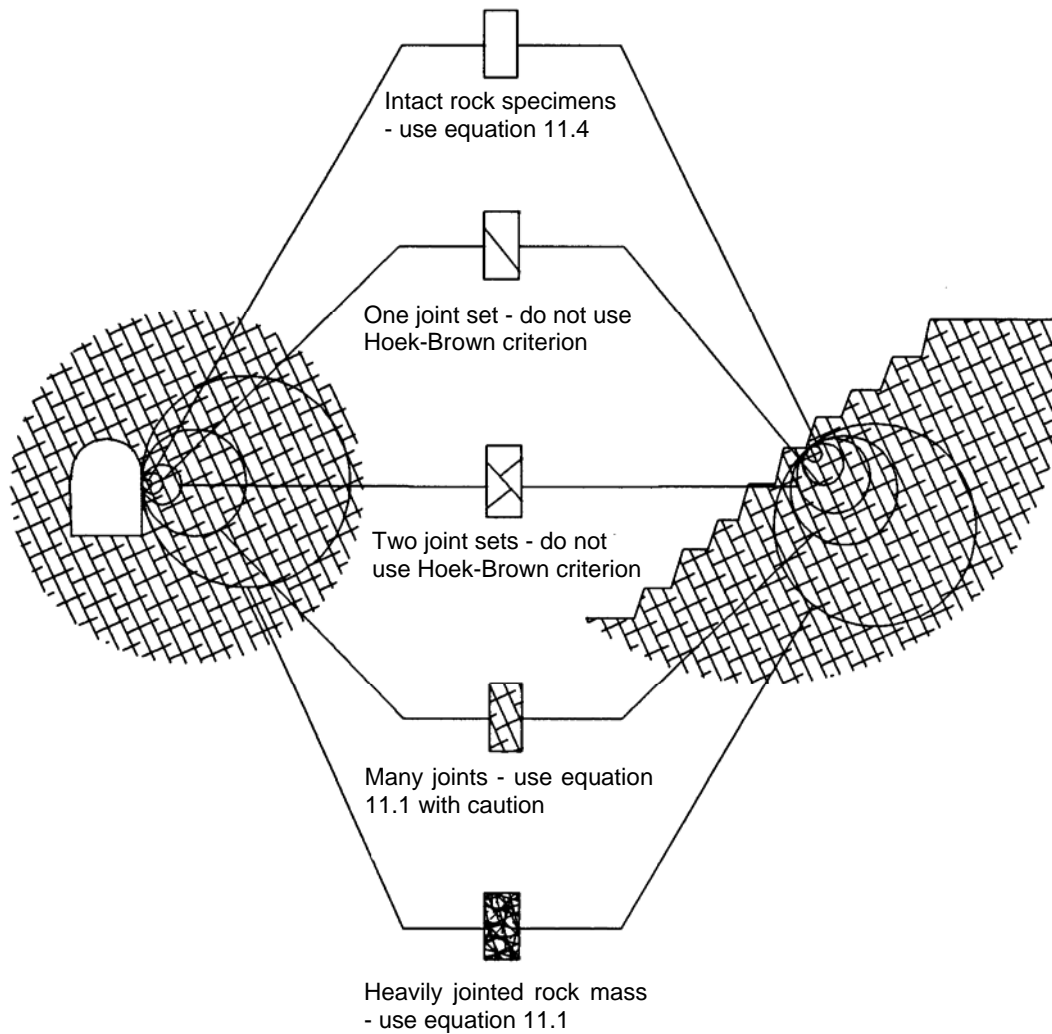
Figure 11.5: Idealised diagram showing the transition from intact to a heavily jointed rock mass with increasing sample size.

11.5 Geological strength Index

The strength of a jointed rock mass depends on the properties of the intact rock pieces and also upon the freedom of these pieces to slide and rotate under different stress conditions. This freedom is controlled by the geometrical shape of the intact rock pieces as well as the condition of the surfaces separating the pieces. Angular rock pieces with clean, rough discontinuity surfaces will result in a much stronger rock mass than one which contains rounded particles surrounded by weathered and altered material.

The Geological Strength Index (GSI), introduced by Hoek (1995) and Hoek, Kaiser and Bawden (1995) provides a system for estimating the reduction in rock mass strength for different geological conditions. This system is presented in Table 11.5 and Table 11.6. Experience has shown that Table 11.5 is sufficient for field

observations since the letter code that identifies each rock mass category can be entered into a field log. Later, these codes can be used to estimate the GSI value from Table 11.6.

Once the Geological Strength Index has been estimated, the parameters that describe the rock mass strength characteristics, are calculated as follows:

$$m_b = m_i \exp\left(\frac{GSI - 100}{28}\right) \quad (11.10)$$

For GSI > 25, i.e. rock masses of good to reasonable quality, the original Hoek-Brown criterion is applicable with

$$s = \exp\left(\frac{GSI - 100}{9}\right) \quad (11.11)$$

and

$$a = 0.5 \quad (11.12)$$

For GSI < 25, i.e. rock masses of very poor quality, the modified Hoek-Brown criterion applies with

$$s = 0 \quad (11.13)$$

and

$$a = 0.65 - \frac{GSI}{200} \quad (11.14)$$
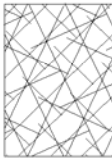
The choice of GSI = 25 for the switch between the original and modified criteria is purely arbitrary. It could be argued that a switch at GSI = 30 would not introduce a discontinuity in the value of *a*, but extensive trials have shown that the exact location of this switch has negligible practical significance.

For better quality rock masses (GSI > 25), the value of GSI can be estimated directly from the 1976 version of Bieniawski's Rock Mass Rating, with the Groundwater rating set to 10 (dry) and the Adjustment for Joint Orientation set to 0 (very favourable) (Bieniawski 1976). For very poor quality rock masses the value of RMR is very difficult to estimate and the balance between the ratings no longer gives a reliable basis for estimating rock mass strength. Consequently, Bieniawski's RMR classification should not be used for estimating the GSI values for poor quality rock masses.

If the 1989 version of Bieniawski's RMR classification (Bieniawski 1989) is used, then GSI = RMR_{89}' - 5 where RMR_{89}' has the Groundwater rating set to 15 and the Adjustment for Joint Orientation set to zero.

One of the practical problems which arises when assessing the value of GSI in the field is related to blast damage. As illustrated in Figure 11.6, there is a considerable difference in the appearance of a rock face which has been excavated by controlled blasting and a face which has been damaged by bulk blasting. Wherever possible, the undamaged face should be used to estimate the value of GSI since the overall aim is to determine the properties of the undisturbed rock mass.

Table 11.5: Characterisation of rock masses on the basis of interlocking and joint alteration[1]

ROCK MASS CHARACTERISTICS FOR STRENGTH ESTIMATES Based upon the appearance of the rock, choose the category that you think gives the best description of the 'average' undisturbed in situ conditions. Note that exposed rock faces that have been created by blasting may give a misleading impression of the quality of the underlying rock. Some adjustment for blast damage may be necessary and examination of diamond drill core or of faces created by pre-split or smooth blasting may be helpful in making these adjustments. It is also important to recognize that the Hoek-Brown criterion should only be applied to rock masses where the size of individual blocks is small compared with the size of the excavation under consideration. STRUCTURE	SURFACE CONDITIONS	VERY GOOD Very rough, fresh unweathered surfaces	GOOD Rough, slightly weathered, iron stained surfaces	FAIR Smooth, moderately weathered or altered surfaces	POOR Slickensided, highly weathered surfaces with compact coatings or fillings of angular fragments	VERY POOR Slickensided, highly weathered surfaces with soft clay coatings or fillings
				DECREASING SURFACE QUALITY ⟹		
BLOCKY - very well interlocked undisturbed rock mass consisting of cubical blocks formed by three orthogonal discontinuity sets	DECREASING INTERLOCKING OF ROCK PIECES	B/VG	B/G	B/F	B/P	B/VP
VERY BLOCKY - interlocked, partially disturbed rock mass with multifaceted angular blocks formed by four or more discontinuity sets		VB/VG	VB/G	VB/F	VB/P	VB/VP
BLOCKY/DISTURBED- folded and/or faulted with angular blocks formed by many intersecting discontinuity sets		BD/VG	BD/G	BD/F	BD/P	BD/VP
DISINTEGRATED - poorly inter-locked, heavily broken rock mass with a mixture or angular and rounded rock pieces		D/VG	D/G	D/F	D/P	D/VP

---

[1] In earlier versions of this table the terms BLOCKY/SEAMY and CRUSHED were used, following the terminology used by Terzaghi (1946). However, these terms proved to be misleading and they have been replaced, in this table by BLOCKY/DISTURBED, which more accurately reflects the increased mobility of a rock mass which has undergone some folding and/or faulting, and DISINTEGRATED which encompasses a wider range of particle shapes.

Table 11.6: Estimate of Geological Strength Index GSI based on geological descriptions.

Figure 11.6: Comparison between the results achieved using controlled blasting (on the left) and normal bulk blasting for a surface excavation in gneiss.

Where all the visible faces have been damaged by blasting, some attempt should be made to compensate for the lower values of GSI obtained from such faces. In recently blasted faces, new discontinuity surfaces will have been created by the blast and these will give a GSI value that may be as much as 10 points lower than that for the undisturbed rock mass. In other words, severe blast damage can be allowed for by moving up one row in Table 11.5 and Table 11.6.

Where blast damaged faces have been exposed for a number of years, it may also be necessary to step as much as one column to the left in order to allow for surface weathering which will have occurred during this exposure. Hence, for example, a badly blast damaged weathered rock surface which has the appearance of a BLOCKY/DISTURBED and FAIR (BD/F in Table 11.5) rock mass may actually be VERY BLOCKY and GOOD (VB/G) in its unweathered and undisturbed in situ state.

An additional practical question is whether borehole cores can be used to estimate the GSI value behind the visible faces? For reasonable quality rock masses (GSI > 25) the best approach is to evaluate the core in terms of Bieniawski's RMR classification and then, as described above, to estimate the GSI value from RMR. For poor quality rock masses (GSI < 25), relatively few intact core pieces longer than 100 mm are recovered and it becomes difficult to determine a reliable value for RMR. In these circumstances, the physical appearance of the material recovered in the core should be used as a basis for estimating GSI.

11.6 Mohr-Coulomb parameters

Most geotechnical software is written in terms of the Mohr-Coulomb failure criterion in which the rock mass strength is defined by the cohesive strength c' and the angle of friction ϕ'. The linear relationship between the major and minor principal stresses, σ_1' and σ_3', for the Mohr-Coulomb criterion is

$$\sigma_1' = \sigma_{cm} + k\sigma_3' \tag{11.15}$$

where σ_{cm} is the uniaxial compressive strength of the rock mass and k is the slope of the line relating σ_1' and σ_3'. The values of ϕ' and c' can be calculated from

$$\sin\phi' = \frac{k-1}{k+1} \tag{11.16}$$

$$c' = \frac{\sigma_{cm}(1-\sin\phi')}{2\cos\phi'} \tag{11.17}$$

There is no direct correlation between equation 11.15 and the non-linear Hoek-Brown criterion defined by equation 11.1. Consequently, determination of the values of c' and ϕ' for a rock mass that has been evaluated as a Hoek-Brown material is a difficult problem.

The author believes that the most rigorous approach available, for the original Hoek-Brown criterion, is that developed by Dr J.W. Bray and reported by Hoek (1983). For any point on a surface of concern in an analysis such as a slope stability calculation, the effective normal stress is calculated using an appropriate stress analysis technique. The shear strength developed at that value of effective normal stress is then calculated from the equations given in Hoek and Brown (1997). The difficulty in applying this approach in practice is that most of the geotechnical software currently available provides for constant rather than effective normal stress dependent values of c' and ϕ'.

Having evaluated a large number of possible approaches to this problem, it has been concluded that the most practical solution is to treat the problem as an analysis of a set of full-scale triaxial strength tests. The results of such tests are simulated by using the Hoek-Brown equation 11.1 to generate a series of triaxial test values. Equation 11.15 is then fitted to these test results by linear regression analysis and the values of c' and ϕ' are determined from equations 11.17 and 11.16. The steps required to determine the parameters A, B, c' and ϕ' are given below. A spreadsheet for carrying out this analysis, with a listing of all the cell formulae, is given in Figure 11.7.

The relationship between the normal and shear stresses can be expressed in terms of the corresponding principal effective stresses as suggested by Balmer (1952):

$$\sigma_n' = \sigma_3' + \frac{\sigma_1' - \sigma_3'}{\partial\sigma_1'/\partial\sigma_3' + 1} \tag{11.18}$$

$$\tau = (\sigma_1' - \sigma_3')\sqrt{\partial\sigma_1'/\partial\sigma_3'} \tag{11.19}$$

For the *GSI* > 25, when *a* = 0.5:

$$\frac{\partial\sigma_1'}{\partial\sigma_3'} = 1 + \frac{m_b\sigma_{ci}}{2(\sigma_1' - \sigma_3')} \tag{11.20}$$

For *GSI* < 25, when *s* = 0:

$$\frac{\partial\sigma_1'}{\partial\sigma_3'} = 1 + am_b^a\left(\frac{\sigma_3'}{\sigma_{ci}}\right)^{a-1} \tag{11.21}$$

The tensile strength of the rock mass is calculated from:

$$\sigma_{tm} = \frac{\sigma_{ci}}{2}\left(m_b - \sqrt{m_b^2 + 4s}\right) \tag{11.22}$$

The equivalent Mohr envelope, defined by equation 11.2, may be written in the form:

$$Y = \log A + BX \tag{11.23}$$

where

$$Y = \log\left(\frac{\tau}{\sigma_{ci}}\right), \ X = \log\left(\frac{\sigma_n' - \sigma_{tm}}{\sigma_{ci}}\right) \tag{11.24}$$

Using the value of σ_{tm} calculated from equation 11.22 and a range of values of τ and σ_n' calculated from equations 11.19 and 11.18 the values of *A* and *B* are determined by linear regression where :

$$B = \frac{\sum XY - (\sum X \sum Y)/T}{\sum X^2 - (\sum X)^2/T} \tag{11.25}$$

$$A = 10^\wedge\left(\sum Y/T - B(\sum X/T)\right) \tag{11.26}$$

and *T* is the total number of data pairs included in the regression analysis.

The most critical step in this process is the selection of the range of σ_3' values. As far as the author is aware, there are no theoretically correct methods for choosing this range and a trial and error method, based upon practical compromise, has been used for selecting the range included in the spreadsheet presented in Figure 11.7.

For a Mohr envelope defined by equation 11.2, the friction angle ϕ_i' for a specified normal stress σ_{ni}' is given by:

$$\phi_i' = \arctan\left(AB\left(\frac{\sigma_{ni}' - \sigma_{tm}}{\sigma_{ci}}\right)^{B-1}\right) \qquad (11.27)$$

The corresponding cohesive strength c_i' is given by:

$$c_i' = \tau - \sigma_{ni}' \tan\phi_i' \qquad (11.28)$$

and the corresponding uniaxial compressive strength of the rock mass is :

$$\sigma_{cmi} = \frac{2c_i' \cos\phi_i'}{1 - \sin\phi_i'} \qquad (11.29)$$

Note that the cohesive strength c_i' given by equation 11.29 is an upper bound value and that it is prudent to reduce this to about 75% of the calculated value for practical applications.

The values of c' and ϕ' obtained from this analysis are very sensitive to the range of values of the minor principal stress σ_3' used to generate the simulated full-scale triaxial test results. On the basis of trial and error, it has been found that the most consistent results are obtained when 8 equally spaced values of σ_3' are used in the range $0 < \sigma_3' < 0.25\sigma_{ci}$.

An example of the results, which are obtained from this analysis, is given in Figure 11.8. Plots of the values of the ratio c'/σ_{ci} and the friction angle ϕ', for different combinations of GSI and m_i are given in Figure 11.9.

The spreadsheet includes a calculation for a tangent to the Mohr envelope defined by equation 11.2. A normal stress has to be specified in order to calculate this tangent and, in Figure 11.8, this stress has been chosen so that the friction angle ϕ' is the same for both the tangent and the line defined by $c' = 3.3$ MPa and $\phi' = 30.1°$, determined by the linear regression analysis described earlier. The cohesion intercept for the tangent is $c' = 4.1$ MPa which is approximately 25% higher than that obtained by linear regression analysis of the simulated triaxial test data.

Fitting a tangent to the curved Mohr envelope gives an upper bound value for the cohesive intercept c'. It is recommended that this value be reduced by about 25% in order to avoid over-estimation of the rock mass strength.

There is a particular class of problem for which extreme caution should be exercised when applying the approach outlined above. In some rock slope stability problems, the effective normal stress on some parts of the failure surface can be quite low, certainly less than 1 MPa. It will be noted that in the example given in Figure 11.8, for values of σ_n' of less than about 5 MPa, the straight line, constant c' and ϕ' method overestimates the available shear strength of the rock mass by increasingly significant amounts as σ_n' approaches zero. Under such circumstances, it would be prudent to use values of c' and ϕ' based on a tangent to the shear strength curve in the range of σ_n' values applying in practice.

Figure 11.7 Spreadsheet for calculation of Hoek-Brown and equivalent Mohr-Coulomb parameters

Hoek-Brown and equivalent Mohr Coulomb failure criteria

Input:	sigci =	85	MPa	mi =	10		GSI =	45

Output:	mb =	1.40		s =	0.0022		a =	0.5	
	sigtm =	-0.13	MPa	A =	0.50		B =	0.70	
	k =	3.01		phi =	30.12	degrees	coh =	3.27	MPa
	sigcm =	11.36	MPa	E =	6913.7	MPa			

Tangent:	signt =	15.97	MPa	phit=	30.12	degrees	coht =	4.12	MPa

Calculation:

									Sums
sig3	1E-10	3.04	6.07	9.1	12.14	15.18	18.21	21.25	85.00
sig1	4.00	22.48	33.27	42.30	50.40	57.91	64.98	71.74	347.08
ds1ds3	15.89	4.07	3.19	2.80	2.56	2.40	2.27	2.18	35.35
sign	0.24	6.87	12.56	17.85	22.90	27.76	32.50	37.13	157.80
tau	0.94	7.74	11.59	14.62	17.20	19.48	21.54	23.44	116.55
x	-2.36	-1.08	-0.83	-0.67	-0.57	-0.48	-0.42	-0.36	-6.77
y	-1.95	-1.04	-0.87	-0.76	-0.69	-0.64	-0.60	-0.56	-7.11
xy	4.61	1.13	0.71	0.52	0.39	0.31	0.25	0.20	8.12
xsq	5.57	1.17	0.68	0.45	0.32	0.23	0.17	0.13	8.74
sig3sig1	0.00	68.23	202.01	385.23	612.01	878.92	1183.65	1524.51	4855
sig3sq	0.00	9.22	36.86	82.94	147.45	230.39	331.76	451.56	1290
taucalc	0.96	7.48	11.33	14.45	17.18	19.64	21.91	24.04	
sig1sig3fit	11.36	20.51	29.66	38.81	47.96	57.11	66.26	75.42	
signtaufit	3.41	7.26	10.56	13.63	16.55	19.38	22.12	24.81	
tangent	4.25309	8.10321	11.4032	14.4729	17.3991	20.2235	22.9702	25.655	

Cell formulae:

```
    mb = mi*EXP((GSI-100)/28)
     s = IF(GSI>25,EXP((GSI-100)/9),0)
     a = IF(GSI>25,0.5,0.65-GSI/200)
 sigtm = 0.5*sigci*(mb-SQRT(mb^2+4*s))
     A =  acalc =  10^(sumy/8 - bcalc*sumx/8)
     B =  bcalc =  (sumxy - (sumx*sumy)/8)/(sumxsq - (sumx^2)/8)
     k = (sumsig3sig1 - (sumsig3*sumsig1)/8)/(sumsig3sq-(sumsig3^2)/8)
   phi = ASIN((k-1)/(k+1))*180/PI()
   coh = (sigcm*(1-SIN(phi*PI()/180)))/(2*COS(phi*PI()/180))
 sigcm = sumsig1/8 - k*sumsig3/8
     E = IF(sigci>100,1000*10^((GSI-10)/40),SQRT(sigci/100)*1000*10^((GSI-10)/40))
  phit = (ATAN(acalc*bcalc*((signt-sigtm)/sigci)^(bcalc-1)))*180/PI()
  coht = acalc*sigci*((signt-sigtm)/sigci)^bcalc-signt*TAN(phit*PI()/180)
  sig3 = Start at 1E-10 (to avoid zero errors) and increment in 7 steps of  sigci/28 to 0.25*sigci
  sig1 = sig3+sigci*(((mb*sig3)/sigci)+s)^a
ds1ds3 = IF(GSI>25,(1+(mb*sigci)/(2*(sig1-sig3))),1+(a*mb^a)*(sig3/sigci)^(a-1))
  sign = sig3+(sig1-sig3)/(1+ds1ds3)
   tau = (sign-sig3)*SQRT(ds1ds3)
     x = LOG((sign-sigtm)/sigci)
     y = LOG(tau/sigci)
    xy = x*y         x sq = x^2        sig3sig1= sig3*sig1                sig3sq = sig3^2
taucalc = acalc*sigci*((sign-sigtm)/sigci)^bcalc
 s3sifit = sigcm+k*sig3
sntaufit = coh+sign*TAN(phi*PI()/180)
tangent = coht+sign*TAN(phit*PI()/180)
```

$$\sigma_1^{'} = \sigma_{cm} + \frac{1 + \sin \phi^{'}}{1 - \sin \phi^{'}} \sigma_3^{'}$$

$$\sigma_1^{'} = \sigma_3^{'} + \sigma_{ci} \left(m_b \frac{\sigma_3^{'}}{\sigma_{ci}} + s \right)^a$$

σ_{cm}

$$\tau = A\sigma_{ci} \left(\frac{\sigma_n^{'} - \sigma_{tm}}{\sigma_{ci}} \right)^B$$

$$\tau = c^{'} + \sigma_n^{'} \tan \phi^{'}$$
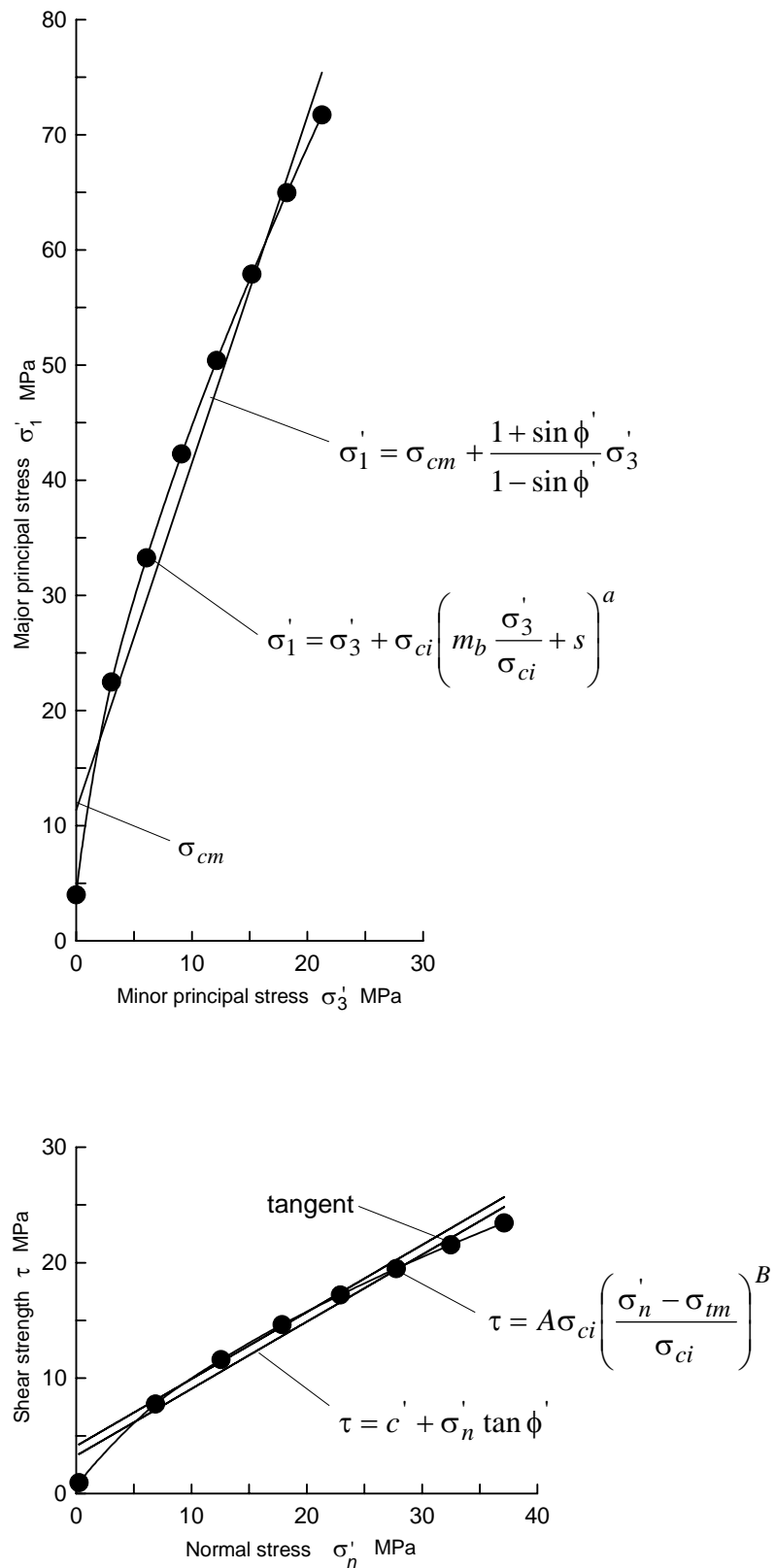
Figure 11.8: Plot of results from simulated full scale triaxial tests on a rock mass defined by a uniaxial compressive strength σ_{ci} = 85 MPa, a Hoek -Brown constant m_i = 10 and a Geological Strength Index GSI = 45.
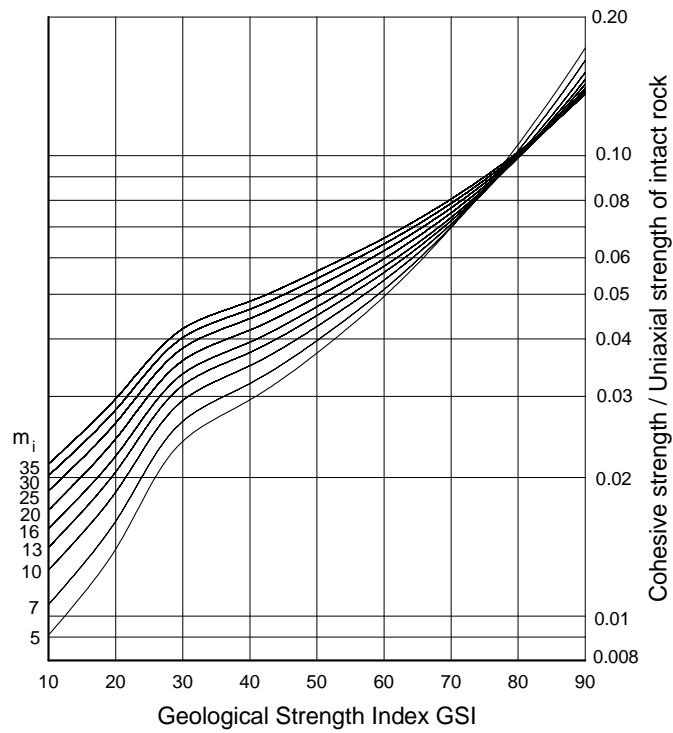
a. Plot of ratio of cohesive strength c' to uniaxial compressive strength σ_{ci} .
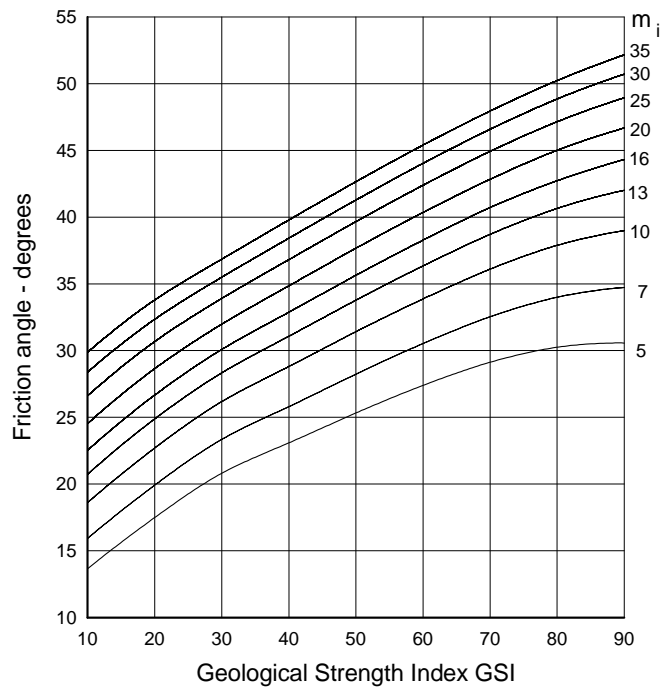
b.   Plot of friction angle ϕ'

Figure 11.9: Plots of cohesive strength and friction angles for different GSI and m_i values.

11.7 Deformation modulus

Serafim and Pereira (1983) proposed a relationship between the in situ modulus of deformation and Bieniawski's RMR classification. This relationship is based upon back analysis of dam foundation deformations and it has been found to work well for better quality rocks. However, for many of the poor quality rocks it appears to predict deformation modulus values which are too high. Based upon practical observations and back analysis of excavation behaviour in poor quality rock masses, the following modification to Serafim and Pereira's equation is proposed for $\sigma_{ci} < 100$:

$$E_m = \sqrt{\frac{\sigma_{ci}}{100}} 10^{\left(\frac{GSI-10}{40}\right)}$$

(11.30)

Note that GSI has been substituted for RMR in this equation and that the modulus E_m is reduced progressively as the value of σ_{ci} falls below 100. This reduction is based upon the reasoning that the deformation of better quality rock masses is controlled by the discontinuities while, for poorer quality rock masses, the deformation of the intact rock pieces contributes to the overall deformation process.

Based upon measured deformations, equation 11.30 appears to work reasonably well in those cases where it has been applied. However, as more field evidence is gathered it may be necessary to modify this relationship.

11.8 Post-failure behaviour

When using numerical models to study the progressive failure of rock masses, estimates of the post-peak or post-failure characteristics of the rock mass are required. In some of these models, the Hoek-Brown failure criterion is treated as a yield criterion and the analysis is carried out using plasticity theory (e.g. Pan and Hudson 1988). No definite rules for dealing with this problem can be given but, based upon experience in numerical analysis of a variety of practical problems, the post-failure characteristics illustrated in Figure 11.10 are suggested as a starting point.

11.8.1 *Very good quality hard rock masses*

For very good quality hard rock masses, such as massive granites or quartzites, the analysis of spalling around highly stressed openings (Hoek, Kaiser and Bawden 1995) suggests that the rock mass behaves in an elastic brittle manner as shown in Figure 11.10(a). When the strength of the rock mass is exceeded, a sudden strength drop occurs. This is associated with significant dilation of the broken rock pieces. If this broken rock is confined, for example by rock support, then it can be assumed to behave as a rock fill with a friction angle of approximately $\phi' = 38°$ and zero cohesive strength.

Typical properties for this very good quality hard rock mass may be as shown in Table 11.7. Note that, in some numerical analyses, it may be necessary to assign a very small cohesive strength in order to avoid numerical instability.
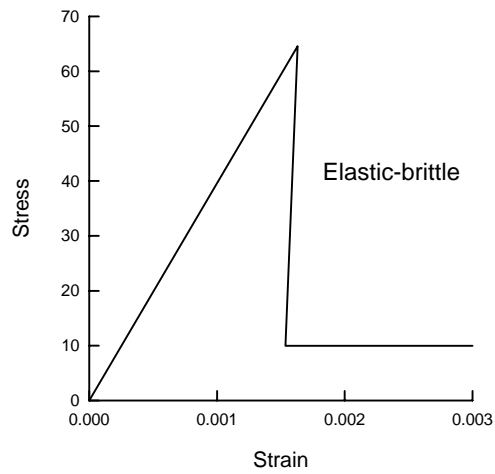
(a) Very good quality hard rock mass
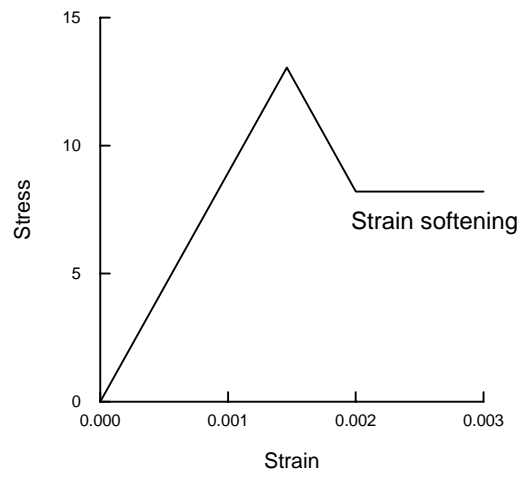
(b) Average quality rock mass
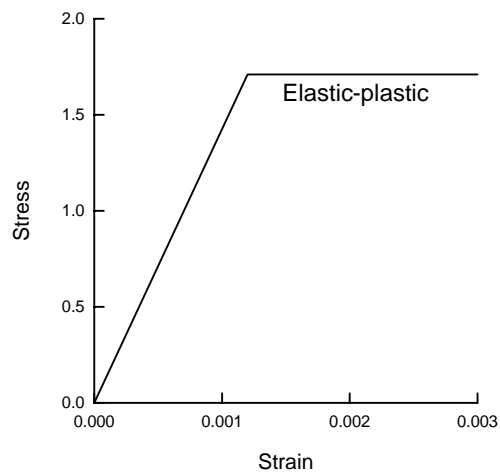
(c) Very poor quality soft rock mass

Figure 11.10: Suggested post failure characteristics for different quality rock masses.

Table 11.7: Typical properties for a very good quality hard rock mass

Intact rock strength	σ_{ci}	150 MPa
Hoek-Brown constant	m_i	25
Geological Strength Index	GSI	75
Friction angle	ϕ'	46°
Cohesive strength	c'	13 MPa
Rock mass compressive strength	σ_{cm}	64.8 MPa
Rock mass tensile strength	σ_{tm}	-0.9 MPa
Deformation modulus	E_m	42000 MPa
Poisson's ratio	ν	0.2
Dilation angle	α	$\phi'/4 = 11.5°$
Post-peak characteristics		
Friction angle	ϕ_f'	38°
Cohesive strength	c_f'	0
Deformation modulus	E_{fm}	10000 MPa

11.8.2   Average quality rock mass

In the case of an average quality rock mass it is reasonable to assume that the post-failure characteristics can be estimated by reducing the GSI value from the in situ value to a lower value which characterises the broken rock mass.

The reduction of the rock mass strength from the in situ to the broken state corresponds to the strain softening behaviour illustrated in Figure 11.10(b). In this figure it has been assumed that post failure deformation occurs at a constant stress level, defined by the compressive strength of the broken rock mass. The validity of this assumption is unknown.

Typical properties for this average quality rock mass may be as follows:

Table 10.8: Typical properties for an average rock mass.

Intact rock strength	σ_{ci}	80 MPa
Hoek-Brown constant	m_i	12
Geological Strength Index	GSI	50
Friction angle	ϕ'	33°
Cohesive strength	c'	3.5 MPa
Rock mass compressive strength	σ_{cm}	13 MPa
Rock mass tensile strength	σ_{tm}	-0.15
Deformation modulus	E_m	9000 MPa
Poisson's ratio	ν	0.25
Dilation angle	α	$\phi'/8 = 4°$
Post-peak characteristics		
Broken rock mass strength	σ_{fcm}	8 MPa
Deformation modulus	E_{fm}	5000 MPa

11.8.3   Very poor quality rock mass

Analysis of the progressive failure of very poor quality rock masses surrounding tunnels suggests that the post-failure characteristics of the rock are adequately represented by assuming that it behaves perfectly plastically. This means that it

continues to deform at a constant stress level and that no volume change is associated with this ongoing failure. This type of behaviour is illustrated in Figure 10.10(c). Typical properties for this very poor quality rock mass may be as follows:

Table 11.9: Typical properties for a very poor quality rock mass

Intact rock strength	σ_{ci}	20 MPa
Hoek-Brown constant	m_i	8
Geological Strength Index	GSI	30
Friction angle	ϕ'	24°
Cohesive strength	c'	0.55 MPa
Rock mass compressive strength	σ_{cm}	1.7 MPa
Rock mass tensile strength	σ_{tm}	-0.01 MPa
Deformation modulus	E_m	1400 MPa
Poisson's ratio	ν	0.3
Dilation angle	α	zero
Post-peak characteristics		
Broken rock mass strength	σ_{fcm}	1.7 MPa
Deformation modulus	E_{fm}	1400 MPa

11.9 Reliability of rock mass strength estimates

The techniques described in the preceding sections of this chapter can be used to estimate the strength and deformation characteristics of isotropic jointed rock masses. When applying this procedure to rock engineering design problems, most users consider only the 'average' or mean properties. In fact, all of these properties exhibit a distribution about the mean, even under the most ideal conditions, and these distributions can have a significant impact upon the design calculations.

In the text that follows, a slope stability calculation and a tunnel support design calculation are carried out in order to evaluate influence of these distributions. In each case the strength and deformation characteristics of the rock mass are estimated by means of the Hoek-Brown procedure, assuming that the three input parameters are defined by normal distributions.

11.9.1 Input parameters

Figure 11.11 has been used to estimate the value of the value of GSI from field observations of blockiness and discontinuity surface conditions. Included in this figure is a crosshatched circle representing the 90% confidence limits of a GSI value of 25 ± 5 (equivalent to a standard deviation of approximately 2.5). This represents the range of values that an experienced geologist would assign to a rock mass described as BLOCKY/DISTURBED or DISINTEGRATED and POOR. Typically, rocks such as flysch, schist and some phyllites may fall within this range of rock mass descriptions.

Figure 11.11: Estimate of Geological Strength Index GSI based on geological descriptions.
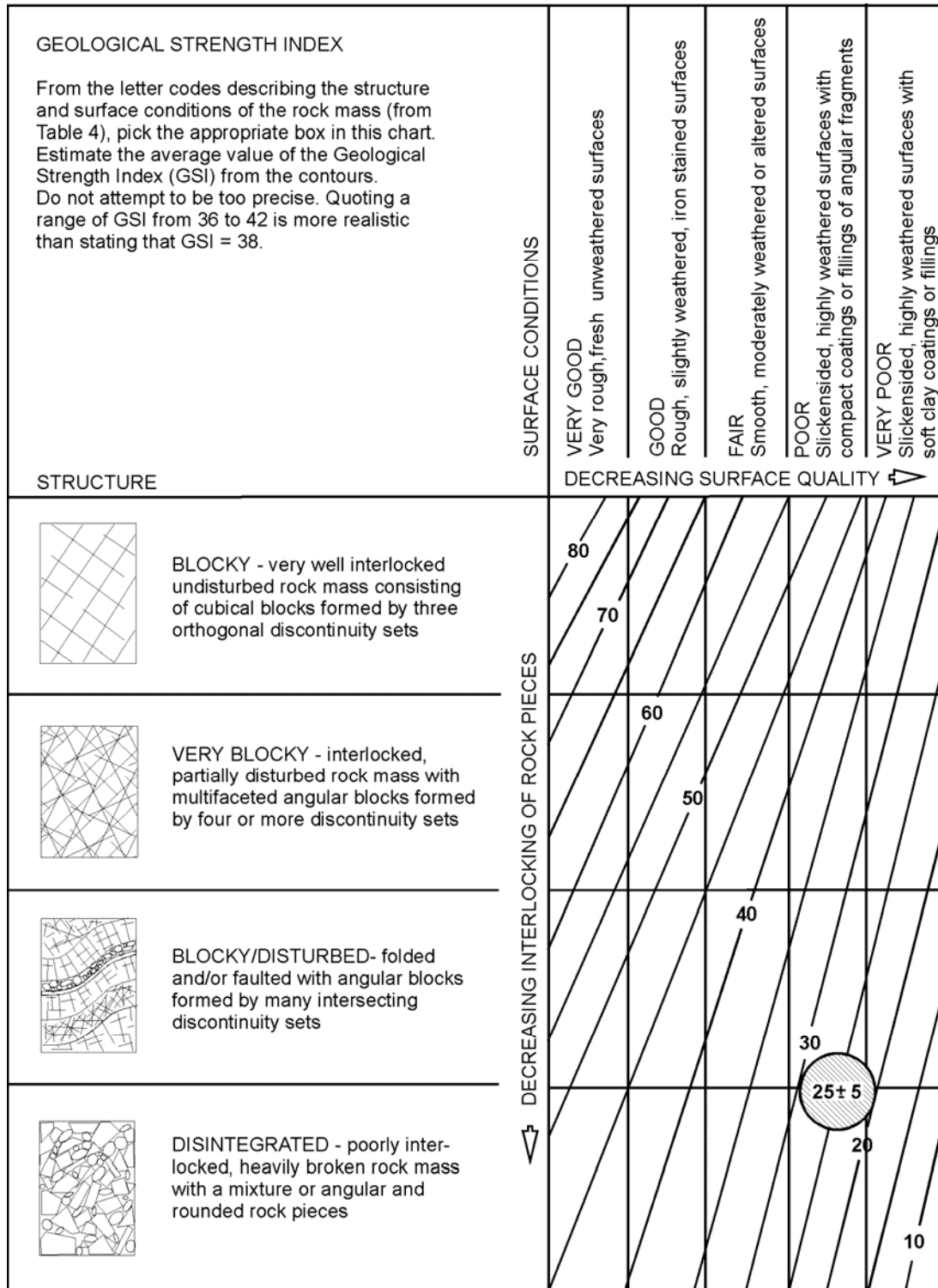
In the author's experience, some geologists go to extraordinary lengths to try to determine an 'exact' value of GSI (or RMR). Geology does not lend itself to such precision and it is simply not realistic to assign a single value. A range of values, such as that illustrated in Figure 11.11 is more appropriate. In fact, in some complex geological environments, the range indicated by the crosshatched circle may be too optimistic.

The two laboratory properties required for the application of the Hoek-Brown criterion are the uniaxial compressive strength of the intact rock (σ_{ci}) and the intact rock material constant m_i. Ideally these two parameters should be determined by triaxial tests on carefully prepared specimens as described by Hoek and Brown (1997).

It is assumed that all three input parameters can be represented by normal distributions as illustrated in Figure 11.12. The standard deviations assigned to these three distributions are based upon the author's experience of geotechnical programs for major civil and mining projects where adequate funds are available for high quality investigations. For preliminary field investigations or 'low budget' projects, it is prudent to assume larger standard deviations for the input parameters.

11.9.2   Output parameters

The values of the friction angle ϕ, the cohesive strength c', the uniaxial compressive strength of the rock mass σ_{cm} and the deformation modulus E_m of the rock mass were calculated by the procedure described in previous sections of this chapter. The Excel add-on program @RISK[2] was used for a Monte Carlo analysis in which 1000 calculations were carried out for randomly selected values of the input parameters. The results of these calculations were analysed using the program BESTFIT[1] and it was found that all four output parameters could be adequately described by the normal distributions illustrated in Figure 11.12.

In several trials it was found that the output parameters ϕ, c' and σ_{cm} were always well represented by normal distributions. On the other hand, for *GSI* values of more than 40, the deformation modulus E_m was better represented by a lognormal distribution.

11.9.3   Slope stability calculation

In order to assess the impact of the variation in output parameters, illustrated in Figure 11.12, a calculation of the factor of safety for a homogeneous slope was carried out using Bishop's circular failure analysis in the program SLIDE[3]. The geometry of the slope and the phreatic surface, the rock mass properties and the critical failure surface for the 'average' properties are shown in Figure 11.13.

---

[2] From Palisade Corporation, 31 Decker Road, Newfield, New York 14867, USA.

[3] Available from Available from Rocscience Inc., 31 Balsam Avenue, Toronto, Ontario, Canada M4E 3B5, Fax 1 416 698 0908, Phone 1 416 698 8217, Email: software@rocscience.com, Internet http://www.rocscience.com.
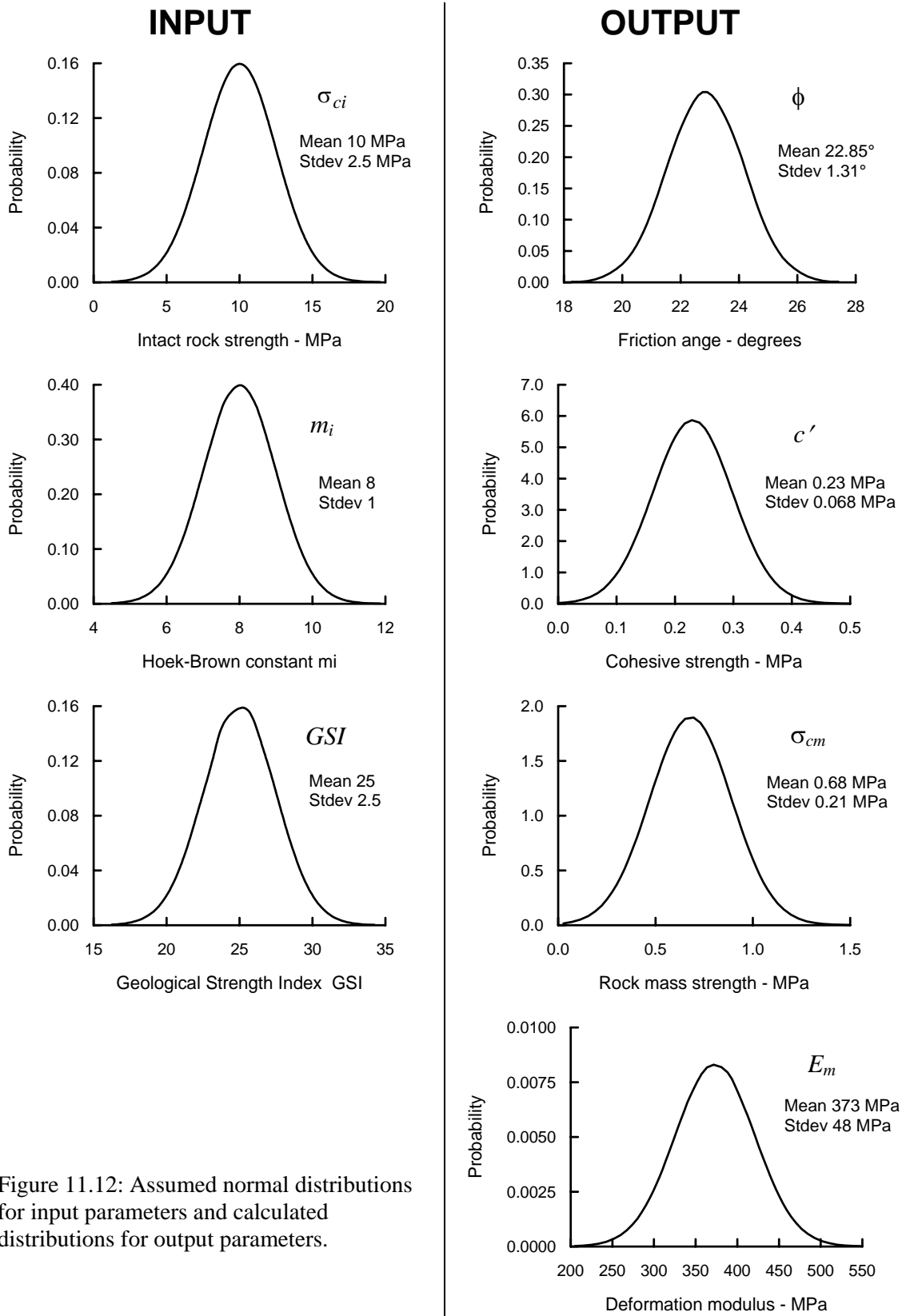
INPUT

OUTPUT

Figure 11.12: Assumed normal distributions for input parameters and calculated distributions for output parameters.
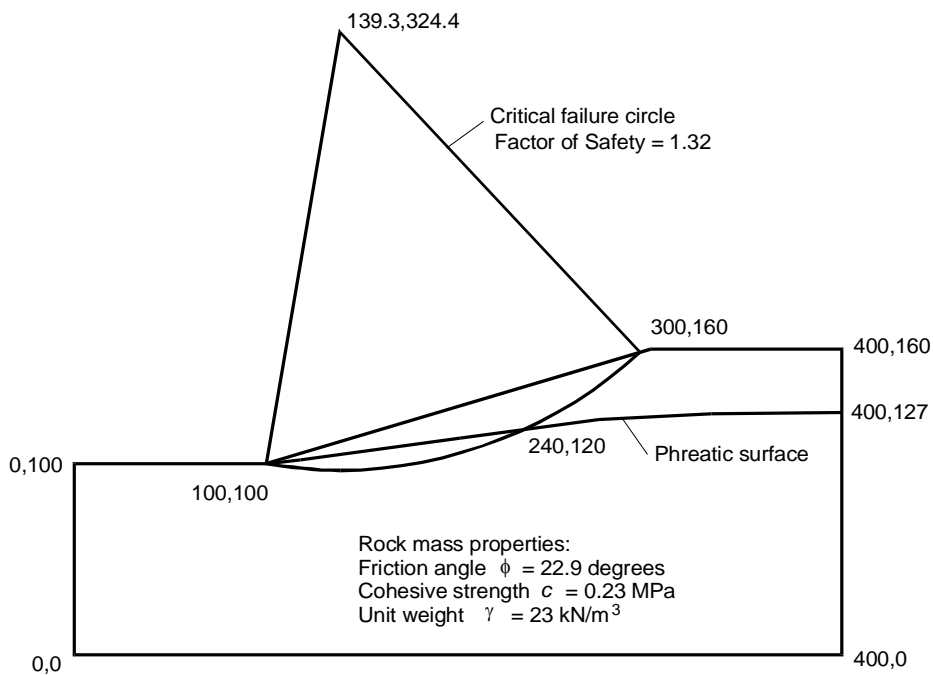
Figure 11.13: Slope and phreatic surface geometry, rock mass properties and critical failure surface for a homogeneous slope.

The distribution of the factor of safety was determined by Rosenbleuth's Point Estimate method (Rosenbleuth 1976, Harr 1987) in which the two values are chosen at one standard deviation on either side of the mean for each variable. The factor of safety is calculated for every possible combination of point estimates, producing 2^m solutions, where m is the number of variables considered. The mean and standard deviation of the factor of safety are then calculated from these 2^m solutions.

This calculation of the mean and standard deviation is given in Table 11.10. Based upon the fact that the two variables included in this analysis are defined by normal distributions and considering the form of the equations used to calculate the factor of safety, it is reasonable to assume that the factor of safety will be adequately represented by a normal distribution. This distribution is illustrated in Figure 11.13.

Table 11.10: Calculations for Rosenbleuth's Point Estimate method using ± one standard deviation.

Case	Friction Angle	Cohesion	Safety Factor	$(SF\text{-}SF_i)^2$
ϕ_-,c_-	21.19	0.162	1.215	0.00922
ϕ_+,c_+	24.16	0.298	1.407	0.00922
ϕ_-, c_+	21.19	0.298	1.217	0.00884
ϕ_+, c_-	24.16	0.162	1.406	0.00912
		sums	5.245	0.0364

$$\text{Mean Safety Factor} = \bar{SF} = \frac{1}{n}\sum_{i=1}^{n} SF_i = 1.31$$

$$\text{Standard deviation} = S^2 = \frac{1}{n-1}\sum_{i=1}^{n}(\bar{SF} - SF_i)^2 = 0.11$$
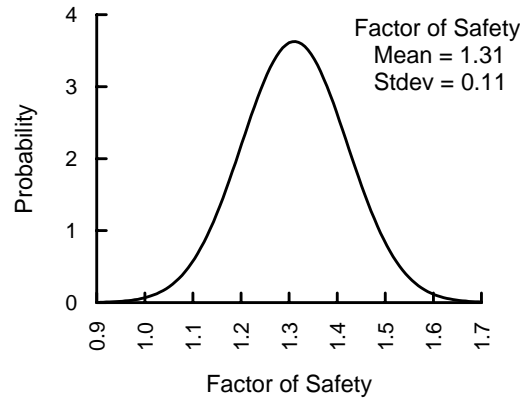
Figure 11.14: Normal distribution of the factor of safety of the slope defined in Figure 11.13.

The mean factor of safety for this slope is 1.3 that is a value frequently used in the design of slopes for open pit mines. It is interesting that the probability of failure, given by the portion of the distribution curve for SF < 1, is very small. This suggests that, for a high quality geotechnical investigation such as that assumed in this study, a safety factor of 1.3 is adequate to ensure stability under the assumed conditions.

11.9.4 Tunnel stability calculations

Consider a circular tunnel of radius r_o in a stress field in which the horizontal and vertical stresses are both p_o. If the stresses are high enough, a 'plastic' zone of damaged rock of radius r_p surrounds the tunnel. A uniform support pressure p_i is provided around the perimeter of the tunnel. This situation is illustrated in Figure 11.15.

Assuming that the rock mass fails with zero plastic volume change, the critical stress level p_{cr} at which failure initiates is given by :

$$p_{cr} = \frac{2p_o - \sigma_{cm}}{1+k} \tag{11.31}$$

where

$$k = \frac{1+\sin\phi}{1-\sin\phi} \tag{11.32}$$

Where the support pressure p_i is less than the critical pressure p_{cr}, the radius r_p of the plastic zone and the inward deformation of the tunnel wall u_{ip} are given by:

$$\frac{r_p}{r_o} = \left[\frac{2(p_o(k-1)+\sigma_{cm})}{(1+k)((k-1)p_i+\sigma_{cm})} \right]^{\frac{1}{(k-1)}} \tag{11.33}$$

$$\frac{u_{ip}}{r_o} = \frac{(1+\nu)}{E}\left[2(1-\nu)(p_o-p_{cr})\left(\frac{r_p}{r_o}\right)^2 - (1-2\nu)(p_o-p_i) \right] \tag{11.34}$$
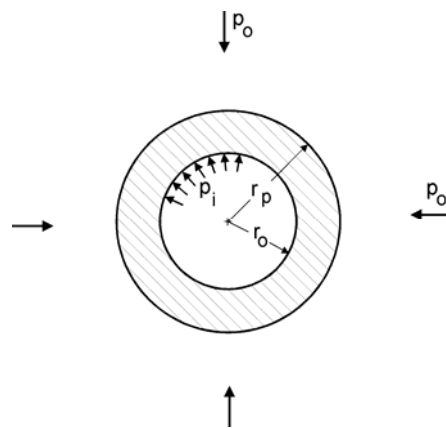
Figure 11.15: Development of a plastic zone around a circular
tunnel in a hydrostatic stress field.

In order to study the influence of the variation in the input parameters, a Monte Carlo analysis was performed using the program @RISK in an Excel spreadsheet that had been programmed to perform the analysis defined above. It was assumed that a 5 m diameter tunnel (r_o = 2.5 m) was subjected to uniform in situ stress of p_o = 2.5 MPa. The rock mass properties were defined by the normal distributions for ϕ, c, σ_{cm} and E defined in Figure 11.12.

   This analysis was carried out for a tunnel with no support. A second analysis was performed for a tunnel with a support pressure of p_i = 0.3 MPa which is approximately that which can be achieved with a closed ring of 50 mm thick shotcrete with a uniaxial compressive strength of 14 MPa (after 1 day of curing). This would represent the early support that would be achieved by the immediate application of shotcrete behind the advancing face. A third analysis was performed for a support pressure p_i = 0.8 MPa. This is approximately the support which can be achieved in this size of tunnel by a 75 mm thick shotcrete lining with a uniaxial compressive strength of 35 MPa (cured for 28 days). The results of these analyses are summarised graphically in Figures 11.16 and 11.17.

   Figures 11.16 and 11.17 show that the size of the plastic zone and the tunnel deformation can be represented by lognormal distributions. As would be expected, the mean values for the size of the plastic zone and the magnitude of the sidewall displacements are reduced significantly by the installation of support.

   What is surprising is the dramatic reduction in the standard deviations with increasing support pressure. This is because of the strong dependence of the size of the plastic zone upon the difference between the critical pressure p_{cr} and the support pressure p_i. A detailed discussion on this dependence is beyond the scope of this technical note and is the subject of ongoing research by the author.

   From the results of the analysis described above it is evident that the installation of a relatively simple support system is very effective in controlling the behaviour of this tunnel. Without support there is an approximate 50% probability of severe instability and possible collapse of the tunnel. A plastic zone diameter of 15 m and a tunnel closure of 50 mm in a 5 m diameter tunnel would certainly cause visible signs of distress. The fact that a relatively thin shotcrete lining can control the size of the

plastic zone and the closure of the tunnel provides confirmation of the effectiveness of support.

A word of warning is required at this point. The example described above is for a 5 m diameter tunnel at a depth of approximately 100 m below surface. For larger tunnels at greater depths, the plastic zone and the displacements can be significantly larger. The demands on the support system may be such that it may be very difficult to support a large tunnel in poor ground at considerable depth below surface.
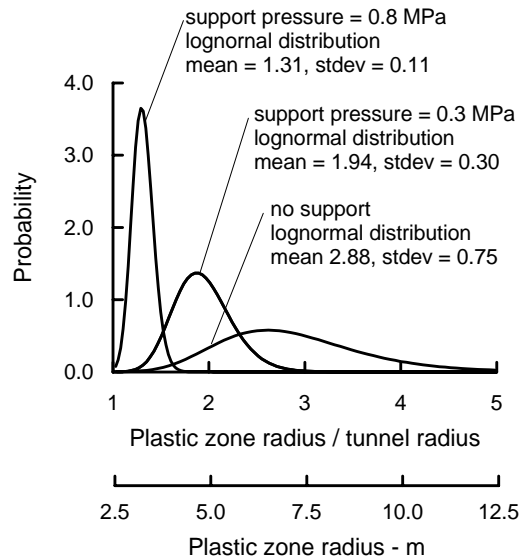
Figure 11.16: Lognormal distributions representing the range of plastic zone radii for different supporting pressures.
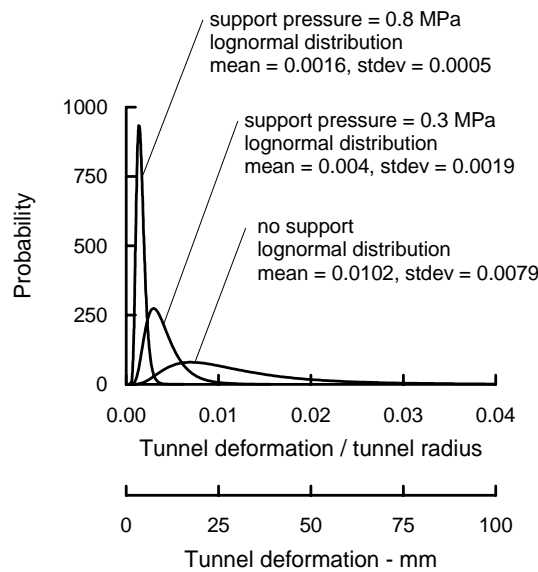
Figure 11.17: Lognormal distributions representing the range of tunnel deformations for different support pressures.

11.9.5   Conclusions

The uncertainty associated with estimating the properties of in situ rock masses has a significant impact or the design of slopes and excavations in rock. The examples that have been explored in this section show that, even when using the 'best' estimates currently available, the range of calculated factors of safety or tunnel behaviour are uncomfortably large. These ranges become alarmingly large when poor site investigation techniques and inadequate laboratory procedures are used.

Given the inherent difficulty of assigning reliable numerical values to rock mass characteristics, it is unlikely that 'accurate' methods for estimating rock mass properties will be developed in the foreseeable future. Consequently, the user of the Hoek-Brown procedure or of any other equivalent procedure for estimating rock mass properties should not assume that the calculations produce unique reliable numbers. The simple techniques described in this section can be used to explore the possible range of values and the impact of these variations on engineering design.

11.10   Practical examples of rock mass property estimates

The following examples are presented in order to illustrate the range of rock mass properties that can be encountered in the field and to give the reader some insight of how the estimation of rock mass properties was tackled in a number of actual projects.

11.10.1 Massive weak rock

Karzulovic and Diaz (1994) have described the results of a program of triaxial tests on a cemented breccia known as Braden Breccia from the El Teniente mine in Chile. In order to design underground openings in this rock, attempts were made to classify the rock mass in accordance with Bieniawski's RMR system. However, as illustrated in Figure 11.18, this rock mass has very few discontinuities and so assigning realistic numbers to terms depending upon joint spacing and condition proved to be very difficult. Finally, it was decided to treat the rock mass as a weak but homogeneous 'almost intact' rock and to determine its properties by means of triaxial tests on large diameter specimens.

A series of triaxial tests was carried out on 100 mm diameter core samples, illustrated in Figure 11.19. The results of these tests were analysed by means of the regression analysis presented in Section 11.3. Back analysis of the behaviour of underground openings in this rock indicate that the in-situ GSI value is approximately 75. From the spreadsheet presented in Figure 11.7 the following parameters were obtained:

Intact rock strength	σ_{ci}	51 MPa	Friction angle	ϕ'	42°
Hoek-Brown constant	m_i	16.3	Cohesive strength	c'	4.32 MPa
Geological Strength Index	GSI	75	Deformation modulus	E_m	30000 MPa
Hoek-Brown constant	s	0.062			

Figure 11.18: Braden Breccia at El Teniente Mine in Chile. This rock is a cemented breccia with practically no joints. It was dealt with in a manner similar to weak concrete and tests were carried out on 100 mm diameter specimens illustrated in Figure 11.19.

Fig. 11.19. 100 mm diameter by 200 mm long specimens of Braden Breccia from the El Teniente mine in Chile.

11.10.2 *Massive strong rock masses*

The Rio Grande Pumped Storage Project in Argentina includes a large underground powerhouse and surge control complex and a 6 km long tailrace tunnel. The rock mass surrounding these excavations is a massive gneiss with very few joints. A typical core from this rock mass is illustrated in Figure 11.20. The appearance of the rock at the surface is illustrated in Figure 11.6, which shows a cutting for the dam spillway.

Figure 11.20: Excellent quality core with very few discontinuities from the massive gneiss of the Rio Grande project in Argentina.

Figure 11.21: Top heading of the 12 m span, 18 m high tailrace tunnel for the Rio Grande Pumped Storage Project.

The rock mass can be described as BLOCKY/VERY GOOD and the GSI value, from Table 11.6, is 75. Typical characteristics for the rock mass are as follows:

Intact rock strength	σ_{ci}	110 MPa	Friction angle	ϕ'	43°	
Hoek-Brown constant	m_i	17.7	Cohesive strength	c'	9.4 MPa	
Geological Strength Index	GSI	75	Rock mass compressive strength	σ_{cm}	43 MPa	
Hoek-Brown constant	m_b	7.25	Rock mass tensile strength	σ_{tm}	-0.94 MPa	
Hoek-Brown constant	s	0.062	Deformation modulus	E_m	42000 MPa	
Constant	a	0.5				

Figure 11.21 illustrates the 8 m high 12 m span top heading for the tailrace tunnel. The final tunnel height of 18 m was achieved by blasting two 5 m benches. The top heading was excavated by full-face drill and blast and, because of the excellent quality of the rock mass and the tight control on blasting quality, most of the top heading did not require any support.

Details of this project are to be found in Moretto et al (1993). Hammett and Hoek (1981) have described the design of the support system for the 25 m span underground powerhouse in which a few structurally controlled wedges were identified and stabilised during excavation.

11.10.3 Average quality rock mass

The partially excavated powerhouse cavern in the Nathpa Jhakri Hydroelectric project in Himachel Pradesh, India is illustrated in Fig. 14. The rock is a jointed quartz mica schist, which has been extensively evaluated by the Geological Survey of India as described by Jalote et al [23]. An average GSI value of 65 was chosen to estimate the rock mass properties which were used for the cavern support design. Additional support, installed on the instructions of the Engineers, was placed in weaker rock zones.

The assumed rock mass properties are as follows:

Intact rock strength	σ_{ci}	30 MPa	Friction angle	ϕ'	40°
Hoek-Brown constant	m_i	15.6	Cohesive strength	c'	2.0 MPa
Geological Strength Index	GSI	65	Rock mass compressive strength	σ_{cm}	8.2 MPa
Hoek-Brown constant	m_b	4.5	Rock mass tensile strength	σ_{tm}	-0.14 MPa
Hoek-Brown constant	s	0.02	Deformation modulus	E_m	13000 MPa
Constant	a	0.5			

Two and three dimensional stress analyses of the nine stages used to excavate the cavern were carried out to determine the extent of potential rock mass failure and to provide guidance in the design of the support system. An isometric view of one of the three dimensional models is given in Figure 11.23.

Figure 11.22: Partially completed 20 m span, 42.5 m high underground powerhouse cavern of the Nathpa Jhakri Hydroelectric Project in Himachel Pradesh, India. The cavern is approximately 300 m below the surface.
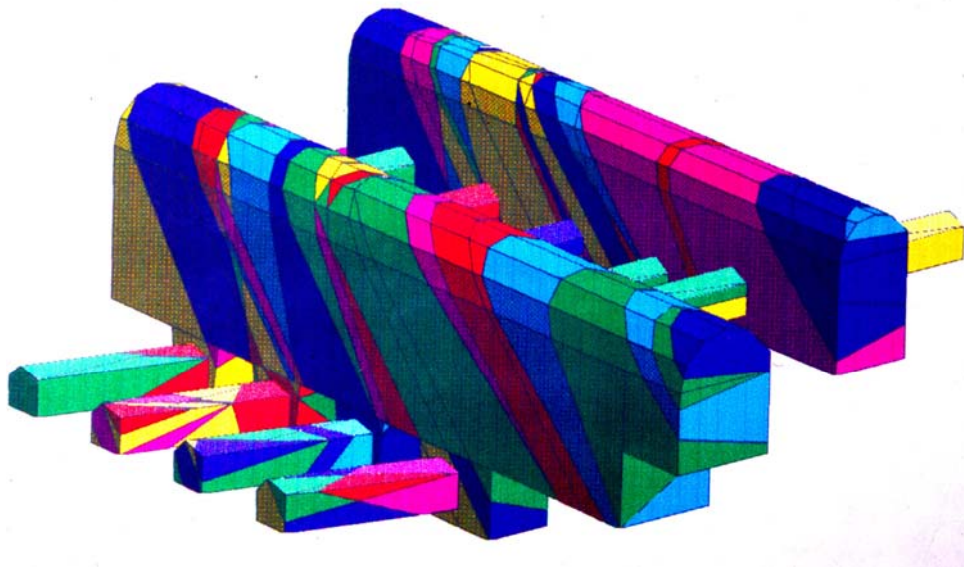
Figure 11.23: Isometric view of the 3DEC[4] model of the underground powerhouse cavern and transformer gallery of the Nathpa Jhakri Hydroelectric Project, analysed by Dr. B. Dasgupta[5].

---

[4] Available from ITASCA Consulting Group Inc., Thresher Square East, 708 South Third Street, Suite 310, Minneapolis, Minnesota 55415, USA. Fax 1 612 371 4717

[5] Formerly at the Institute of Rock Mechanics (Kolar), Kolar Gold Fields, Karnataka, now with of Advanced Technology and Engineering Services, Delhi. India.

The support for the powerhouse cavern consists of rockbolts and mesh reinforced shotcrete. Alternating 6 and 8 m long 32 mm diameter bolts on 1 x 1 m and 1.5 x 1.5 m centres are used in the arch. Alternating 9 and 7.5 m long 32 mm diameter bolts are used in the upper and lower sidewalls with alternating 9 and 11 m long 32 mm rockbolts in the centre of the sidewalls, all at a grid spacing of 1.5 m. Shotcrete consists of two 50 mm thick layers of plain shotcrete with an interbedded layer of weldmesh. The support provided by the shotcrete was not included in the support design analysis, which relies upon the rockbolts to provide all the support required.

In the headrace tunnel, some zones of sheared quartz mica schist have been encountered and these have resulted in large displacements as illustrated in Figure 11.24. This is a common problem in hard rock tunnelling where the excavation sequence and support system have been designed for 'average' rock mass conditions. Unless very rapid changes in the length of blast rounds and the installed support are made when an abrupt change to poor rock conditions occurs, for example when a fault is encountered, problems with controlling tunnel deformation can arise.

The only effective way known to the authors for anticipating this type of problem is to keep a probe hole ahead of the advancing face at all times. Typically, a long probe hole is percussion drilled during a maintenance shift and the penetration rate, return water flow and chippings are constantly monitored during drilling. Where significant problems are indicated by this percussion drilling, one or two diamond-drilled holes may be required to investigate these problems in more detail. In some special cases, the use of a pilot tunnel may be more effective in that it permits the ground properties to be defined more accurately than is possible with probe hole drilling. In addition, pilot tunnels allow pre-drainage and pre-reinforcement of the rock ahead of the development of the full excavation profile.
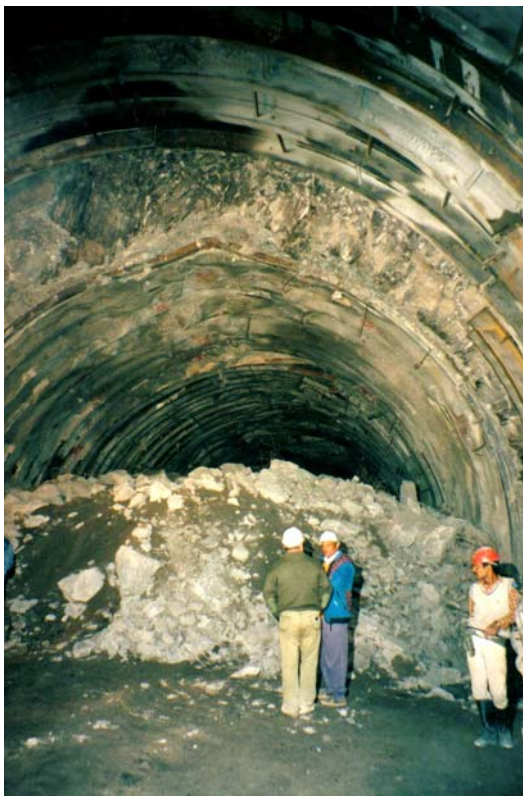
Figure 11.24: Large displacements in the top heading of the headrace tunnel of the Nathpa Jhakri Hydroelectric project. These displacements are the result of deteriorating rock mass quality when tunnelling through a fault zone.

11.10.4 Poor quality rock mass at shallow depth

Kavvadas et al (1996) have described some of the geotechnical issues associated with the construction of 18 km of tunnels and the 21 underground stations of the Athens Metro. These excavations are all shallow with typical depths to tunnel crown of between 15 and 20 m. The principal problem is one of surface subsidence rather than failure of the rock mass surrounding the openings.

The rock mass is locally known as Athenian schist which is a term erroneously used to describe a sequence of Upper Cretaceous flysch-type sediments including thinly bedded clayey and calcareous sandstones, siltstones (greywackes), slates, shales and limestones. During the Eocene, the Athenian schist formations were subjected to intense folding and thrusting. Later extensive faulting caused extensional fracturing and widespread weathering and alteration of the deposits.

The GSI values, estimated from Bieniawski's 1976 RMR classification, modified as recommended by Hoek, Kaiser and Bawden (1995) ranges from about 15 to about 45. The higher values correspond to the intercalated layers of sandstones and limestones, which can be described as BLOCKY/DISTURBED and POOR (Table 11.6). The completely decomposed schist can be described as DISINTEGRATED and VERY POOR and has GSI values ranging from 15 to 20. Rock mass properties for the completely decomposed schist, using a GSI value of 20, are as follows:

Intact rock strength	σ_{ci}	5-10 MPa	Constant	a	0.55
Hoek-Brown constant	m_i	9.6	Friction angle	ϕ'	22.4°
Geological Strength Index	GSI	20	Cohesive strength	c'	0.09-0.18 MPa
Hoek-Brown constant	m_b	0.55	Rock mass strength	σ_{cm}	0.27-0.53 MPa
Hoek-Brown constant	s	0	Deformation modulus	E_m	398-562 MPa

The Academia, Syntagma, Omonia and Olympion stations were constructed using the New Austrian Tunnelling Method twin side drift and central pillar method as illustrated in Figure 11.25. The more conventional top heading and bench method, illustrated in Figure 11.26, was used for the excavation of the Ambelokipi station. These stations are all 16.5 m wide and 12.7 m high. The appearance of the rock mass in one of the Olympion station side drift excavations is illustrated in Figures 11.27 and 11.28.

Numerical analyses of the two excavation methods showed that the twin side drift method resulted in slightly less rock mass failure in the crown of the excavation. However, the final surface displacements induced by the two excavation methods were practically identical.

Maximum vertical displacements of the surface above the centre-line of the Omonia station amounted to 51 mm. Of this, 28 mm occurred during the excavation of the side drifts, 14 mm during the removal of the central pillar and a further 9 mm occurred as a time dependent settlement after completion of the excavation. According to Kavvadas et al (1996), this time dependent settlement is due to the dissipation of excess pore water pressures which were built up during excavation. In the case of the Omonia station, the excavation of recesses towards the eastern end of

the station, after completion of the station excavation, added a further 10 to 12 mm of vertical surface displacement at this end of the station.
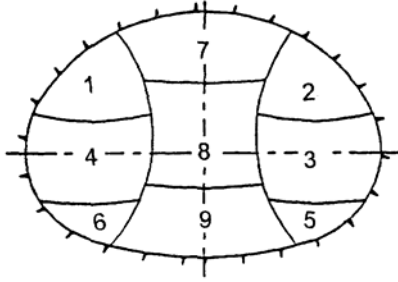
Figure 11.25: Twin side drift and central pillar excavation method. Temporary support consists of double wire mesh reinforced 250 - 300 mm thick shotcrete shells with embedded lattice girders or HEB 160 steel sets at 0.75 - 1 m spacing.
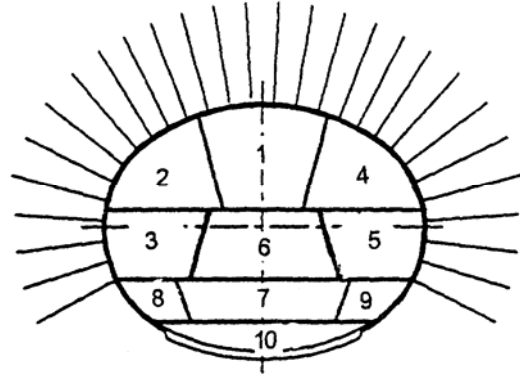
Figure 11.26: Top heading and bench method of excavation. Temporary support consists of a 200 mm thick shotcrete shell with 4 and 6 m long untensioned grouted rockbolts at 1.0 - 1.5 m spacing

Figure 11.27: Side drift in the Athens Metro Olympion station excavation that was excavated by the method illustrated in Figure 11.25. The station has a cover depth of approximately 10 m over the crown.
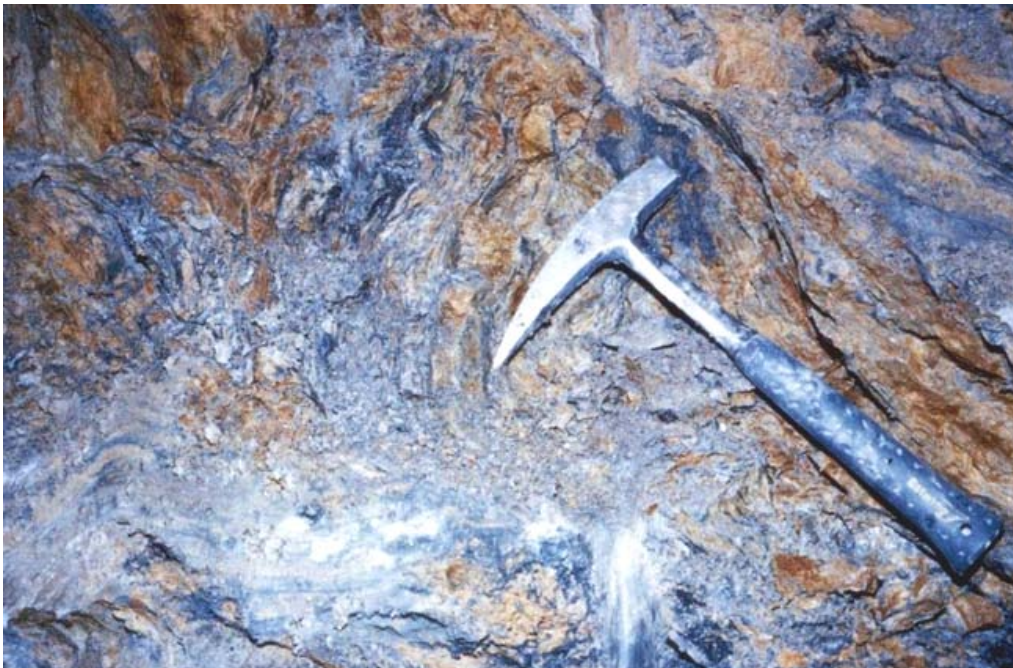
Figure 11.28: Appearance of the very poor quality Athenian Schist at the face of the side heading illustrated in Figure 11.27.

11.10.5 Poor quality rock mass under high stress

The Yacambú Quibor tunnel in Venezuela is considered to be one of the most difficult tunnels in the world. This 26 km long water supply tunnel through the Andes is being excavated in sandstones and phyllites at depths of up to 1200 m below surface. The graphitic phyllite is a very poor quality rock and gives rise to serious squeezing problems which, without adequate support, result in complete closure of the tunnel. A full-face tunnel-boring machine was completely destroyed in 1979 when trapped by squeezing ground conditions.

At its worst, the graphitic phyllite has an unconfined compressive strength of about 15 MPa and the estimated GSI value is about 24. Typical rock mass properties are as follows:

Intact rock strength	σ_{ci}	15 MPa	Constant	a	0.53
Hoek-Brown constant	m_i	10	Friction angle	ϕ'	24°
Geological Strength Index	GSI	24	Cohesive strength	c'	0.34 MPa
Hoek-Brown constant	m_b	0.66	Rock mass strength	σ_{cm}	1 MPa
Hoek-Brown constant	s	0	Deformation modulus	E_m	870 MPa

Various support methods have been used on this tunnel and only one will be considered here. This was a trial section of tunnel, at a depth of about 600 m, constructed in 1989. The support of the 5.5 m span tunnel was by means of a complete ring of 5 m long, 32 mm diameter untensioned grouted dowels with a 200 mm thick shell of reinforced shotcrete. This support system proved to be very effective but was later abandoned in favour of yielding steel sets (steel sets with sliding joints) because of construction schedule considerations.

Examples of the results of a typical numerical stress analysis of this trial section, carried out using the program PHASE[2], are given in Figures 11.28 and 11.29. Figure 11.28 shows the extent of failure, with and without support, while Figure 11.29 shows the displacements in the rock mass surrounding the tunnel. Note that the criteria used to judge the effectiveness of the support design are that the zone of failure surrounding the tunnel should lie within the envelope of the rockbolt support, the rockbolts should not be stressed to failure and the displacements should be of reasonable magnitude and should be uniformly distributed around the tunnel. All of these objectives were achieved by the support system described earlier.
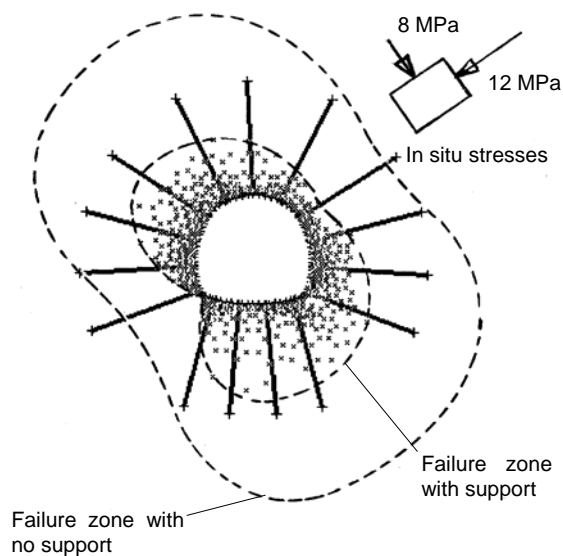
Figure 11.28: Results of a numerical analysis of the failure of the rock mass surrounding the Yacambu-Quibor tunnel when excavated in graphitic phyllite at a depth of about 600 m below surface.
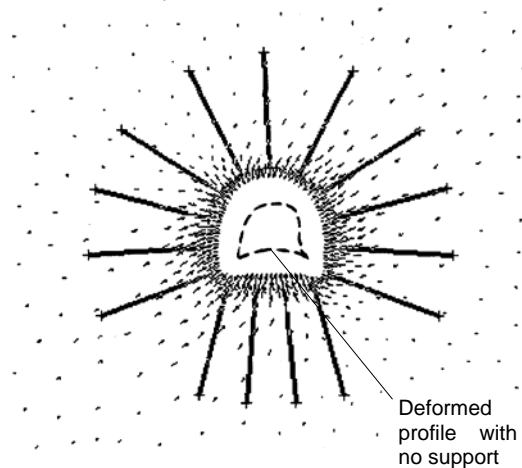
Figure 11.29: Displacements in the rock mass surrounding the Yacambu-Quibor tunnel. The maximum calculated displacement is 258 mm with no support and 106 mm with support.

11.10.6 Slope stability considerations

When dealing with slope stability problems in rock masses, great care has to be taken in attempting to apply the Hoek-Brown failure criterion, particularly for small steep slopes. As illustrated in Figure 11.30, even rock masses that appear to be good candidates for the application of the criterion can suffer shallow structurally controlled failures under the very low stress conditions which exist in such slopes.

As a general rule, when designing slopes in rock, the initial approach should always be to search for potential failures controlled by adverse structural conditions. These may take the form of planar failures on outward dipping features, wedge failures on intersecting features, toppling failures on inward dipping failures or complex failure modes involving all of these processes. Only when the potential for structurally controlled failures has been eliminated should consideration be given to treating the rock mass as an isotropic material as required by the Hoek-Brown failure criterion.

Figure 11.30: Structurally controlled failure in the face of a steep bench in a heavily jointed rock mass.

Figure 11.31 illustrates a case in which the base of a slope failure is defined by an outward dipping fault which does not daylight at the toe of the slope. Circular failure through the poor quality rock mass overlying the fault allows failure of the toe of the slope. Analysis of this problem was carried out by assigning the rock mass at the toe properties that had been determined by application of the Hoek-Brown criterion. A search for the critical failure surface was carried out utilising the program XSTABL[6] which allows complex failure surfaces to be analysed and which includes facilities for the input of non-linear failure characteristics as defined by equation 11.2.
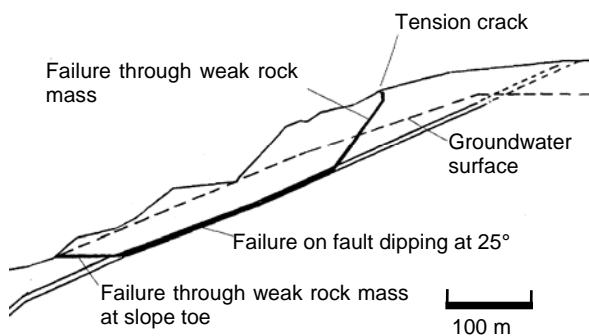
Figure 11.31: Complex slope failure controlled by an outward dipping basal fault and circular failure through the poor quality rock mass overlying the toe of the slope.

---

[6] Available from Interactive Software Designs, Inc., 953 N. Cleveland Street, Moscow, Idaho, USA 83843, Fax + 1 208 885 6608

12

Tunnels in weak rock

12.1 Introduction

Tunnelling in weak rock presents some special challenges to the geotechnical engineer since misjudgements in the design of support systems can lead to very costly failures. In order to understand the issues involved in the process of designing support for this type of tunnel it is necessary to examine some very basic concepts of how a rock mass surrounding a tunnel deforms and how the support systems acts to control this deformation. Once these basic concepts have been explored, examples of practical support designs for different conditions will be considered.

12.2 Deformation around an advancing tunnel

Figure 12.1 shows the results of a three-dimensional finite element analysis of the deformation of the rock mass surrounding a circular tunnel advancing through a weak rock mass subjected to equal stresses in all directions. The plot shows displacement vectors in the rock mass as well as the shape of the deformed tunnel profile. Figure 12.2 gives a graphical summary or the most important features of this analysis.

Deformation of the rock mass starts about one half a tunnel diameter ahead of the advancing face and reaches its maximum value about one and one half diameters behind the face. At the face position about one third of the total radial closure of the tunnel has already occurred and the tunnel face deforms inwards as illustrated in Figures 12.1 and 12.2. Whether or not these deformations induce stability problems in the tunnel depends upon the ratio of rock mass strength to the in situ stress level, as will be demonstrated in the following pages.

Note that it is assumed that deformation process described occurs immediately upon excavation of the face. This is a reasonable approximation for most tunnels in rock. The effects of time dependent deformations upon the performance of the tunnel and the design of the support system will be not be discussed in this chapter.

12.3 Tunnel deformation analysis

In order to explore the concepts of rock support interaction in a form which can readily be understood, a very simple analytical model will be utilised. This model involves a circular tunnel subjected to a hydrostatic stress field in which the horizontal and vertical stresses are equal.
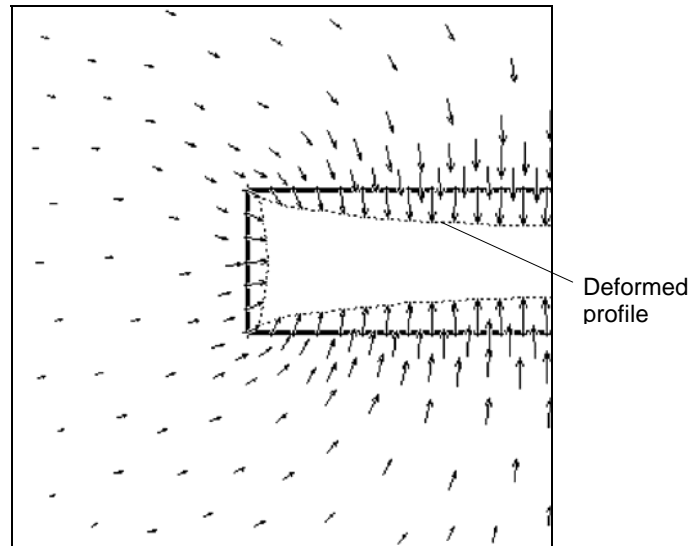
Figure 1: Vertical section through a three-dimensional finite element model of the failure and deformation of the rock mass surrounding the face of an advancing circular tunnel. The plot shows displacement vectors as well as the shape of the deformed tunnel profile.
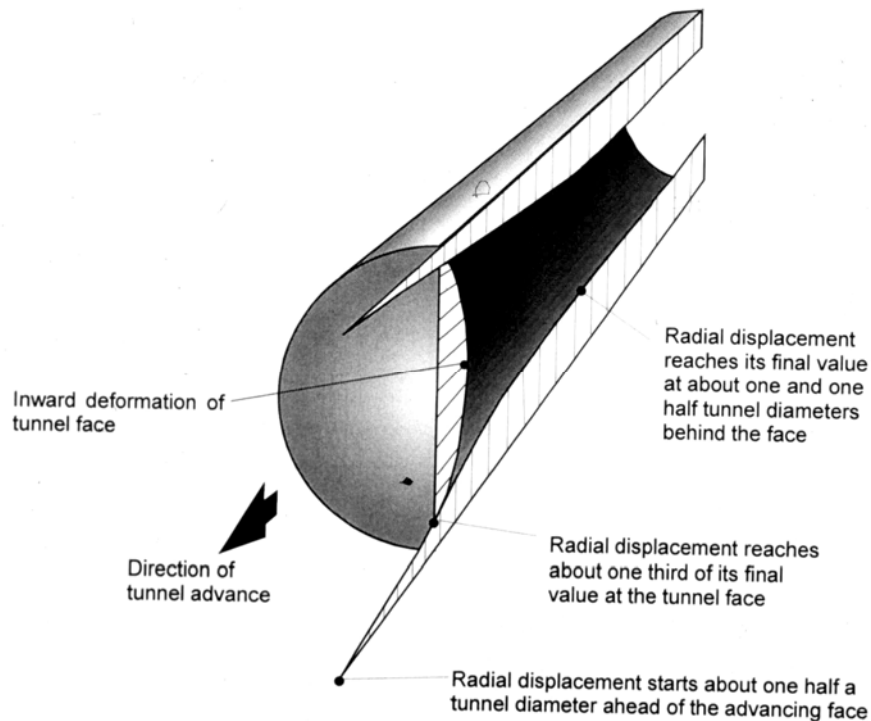
Figure 2: Pattern of deformation in the rock mass surrounding an advancing tunnel.

In this analysis it is assumed that the surrounding heavily jointed rock mass behaves as an elastic-perfectly plastic material in which failure involving slip along intersecting

discontinuities is assumed to occur with zero plastic volume change (Duncan Fama, 1993). Support is modelled as an equivalent internal pressure and, although this is an idealised model, it provides useful insights on how support operates.

12.3.1 Definition of failure criterion

It is assumed that the onset of plastic failure, for different values of the effective confining stress σ_3', is defined by the Mohr-Coulomb criterion and expressed as:

$$\sigma_1' = \sigma_{cm} + k\sigma_3' \tag{12.1}$$

The uniaxial compressive strength of the rock mass σ_{cm} is defined by:

$$\sigma_{cm} = \frac{2c'\cos\phi'}{(1-\sin\phi')} \tag{12.2}$$

and the slope k of the σ_1' versus σ_3' line as:

$$k = \frac{(1+\sin\phi')}{(1-\sin\phi')} \tag{12.3}$$

where σ_1' is the axial stress at which failure occurs

σ_3' is the confining stress

c' is the cohesive strength and

ϕ' is the angle of friction of the rock mass

In order to estimate the cohesive strength c' and the friction angle ϕ' for an actual rock mass, the Hoek-Brown criterion (Hoek and Brown 1997) can be utilised. Having estimated the parameters for failure criterion, values for c' and ϕ' can be calculated as described in Chapter 11.

12.3.2 Analysis of tunnel behaviour

Assume that a circular tunnel of radius r_o is subjected to hydrostatic stresses p_o and a uniform internal support pressure p_i as illustrated in Figure 12.3. Failure of the rock mass surrounding the tunnel occurs when the internal pressure provided by the tunnel lining is less than a critical support pressure p_{cr}, which is defined by:

$$p_{cr} = \frac{2p_o - \sigma_{cm}}{1+k} \tag{12.4}$$
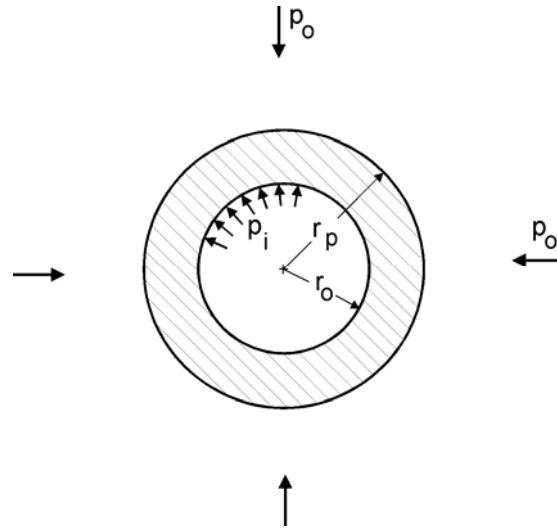
Figure 12.3: Plastic zone surrounding a circular tunnel.

If the internal support pressure p_i is greater than the critical support pressure p_{cr}, no failure occurs, the behaviour of the rock mass surrounding the tunnel is elastic and the inward radial elastic displacement of the tunnel wall is given by:

$$u_{ie} = \frac{r_o(1+\nu)}{E_m}(p_o - p_i) \tag{12.5}$$

where E_m is the Young's modulus or deformation modulus and
ν is the Poisson's ratio.

When the internal support pressure p_i is less than the critical support pressure p_{cr}, failure occurs and the radius r_p of the plastic zone around the tunnel is given by:

$$r_p = r_o \left[\frac{2(p_o(k-1)+\sigma_{cm})}{(1+k)((k-1)p_i+\sigma_{cm})} \right]^{\frac{1}{(k-1)}} \tag{12.6}$$

For plastic failure, the total inward radial displacement of the walls of the tunnel is:

$$u_{ip} = \frac{r_o(1+\nu)}{E} \left[2(1-\nu)(p_o-p_{cr})\left(\frac{r_p}{r_o}\right)^2 - (1-2\nu)(p_o-p_i) \right] \tag{12.7}$$

A spreadsheet for the determination of the strength and deformation characteristics of the rock mass and the behaviour of the rock mass surrounding the tunnel is given in Figure 12.4.

Input:	sigci =	10	MPa		mi =	10			GSI =	25	
	mu =	0.30			ro =	3.0	m		po =	2.0	Mpa
	pi =	0.0	MPa		pi/po =	0.00					

Output:	mb =	0.69			s =	0.0000			a =	0.525	
	k =	2.44			phi =	24.72	degrees		coh =	0.22	MPa
	sigcm =	0.69	MPa		E =	749.9	MPa		pcr =	0.96	MPa
	rp =	6.43	m		ui =	0.0306	m		ui=	30.5957	mm

sigcm/po	0.3468		rp/ro = 2.14		ui/ro =	0.0102

Calculation:

									Sums
sig3	1E-10	0.36	0.71	1.1	1.43	1.79	2.14	2.50	10.00
sig1	0.00	1.78	2.77	3.61	4.38	5.11	5.80	6.46	29.92
sig3sig1	0.00	0.64	1.98	3.87	6.26	9.12	12.43	16.16	50
sig3sq	0.00	0.13	0.51	1.15	2.04	3.19	4.59	6.25	18

Cell formulae:

mb = mi*EXP((GSI-100)/28)

s = IF(GSI>25,EXP((GSI-100)/9),0)

a = IF(GSI>25,0.5,0.65-GSI/200)

sig3 = Start at 1E-10 (to avoid zero errors) and increment in 7 steps of sigci/28 to 0.25*sigci

sig1 = sig3+sigci*(((mb*sig3)/sigci)+s)^a

k = (sumsig3sig1 - (sumsig3*sumsig1)/8)/(sumsig3sq-(sumsig3^2)/8)

phi = ASIN((k-1)/(k+1))*180/PI()

coh = (sigcm*(1-SIN(phi*PI()/180)))/(2*COS(phi*PI()/180))

sigcm = sumsig1/8 - k*sumsig3/8

E = IF(sigci>100,1000*10^((GSI-10)/40),SQRT(sigci/100)*1000*10^((GSI-10)/40))

pcr = (2*po-sigcm)/(k+1)

rp = IF(pi<pcr,ro*(2*(po*(k-1)+sigcm)/((1+k)*((k-1)*pi+sigcm)))^(1/(k-1)),ro)

ui = IF(rp>ro,ro*((1+mu)/E)*(2*(1-mu)*(po-pcr)*((rp/ro)^2)-(1-2*mu)*(po-pi)),ro*(1+mu)*(po-pi)/E)

Figure 12.4: Spreadsheet for the calculation of rock mass characteristics and the behaviour of the rock mass surrounding a circular tunnel in a hydrostatic stress field.

12.4 Dimensionless plots of tunnel deformation

A useful means of studying general behavioural trends is to create dimensionless plots from the results of parametric studies. Two such dimensionless plots are presented in Figures 12.5 and 12.6. These plots were constructed from the results of a Monte Carlo analysis in which the input parameters for rock mass strength and tunnel deformation were varied at random in 2000 iterations [1]. It is remarkable that, in spite of the very wide range of conditions included in these analyses, the results follow a very similar trend and that it is possible to fit curves which give a very good indication of the average trend.

---

[1] Using the program @RISK in conjunction with a Microsoft Excel spreadsheet for estimating rock mass strength and tunnel behaviour (equations 4 to 7). Uniform distributions were sampled for the following input parameters, the two figures in brackets define the minimum and maximum values used: Intact rock strength σ_{ci} (1,30 MPa), Hoek-Brown constant m_i (5,12), Geological Strength Index GSI (10,35), In situ stress (2, 20 MPa), Tunnel radius (2, 8 m).

The equation shown on the plot:

$$\frac{r_p}{r_o} = 1.25\left(\frac{\sigma_{cm}}{p_o}\right)^{-0.57}$$
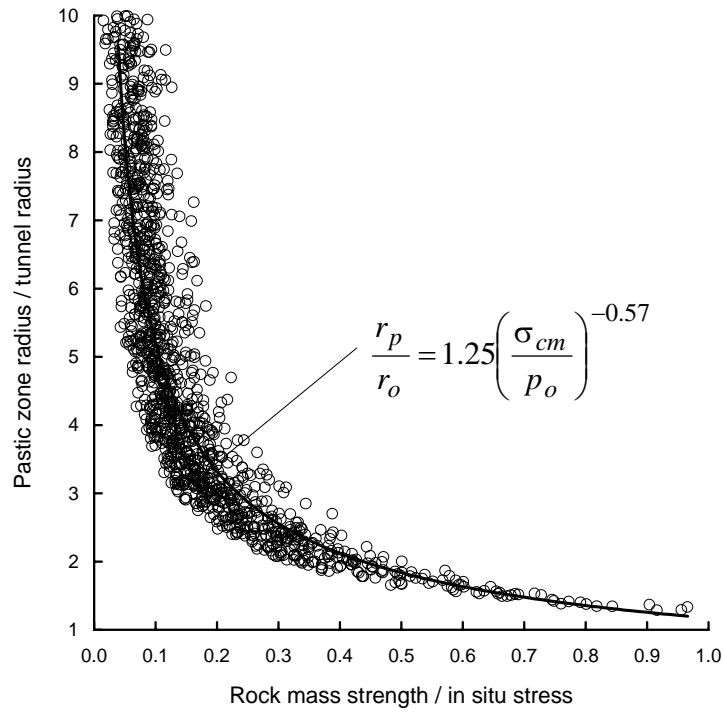
Figure 12.5: Relationship between size of plastic zone and ratio of rock mass strength to in situ stress.

The equation shown on the plot:

$$\frac{u_i}{r_o} = 0.002\left(\frac{\sigma_{cm}}{p_o}\right)^{-2}$$
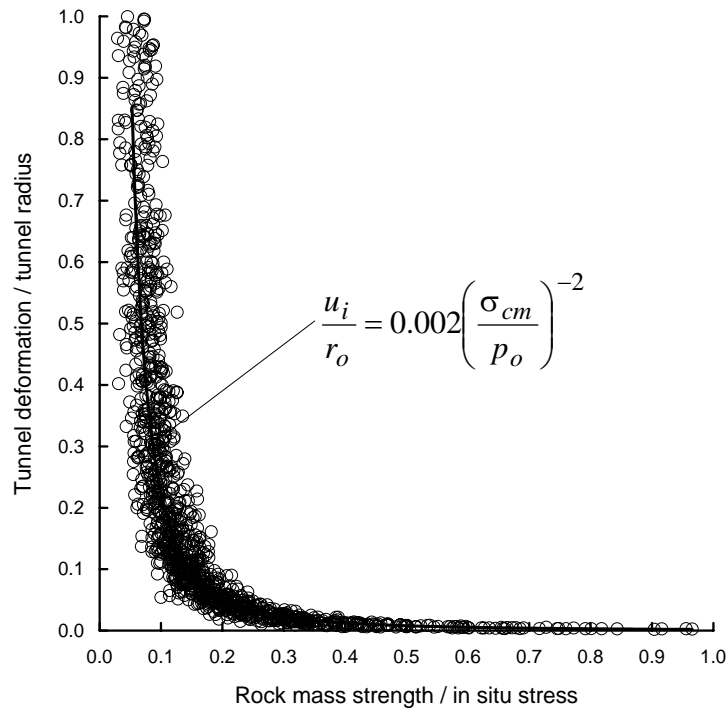
Figure 12.6: Tunnel deformation versus ratio of rock mass strength to in situ stress.

Figure 12.5 gives a plot of the ratio to plastic zone radius to tunnel radius versus the ratio of rock mass strength to in situ stress. This plot shows that the plastic zone size increases very rapidly once the rock mass strength falls below 20% of the rock mass strength. Practical experience suggests that, once this rapid growth stage is reached it becomes very difficult to control the stability of the tunnel.

Figure 12.6 is a plot of the ratio of tunnel deformation to tunnel radius against the ratio of rock mass strength to in situ stress. Once the rock mass strength falls below 20% of the in situ stress level, deformations increase substantially and, unless these deformations are controlled, collapse of the tunnel is likely to occur.

Figures 12.5 and 12.6 are for the condition of zero support pressure ($p_i = 0$). Similar analyses were run for a range of support pressure versus in situ stress ratios (p_i/p_o) and a statistical curve fitting process was used to determine the best fit curves for the generated data for each p_i/p_o value. These curves are given in Figures 12.7 and 12.8.

The series of curves shown in Figures 12.7 and 12.8 are defined by the equations:

$$\frac{rp}{ro} = \left(1.25 - 0.625\frac{p_i}{p_o}\right)\frac{\sigma_{cm}}{p_o}^{\left(\frac{p_i}{p_o}-0.57\right)}$$

(12.8)

$$\frac{ui}{ro} = \left(0.002 - 0.0025\frac{p_i}{p_o}\right)\frac{\sigma_{cm}}{p_o}^{\left(2.4\frac{p_i}{p_o}-2\right)}$$

(12.9)

where rp = Plastic zone radius
       u_I = Tunnel sidewall deformation
       r_o = Original tunnel radius in metres
       p_I = Internal support pressure
       p_o = In situ stress = depth below surface × unit weight of rock mass
       σ_{cm}=   Rock mass strength = $2c'\cos\phi'/(1-\sin\phi')$

An alternative plot of the data used to construct Figure 12.8 is given in Figure 12.9. For readers who have studied rock support interaction analyses this plot will be familiar and it gives a good indication of the influence of support pressures on tunnel deformation.

12.5   Estimates of support capacity

Hoek and Brown (1980a) and Brady and Brown (1985) have published equations which can be used to calculate the capacity of mechanically anchored rockbolts, shotcrete or concrete linings or steel sets for a circular tunnel. No useful purpose would be served by reproducing these equations here but they have been used to estimate the values plotted in Figure 12.10. This plot gives maximum support pressures (p_{sm}) and maximum elastic displacements (u_{sm}) for different support systems installed in circular tunnels of different diameters. Note that, in all cases, the support is assumed to act over the entire surface of the tunnel walls. In other words, the shotcrete and concrete linings are closed rings; the steel sets are complete circles; and the mechanically anchored rockbolts are installed in a regular pattern that completely surrounds the tunnel.
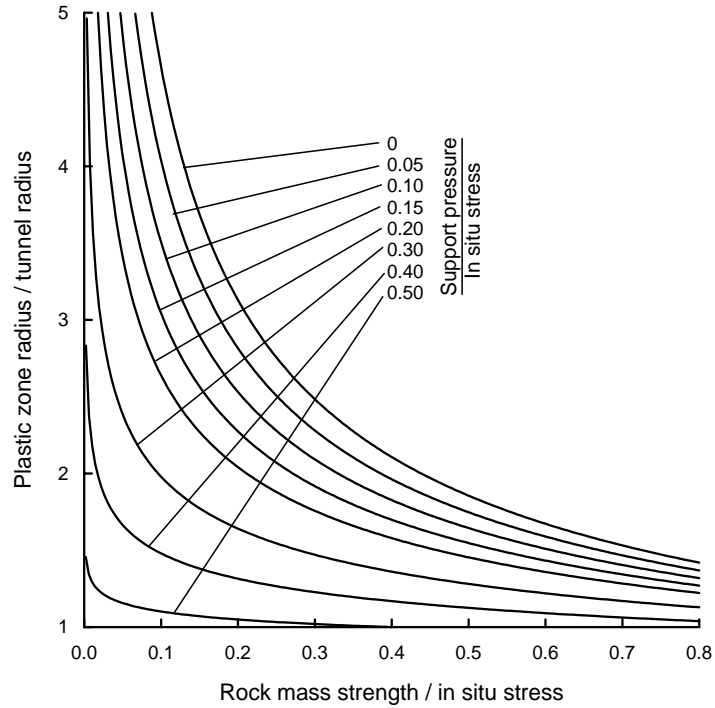
Figure 12.7: Ratio of plastic zone to tunnel radius versus the ratio of rock mass strength to in situ stress for different support pressures.
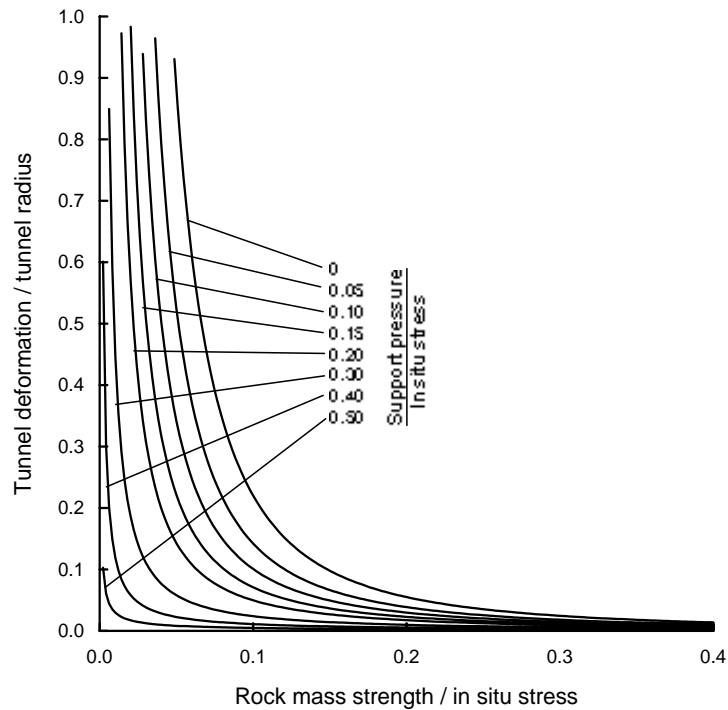
Figure 12.8: Ratio of tunnel deformation to tunnel radius versus the ratio of rock mass strength to in situ stress for different support pressures.
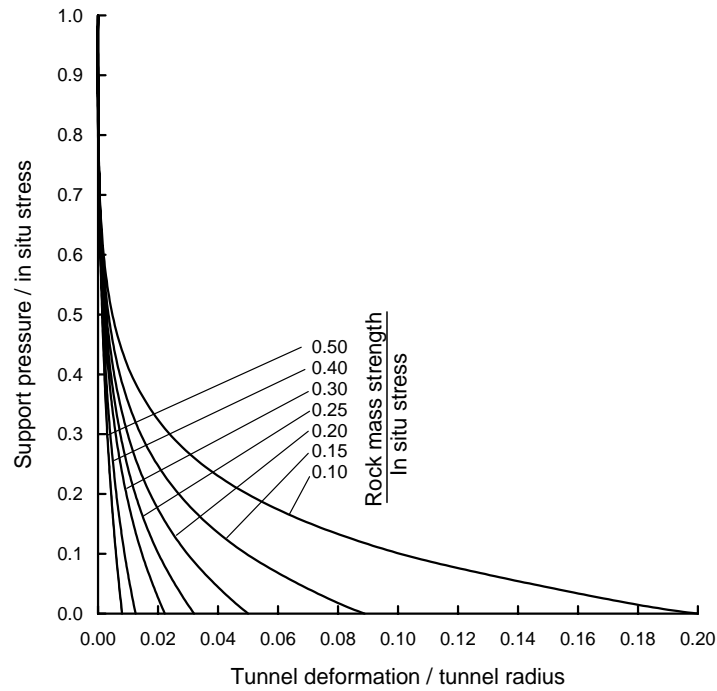
Figure 12.9: Relationship between support pressure and tunnel
deformation for different ratios of rock mass strength to in situ stress.
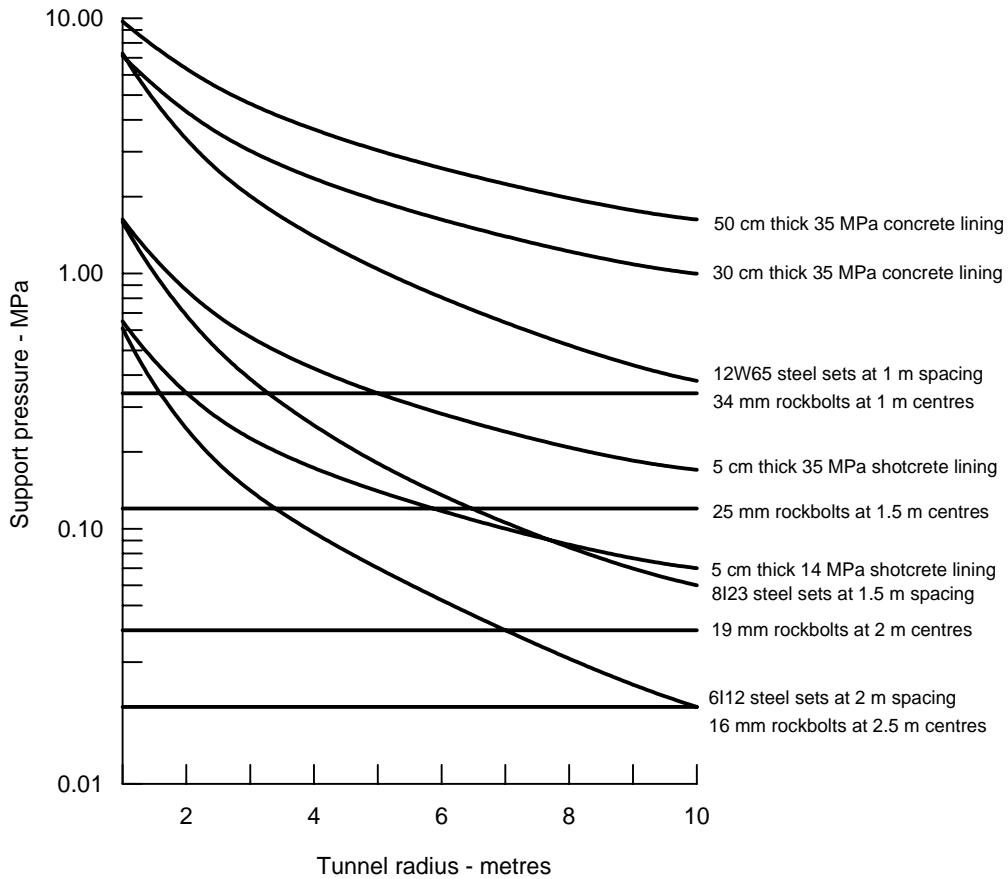
Figure 12.10: Estimates of support capacity for tunnels of different sizes.

Because this model assumes perfect symmetry under hydrostatic loading of circular tunnels, no bending moments are induced in the support. In reality, there will always be some asymmetric loading, particularly for steel sets and shotcrete placed on rough rock surfaces. Hence, induced bending will result in support capacities that are lower than those given in Figure 12.10. Furthermore, the effect of not closing the support ring, as is frequently the case, leads to a drastic reduction in the capacity and stiffness of steel sets and concrete or shotcrete linings.

12.6   Practical example

In order to illustrate the application of the concepts presented in this chapter, the following practical example is considered.

A 4 m span drainage tunnel is to be driven in the rock mass behind the slope of an open pit mine. The tunnel is at a depth of approximately 150 m below surface and the general rock is a granodiorite of fair quality. A zone of heavily altered porphyry associated with a fault has to be crossed by the tunnel and the properties of this zone, which has been exposed in the open pit, are known to be very poor. Mine management has requested an initial estimate of the behaviour of the tunnel and of the probable support requirements. The tunnel is to link up with an old mine drainage tunnel that was constructed several decades ago.

12.6.1 Estimate of rock mass properties

Figures 12.6 and 12.7 show that a crude estimate of the behaviour of the tunnel can be made if the ratio of rock mass strength to in situ stress is available. For the purpose of this analysis the in situ stress is estimated from the depth below surface and the unit weight of the rock. For a depth of 150 m and a unit weight of 0.027 MN/m^3, the vertical in situ stress is approximately 4 MPa. The fault material is considered incapable of sustaining high differential stress levels and it is assumed that the horizontal and vertical stresses are equal within the fault zone.

It has been found that the ratio of the uniaxial compressive strengths in the field and the laboratory $(\sigma_{cm}/\sigma_{ci})$, calculated by means of the spreadsheet given in Figure 11.7 in Chapter 11 and shown in Figure 12.11, can be estimated from the following equation:

$$\sigma_{cm} = (0.0034 m_i^{0.8})\sigma_{ci}\{1.029 + 0.025 e^{(-0.1 m_i)}\}^{GSI} \qquad (12.10)$$

where *GSI* is the Geological Strength Index and m_i is a material constant as proposed by Hoek and Brown (1997) and discussed in Chapter 11.

In the case of the granodiorite, the laboratory uniaxial compressive strength is approximately 100 MPa. However for the fault material, specimens can easily be broken by hand as shown in Figure 12.12. The laboratory uniaxial compressive strength of this material is estimated at approximately 10 MPa.

Based upon observations in the open pit mine slopes, the granodiorite is estimated to have a GSI value of approximately 55. The fault zone has been assigned GSI = 15. The rock mass descriptions that form the basis of these estimates are illustrated in Figure 12.13.
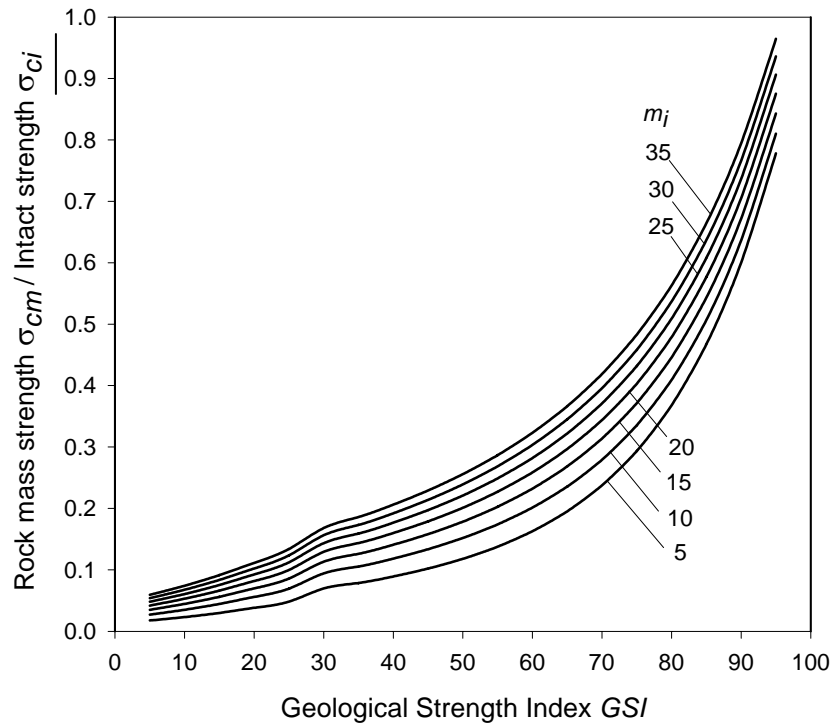
Figure 12.11: Relationship between in situ and laboratory uniaxial compressive strengths and the Geological Strength Index.
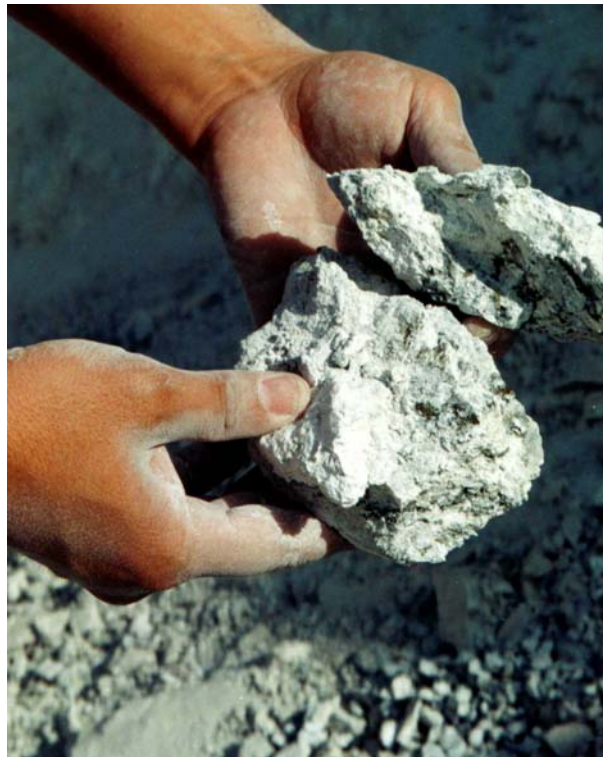
Figure 12.12: Heavily altered porphyry can easily be broken by hand.

Figure 12.13: Table for estimating GSI value (Hoek and Brown 1997) showing ranges of values for granodiorite and fault zone.
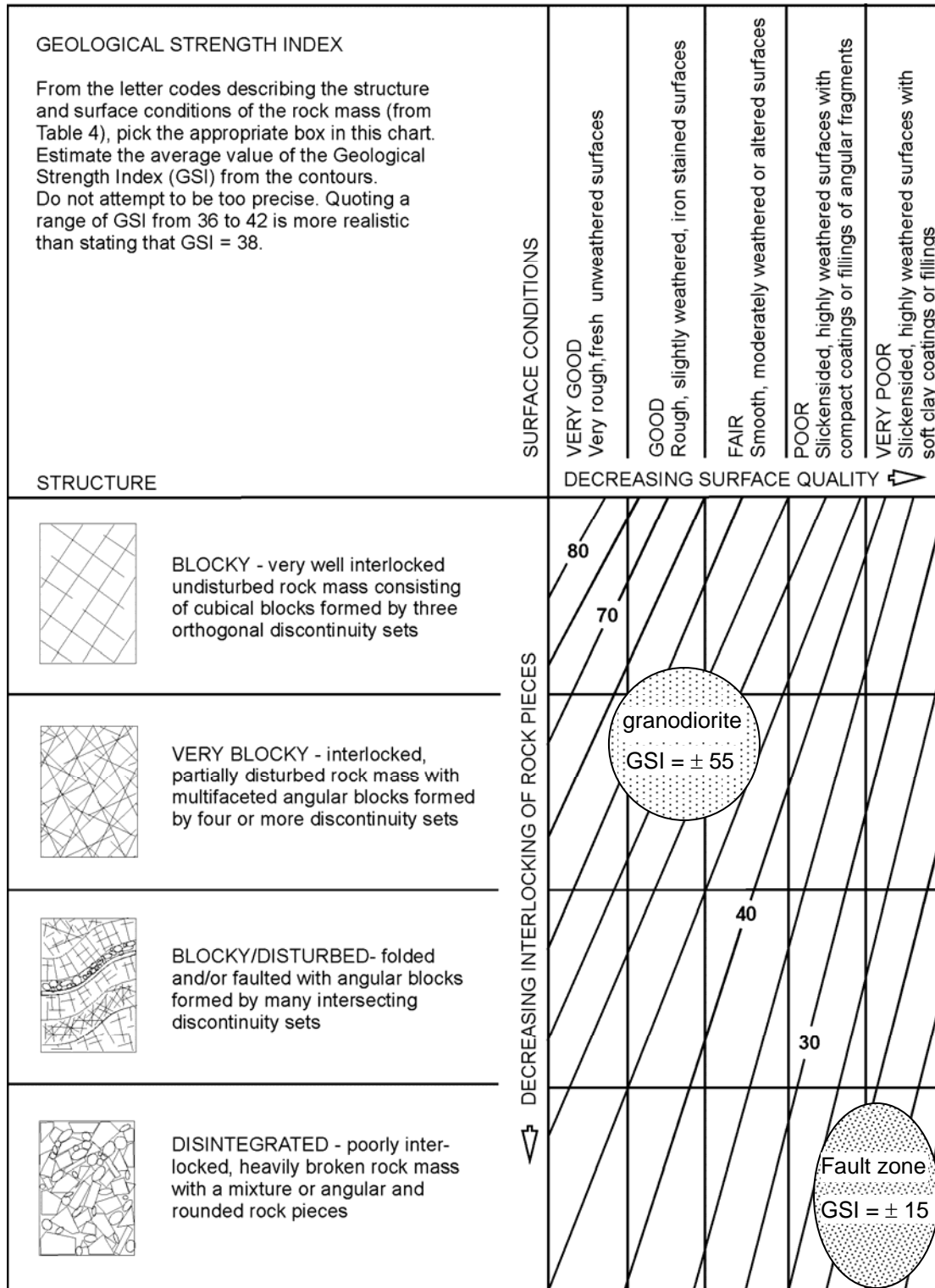
For the granodiorite, substitution of GSI = 55, m_i = 30 and σ_{ci} = 100 MPa into equation 12.10 gives an approximate value for the uniaxial compressive strength of the rock mass as 23 MPa. For an in situ stress of 4 MPa, this gives a ratio of rock mass strength to in situ stress in excess of 5. Figures 12.5 and 12.6 show that the size of the plastic zone and also the induced deformations will be negligibly small for is ratio. This conclusion is confirmed by the appearance of the old drainage tunnel that has stood for several decades without any form of support.

Based upon this evaluation, no permanent support should be required for the tunnel in the fair quality granodiorite. Temporary support in the form of spot bolts and shotcrete may be required for safety where the rock mass is heavily jointed.

In the case of the altered porphyry and fault material, substitution of GSI = 15, m_i = 12 and σ_{ci} = 10 MPa into equation 12.10 gives a rock mass strength of approximately 0.4. This, in turn, gives a ratio of rock mass strength to in situ stress of 0.1.

From Figure 12.5, the radius of plastic zone for a 2 m radius tunnel in this material is approximately 9.5 m without support. The tunnel deformation in approximately 0.4 m, giving a closure of 0.8 m. These conditions are clearly unacceptable and substantial support is required in order to prevent convergence and possible collapse of this section. Since this is a drainage tunnel, the final size is not a major issue and a significant amount of closure can be tolerated. However, experience suggests that the ratio of tunnel deformation to tunnel radius should be kept below about 0.02 in order to avoid serious instability problems. Figure 12.9 indicates that a ratio of support pressure to in situ stress of approximately 0.35 is required to restrain the deformation to this level for a rock mass with a ratio of rock mass strength to in situ stress of 0.1. This translates into a required support pressure of 1.4 MPa.

Because of the very poor quality of the rock mass and the presence of significant amount of clay, the use of rockbolts or cables is not appropriate because of the difficulty of achieving adequate anchorage. Consequently, support has to be in the form of shotcrete or concrete lining or closely spaced steel sets as suggested by Figure 12.10. Obviously, placement of a full concrete lining during tunnel driving is not practical and hence the remaining choice for support is the use of steel sets.

The problem of using heavy steel sets in a small tunnel is that bending of the sets is difficult. A practical rule of thumb is that an H or I section can only be bent to a radius of about 14 times the depth of the section. This problem is illustrated in Figure 12.14 that shows a heavy H section set being bent. In spite of the presence of temporary stiffeners, there is significant buckling of the inside flange of the set and a lot of additional work is required before the set can be sent underground.

The practical solution adopted in the actual case upon which this example is based was to use sliding joint top hat section sets. These sets, as delivered to site, are shown in Figure 12.15 which illustrates how the sections fit into each other. The assembly of these sets to form a sliding joint is illustrated in Figure 12.16 and the installation of the sets in the tunnel is illustrated in Figure 12.17.

The sets are installed immediately behind the advancing face which, in a rock mass such as that considered here, is usually excavated by hand. The clamps holding the joints are tightened to control the frictional force in the joints which slide progressively as the face is advanced and the rock load is applied to the sets.

Figure 12.14: Buckling of an H section steel set being bent to a small a radius. Temporary stiffeners have been tack welded into the section to minimise buckling but a considerable amount of work is required to straighten the flanges after these stiffeners have been removed.

Figure 12.15: Top hat section steel sets delivered to site ready to be transported underground.
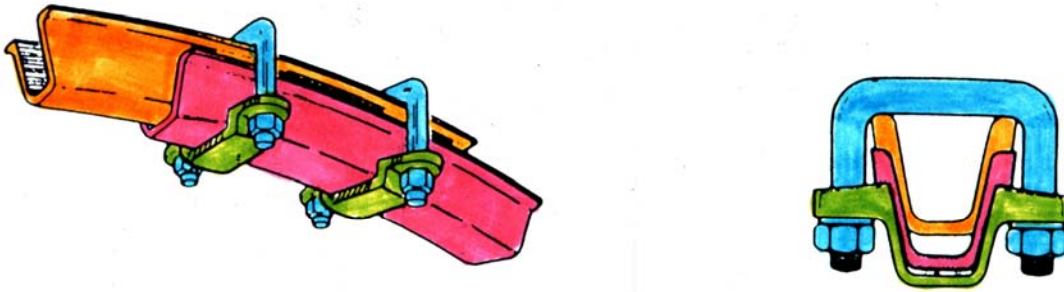
Figure 12.16: Assembly of a friction joint in a top hat section steel set.

Figure 12.17: Installation of sliding joint top hat section steel sets immediately behind the face of a tunnel being advanced through very poor quality rock.

The use of sliding joints in steel sets allows very much lighter section sets to be used than would be the case for sets with rigid joints. These sets provide immediate protection for the workers behind the face but they permit significant deformation of the tunnel to take place as the face is advanced. In most cases, a positive stop is welded onto the sets so that, after a pre-determined amount of deformation has occurred, the joint locks and the set becomes rigid. A trial and error process has to be used to find the amount of deformation that can be permitted before the set locks. Too little deformation will result in obvious buckling of the set while too much deformation will result in loosening of the surrounding rock mass.

In the case of the tunnel illustrated in Figure 12.17, lagging behind the sets consists of wooden poles of about 100 mm diameter. A variety of materials can be used for lagging but wood, in the form of planks or poles, is still the most common. In addition to the lagging, a timber mat has been propped against the face to improve the stability of the face. This is an important practical precaution since instability of the tunnel face can result in progressive ravelling ahead of the steel sets and, in some cases, collapse of the tunnel.

As an alternative to supporting the face, as illustrated in Figure 12.17, uses spiles to create an umbrella of reinforced rock ahead of the advancing face. Figures 12.18 illustrate the general principles of the technique. In the example illustrated, spiling is being used to advance a 7 m span, 3 m high tunnel top heading through a clay-rich fault zone material in a tunnel in India. The spiles, consisting of 25 mm steel bars, were driven in by means of a heavy sledgehammer.

Figure 12.18: Spiling in very poor quality clay-rich fault zone material.

Direction of face advance
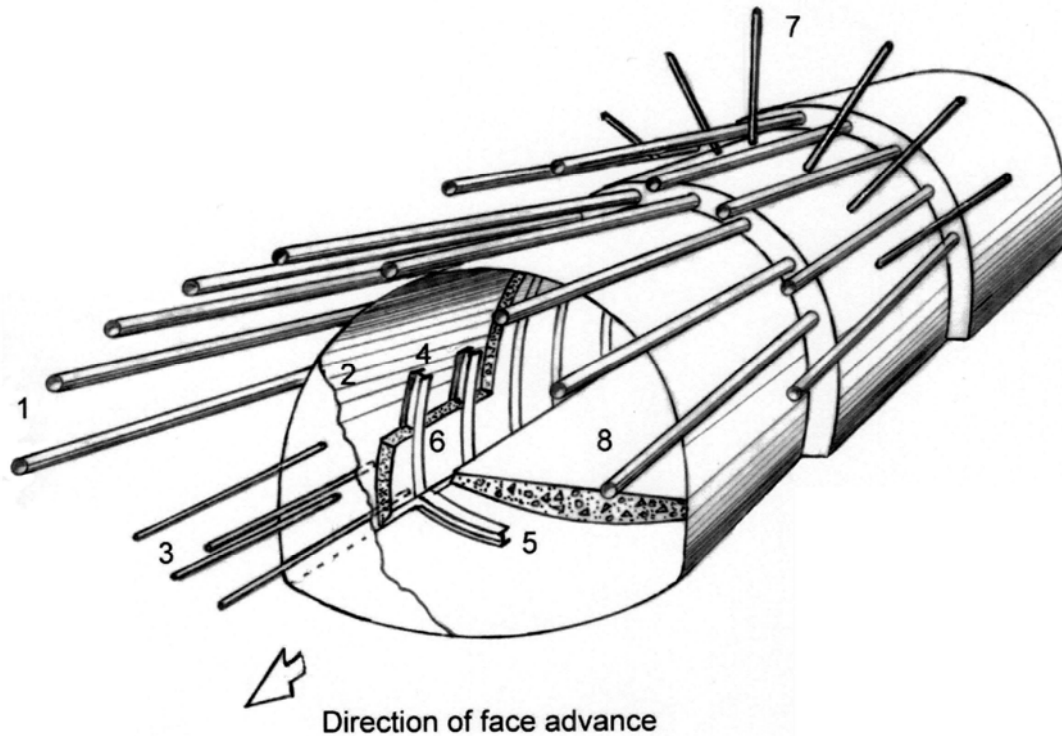
1   Forepoles – typically 75 or 114 mm diameter pipes, 12 m long installed every 8 m to create a 4 m overlap between successive forepole umbrellas.

2   Shotcrete – applied immediately behind the face and to the face, in cases where face stability is a problem. Typically, this initial coat is 25 to 50 mm thick.

3   Grouted fiberglass dowels – Installed midway between forepole umbrella installation steps to reinforce the rock immediately ahead of the face. These dowels are usually 6 to 12 m long and are spaced on a 1 m x 1 m grid.

4   Steel sets – installed as close to the face as possible and designed to support the forepole umbrella and the stresses acting on the tunnel.

5   Invert struts – installed to control floor heave and to provide a footing for the steel sets.

6   Shotcrete – typically steel fiber reinforced shotcrete applied as soon as possible to embed the steel sets to improve their lateral stability and also to create a structural lining.

7   Rockbolts as required. In very poor quality ground it may be necessary to use self-drilling rockbolts in which a disposable bit is used and is grouted into place with the bolt.

8   Invert lining – either shotcrete or concrete can be used, depending upon the end use of the tunnel.

Figure 12.19: Full face 10 m span tunnel excavation through weak rock under the protection of a forepole umbrella. The final concrete lining is not included in this figure.

For larger tunnels in very poor ground, forepoles are usually used to create a protective umbrella ahead of the face. These forepoles consist of 75 to 140 mm diameter steel pipes through which grout is injected. In oder for the forepoles to work effectively the rock mass should behave in a frictional manner so that arches or bridges can form between individual forepoles. The technique is not very effective in fault gouge material containing a siginifcant proportion of clay unless the forepole spacing is very close. The forepoles are in installed by means of a special drilling maching as illustrated in Figure 12.20.

Where the rock mass is suitable for the application of forepoles, consideration can be given to stabilising the face by means of fibreglass dowels grouted into the face as illustrated in Figure 12.19.

Figure 12.20: Installation of 12 m long 75 mm diameter pipe forepoles in an 11 m span tunnel top heading in a fault zone.

13

Large Powerhouse caverns in weak rock

13.1   Introduction

In the context of this discussion, weak rock is rock that will fail when subjected to the stress levels induced by the excavation of large underground caverns at depths of 100 to 300 m below surface. Sedimentary rocks such as bedded sandstones, shales, siltstones and mudstones are amongst the rocks which fall into this category. Tunnels and caverns associated with underground hydroelectric projects are sometimes excavated in rock masses of this type.

The design concepts discussed are based upon experience drawn from a number of hydroelectric projects. The choice of the size and shape of power and transformer caverns, the location of these caverns relative to each other and to the ground surface, the influence of joints and bedding planes on the stability of the excavations and the choice of the most appropriate support systems are issues which are common to all of these schemes. In applying these principles to a new scheme, the reader should be aware that each scheme will have its own set of rock mass properties, in situ stress conditions and design constraints imposed by mechanical, electrical and hydraulic considerations. Consequently, the general design concepts outlined here have to be modified to suit each scheme.

13.2   Rock mass strength

In most strong igneous and metamorphic rocks such as dolerites, basalts, granites, gneisses and quartzites, the stability of large caverns at depths of less than 500 m below surface depends almost entirely upon structurally controlled wedges and blocks that are released by the creation of the excavations. In these conditions, the excavation profile can be controlled with good blasting procedures, and the rock mass and any support placed in it are subjected to relatively small displacements. The strength of the rock itself plays a minor role in the behaviour of the rock mass which is controlled by intersecting joints, schistosity, bedding planes, shear zones and faults. Away from the major structures, the rock may be capable of standing unsupported during excavation for considerable periods of time, and the excavation and support of tunnel intersections with the cavern poses no particular problem. The evaluation of the stability of these excavations is carried out by means of limit equilibrium analyses. The factor of safety is calculated by comparing the shear strength of the discontinuities, which bound the potentially unstable blocks and wedges, with the driving forces due to the gravitational weight of these blocks and wedges as discussed in Chapter 5.

In the case of weaker sedimentary rocks, the strength of the rock material is generally lower and the rock mass is frequently more heavily jointed and more deeply weathered. The control of overbreak during excavation by drilling and blasting will be more difficult, and the rock mass and the supports placed in it may be subjected to deformations of up to 50 or 100 mm at the surface of the excavation. The sequence of excavation and support of tunnel intersections with the cavern will have to be controlled and will require careful engineering design. For these caverns, support will usually be required immediately after excavation. In designing these supports, failure of the rock material and sliding and rotation of individual blocks of rock within the rock mass have to be considered in addition to failure along structural features such as bedding planes, shear zones and faults.

The Hoek and Brown failure criterion, described in Chapter 11, provides a basis for estimating the strength of rock masses of the type under consideration here. For all the examples discussed, it has been assumed that the rock mass is a fair to poor quality siltstones and that its properties are defined by:

Uniaxial compressive strength of intact rock	$\sigma_c = 100$ MPa
Constant m_i for intact siltstone	$m_i = 10$
Geological Strength Index	$GSI = 48$
Rock mass constant	$m_b = 1.56$
Rock mass constant	$s = 0.003$
Deformation modulus	$E = 8900$ MPa
Poisson's ratio	$\nu = 0.3$
Friction angle	$\phi = 31°$
Cohesive strength	$c' = 4$ MPa

Figure 13.1 gives plots of the relationship between the maximum and minimum principal stresses and the shear and normal stresses at failure defined by the Hoek-Brown failure criterion.

13.3   In situ stress conditions

A study of the results of in situ stress measurements from around the world suggests that the horizontal stress is generally significantly greater than the vertical stress at depths below surface of less than 1000 m (Brown and Hoek (1978), Sheory (1994)). The vertical stress is normally assumed to be equal to the product of the unit weight of the rock mass and the depth below surface and measured in situ stresses are usually in reasonable agreement with this assumption. The ratio of average horizontal stress to vertical stress can be as high as 3 and values of 1.5 or 2 are frequently assumed for preliminary analyses.

It is always advisable to measure the in situ stresses in the vicinity of major underground caverns as early in the project feasibility study as possible. During early site investigations, when no underground access is available, the most commonly used method for measuring in situ stresses is hydrofracturing (Haimson (1978)). The hydraulic pressure required to produce fresh cracks and subsequently close and re-open them is used to estimate in situ stress levels. Once underground access is available, overcoring techniques can be used, as discussed in Chapter 10.
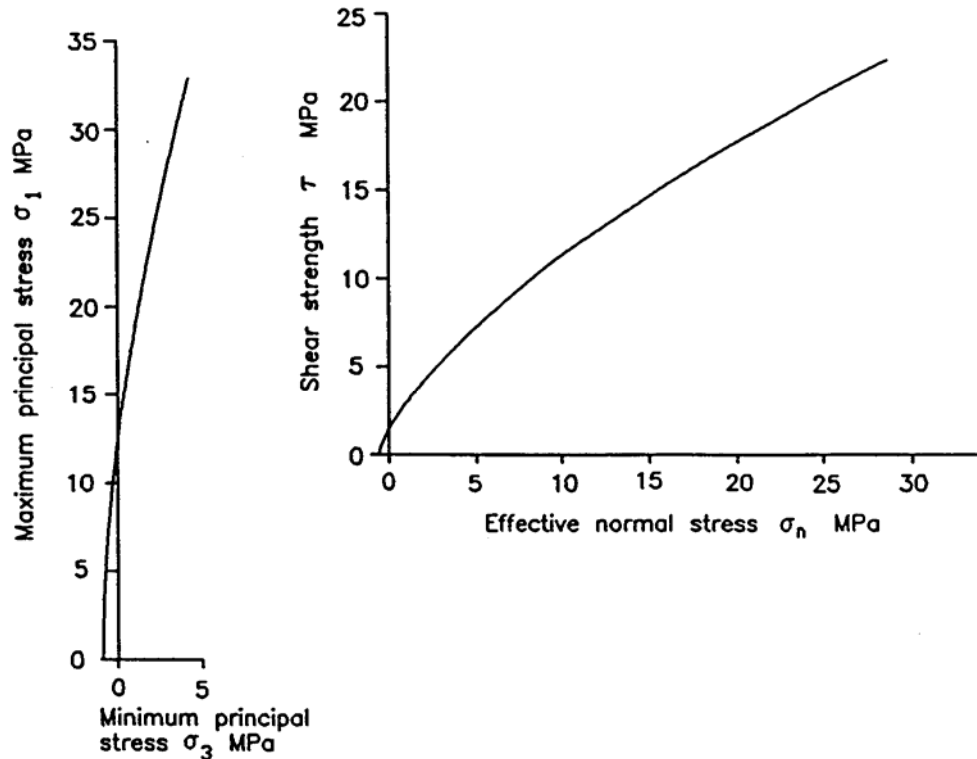
Figure 13.1: Plot of relationships between maximum and minimum principal stresses and normal and shear stresses for failure of a fair to poor quality siltstone. The properties of the siltstone are defined on the previous page.

13.3.1 Stresses around underground caverns near the toes of slopes

Since hydroelectric projects are frequently located in mountainous areas, the influence of surface topography upon the in situ stress field has to be taken into account in deciding upon the exact location of the underground powerhouse.

Figure 13.2 shows the maximum and minimum principal stresses in a gravitationally loaded slope with a far field horizontal to vertical in situ stress ratio of 3 : 1. The in situ stresses, particularly the minimum principal stress σ_3, are significantly altered in the vicinity of the slope face as compared with the far field stresses. These local changes in the in situ stress field influence the stresses induced in the rock mass surrounding an underground cavern located near the slope toe[1].

Figure 13.3 illustrates the results of a boundary element analysis in which an underground powerhouse cavern has been located at different distances from the toe of the slope analysed in Figure 13.2. Contours showing zones in which the tensile and shear strength of the rock mass have been exceeded are plotted in this figure. Failure trajectories in these overstressed zones indicate the direction in which failure of the rock would propagate, assuming the rock mass to be homogeneous.

---

[1]These analyses were carried out using the elastic boundary element program EXAMINE[2D] developed in the Department of Civil Engineering at the University of Toronto. The program is available from Rocscience Inc., 31 Balsam Avenue, Toronto, Ontario, Canada M4E 3B5, Fax 1 416 698 0908, Phone 1 416 698 8217, Email: software@rocscience.com, Internet http://www.rocscience.com.
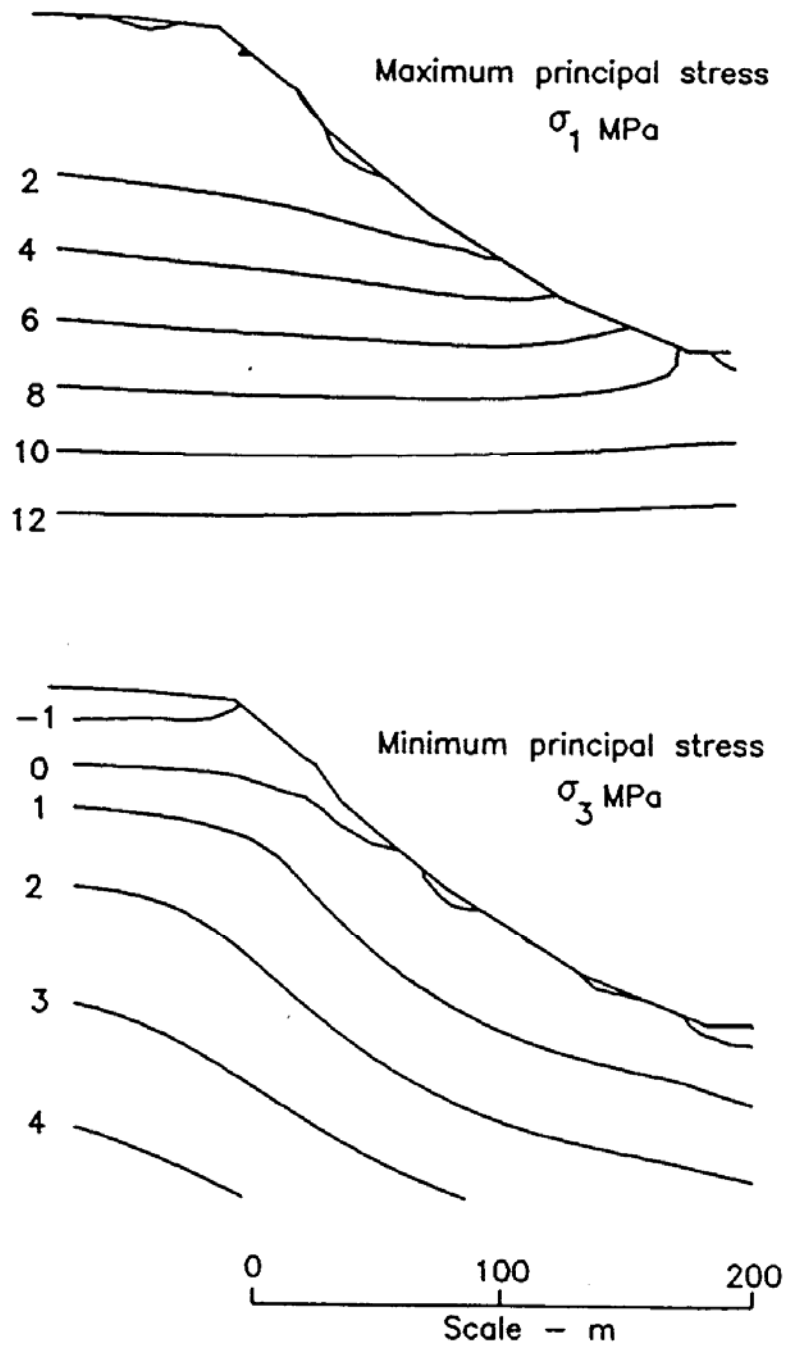
Figure 13.2: Distribution of maximum and minimum principal stresses in a gravitationally loaded slope with far field in situ stresses defined by a ratio of horizontal to vertical stress of 3:1
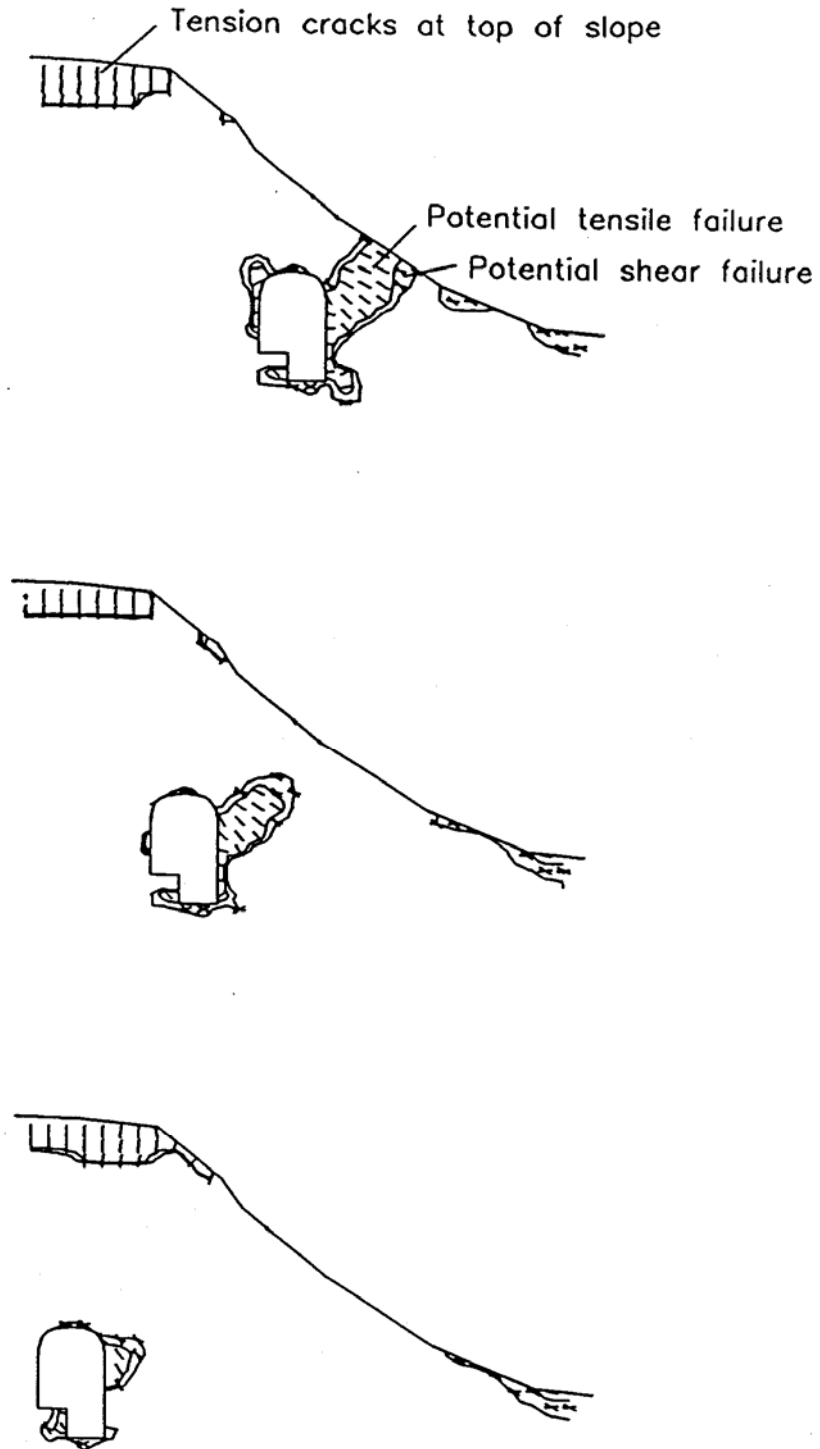
Figure 13.3: Zones of overstress and failure trajectories for a siltstone rock mass surrounding an underground cavern at different distances from the toe of the slope.

In all cases, vertical tension cracks would be generated at the crest of this particular slope and a minor amount of shear failure would occur near the toe. Such failures are common in slopes in weak rock masses and, once formed, are generally not a cause for concern since they are local in nature and result in stress relief and the re-establishment of equilibrium. Tension cracks, running parallel to the crests of slopes in sedimentary rock masses are common and have been observed to remain stable for many years. Usually, they have had no significant influence on the overall behaviour of the slope.

The zones of overstress in the rock surrounding the cavern are significantly different in the three cases illustrated. For the case in which the power cavern is closest to the slope toe, the extension of the overstressed zone to the slope face could result in the generation of local slope instability and could also result in the formation of a highly permeable zone between the slope face and the downstream wall of the cavern. In addition, the extent and the asymmetrical shape of the zone of overstressed rock suggests that substantial support in the form of long grouted cables would be required to stabilise the rock mass surrounding the cavern. The author considers this cavern to be too close to the toe of the slope and would recommend moving it further into the rock mass.

The zones of overstress in the case of the cavern located furthest from the slope toe are much smaller than for the other two cases and the rock mass surrounding this cavern could probably be stabilised with a relatively modest array of grouted cables.

In considering the three options illustrated in Figure 13.3, it must be remembered that geotechnical factors are not the only items which have to be considered in deciding upon the cavern location. Another important factor is the length of the tailrace tunnels. Hydraulic engineers usually want to keep these as short as possible in order to avoid the need for a downstream surge shaft to compensate for pressure fluctuations. Once the tailrace tunnel length approaches 100 m the need for a downstream surge shaft has to be considered.

13.3.2 *Determination of steel lining length for pressure tunnels*

Although not related to cavern design, the determination of the length of steel linings for pressure tunnels is an in situ stress related problem that deserves special consideration. The very high cost of pressure tunnel steel linings can sometimes impose significant constraints upon the feasibility of hydroelectric projects.

In most weak rock masses, concrete linings are required in all hydraulic conduits in order to provide protection against erosion of weak seams and to improve the hydraulic characteristics of the tunnels. Assuming that the tunnels have been correctly supported by means of grouted rockbolts and cables during construction, the concrete linings can be of minimum thickness and lightly reinforced. It is assumed that these concrete linings will crack under operating pressure and that they will be slightly leaky. Provided that the cracks do not propagate a significant distance into the rock mass and cause hydraulic jacking, the slight amount of leakage is not a problem. However, conditions which give rise to hydraulic jacking have to be avoided and this is usually achieved by the provision of an internal steel lining in the tunnel.

The criterion for deciding when a tunnel should be steel lined is when the minimum principal stress in the rock mass falls below the maximum dynamic water pressure in the tunnel. This is a function of the maximum static head of water in the tunnel, the operation of the gates and the characteristics of the turbines. An allowance of 20% over

the maximum static head is usually considered adequate for a pressure tunnel associated with the operation of a Pelton wheel since this does not induce large pressure fluctuations. In the case of a Francis turbine, larger pressure fluctuations can be induced and an allowance of 30% above the maximum static head is normally used.

Figure 13.4 illustrates the case of a proposed pressure tunnel arrangement for a surface powerhouse at the toe of a slope. A headrace tunnel at elevation 680 m feeds water into a vertical shaft and then into a horizontal pressure tunnel at elevation 550 m.   The maximum reservoir pool level is 780 m and this results in an internal static pressure in the upper headrace tunnel of (780 - 680) x 0.01 = 1.0 MPa, where the unit weight of water is 0.01 MN/m^3. Assuming that an allowance of 30% over this static pressure is required for a Francis turbine system, a steel lining will be required for any section of the upper headrace tunnel where the minimum principal stress in the rock mass is less than 1.3 x 1.0 = 1.3 MPa. As shown in Figure 13.4, these conditions require about 80 m of steel lining where the headrace tunnel passes beneath the valley upstream of the surge tank. An option which should be considered in this case would be to increase the grade of the headrace tunnel so that the cover depth in the vicinity of the valley is increased. A relatively modest increase of 15 to 20 m in cover depth would probably eliminate the need for the steel lining resulting in significant cost savings and the removal of a construction impediment.

For the lower elevation tunnel, the internal static pressure in the tunnel is given by (780 - 550) x 0.01 = 2.3 MPa. Allowing an additional 30% for dynamic pressure, the minimum principal stress at which the steel lining should commence is 3 MPa. As shown in Figure 13.4, the lower pressure tunnel should be lined from x co-ordinate 500 m to the surface powerhouse.

The minimum principal stress contours plotted in Figure 13.4 were determined by means of a boundary element analysis assuming a gravitational loading of the slope and a far field horizontal to vertical in situ stress ratio of 1.5:1. This analysis assumes that the rock mass is homogeneous and isotropic and that the minimum principal stress lies in the plane of the drawing. It is essential that an accurate topographic map of the surrounding area be checked to ensure that there are no valleys or low points in a direction normal to the plane of the drawing which could give rise to stress relief in that direction. If in doubt, similar stress analyses to that illustrated in Figure 13.4 should be carried out for other sections perpendicular to the tunnel axis to check whether the minimum principal stresses are low enough to cause problems.

Since these stress analyses assume ideal rock conditions and do not take into account possible leakage paths along faults, shear zones or other geological discontinuities, I strongly recommend that the findings of the type of stress analysis illustrated in Figure 13.4 be confirmed by hydraulic acceptance tests. These involve drilling boreholes from the surface to the points at which the steel linings are to be terminated, packing off the lower 1 to 3 m of the borehole and then subjecting the packed-off sections to hydraulic pressures increased incrementally up to the maximum dynamic pressure anticipated in the tunnel. The pump pressures and flow rates should be carefully monitored to determine whether any excessive joint opening or hydraulic fracturing occurs during the pressure tests. The test pressure should be maintained for at least an hour to establish that there is no significant leakage through the rock mass from the points at which the steel linings are to be terminated. Only when these tests have confirmed the theoretical calculations can the steel lining lengths be established with confidence. I am aware of several pressure tunnel failures where lining length calculations were carried out but no pressure

acceptance tests were performed. Had such tests been done, they would have revealed anomalies or deviations from the conditions assumed in the calculations and these deficiencies could have been allowed for in deciding upon the steel lining lengths.
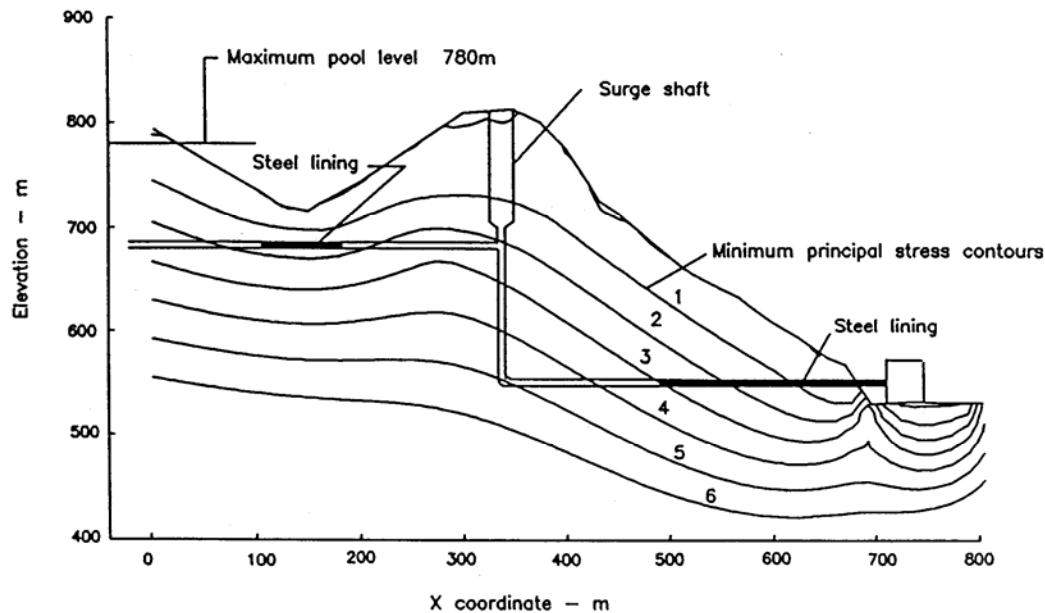
Figure 13.4: Contours of minimum principal stress σ_3 (MPa) in a gravitationally loaded slope with a far field in situ stress field defined by a ratio of horizontal to vertical stress of 1.5 : 1. Lengths of steel lining required in the pressure tunnel are shown.

13.4   Pillar size between excavations

In some cases, more than one cavern is required in an underground hydroelectric project. For example, the transformers may be placed in a smaller cavern parallel to the power cavern. This has the advantage of reducing the size of the main cavern and of isolating the transformers in case of fire. When this arrangement is used, there is frequently a demand from the electrical engineers to place the two caverns as close together as possible in order to reduce the length and hence the cost of the busbars that link the generators to the transformers. However, placing the two caverns close together may give rise to unfavourable stress conditions in the pillar between the caverns.

Figure 13.5 illustrates the results of a series of analyses in which the distances between two parallel caverns were varied. These analyses assume that the rock mass is a fair to poor quality siltstone, as defined earlier in this chapter, and that the ratio of horizontal to vertical in situ stress is 1.5:1. The caverns are located at a depth of 280 m below surface.

The contours plotted in Figure 13.5 define the ratios of the rock mass strength to the maximum principal stress induced in the rock mass surrounding the caverns. Zones defined by contours with strength/stress ratios of less than 1 are zones of potential rock mass failure. Because of the complex process of stress re-distribution associated with

progressive failure of the rock mass surrounding the excavations, these zones of overstressed rock do not necessarily coincide with the actual extent of rock fracture. The zones of overstress do, however, give a reasonable basis for comparison and experience suggests that the designer should attempt to keep these zones as small as possible with a priority on minimising the extent of potential zones of tensile fracture[2].

In the case of the upper plot in Figure 13.5, the distance between the two caverns is approximately equal to one half of the height of the larger of the two caverns and the zone of overstress extends across the entire pillar. Note that the central portion of the overstressed zone has strength/stress values of less than zero and will be prone to tensile failure. This pillar would almost certainly suffer severe damage and would require very substantial support in the form of tensioned grouted cables spanning the width of the pillar.

The lower plot in Figure 13.5, with the pillar width approximately equal to 1.5 times the height of the larger of the two caverns, shows that the zones of overstress are of limited extent and that the core of the pillar has strength/stress ratios in excess of 4. This means that the stress fields surrounding the two caverns are almost independent of one another. The extent of the overstressed zones suggests that a relatively modest amount of support would be required to stabilise the rock mass surrounding the caverns.

The plot in the middle of Figure 13.5 represents a situation that could be considered a reasonable compromise for many underground hydroelectric projects. The distance between the two caverns is approximately equal to the height of the larger of the two caverns and this is generally acceptable in terms of busbar length. The stress fields surrounding the two caverns obviously interact to a certain extent but the zones of overstress are not so large that major changes in the support pattern would be required. The zone of potential tensile failure between the two caverns has been eliminated in this layout.

For caverns in weak rock masses such as those considered in this chapter, I recommend that pillar widths should not be less than the height of the larger of the two caverns, and that, wherever possible, they should be slightly greater. In very poor quality rock masses, in which the overstressed zones are larger, it may be advisable to increase the pillar width to 1.5 times the height of the larger cavern. In all cases, a comparative study similar to that illustrated in Figure 13.5 should be carried out in order to confirm these decisions.

13.5   Problems in using a concrete arch in weak rock

Many underground caverns have been constructed with roof support provided by a cast-in-place concrete arch. As illustrated in Figure 13.6, the cavern arch is excavated to its full width and inclined haunches are provided to carry the reaction of the concrete arch. The reinforced concrete arch is cast in place when the floor of the excavation is level with the bottom of the inclined haunches. The lower part of the cavern is then excavated, usually by benching downwards.

---

[2] This analysis was originally carried out using the program EXAMINE[2D] that is only suitable for elastic analyses. Since that time, new programs such as PHASE[2] have become available and these can be used for a full progressive failure analysis. It is recommended that analyses of the type described here should be carried out with a program such as PHASE[2], which is available from Rocscience Inc., 31 Balsam Avenue, Toronto, Ontario, Canada M4E 3B5, Fax 1 416 698 0908, Phone 1 416 698 8217, Email: software@rocscience.com, Internet http://www.rocscience.com.
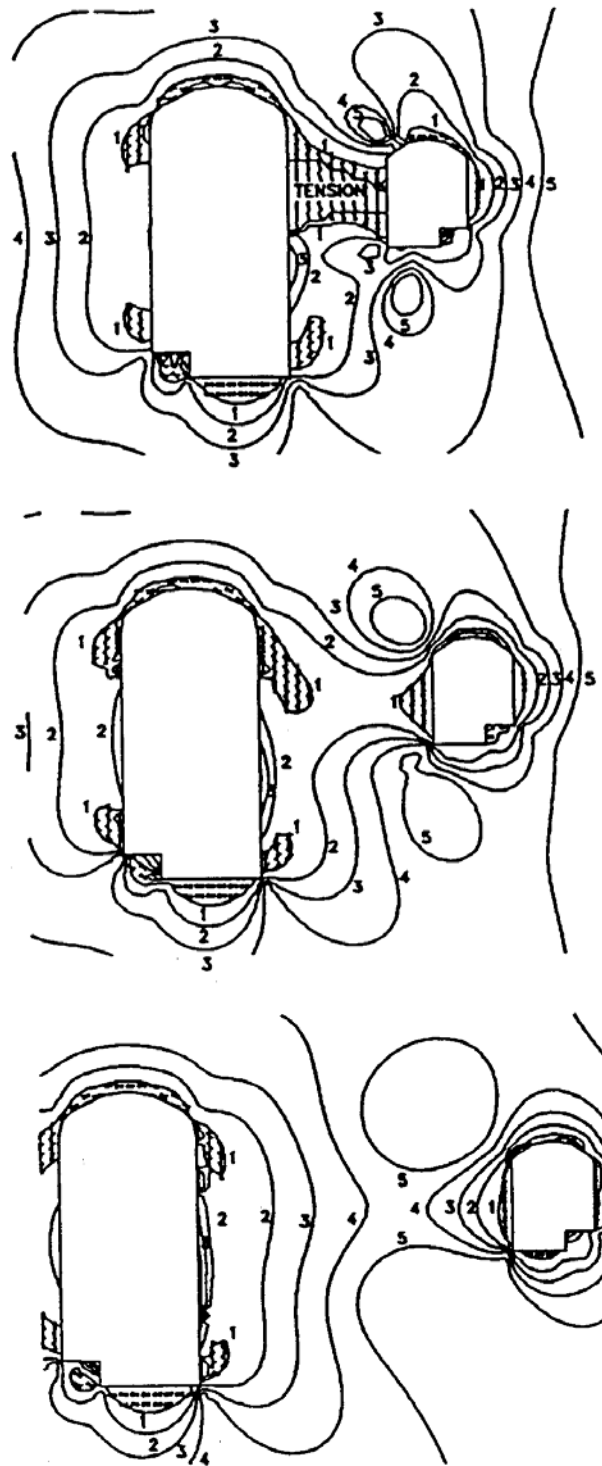
Figure 13.5: Contours of strength/stress ratios and failure trajectories in the rock mass surrounding two adjacent caverns in a siltstone rock mass with different spacing between the caverns.
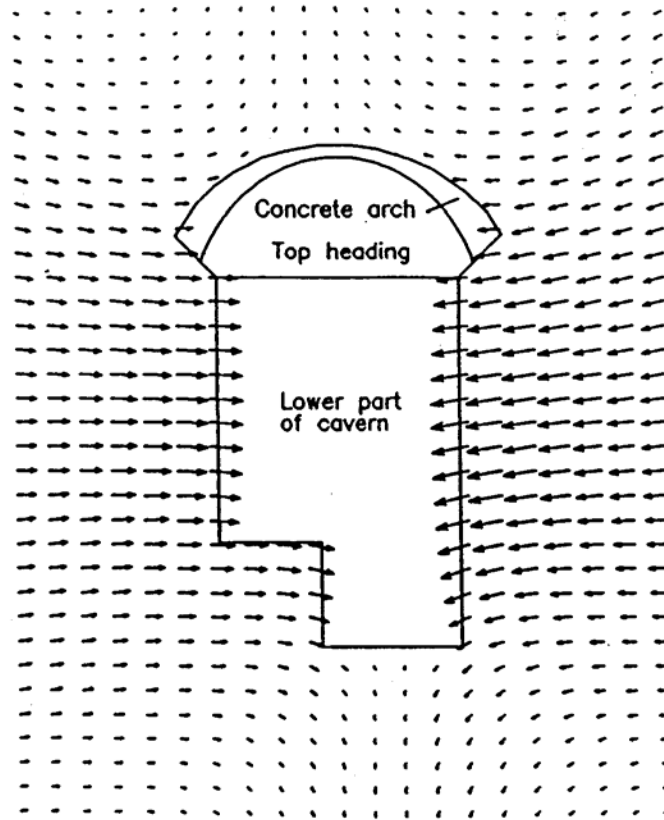
Figure 13.6: Plot of net displacements induced by excavation of the lower part of a large cavern in which the roof support is provided by means of a cast-in-place concrete arch.
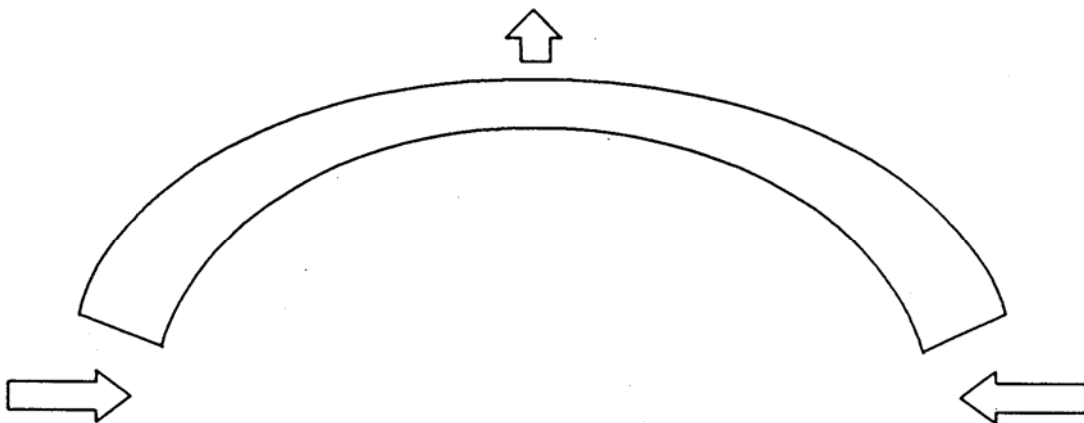
Figure 13.7: Displacements imposed on a cast-in-place concrete arch as a result of excavation of the lower part of the cavern

The concrete arch provides support for any rock that may become loosened in the cavern roof. The problem with this arch is that, if it is very rigid as compared with the surrounding rock mass, the deformations induced as a result of the excavation of the lower part of the cavern can cause excessive bending in the concrete arch. In addition, large amounts of temporary support in the form of rock reinforcement may be required to allow excavation to proceed to the stage where the concrete arch can be constructed. This reinforcement will have to be placed in the same manner as would normally be employed if it formed the permanent support of the rock arch. This would involve excavating a small top heading in the central crown, installing the reinforcement, widening the heading out into the haunches, installing more reinforcement, and so on. An example where pre-treatment and pre-support of a very poor quality rock mass was carried out to avoid temporary support problems during arch excavation is presented in a paper by Cheng and Liu (1990).

Figure 13.6 is a plot of the displacements induced by excavation of the lower part of the cavern. This plot was obtained by subtracting the displacements induced by the creation of the top heading from the displacements induced by the excavation of the entire cavern. These displacement vectors show that the upper part of the sidewalls displace inwards about 60 mm while the centre of the arch displaces upwards about 10 mm. Figure 13.7 is a diagrammatic representation of the displacements imposed on the concrete arch as a result of the displacements in the rock mass. Depending upon the magnitude of the displacements in the rock mass and the curvature and thickness of the concrete arch, the stresses in the concrete and in the reinforcing steel can exceed the safe working loads in these materials. This can give rise to critical conditions during construction since the repair of a damaged concrete roof arch is an extremely difficult and expensive process. Cases exist where severe cracking of the concrete arch led to the installation of additional steel arch support in local areas of the power cavern roof.

In general, I consider that the use of concrete roof arches should be avoided when designing large underground powerhouse caverns in weak rock masses. Experience has shown that the use of a more flexible support system such as that provided by grouted cables and a surface layer of shotcrete provides a more satisfactory solution. Where local problems occur, these can usually be dealt with by the installation of additional cables or the application of an additional layer of shotcrete. As long as access to the roof is maintained, remedial works can be carried out without disrupting the other construction activities in the cavern. Two schemes, with which I have been involved, have utilised platforms on top of a temporary crane to ensure that such access is available.

13.6   Crane beams

Underground powerhouse and transformer caverns require cranes of significant capacity to move heavy pieces of equipment around during installation and maintenance operations. Since these cranes are designed by structural engineers, it has been the practice that the cranes are supported on beams supported by columns. In many cases these structures are designed to be completely independent of the surrounding rock mass, just as they would be in a surface powerhouse structure. In my opinion, this is an inappropriate design approach since it does not utilise the enormous carrying capacity of the rock mass surrounding the cavern. Whenever possible the cranes beams should be suspended directly from the cavern walls as described in the examples given below.

The concerns which are normally expressed by designers, who are not familiar with the installation of suspended crane beams, are:

1. What capacity and length of cables or rockbolts are required to support the beams and what assurance can be given about the security of this support system?
2. How can displacements in the rock mass surrounding the cavern be accommodated in the case of crane beams attached to the walls?

The design of the rockbolts or cables required to support the beams follows the same procedure as would be used for the stabilisation of wedges in the roof or sidewalls of the cavern. The forces that have to be supported by the bolts or cables are calculated from the dead-weight of the beams themselves and the crane, loaded to maximum capacity. The crane load is distributed over the distance covered by the crane wheels along the beam. In addition, forces must be added to allow for the dynamic effects of the starting and braking of the crane, both along and across the cavern. These are simple force calculations that have to be carried out for any crane design.

Once the forces to be resisted by the rockbolts or cables are known, the capacity, length, number and orientation of the support elements can be chosen as would be done for the support of a rock wedge. The most important component of this support design is a thorough assessment of the geological conditions in the walls to which to beams are to be attached. The walls themselves should be stable and there should be no geological conditions, such as unfavourable oriented shear seams, which could cause instability as a result of the additional forces to be applied by the crane beam support.

Normally, long post-stressed cables are used for supporting the crane beams. However, there are several cases in which normal tensioned and grouted rockbolts have been used. Provided that the rock conditions are suitable, there should be no objection to the use of rockbolts for this purpose.

Many suspended crane beams have been used throughout the world and, provided that the design is carried out in a responsible manner, as described above, there is absolutely no reason why the system should be any less secure than a more traditional column crane.

On the question of displacements, this is very easily dealt with by providing the facilities for adjusting the position of the crane rail on top of the beam. The crane beams are normally cast in place when the cavern crown has been fully excavated and when the first bench has been taken. At this stage about 50 % of the displacement in the rock mass surrounding the cavern has already taken place. If the crane rails are installed at this stage, so that a construction crane can be used, provision must be made for the additional displacements that are induced as the cavern is benched downwards to its full height. Typically, these additional displacements will amount to a few centimetres on each wall. If the anchor plates holding the crane rails in place are provided with slotted holes to accommodate this additional displacement, there is no difficulty in adjusting the span between the crane rails as required. The anticipated displacements for each excavation stage can be estimated by numerical analyses as described elsewhere in these notes.

Some examples of typical suspended crane beans are given in Figures 13.8, 13.9 and 13.10.

In the Drakensberg Pumped Storage Project in South Africa, anchored crane beams were installed in about 1975 during excavation of the cavern. These beams were cast in place directly against the shotcrete layer which, along with rockbolts, formed part of the cavern support system. The rock in this case is a very poor quality interbedded

sedimentary sequence of sandstones, mudstones, siltstones and shales. Corrosion protected cables, 15 m long and of 100 ton capacity, were installed at approximately 1.5 m spacing along the beam. Lateral displacement of the beams, both during and after construction, was accommodated by providing slotted holes in the crane rail fixtures. The system has operated without problems for over 20 years.

Figure 13.8: Example of a cast in place crane beam in the Drakensberg Pumped storage project in South Africa. The beam is supported against a vertical face of interbedded sandstone, siltstone and mudstone by means of stressed and grouted cables. A temporary construction crane that was used to access the roof is shown in the photograph.

In the Singkarak Hydroelectric Project in Indonesia, anchored crane beams have been installed directly against the rock face, which is gneiss of reasonable quality. This installation is shown in the photograph reproduced in Figure 13.9, taken during construction of the cavern.

In the case of the Thissavros project in Greece, illustrated in Figure 13.10, the rock mass is gneiss but the cavern is oriented parallel to the strike of two major discontinuity systems. Hence, while the cavern walls were supported by 6 m long rockbolts, it was felt that the additional forces from the fully loaded crane could induce wedge instability in the walls. For this reason, the cast in place suspended crane beams were used only for a light construction crane, as illustrated in Figure 13.10. Concrete columns were then added, once the benching of the cavern was completed, to carry the full crane loads.

The principal reason for the choice of this system on many projects is that it allows for early installation of the cranes. Frequently, a light construction gantry, which runs on the crane rails, is installed immediately after the construction of the crane beams. This provides access for the monitoring of instruments in the cavern roof and for repair work to the roof support system if required. The main crane can be assembled early in the schedule and it is then available to assist in excavation of the lower benches and in the concrete work in the base of the cavern. These scheduling advantages offer considerable benefits when compared with a normal column supported crane.

Figure 13.9: Example of suspended crane beams in the powerhouse cavern of the Singkarak Hydroelectric Project in Indonesia.

Figure 13.10: Example of anchored crane beams in the underground powerhouse cavern for the Thissavros Hydroelectric project in Greece. In this case the beams shown were used for a construction crane and concrete columns were added later to carry the full crane loads.

13.7 Choice of cavern shapes

In strong rock masses, for which rock mass failure is not a problem, the conventional shape chosen for an underground powerhouse cavern is similar to that illustrated in Figure 13.11. The arched roof provides stability in the rock above the cavern roof and also provides convenient headroom for an overhead crane. The sidewalls are simple to excavate by vertical drill-and-blast benching and provide clean uncomplicated walls for crane column location and the accommodation of services.

The problem with this cavern shape when used in weak rock masses, particularly with high horizontal in situ stresses, is that tall straight sidewalls are deflected inwards (see Figure 13.6) and tensile failure is induced as shown in Figure 13.11. Zones of failure are illustrated in this figure and the maximum sidewall movement is 38.5 mm. The stabilisation of the rock mass surrounding this cavern will require significant reinforcement in the form of grouted cables or rockbolts.

An alternative cavern shape is illustrated in Figure 13.12. This elliptical shape has been used on schemes such as Waldeck II in Germany (Lottes, (1972)) and Singkarak in Indonesia (see Figure 13.9). As shown in Figure 13.12, the dept of the failure zones in the sidewalls has been reduced as compared to that in the conventional cavern. This results in a more stable overall cavern and a reduced support requirement.

While this cavern shape is better from a geotechnical point of view, it has some practical disadvantages. The cavern shape is such that the construction has to be more carefully executed than the conventional straight-walled cavern and items such as the cranes and services have to be designed to fit into the cavern shape. These differences can create significant problems where the skill of the labour force is limited.

In the weak rock schemes in which I have been involved, the conventional cavern shape has been chosen in preference to the elliptical shape because the overall advantages of the elliptical cavern have not been considered of critical importance when compared with the simplicity of the conventional cavern shape. Present support design techniques, discussed later in this chapter, are relatively unsophisticated and the stress changes resulting from a change in cavern shape are probably too small to have very much impact upon the support design. Consequently, it is doubtful whether the overall costs and time involved in the construction of conventionally shaped caverns would be higher than those that would be incurred in constructing elliptical caverns.

I recommend that each scheme should be investigated on its own merits, taking into account construction problems as well as geotechnical factors. In some cases, the use of an elliptical cavern shape may be justified but, in general, the conventional cavern shape illustrated in Figure 13.11 will be found suitable for all but the very weakest rock masses.

Before leaving this topic, attention is drawn to the unfavourable stress and potential failure conditions created by the stepped base of the cavern. A step of some sort is generally required to house the draft tubes and the lower parts of the turbines. It could be argued that this step should be created by cast-in-place concrete after a cavern of optimum shape has been excavated. In practice, this somewhat theoretical approach is found to be both unnecessary and uneconomical since failure in the base of the cavern is relatively easy to control. The instability of this bench is due to stress relief resulting from the creation of an unsupported vertical face and minimal support in the form of untensioned grouted steel rods (dowels), installed from the cavern floor before excavation of the lower benches, will counteract this instability.
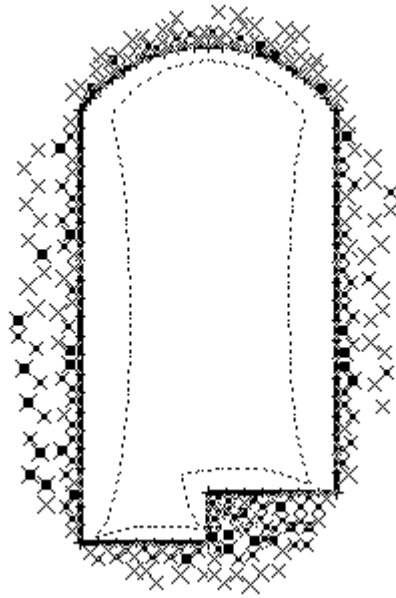
Figure 13.11: Conventional arched roof cavern shape showing zones of failure at a depth below surface of 280 m with a horizontal stress of 1.5 times the vertical stress. The deformed excavation shape is shown and maximum sidewall displacement is 38.5 mm. Analysed using PHASE[2].
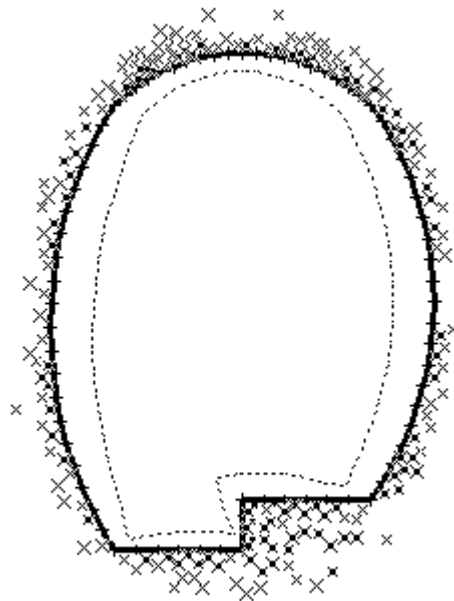
Figure 13.12: Elliptical cavern showing zones of failure for the same rock mass strength and in situ stress conditions as for the conventional cavern illustrated in Figure 13.11. The maximum sidewall displacement is 33 mm.

Good blasting practice is helpful here as damage to the bench can be reduced significantly by pre-splitting the bench face when the general level of excavation is still 2 or 3 m above the top of the step. Damage caused by pre-split blasting is confined to the rock above the step that is removed subsequently by the final blast down to the elevation of the step. The potential shear failure of the cavern floor and the lower part of the downstream sidewall does not pose any serious threat since it is self-supporting and because the lower part of the cavern is generally filled with concrete to form the turbine foundations, drainage tunnels and other service structures.

13.8   Influence of joints and bedding planes

In all of the analyses presented so far it has been assumed that the rock mass is weak but that it is isotropic and homogeneous. In other words, there are no dominant weakness directions in the rock mass. These assumptions are seldom valid in actual rock masses since joints and bedding planes are usually present, particularly in the case of sedimentary rocks. While these features do not have the same impact as faults or shear zones, they can introduce a directional pattern of weakness in the rock mass and this should be taken into account in the cavern design.

Since each rock mass will have its own unique set of structural features, it is essential that an analysis be carried out for each and every project. This chapter is concerned with general concepts rather than specific details and a simple example that illustrates these concepts is presented in Figure 13.13.
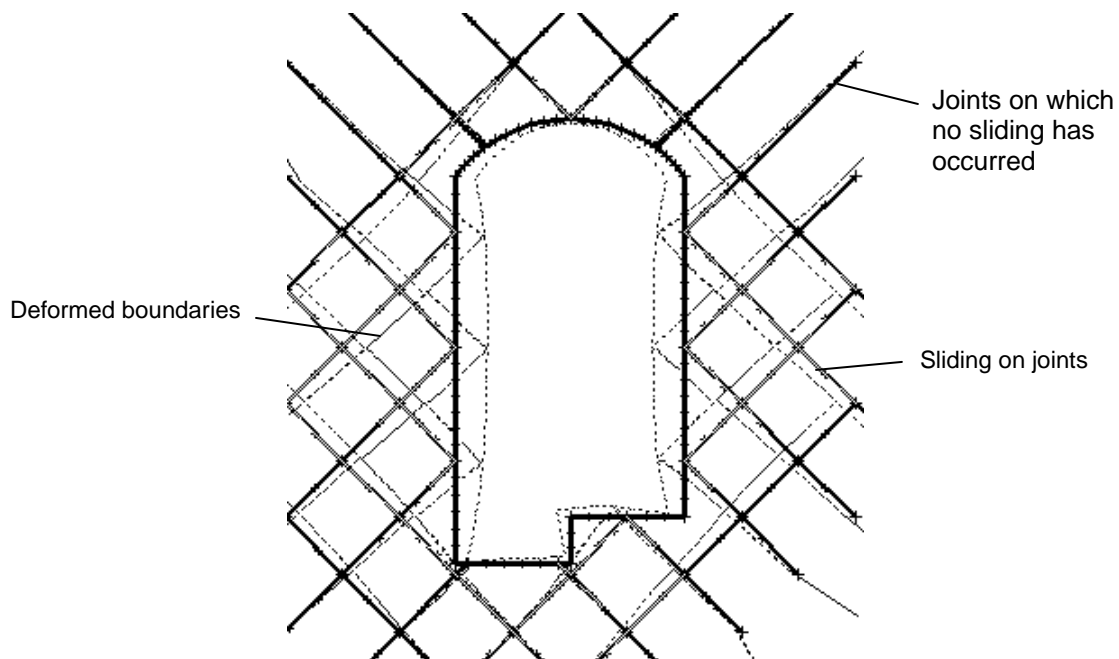
Figure 13.13: Influence of two sets of joints, inclined at 45°, on the displacements on the rock mass surrounding a conventional cavern. The rock mass properties and the in situ stresses are the same as those assumed in the previous section. The joints have a cohesive strength of 0.2 MPa and a friction angle of 30°.

The rock mass is assumed to be the same fair to poor quality siltstone as defined earlier and used in all previous analyses. Two sets of joints have been assumed and the shear strength of these discontinuities is defined by a Mohr-Coulomb angle of friction $\phi = 30°$ and cohesive strength of $c = 0.2$ MPa.

The influence of the joints in this case is dramatic in that all failure has been concentrated on the joints and there is no yield in the blocks separated by the joints. In other words, the problem has been transformed into one of structurally controlled failure as discussed in Chapter 6.

This transformation is controlled by the low shear strength of the joints as compared with that of the rock material. While the friction angles are almost the same, the cohesive strength of the joints is 0.2 MPa while that of the rock is 4 MPa. This means that the failure will occur preferentially on the joints whenever it has the chance to do so. However, in situations in which the joint strength is closer to that of the rock material forming the blocks in between the joints, the failure will tend to be more evenly spread between the two.

The inclination of the joints with respect to the principal stress directions is also important. Joints inclined to the direction of the maximum principal stress will tend to slide more easily than those parallel and normal to this direction.

The lessons to be learned from this rather simple example are that each case has to be considered carefully to establish whether it should be treated as a structural failure problem or whether it can be assumed that the rock mass is sufficiently homogeneous that the concepts discussed earlier in this chapter can be applied.

13.9   Design of reinforcement

The aim of any underground support design should be to help the rock mass to support itself to the greatest extent possible. This involves ensuring that the shapes and layout of excavations have been optimised, that the rock is damaged as little as possible during excavation, that the support characteristics have been carefully chosen to match the behaviour of the rock and that the sequence of excavation and support installation have been taken into account in the support design. There is no one 'correct' way to design support and there are many possible solutions which could be applied equally successfully to each underground cavern project. The support design concepts presented in this chapter are those which I have found to work effectively and economically in both mining and civil engineering applications.

A good starting point for any support design is a study of the literature to determine what others have done in similar circumstances. These precedents have also been usefully summarised in the rock mass classification schemes of Bieniawski (1989) and Barton, Lien and Lunde (1974). Figure 13.14, adapted from Barton (1989), gives the type of support which has been successfully used in underground excavations in weak rock masses. In this figure, *fibercrete* is an abbreviation for steel fibre reinforced shotcrete and *bolts* refer to either grouted bolts or cables which may or may not be tensioned, depending upon the sequence of installation.

Note that the design of cast concrete linings, shown in the upper left hand segment of Figure 13.14, must take into account the relative deformability of the concrete and the surrounding rock mass. As discussed earlier, the choice of an inappropriate shape and thickness for a concrete lining can result in serious overstressing of the concrete. This

problem is more acute for a cavern roof than for a tunnel lining. The roof arch is vulnerable to deformations resulting from benching after its construction and there is no opportunity to close the arch by constructing a concrete invert, as is commonly done for a tunnel lining.
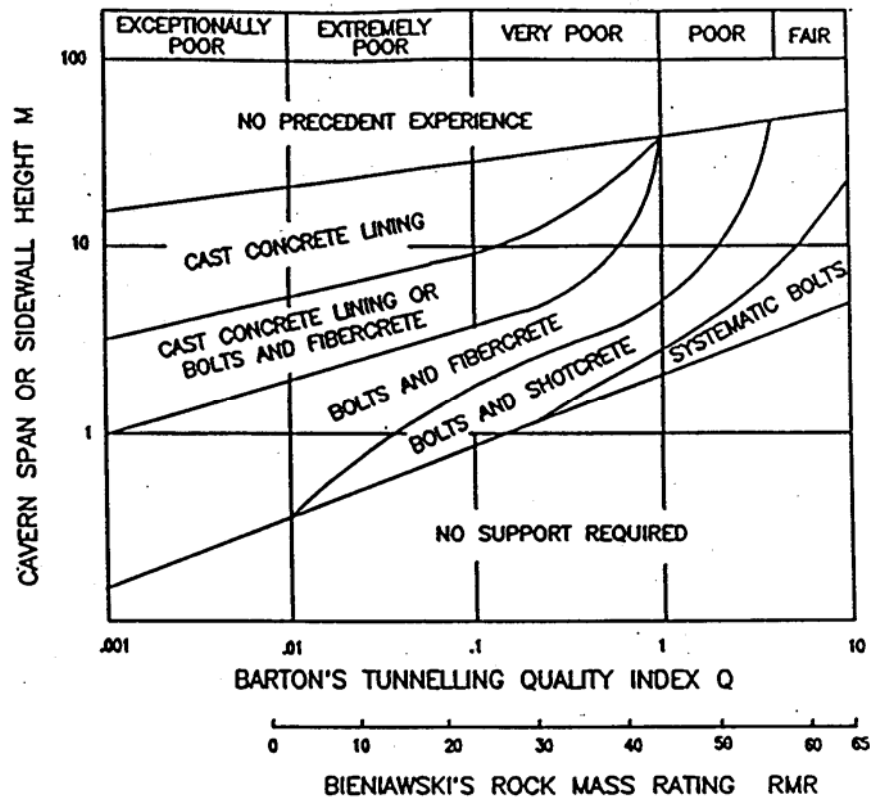
Figure 13.14: Summary of precedent experience on support of weak rocks in terms of rock mass classifications. Adapted from Barton (1989).

I unreservedly recommend the use of one of the existing classification schemes to obtain a first approximation to the level of support necessary for a large cavern in a weak rock mass. However, caution is advised against the uncritical acceptance of the recommendations coming from them. The collection of the data necessary to calculate RMR or Q values for a rock mass usually provides enough information for the design engineer to formulate a clear impression of the particular modes of failure that his design must resist. Careful consideration of the potential behaviour patterns of the rock mass, particularly the influence of geological structures, may lead to significant modification of the support recommendations obtained from the application of classification systems.

13.9.1 Estimating support pressures

One approach in estimating support pressure is to consider the extent of the zones of overstressed and blast damaged rock above the cavern roof and to assume that this rock acts as a dead weight which has to be supported. Considering the example illustrated in

Figure 13.11 for a rock mass with an RMR value of 48 and Q = 1.5, the zone of overstress extends approximately 3 m into the rock mass above the crown of this 20 m span cavern.

In addition to the stress induced fracturing that may occur, the fracturing and loosening of the rock mass due to blasting should also be considered. From experience it is suggested that blast damage may extend 1.5 to 3 m into the rock adjacent to the roof depending upon how much care has been taken to control the blasting.

Assuming that 3 m of rock have been damaged by either stress induced or blast induced fracturing, a dead weight of broken rock of up to 8 tonnes/m^2 of exposed surface of the cavern roof has to be supported. Where this support is to be provided by means of rockbolts or cables, a factor of safety of 1.5 to 2 is usually allowed to account for installation problems and to provide some reserve support capacity. Hence, the total capacity of the installed bolts or cables should be of the order of 12 to 16 tonnes/m^2 (0.12 to 0.16 MPa).

Figure 13.15, adapted from a paper by Barton (1989), shows that this estimate of a support pressure of 12 to 16 tonnes/m^2 for a rock mass with Q = 1.5 is in line with recommendations based upon previous experience.
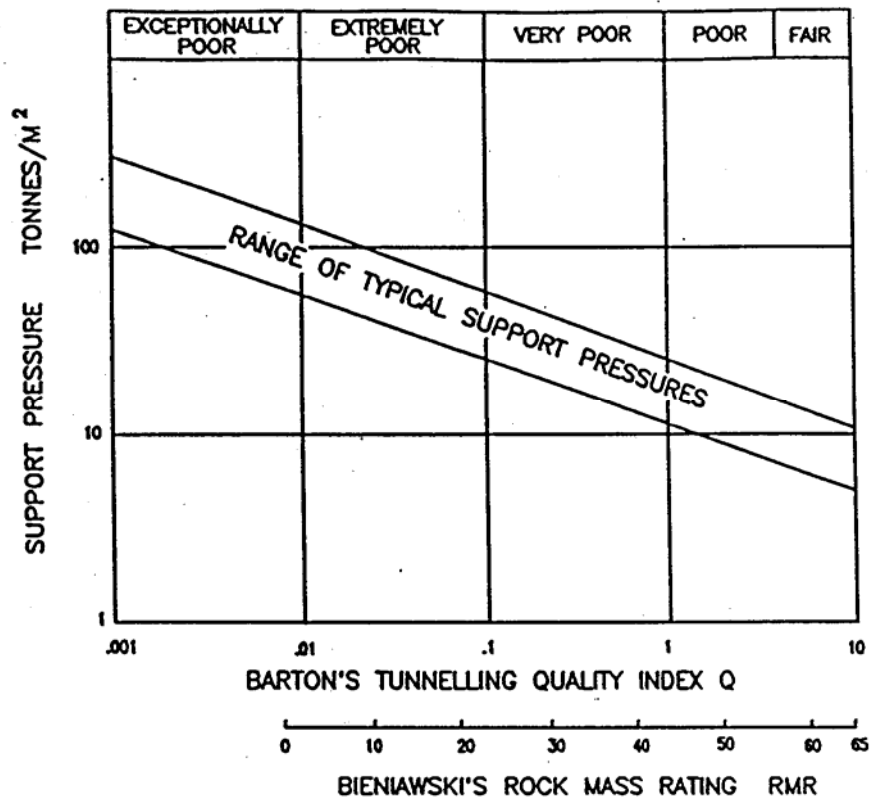
Figure 13.15: Relationship between support pressure and rock mass quality. Adapted from Barton (1989).

Some simplified closed form theoretical solutions have been developed which permit the study of the interaction of different types of support with the zone of failed rock surrounding underground excavations, and these solutions have been summarised by

Brown et al (1983). All of these solutions consider the development of a 'plastic' failure zone in a homogeneous rock mass surrounding a circular tunnel in a hydrostatic stress field and these assumptions impose severe limitations upon the application of these solutions to practical rock support design. Nevertheless, these simplified models have proved to be very useful in the development of an understanding of the basic concepts of rock support interaction and I urge interested readers to become familiar with these models and concepts. A discussion on this topic together with a listing of the simple calculation steps required can be found in Hoek and Brown (1988).

Today, the availability of powerful numerical analysis tools such as FLAC and PHASE^2 makes it possible to study support options in great detail. Such analyses are no longer constrained by the capability of the programs but rather by the quality of the input information. The reader should avoid the temptation to believe the results of a single analysis, however convincing the output may appear. It is always necessary to carry out parametric studies to cover the range of possible input parameters. It is only in this way that a sound understanding of the behaviour of the rock mass surrounding the excavation can be established.

13.9.2 *Design of rockbolt and cable support*

The excavation of a large cavern in weak rock will usually require the installation of systematic rock support or reinforcement during excavation as an integral part of the excavation cycle. Even when the use of cast concrete arches and/or sidewalls is envisaged for final support, consideration must be given to the requirements of temporary stability during excavation, which will often require extensive support if safe and controlled excavation is to be achieved. In many cases, the only significant difference between supports used for temporary and permanent purposes relates to corrosion protection requirements. Corrosion protection is an important design consideration in environments where corrosive water is encountered during preliminary investigation or excavation. In modern practice, corrosion protection measures usually require at least one physical barrier (single corrosion protection) to protect the individual rockbolts or rock anchors against corrosion (British Standards, 1987). This physical barrier often takes the form of a corrugated plastic sheath which completely encapsulates the steel bar or cable from which the anchor is formed.

Rock mass reinforcement for large caverns usually involves the installation of rockbolts formed from deformed steel bar or cables made from pre-stressing strand. Rock bolts are generally cheaper and quicker to install but cables can provide higher capacity and may be easier to install when long reinforcement elements are required. Combinations of rockbolts and cables are commonly used to combine the best features of both systems. The rockbolts are installed close to the face for immediate support while the cables are installed subsequently as the primary reinforcement system.

The possibility has to be considered that, during excavation, cables will pick up excess load over their installation load to the extent that they become seriously overstressed. In this circumstance, prediction of the final cable load is an important input into decisions on the appropriate installed load, the timing of the installation and tensioning and the choice between fully grouted or adjustable cables. In the author's experience, fully grouted cables are more convenient for the contractor and provide stiffer support, particularly in response to deformations occurring at a large angle to the cables.

However, the use of adjustable (i.e. re-tensionbable) cables may be appropriate in circumstances where very large deformations are anticipated. These cables are made by placing a plastic sheath over a significant portion of the length of the cable. This sheath breaks the bond between the cable and the grout and allows the cable to deform independently of the surrounding rock.

It is important to recognise that there are two types of rockbolt or cable support commonly used in underground excavations. In good quality rock masses in which the stability is controlled by intersecting joints, bedding planes, shear zones and faults, the support has to be designed to reinforce specific blocks and wedges which may fall or slide into the excavation. This type of support, frequently referred to as 'spot bolting', involves the installation of a few bolts or cables at clearly defined locations, with their length, orientation and capacity chosen to provide adequate support for the wedge or block under consideration.

While 'spot bolting' may be required for isolated blocks or wedges in weak rock masses, it is the second type of support, frequently called 'pattern bolting', which is more relevant to this chapter. 'Pattern bolting' involves the installation of rockbolts or cables in a regular pattern that is designed to reinforce the entire rock mass in much the same way as reinforcing steel acts in reinforced concrete. Typically, 5 m long 20 tonne capacity rockbolts installed in a 2 m x 2 m grid pattern could be used over the entire roof and wall area of a large underground cavern. These bolts would provide a support pressure of 2.5 tonnes/m^2 if loaded to 50% of their capacity.

The first question to be decided is the length of the rockbolts or cables. Analyses of the extent of zones of overstressed rock, such as those presented in Figures 13.11 and 12.12, are useful in determining the approximate extent of rock requiring support. Generally, the bolts or cables should extend 2 or 3 m beyond the limit of the zone of overstressed material. As previously stated, great care must be taken in using this approach to select reinforcement lengths since relatively modest changes in rock mass properties or in situ stresses can result in significant changes in the zones of overstress. Consequently, parametric studies in which these input data are varied over the maximum credible range are essential if the reinforcement lengths are to be based upon such studies.

An alternative approach is to use previous experience. Figures 13.16 and 13.17 give the lengths of roof and sidewall rockbolts and cables in some typical large powerhouse caverns in weak rock masses. Plotted on the same graphs are empirical relationships suggested by Barton (1989) for bolts and cables. For underground powerhouse excavations these relationships are simplified to :

Roof	rockbolts	L = 2 + 0.15 x SPAN m
	cables	L = 0.4 x SPAN m
Walls	rockbolts	L = 2 + 0.15 x HEIGHT m
	cables	L = 0.35 x HEIGHT m

The choice of rockbolt and cable spacing is based upon the following considerations:

a) In order to ensure that the bolts or cables interact with each other to form a zone of uniformly reinforced rock (Lang, 1961), the spacing S of the bolts or cables should be less than one half of the length L, i.e. S < L/2.

b) For a support pressure P and a working load in the bolt or cable T, the spacing for a square grid is given by $S = \sqrt{T/P}$.
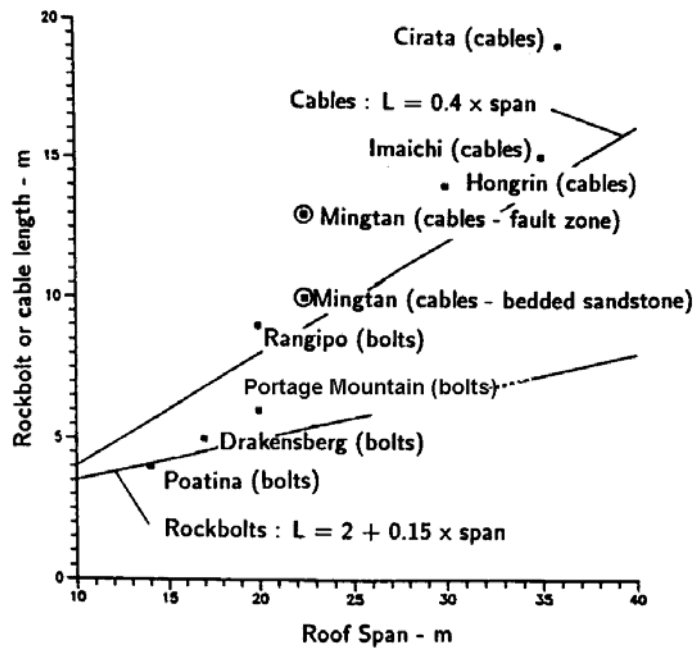
Figure 13.16: Rockbolt and cable lengths for roof support in some large caverns in weak rock.
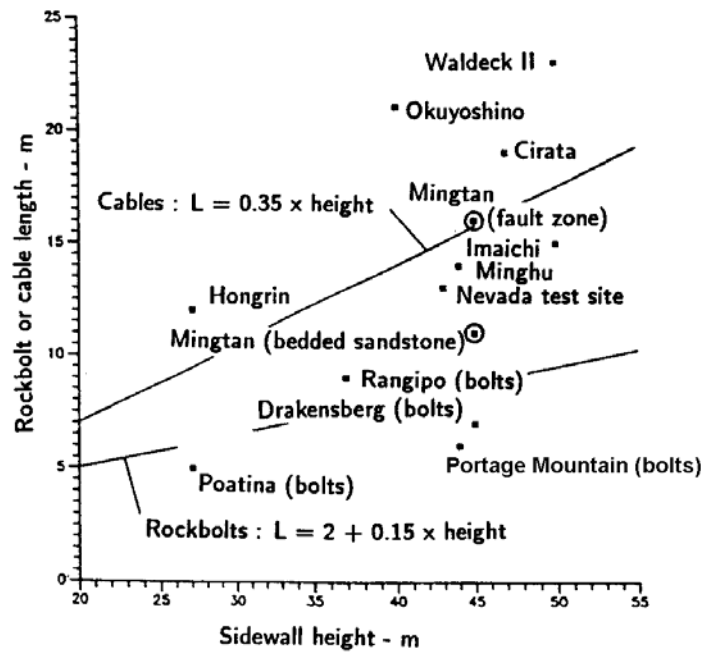
Figure 13.17: Rockbolt and cable lengths for sidewall support in some large caverns in weak rock.

Typical bolt and cable spacing range from 1 to 3 m with 1.5 m being a common spacing for bolts and 2 m being widely used for cables. Where additional support capacity is required to support local areas of weaker rock, bolts or cables placed at the centre of each grid square will sometimes suffice. Alternatively, when cables are used, additional strands can be placed in each hole to increase the capacity of the cables.

13.9.3 Use of shotcrete linings

In the past two decades, shotcrete has developed into a versatile support system that is ideally suited to the requirements of cavern support in a deformable rock mass.

Two significant benefits of shotcrete are that it can be applied quickly to freshly exposed rock during excavation and that it develops strength steadily after application. Green shotcrete is resilient to damage from nearby blasting and associated stress redistribution and gains strength at the same time as load is being transferred onto it. High early strength can be achieved by the addition of accelerators without a serious loss in long-term strength. Dosage of the accelerator has to be controlled carefully to ensure good intermixing and avoid local overdosing.

When used in combination with systematic rock reinforcement, shotcrete can provide immediate temporary support during excavation or form the permanent lining for the roof and sidewalls during the design life of the cavern. Irrespective of the form of temporary support, shotcrete application for permanent support purposes can often be delayed until all adjacent excavation has been completed. This allows the permanent lining to be sprayed in a better working environment than that existing close to the working face and this allows better control over thickness and quality. Some designers prefer to utilise additive free shotcrete for final lining application on the grounds that high early strength is not needed for the final lining and the addition of additives may be detrimental to the long-term performance of the shotcrete.

Research and development into shotcrete mixes, additives and equipment have progressed to the stage that shotcrete quality now rests almost entirely with the choice of compatible equipment and the equipment operators. Wet mix application requires careful attention to the supply of mix and air to ensure that the material leaves the nozzle in a continuous uninterrupted stream that can be applied by the operator or nozzleman in such a fashion as to maximise compaction and minimise rebound. With the dry mix method the supply of water also has to be controlled by the nozzleman.

For the engineer who is not an expert in shotcrete technology, there is a bewildering choice of equipment and additives, starting with the basic selection of the wet mix or the dry mix method. No hard and fast rules apply to this selection, other than to say that, depending on local circumstances, either system may be suitable to form the temporary or permanent lining of a large cavern. In general, higher production rates are possible with the wet mix processes, but this is not necessarily a major factor in considering the system to be used for cavern lining purposes. Remotely controlled robot applicator systems are widely used, but hand held nozzles will also provide a satisfactory product, if used properly. Liquid plasticizers and water reducing agents are commonly used as an aid to application and dust suppressants have recently been developed to improve the working environment for the nozzleman. It is common policy to limit the total amount of all additives in a mix to a figure of the order of 5 or 6% by weight of cement.

A significant advance in shotcrete technology has been brought about by the introduction of micro silica into the mix at up to 10% by weight of cement. This results

in a significant reduction in rebound, and an increase in the thickness that can be built up in a single application. It is also beneficial for application onto damp or wet surfaces. The addition of micro silica produces a denser product with an increase in early strength, and does not appear to have a detrimental effect on long-term strength. Problems with the use of steel fibre reinforced shotcrete have been greatly reduced by the use of micro silica. Rebound of both shotcrete and the fibres is significantly less than it used to be. Balling of the steel fibres and excessive equipment wear have also been largely overcome so that, over the last five years, micro silica fibre reinforced shotcrete technology has become a viable and frequently preferable option to the accepted use of steel mesh embedded in plain shotcrete.

For steel fibre shotcrete, the number of shotcrete applications can sometimes be reduced when compared with the more complex installation of layers of plain and/or mesh reinforced shotcrete. Although the initial bending strength of the two products is similar, performance is improved because the post crack load bearing capacity is significantly better in the case of steel fibre shotcrete. Typical current practice involves the use of fibres in the range of 20 to 40 mm long and approximately 0.5 mm diameter. Current research is examining the use of longer fibres (to improve post crack strength further) and materials other than steel.

Decisions on lining thickness are usually based on a combination of empirical and practical considerations rather than concern about stress levels in the lining. Where concern about stress does exist, delayed application of the final layer or the application of an additional layer are available options. The thickness built up in a single application is typically of the order of 40 to 80 mm and total thickness of the order 100 to 200 mm. With layers less than 40 mm thick concern will sometimes exist that an effectively continuous layer will not be achieved if application to a very irregular surface is required.

When designing permanent shotcrete linings, it is important to specify quality control or acceptance tests as a design requirement. The use of steel fibre shotcrete does not readily allow rigorous checking during the execution of the work in the manner that rockbolt work or reinforced concrete construction does, since it is dependent on the skill of the operator. Thus, it is essential to do routine acceptance testing by coring through the completed lining in order to check the density and strength of the sprayed product, the adhesion to the rock surface, the inter-layer adhesion where two or more layers have been applied, and the total thickness achieved. Inter-layer adhesion can be a particular problem if a long time period elapses between the application of temporary support and permanent support shotcrete, since it is difficult to remove the grime that accumulates on the surface of the initial layer if diesel powered equipment is used in association with blasting, mucking and support activities. Where large deformations are expected after the completion of the final lining, some designers may still prefer a fully engineered solution, with mesh layers incorporated into a shotcrete lining and positive connection of the mesh to rockbolts and cables, over the use of simple fibre reinforced linings.

Uncertainties of this type in relation to shotcrete linings give rise to a tendency to overspecify the product in terms of the strength properties to be achieved at 3 days or 7 days. While it is generally true that high early strength is a desirable feature of shotcrete, nothing is gained by forcing the contractor to produce higher strengths than are needed. For example, a permanent lining sprayed onto a rock surface, which already had a reasonable level of support for temporary purposes, may not need to be accelerated at all. In this circumstance, the 7 and 28 day strengths generally accepted in structural concrete

usage may be as good a criterion as the 3 and 7 day strengths which have come to be associated with shotcrete usage. It has already been stated that concern about the long-term effects of additives on strength has caused some designers to opt for an additive free shotcrete for final lining purposes.

13.9.4 Support installation sequences

Should rockbolts and cables be tensioned and at what stage of the excavation sequence should a shotcrete layer be applied? These are questions which arise during discussions on the design of support for underground excavations in weak rock masses. They are dealt with here by means of a practical example based upon the support installation sequence for the power cavern of the Mingtan Pumped Storage Project in Taiwan. This project is described in detail by Cheng and Liu (1990) and further details can be found in a paper by Moy and Hoek (1989). Figure 13.18 gives a summary of the principal support installation stages for this 25 m span 46 m high cavern in fair to poor quality bedded sandstone.

During a preliminary contract an existing exploration/drainage gallery and two longitudinal working galleries were utilised to install grouted cables in the pattern illustrated in Figure 13.18a. These 50 tonne capacity cables were double corrosion protected and installed downwards from the exploration/drainage gallery, located 10 m above the crown of the arch, and upwards from the two working galleries. A light straightening load of 5 tonnes was applied to each cable before grouting and hence the cables were effectively untensioned but straight and fully grouted into the rock mass. Since these cables were installed before any excavation of the cavern had taken place, no significant displacements had occurred in the rock mass at the time of cable grouting.

Excavation of the cavern roof, illustrated in Figure 13.18b, induced significant displacements (Moy and Hoek (1989)) and these tensioned the grouted cables.   Had the cables been tensioned before grouting, the additional tension induced by the displacements in the rock mass could have resulted in overstressing of the cables. The purpose behind the installation of these untensioned grouted cables was to reinforce the rock mass in much the same way as the placement of reinforcing bars in concrete acts to strengthen the concrete. The process was intended to improve the overall quality of the rock mass so that the main excavation contract could proceed with fewer rock stability problems than would have been the case had the pre-reinforcement not been in place.

The cavern roof was excavated by means of a central 6 m x 6 m heading which was subsequently slashed out to the full cavern width as illustrated in Figure 13.18b. Upon exposure of the final roof surface at each stage of this excavation process, a 50 mm layer of steel fibre reinforced micro-silica shotcrete was applied within 5 to 10 m of the face. The purpose of this shotcrete layer was to provide support for the small blocks and wedges which would otherwise have been free to fall from between the reinforcing cables. In addition, the shotcrete provided immediate sealing against moisture changes which could cause slaking in some of the siltstone rock units exposed on the surface.

A relatively thin shotcrete layer was used at this stage in order to allow for displacements which would be induced by adjacent excavation of the upper part of the cavern.   Even if minor cracking of the shotcrete had been induced by these displacements, the presence of the steel fibre reinforcement provided a high post- crack deformation capacity for the shotcrete and hence maintained its support capacity.
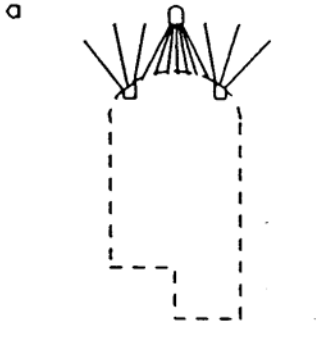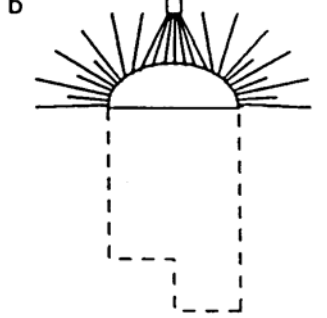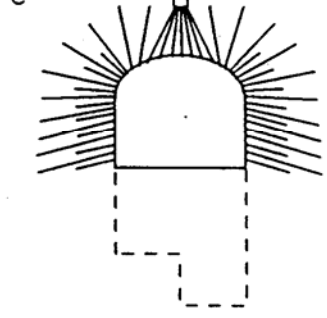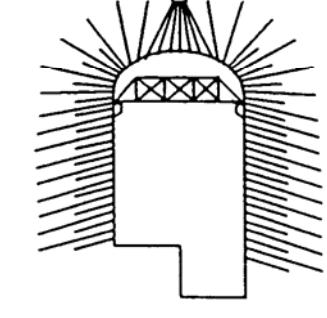
a Installation of double corrosion protected cables from exploration/drainage gallery located 10 m above center of roof arch and from two longitudinal working galleries. The 50 tonne capacity cables were installed on a 2 m x 2 m grid pattern and a small straightening load of 5 tonnes was applied before grouting.

Dashed lines show cavern profile before excavation.

b Excavation of cavern roof by center heading and slashing with application of first 50 mm thick layer of steel fiber reinforced micro-silica shotcrete. Faceplates were added to projecting ends of cables and tensioned to 20% of ultimate capacity to ensure positive anchorage. Where required, 5 m long 25 mm diameter mechanically anchored, tensioned and grouted rockbolts installed at centers of 2 m x 2 m grid of cable reinforcement.

c Excavation of cavern by 2.5 m vertical benches. Double corrosion protected 112 tonne cables, inclined downwards at 15° to cross bedding planes, were installed on a 3 m x 3 m grid in the sidewalls. Before grouting, these were tensioned to 38 to 45% of yield strength, depending upon their location relative to the bench. Intermediate 6 m long 25 mm diameter tensioned and grouted rockbolts were installed between cables. Final shotcreting of the roof was carried out at an early stage of benching.

d Complete excavation of the cavern with 150 mm total thickness of steel fiber reinforced micro-silica shotcrete on the roof and upper sidewalls and 50 mm thickness on the lower sidewalls. Access to roof for inspection and minor remedial bolting maintained from temporary crane.

Figure 13.18: Support installation sequence for the power cavern of the Mingtan Pumped Storage Project in Taiwan.

Figure 13.19: Cables and shotcrete were used to support the roof of the power cavern in the Mingtan Pumped Storage Project in Taiwan.

Figure 14.30: Installation of cables in the sidewall of the power cavern in the Mingtan Pumped Storage Project in Taiwan.

As soon as the ends of the pre-placed reinforcing cables were exposed, faceplates were installed on them and a tension of 20% of the ultimate capacity of the cable was applied to ensure positive anchorage. Note that this tension acts over a very short length of each cable near its exposed end since the remainder of the cable is fully grouted into the rock mass. Experience in the mining industry has shown that the installation of faceplates on pre-placed untensioned grouted cables is very beneficial in providing support for the near surface blast damaged material which otherwise tends to fall away from the ends of the cable. In most areas in the Mingtan cavern, 5 m long 25 mm diameter mechanically anchored rockbolts were placed at the centre of each square in the 2 m x 2 m grid of cables. These bolts were tensioned to 70% of their yield load before grouting since they would not be subjected to significant displacements during the excavation of the lower part of the cavern.Excavation of the lower part of the cavern was carried out by means of 2.5 m high vertical benches. Sidewall support was provided by a 3 m x 3 m pattern of tensioned, grouted, double corrosion protected 75, 112 or 131 tonne cables, installed at a downward angle of 15° to ensure crossing of bedding planes which strike across the cavern axis (Moy and Hoek (1989)). These cables were tensioned at between 38 and 45% of their yield load, depending upon their level in the cavern sidewall and their location in relationship to the position of the bench floor at the time of installation. The tension was reduced for those cables which were installed close to the bench floor in the lower walls of the cavern. Mechanically anchored rockbolts, 6 m long and 25 mm in diameter, were installed between the cables as illustrated in Figure 13.18c. These bolts were tensioned to 70% of their yield load before grouting.

At an early stage of benching, when excavation had progressed to a stage beyond which further deformations induced in the roof were relatively small, an additional thickness of 100 mm of steel fibre reinforced micro-silica shotcrete was applied to the roof and upper sidewalls. The total thickness of 150 mm of shotcrete represents the final lining for the roof and upper sidewalls of this cavern. Full details of the shotcrete specifications and mix design have been given by Moy, Hsieh and Li (1990).

The lower cavern sidewalls were reinforced with cables in the same way as the upper sidewalls shown in Figure 13.18c. Only 50 mm of steel fibre reinforced micro-silica shotcrete was used on the lower sidewalls since most of these surfaces were subsequently covered by concrete as the turbine foundations were cast in place.

13.10 Excavation methods

The stability of a large underground excavation is very much dependent upon the integrity of the rock immediately surrounding it. In particular, the tendency for roof falls is directly related to the interlocking of the immediate roof strata. For weak rock masses with clay filled joints and localised soft or altered zones, the capacity of the rock mass to contribute to its own support temporarily during excavation can be totally destroyed by careless excavation or poor sequencing of excavation and support activities. Thus, the choice of excavation method assumes a degree of importance which has not always been catered for by specifications and construction procedures.

The most frequently adopted method for cavern excavation is drilling and blasting. Strictly speaking, blasting control is not a cavern design requirement but it exerts the biggest single influence on the outcome of the excavation process, and should be considered accordingly. In a weak rock mass, the sequencing of excavation and support

will typically follow the top heading, slash and 2.5 to 5 m bench procedure described in the previous section.

The control of rockbolting (e.g. maintaining design spacing) and shotcrete operations (e.g. achieving uniform design thickness) is far more easily effected when good control is maintained over excavated profiles, so blasting specifications are normally written in terms of maximum permissible overbreak or the presence of ``half barrels'' (charge hole drill marks) on the profile produced by the blast. Even in weak rocks, some half barrels can be expected with a well-balanced blast, especially if pre-splitting or smooth blasting is utilised, but care should be taken to ensure that the specifications do not demand results which are impossible to achieve in practice. After the initial heading, extensive free faces exist and provide a void into which the broken rock can move. In this circumstance, the blast energy absorbed into the rock mass should be minimal.

For a well-balanced blast, each successive delay should produce even breakage and leave the appropriate burden to be removed by the next delay. Whether a pre-split or a smooth blast is employed, the location and charging of the easier holes drilled closest to the perimeter holes is critical to the outcome of the blast, since overcharging or poor alignment of these holes will result in damage beyond the final perimeter which cannot be rectified once it has occurred. Hole alignment of the perimeter holes themselves is of obvious importance, and can be maintained by the use of parallel drill hole facilities on modern jumbos. Alternatively, drilling inspectors can help the operator maintain the required hole alignment during the early stages of drilling. For vertical drilling, templates made up from flat plates with steel tubes welded onto them to act as a guide for the drill, can be used when the hole is collared.

Where good drilling control and apparently well-balanced charges do not produce good blasting results, it is sometimes useful for the inspection teams to request a piecemeal blast. This requires each delay of holes to be fired individually, so that the profile created by each delay can be inspected to ensure that breakage has occurred in the way it should. If such a process confirms that the holes and charges are well-balanced but the production blasts still do not produce the desired results, then there may be a problem with the initiation system, e.g. excessive scatter on the delay detonators producing out of sequence firing.

The ultimate in damage control is machine excavation, and for cavern excavation, this usually implies the use of road headers. The possibility of using road headers for general cavern excavation should be considered wherever the intact rock strength is less than 60 MPa, and the viability of the method, as opposed to drilling and blasting, will be dependent on a comparison of the costs and required excavation rates rather than the ability of the road header to cut the rock. The absolute limiting rock strength for cutting with a road header has been put at 125 to 130 MPa, and this can only be achieved with great difficulty over short distances with pick destruction being the limiting factor (Pearce, 1988). The lack of disturbance to the rock and the possible reductions in support required are major advantages in the use of road headers.

The use of road headers becomes even more attractive when there is a need to control vibrations induced by blasting. This can be the case when cavern excavation is required adjacent to an existing underground installation, or when caverns are to be excavated relatively close to the surface. Langefors and Khilstrom (1973) and others have published blast damage criteria for building and surface structures. Almost all of these relate blast damage to peak particle velocity resulting from the dynamic stresses induced by the explosion. Where these generally applicable guidelines impose unreasonable restriction

on the blasting requirements of a project, monitoring at the site allows site specific limits of the charge weight to be determined. These limits are defined by the charge weight in the cavern which will produce unsatisfactorily high particle velocities at the surface or the adjacent underground structures. An example of this type of monitoring is described in a paper on the Tai Koo cavern in Hong Kong (Sharp et al (1986)).

13.11 Cavern instrumentation

The installation of rock mass monitoring systems around a large cavern in a weak rock mass is considered essential in order to ensure that control is maintained over stability conditions during and immediately following excavation. The stress redistributions that accompany excavation in a weak rock mass can produce large deformations, which will in turn modify the loads carried by the rock reinforcement system and the stress carried by the shotcrete lining. Given the uncertainties of support design, the design engineer will require confirmation that his assumptions, on the level of deformation and load and stress changes that will occur, are not invalidated by the actual response to excavation.

Of the three effects listed above, the most reliable data usually come from displacement monitoring, since this can be conducted on a scale comparable with the size of the excavation and the volume of rock affected by stress redistribution. By comparison, measurements of stress change in the rock or the lining can only be conducted at isolated points which may not be representative of the average condition. Load monitoring in the rock reinforcement is possible for unbonded bolts and anchors, but the results are of questionable applicability to fully bonded reinforcement for which highly localised strains and load changes may occur where the bolt or cable crosses a specific joint.

Displacement monitoring may be relative or absolute. An example of the former is the installation of a multipoint extensometer in the sidewall of a cavern, with the deepest anchor inside the zone of rock where movement may be expected. Movements beyond the deepest anchor will not be registered by the extensometer. An example of absolute movement monitoring is the measurement of the horizontal convergence of the two sidewalls of the cavern by means of a tape extensometer stretched between the walls. However deep the movement, it will all be registered by the tape extensometer. Where relative displacement is monitored, the opportunity exists to extrapolate to the absolute displacement by calibrating a numerical model against the relative movements monitored, and using the model's predictions outside the monitored zone. Numerical models also allow the estimation of any movements occurring before the installation of the instruments, which are usually installed from inside the excavation. In some circumstances, it is possible to install extensometers, before the commencement of cavern excavation, from adjacent exploration or drainage galleries, and the advisability of doing this should always be assessed. In deciding the layout of extensometers, it is usually advantageous to be able to distinguish between movements inside and outside the reinforced zone, since the former will affect the loads carried by the reinforcement and the latter will not. During the later stages of excavation of a cavern in weak rock, large movements may continue at depth in the upper sidewall, but this may be of no concern to the designer if the reinforced zone has stabilised.

Stress changes in the rock can be calculated from monitored displacements by the assumption of a value for the rock mass modulus. The use of analyses of this kind during

the early stages of excavation sometimes indicates the need for additional supports or modifications of the design requirements during a later stage of excavation. This will be backed up by load change data obtained from load cells fitted to isolated elements of the reinforcement system.

Large stress changes in shotcrete linings are usually fairly apparent from the occurrence of cracks in the lining. For this reason, visual observation maintains its status as an important data gathering method. It is also still the most effective way of assessing the groundwater conditions in the rock mass surrounding an opening. Where groundwater discharges into a cavern, piezometer installations are advisable to check that excessive pressures cannot build up in the roof or behind the sidewalls.

13.12 Summary and conclusions

The design of large powerhouse caverns in weak rock masses differs from that of caverns in stronger rocks in that failure of the rock mass surrounding the excavations and large deformations of the roof and walls will have to be accommodated in the design. This requires an understanding of the behaviour of weak rock masses and of the interaction of the support with these rock masses during excavation and subsequent operation of the caverns.

Estimating the strength and deformation characteristics of weak rock masses is an uncertain process and large variations in properties can be anticipated, particularly in bedded sedimentary rocks. This means that precise analysis of the stresses and deformations induced by the excavation of the caverns is not possible, and the designer has to rely on parametric studies in which the in situ stresses and material properties are varied over their maximum credible range in order to establish general behavioural trends. Examples of such parametric studies, using a two-dimensional elastic boundary element analysis, have been presented in this chapter. More refined studies, using non-linear progressive failure analyses, are only justified when sufficient data have been gathered from the monitoring of actual excavation behaviour to provide realistic input data for such analyses. An example of this more refined type of analysis is presented in Cheng and Liu (1990).

Issues such as the location of the caverns relative to the toes of slopes and the determination of the lengths of steel linings in pressure tunnels, while not central to the question of cavern design, have important practical and financial implications and have been considered briefly in this chapter.

The principal issues which have been addressed are those of the failure and deformations induced in the rock mass surrounding large caverns and how these are dealt with in the choice of the excavation shape and the type of reinforcement used. Concrete arches, traditionally used to provide support for the rock mass above large powerhouse caverns, can suffer from excessive bending as a result of the large deformations which occur in these weak rocks. Consequently, the author recommends that concrete arches should not be used or that, if they are used, very careful attention be given to matching the deformation characteristics of the arch to the displacements which occur in the rock mass. A preferred means of support involves the installation of grouted cables and rockbolts in the rock mass and the application of a surface layer of shotcrete to stabilise the near surface blast-damaged rock. This system is very flexible, as compared with the concrete arch, and can move with the rock mass to accommodate the large displacements associated with cavern excavation. Corrosion protection of the cables is essential since

these provide the primary permanent support for the rock mass and must have a working life in excess of that of the cavern itself.

The sequence of installation of cables, rockbolts and shotcrete is an important issue which has been illustrated by means of a practical example. The questions of whether rockbolts and cables should be tensioned before grouting and when different shotcrete layers should be applied are all related to the development of the deformation pattern in the rock surrounding the excavation. Consequently, the sequence of support installation must be carefully matched to the sequence of excavation in order to provide adequate support without the risk of overstressing the support elements.

All of the care which has been taken in estimating the in situ stresses, the rock mass strength and deformation characteristics and in carrying out the support design can be wasted if excessive damage is inflicted on the rock by careless blasting. Techniques for controlling this blast damage are available and have proved to be very effective when Owners and Engineers work with the Contractor to ensure that these techniques are used during critical stages of a project.

14

Rockbolts and cables

14.1 Introduction

Rockbolts and dowels have been used for many years for the support of underground excavations and a wide variety of bolt and dowel types have been developed to meet different needs which arise in mining and civil engineering.

Rockbolts generally consist of plain steel rods with a mechanical anchor at one end and a face plate and nut at the other. They are always tensioned after installation. For short term applications the bolts are generally left ungrouted. For more permanent applications or in rock in which corrosive groundwater is present, the space between the bolt and the rock can be filled with cement or resin grout.

Dowels or anchor bars generally consist of deformed steel bars which are grouted into the rock. Tensioning is not possible and the load in the dowels is generated by movements in the rock mass. In order to be effective, dowels have to be installed before significant movement in the rock mass has taken place. Figure 14.1 illustrates a number of typical rockbolt and dowel applications that can be used to control different types of failure that occur in rock masses around underground openings.

The move towards larger underground excavations in both mining and civil engineering has resulted in the gradual development of cable reinforcement technology to take on the support duties which exceed the capacity of traditional rockbolts and dowels. Some of the hardware issues that are critical in the successful application of cables in underground excavations are reviewed in this chapter.

14.2 Rockbolts

14.2.1 Mechanically anchored rockbolts

Expansion shell rockbolt anchors come in a wide variety of styles but the basic principle of operation is the same in all of these anchors. As shown in Figure 14.2, the components of a typical expansion shell anchor are a tapered cone with an internal thread and a pair of wedges held in place by a bail. The cone is screwed onto the threaded end of the bolt and the entire assembly is inserted into the hole that has been drilled to receive the rockbolt. The length of the hole should be at least 100 mm longer than the bolt otherwise the bail will be dislodged by being forced against the end of the hole. Once the assembly is in place, a sharp pull on the end of the bolt will seat the anchor. Tightening the bolt will force the cone further into the wedge thereby increasing the anchor force.
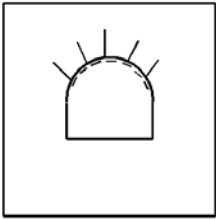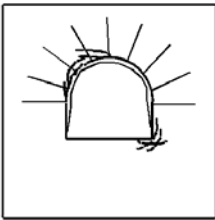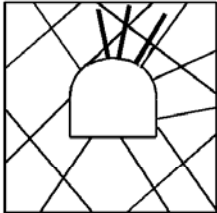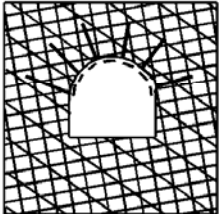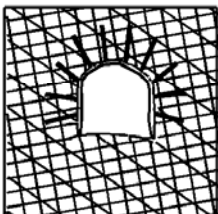
	Low stress levels	High stress levels
Massive rock	Massive rock subjected to low in situ stress levels. No permanent support. Light support may be required for construction safety.	Massive rock subjected to high in situ stress levels. Pattern rockbolts or dowels with mesh or shotcrete to inhibit fracturing and to keep broken rock in place.
Jointed rock	Massive rock with relatively few discontinuities subjected to low in situ stress conditions. 'Spot' bolts located to prevent failure of individual blocks and wedges. Bolts must be tensioned.	Massive rock with relatively few discontinuities subjected to high in situ stress conditions. Heavy bolts or dowels, inclined to cross rock structure, with mesh or steel fibre reinforced shotcrete on roof and sidewalls.
Heavily jointed rock	Heavily jointed rock subjected to low in situ stress conditions. Light pattern bolts with mesh and/or shotcrete will control ravelling of near surface rock pieces.	Heavily jointed rock subjected to high in situ stress conditions. Heavy rockbolt or dowel pattern with steel fibre reinforced shotcrete. In extreme cases, steel sets with sliding joints may be required. Invert struts or concrete floor slabs may be required to control floor heave.

Figure 14.1: Typical rockbolt and dowel applications to control different types of rock mass failure during tunnel driving.
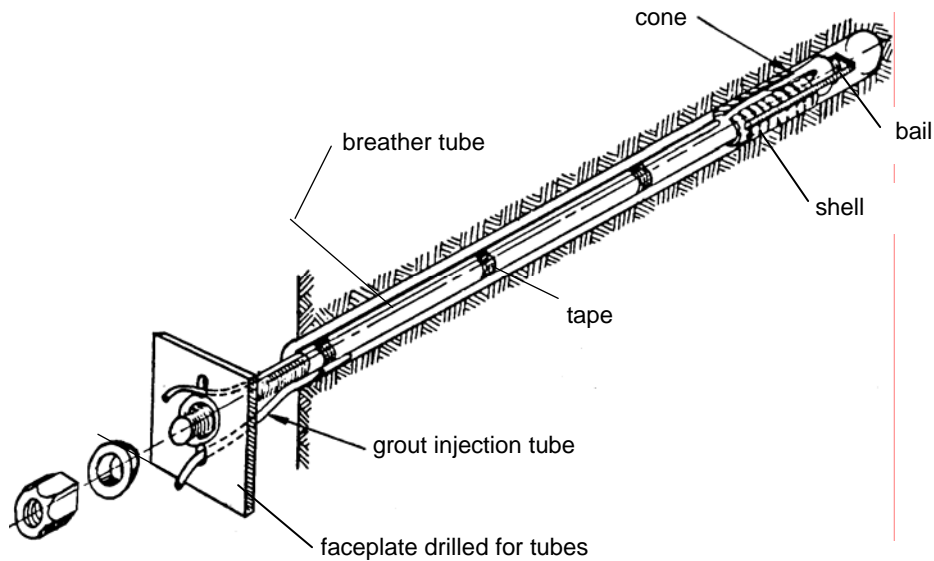
Figure 14.2: Components of a mechanically anchored rockbolt with provision for grouting.

These expansion shell anchors work well in hard rock but they are not very effective in closely jointed rocks and in soft rocks, because of deformation and failure of the rock in contact with the wedge grips. In such rocks, the use of resin cartridge anchors, described later in this chapter, are recommended.

At the other end of the rockbolt from the anchor, a fixed head or threaded end and nut system can be used. In either case, some form of faceplate is required to distribute the load from the bolt onto the rock face. In addition, a tapered washer or conical seat is needed to compensate for the fact that the rock face is very seldom at right angles to the bolt. A wide variety of faceplates and tapered or domed washers are available from rockbolt suppliers.

In general, threads on rockbolts should be as coarse as possible and should be rolled rather than cut. A fine thread is easily damaged and will cause installation problems in a typical underground environment. A cut thread weakens the bolt and it is not unusual to see bolts with cut threads that have failed at the first thread at the back of the nut. Unfortunately, rolled thread bolts are more expensive to manufacture and the added cost tends to limit their application to situations where high strength bolts are required.

Tensioning of rockbolts is important to ensure that all of the components are in contact and that a positive force is applied to the rock. In the case of light 'safety' bolts, the amount of tension applied is not critical and tightening the nut with a conventional wrench or with a pneumatic torque wrench is adequate. Where the bolts are required to carry a significant load, it is generally recommended that a tension of approximately 70% of the capacity of the bolt be installed initially. This provides a known load with a reserve in case of additional load being induced by displacements in the rock mass.

One of the primary causes of rockbolt failure is rusting or corrosion and this can be counteracted by filling the gap between the bolt and the drillhole wall with grout. While this is not required in temporary support applications, grouting should be considered where the ground-water is likely to induce corrosion or where the bolts are required to perform a 'permanent' support function.

The traditional method of grouting uphole rockbolts is to use a short grout tube to feed the grout into the hole and a smaller diameter breather tube, extending to the end of the hole, to bleed the air from the hole. The breather tube is generally taped to the bolt shank and this tends to cause problems because this tube and its attachments can be damaged during transportation or insertion into the hole. In addition, the faceplate has to be drilled to accommodate the two tubes, as illustrated in Figure 14.2. Sealing the system for grout injection can be a problem.

Many of these difficulties are overcome by using a hollow core bolt. While more expensive than conventional bolts, these hollow bolts make the grouting process much more reliable and should be considered wherever permanent rockbolt installations are required. The grout should be injected through a short grout tube inserted into the collar of the hole and the central hole in the bolt should be used as a breather tube. When installing these bolts in downholes, the grout should be fed through the bolt to the end of the hole and the short tube used as a breather tube.

Since the primary purpose of grouting mechanically anchored bolts is to prevent corrosion and to lock the mechanical anchor in place, the strength requirement for the grout is not as important as it is in the case of grouted dowels or cables (to be discussed later). The grout should be readily pumpable without being too fluid and a typical water/cement ratio of 0.4 to 0.5 is a good starting point for a grout mix for this application. It is most important to ensure that the annular space between the bolt and the drillhole wall is completely filled with grout. Pumping should be continued until there is a clear indication that the air has stopped bleeding through the breather tube or that grout is seen to return through this tube.

14.2.2 Resin anchored rockbolts

Mechanically anchored rockbolts have a tendency to work loose when subjected to vibrations due to nearby blasting or when anchored in weak rock. Consequently, for applications where it is essential that the support load be maintained, the use of resin anchors should be considered.

A typical resin product is made up of two component cartridges containing a resin and a catalyst in separate compartments, as shown in Figure 14.3. The cartridges are pushed to the end of the drillhole ahead of the bolt rod that is then spun into the resin cartridges by the drill. The plastic sheath of the cartridges is broken and the resin and catalyst mixed by this spinning action. Setting of the resin occurs within a few minutes (depending upon the specifications of the resin mix) and a very strong anchor is created.

This type of anchor will work in most rocks, including the weak shales and mudstones in which expansion shell anchors are not suitable. For 'permanent' applications, consideration should be given to the use of fully resin-grouted rockbolts, illustrated in Figure 14.4. In these applications, a number of slow-setting resin cartridges are inserted into the drillhole behind the fast-setting anchor cartridges.

Figure 14.3: Typical two-component resin cartridge used for anchoring and grouting rockbolts.
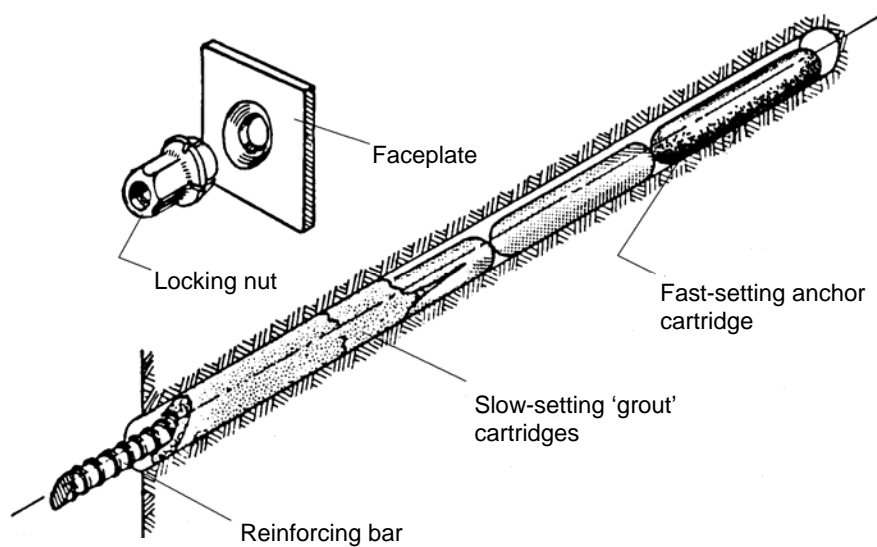
Figure 14.4: Typical set-up for creating a resin anchored and grouted rockbolt. Resin grouting involves placing slow-setting resin cartridges behind the fast-setting anchor cartridges and spinning the bolt rod through them all to mix the resin and catalyst. The bolt is tensioned after the fast-setting anchor resin has set and the slow-setting resin sets later to grout the rod in place.

Spinning the bolt rod through all of these cartridges initiates the chemical reaction in all of the resins but, because the slow-setting 'grout' cartridges are timed to set in up to 30 minutes, the bolt can be tensioned within two or three minutes of installation (after the fast anchor resin has set). This tension is then locked in by the later-setting grout cartridges and the resulting installation is a fully tensioned, fully grouted rockbolt.

The high unit cost of resin cartridges is offset by the speed of installation. The process described above results in a completely tensioned and grouted rockbolt installation in one operation, something that cannot be matched by any other system currently on the market. However, there are potential problems with resins.

Most resin/catalyst systems have a limited shelf life which, depending upon storage temperatures and conditions, may be as short as six months. Purchase of the resin cartridges should be limited to the quantities to be used within the shelf life. Care should be taken to store the boxes under conditions that conform to the manufacturer's recommendations. In critical applications, it is good practice to test the activity of the resin by sacrificing one cartridge from each box, before the contents are used underground. This can be done by breaking the compartment separating the resin and catalyst by hand and, after mixing the components, measuring the set time to check whether this is within the manufacturer's specifications.

Breaking the plastic sheath of the cartridges and mixing the resins effectively can also present practical problems. Cutting the end of the bolt rod at an angle to form a sharp tapered point will help in this process, but the user should also be prepared to do some experimentation to achieve the best results. Note that the length of time or the number of rotations for spinning the resins is limited. Once the setting process has been initiated, the structure of the resin can be damaged and the overall installation weakened by additional spinning. Most manufacturers supply instructions on the number of rotations or the length of time for spinning.

In some weak argillaceous rocks, the drillhole surfaces become clay-coated during drilling. This causes slipping of the resin cartridges during rotation, resulting in incomplete mixing and an unsatisfactory bond. In highly fractured rock masses, the resin may seep into the surrounding rock before setting, leaving voids in the resin column surrounding the rockbolt. In both of these cases, the use of cement grouting rather than resin grouting may provide a more effective solution.

There is some uncertainty about the long-term corrosion protection offered by resin grouts and also about the reaction of some of these resins with aggressive groundwater. For temporary applications, these concerns are probably not an issue because of the limited design life for most rockbolt installations. However, where very long service life is required, current wisdom suggests that cement grouted bolts may provide better long term protection.

14.3 Dowels

14.3.1 Grouted dowels

When conditions are such that installation of support can be carried out very close to an advancing face, or in anticipation of stress changes that will occur at a later excavation stage, dowels can be used in place of rockbolts. The essential difference between these systems is that tensioned rockbolts apply a positive force to the rock,

while dowels depend upon movement in the rock to activate the reinforcing action. Mining drawpoints, which are mined before the overlying stopes are blasted, are good examples of excavations where untensioned grouted dowels will work well.

The simplest form of dowel in use today is the cement grouted dowel as illustrated in Figure 14.5. A thick grout (typically a 0.3 to 0.35 water/cement ratio grout) is pumped into the hole by inserting the grout tube to the end of the hole and slowly withdrawing the tube as the grout is pumped in. Provided that a sufficiently viscous grout is used, it will not run out of the hole. The dowel is pushed into the hole about half way and then given a slight bend before pushing it fully into the hole. This bend will serve to keep the dowel firmly lodged in the hole while the grout sets. Once the grout has set, a face plate and nut can be fitted onto the end of the dowel and pulled up tight. Placing this face place is important since, if the dowel is called on to react to displacements in the rock mass, the rock close to the borehole collar will tend to pull away from the dowel unless restrained by a faceplate.

In mining drawpoints and ore-passes, the flow of broken rock can cause serious abrasion and impact problems. The projecting ends of grouted rebars can obstruct the flow of the rock. Alternatively, the rebar can be bent, broken or ripped out of the rock mass. In such cases, grouted flexible cable, illustrated in Figure 14.6, can be used in place of the more rigid rebar. This will allow great flexibility with impact and abrasion resistance.

Older type grouted dowels such as the Scandinavian 'perfobolt' or dowels, where the grout is injected after the rod has been inserted, tend not to be used. The installation is more complex and time consuming and the end product does not perform any better than the simple grouted dowel described above.
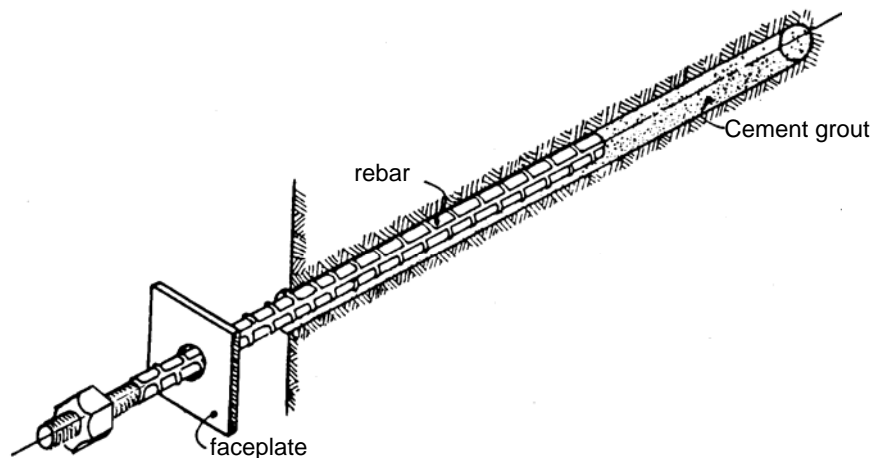
Figure 14.5: Grouted dowel using a deformed bar inserted into a grout-filled hole.
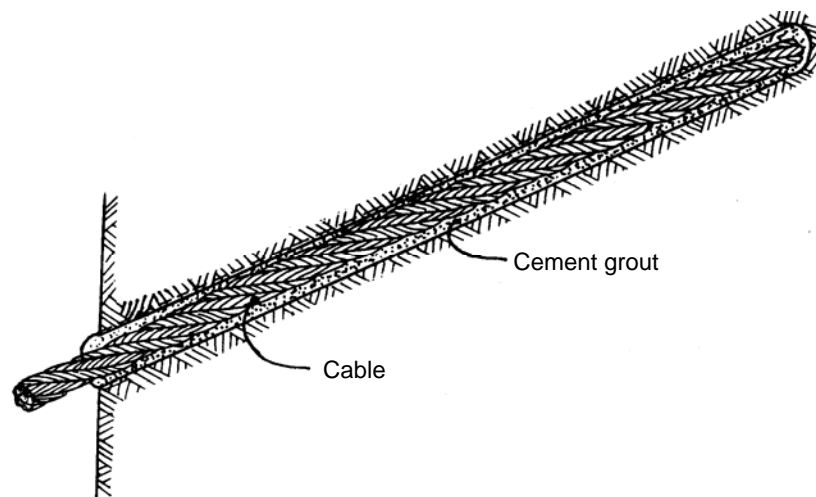
Figure 14.6: Gorouted cables can be used in place of rebar when more flexible support is required or were impact and abrasion can cause problems with rigid support.

14.3.2   *Friction dowels or 'Split Set' stabilisers*

Split Set stabilisers were originally developed by Scott (1976, 1983) and are manufactured and distributed by Ingersoll-Rand. The system, illustrated in Figure 14.7, consists of a slotted high strength steel tube and a face plate. It is installed by pushing it into a slightly undersized hole and the radial spring force generated, by the compression of the C shaped tube, provides the frictional anchorage along the entire length of the hole. A list of typical Split Set stabiliser dimensions and capacities is given in Table 14.1.

Because the system is quick and simple to install, it has gained rapid acceptance by miners throughout the world. The device is particularly useful in mild rockburst environments, because it will slip rather than rupture and, when used with mesh, will retain the broken rock generated by a mild burst. Provided that the demand imposed on Split Sets stabilisers does not exceed their capacity, the system works well and can be considered for many mining applications. They are seldom used in civil engineering applications.

Corrosion remains one of the prime problems with Split Set stabilisers since protection of the outer surface of the dowel is not feasible. Galvanising the tube helps to reduce corrosion, but is probably not a preventative measure which can be relied upon for long term applications in aggressive environments.

14.3.3   *'Swellex' dowels*

Developed and marketed by Atlas Copco, the 'Swellex' system is illustrated in Figure 14.8. The dowel, which may be up to 12 m long, consists of a 42 mm diameter tube which is folded during manufacture to create a 25 to 28 mm diameter unit which can be inserted into a 32 to 39 mm diameter hole. No pushing force is required during insertion and the dowel is activated by injection of high pressure water (approximately 30 MPa or 4,300 psi) which inflates the folded tube into intimate contact with the walls of the borehole.
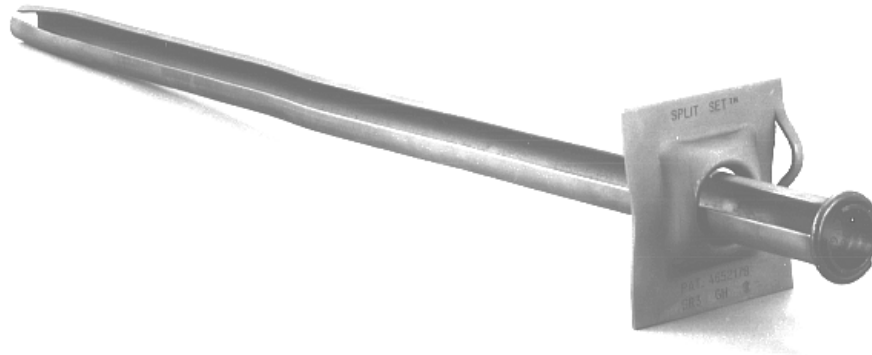
Figure 14.7: Split Set stabiliser. Ingersol-Rand photograph.

Table 14.1: Split Set specifications (After Split Set Division, Ingersol-Rand Company).

Split Set stabiliser model	*SS-33*	*SS-39*	*SS-46*
Recommended nominal bit size	31 to 33 mm	35 to 38 mm	41 to 45 mm
Breaking capacity, average	10.9 tonnes	12.7 tonnes	16.3 tonnes
minimum	7.3 tonnes	9.1 tonnes	13.6 tonnes
Recommended initial anchorage (tonnes)	2.7 to 5.4	2.7 to 5.4	4.5 to 8..2
Tube lengths	0.9 to 2.4 m	0.9 to 3.0 m	0.9 to 3.6 m
Nominal outer diameter of tube	33 mm	39 mm	46 mm
Domed plate sizes	150x150 mm	150x150 mm	150x150 mm
	125x125 mm	125x125 mm	
Galvanised system available	yes	yes	yes
Stainless steel model available	no	yes	no

During 1993 the original Swellex dowel was replaced by the EXL Swellex which is manufactured from a high strength but ductile steel. This steel allows significant displacement without loss of capacity. Stillborg (1994), carried out a series of tests in which bolts and dowels were installed across a simulated 'joint' and subjected to tensile loading. In the EXL Swellex dowel tests, opening of the joint concentrates loading onto the portion of the dowel crossing the joint, causing a reduction in diameter and a progressive 'de-bonding' of the dowel away from the joint. The ductile characteristics of the steel allows the de-bonded section to deform under constant load until, eventually, failure occurs when the total displacement reaches about 140 mm at a constant load of approximately 11 tonnes. These tests are described in greater detail later in this Chapter.

Corrosion of Swellex dowels is a matter of concern since the outer surface of the tube is in direct contact with the rock. Atlas Copco have worked with coating manufacturers to overcome this problem and claim to have developed effective corrosion resistant coatings.
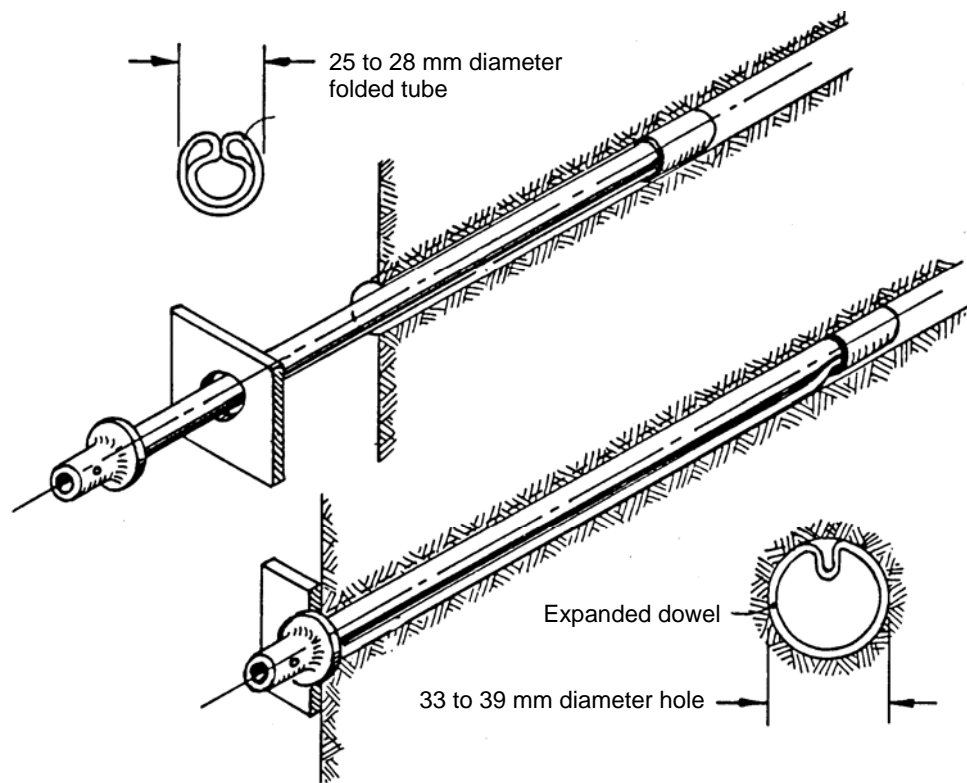
Figure 14.8: Atlas Copco 'Swellex' dowel.

Speed of installation is the principal advantage of the Swellex system as compared with conventional rockbolts and cement grouted dowels. In fact, the total installation cost of Swellex dowels or Spilt Set stabilisers tends to be less than that of alternative reinforcement systems, when installation time is taken into account. Both systems are ideal for use with automated rockbolters.

14.4 Load-deformation characteristics

Stillborg (1994) carried out a number of tests on rockbolts and dowels installed across a simulated 'joint', using two blocks of high strength reinforced concrete. This type of test gives a more accurate representation of conditions encountered underground than does a standard 'pull-out' test.

The rockbolts and dowels tested were installed in percussion drilled holes using the installation techniques used in a normal underground mining operation. The installed support systems were then tested by pulling the two blocks of concrete apart at a fixed rate and measuring the displacement across the simulated 'joint'.

The results of Stillborg's tests are summarised in Figure 14.9 which gives load deformation curves for all the bolts and dowels tested. The configuration used in each test and the results obtained are summarised below:
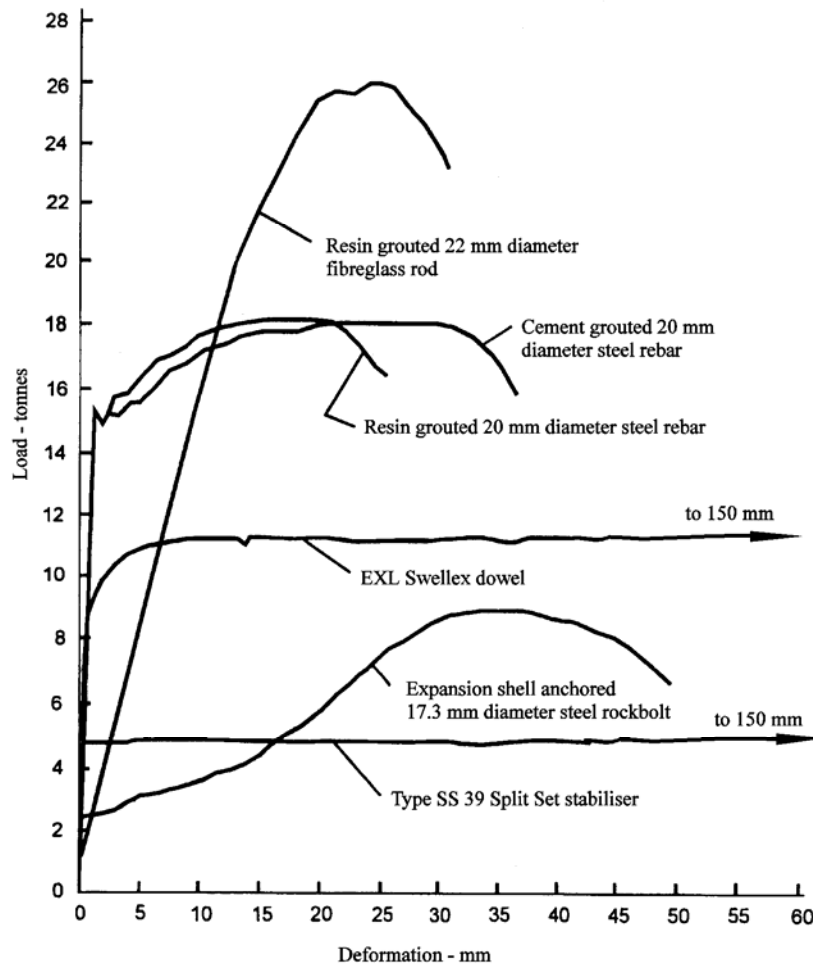
Figure 14.9: Load-deformation results obtained by Stillborg in tests carried out at Luleå University in Sweden. High strength reinforced concrete with a uniaxial compressive strength of 60 MPa was used for the test blocks and holes were drilled with a percussion rig to simulate in situ rock conditions.

1. Expansion shell anchored rockbolt

Steel rod diameter: 17.28 mm
Ultimate tensile strength of bolt shank: approximately 12.7 tonnes
Expansion shell anchor: Bail type three wedge anchor
At the pre-load of 2.25 tonnes, no deformation of the face plate.
At a load of 4 tonnes, the face plate has deformed 9.5 mm and is completely flat, the bolt shank has deformed an additional 3.5 mm giving a total deformation of 13 mm at 4 tonnes load.
Failure initiates at a load of 8 tonnes and a deformation of 25 mm with progressive failure of the expansion shell anchor in which the cone is pulled through the wedge.
Maximum load is 9 tonnes at a deformation of 35 mm.

2. Cement grouted steel rebar

Steel bar diameter: 20 mm

Ultimate tensile strength of steel rebar: 18 tonnes
Faceplate: flat plate
Borehole diameter: 32 mm
Cement grout: 0.35 water/cement ratio grout cured for 11 days

At a load of 15 tonnes and an elastic deformation of about 1.5 mm, a sudden load drop is characteristic of hot rolled rebar steel.
Maximum load is 18 tonnes at a deformation of 30 mm.

3. Resin grouted steel rebar

Steel rebar diameter: 20 mm
Ultimate tensile strength of steel rebar: 18 tonnes
Faceplate: flat plate
Borehole diameter: 32 mm
Resin grout: Five 580 mm long, 27 mm diameter polyester resin cartridges. Curing time 60 minutes. Mixed by rotating rebar through cartridges in the borehole

At a load of 15 tonnes and an elastic deformation of about 1.5 mm, a sudden load drop is characteristic of hot rolled rebar steel.
Maximum load is 18 tonnes at a deformation of 20 mm
The resin is stronger than the cement grout and local fracturing and bond failure in and near the joint is limited as compared with the cement grouted rebar, leading to a reduced ultimate displacement at rebar failure.

4. Resin grouted fibreglass rod

Fibreglass rod diameter: 22 mm
Ultimate tensile strength of fibreglass rod: 35 tonnes
Faceplate: special design by H. Weidmann AG. Switzerland (see margin drawing - after Stillborg)
Borehole diameter: 32 mm
Resin grout: Five 580 mm long, 27 mm diameter polyester resin cartridges. Curing time 60 minutes. Mixed by rotating fibreglass rod through cartridges in the borehole
At approximately 1.5 tonnes load, failure of the fibreglass/resin interface initiates and starts progressing along the rod. As bond failure progresses, the fiberglass rod deforms over a progressively longer 'free' length.
General bond failure occurs at a load of approximately 26 tonnes and a deformation of 25 mm.
The ultimate capacity of this assembly is determined by the bond strength between the resin and the fibreglass rod and by the relatively low frictional resistance of the fibreglass.

5. Split Set stabiliser, type SS 39

Tube diameter: 39 mm
Ultimate tensile strength of steel tube: 11 tonnes
Faceplate: special design by manufacturer (see Figure 12.8)
Borehole diameter: 37 mm

Dowel starts to slide at approximately 5 tonnes and maintains this load for the duration of the test which, in this case, was to a total displacement of 150 mm

6. EXL Swellex dowel

   Tube diameter: 26 mm before expansion
   Ultimate tensile strength of steel tube: 11.5 tonnes (before expansion)
   Type of face plate: Domed plate (see margin drawing - after
     Stillborg)
   Borehole diameter: 37 mm
   Pump pressure for expansion of dowel: 30 MPa
   At 5 tonnes load the dowel starts to deform locally at the joint and, at the same time,
     'bond' failure occurs at the joint and progresses outward from the joint as the load is
     increased. General 'bond' failure occurs at 11.5 tonnes at a deformation of approximately
     10 mm. The dowel starts to slide at this load and maintains the load for the duration of
     the test which, in this case, was to 150 mm.

14.5 Cables

A comprehensive review of cable support in underground mining has been given in a book by Hutchinson and Diederichs (1996). This book is highly recommended for anyone who is concerned with the selection and installation of cable support for either mining or civil engineering applications.

   Some of the main cable types used by mining have been summarised by Windsor (1992) and are illustrated in Figure 14.10.

14.5.1   Bond strength

The forces and displacements associated with a stressed cable grouted into a borehole in rock are illustrated in Figure 14.11.

   As the cable pulls out of the grout, the resultant interference of the spiral steel wires with their associated grout imprints or flutes causes radial displacement or dilation of the interface between the grout and the cable. The radial dilation induces a confining pressure that is proportional to the combined stiffness of the grout and the rock surrounding the borehole. The shear stress, which resists sliding of the cable, is a product of the confining pressure and the coefficient of friction between the steel wires and the grout. Shear strength, therefore, increases with higher grout strength, increases in the grout and the rock stiffness and increases in the confining stresses in the rock after installation of the cable. Conversely, decrease in shear strength can be expected if any of these factors decrease or if the grout crushes.

   Theoretical models of the behaviour of this rock/grout/cable system have been developed by Yazici and Kaiser (1992), Kaiser et al (1992), Hyett et al, (1992). The second of these models has been incorporated into the program PHASE^2.

14.5.2   Grouts and grouting

The question of grout quality has always been a matter of concern in reinforcement systems for underground construction. One of the critical factors in this matter has been the evolution of grout pumps capable of pumping grouts with a low enough water/cement ratio (by weight) to achieve adequate strengths. Fortunately, this problem has now been overcome and there is a range of grout pumps on the market which will pump very viscous grouts and will operate reliably under typical underground conditions.

TYPE	LONGITUDINAL SECTION	CROSS SECTION
Multi-wire tendon (Clifford, 1974)		
Birdcaged multi-wire tendon (Jirovec, 1978)		Antinode Node
Single strand (Hunt & Askew, 1977)		Normal Indented Drawn
Coated single strand (Hunt & Askew, 1977)		Sheathed Coated Encapsulated
Barrel and wedge anchor on strand (Mathews et al, 1984)	Double-acting twin anchor Single anchor	3 component 2 component
Swaged anchor on strand (Schmuck, 1979)		Square Circular
High capacity shear dowel (Mathews et al, 1986)		Steel tube Concrete
Birdcaged strand (Hutchins et al, 1990)		Antinode Node
Bulbed strand (Garford, 1990)		Antinode Node
Ferruled strand (Windsor, 1990)		Antinode Node

Figure 14.10: Summary of the development of cable reinforcing systems for underground mining (Windsor (1992)).
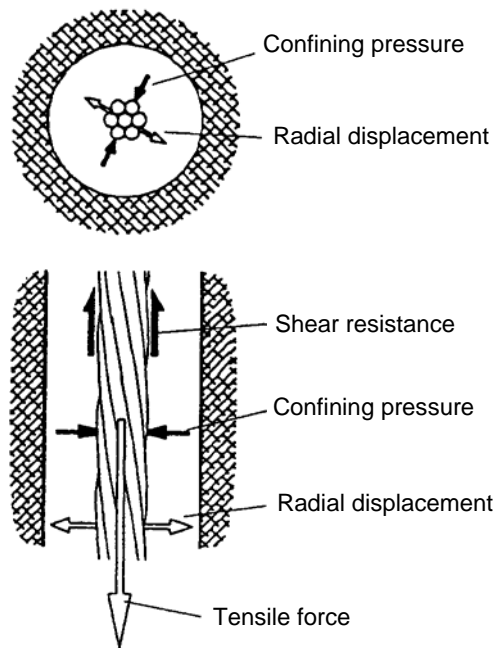
Figure 14.11: Forces and displacements associated with a stressed cable
grouted into a borehole in rock.

The results of a comprehensive testing programme on Portland cement grouts have
been summarised by Hyett et al (1992) and Figures 14.12, and 14.13 are based upon
this summary. Figure 14.12 shows the decrease in both 28 day uniaxial compressive
strength and deformation modulus with increasing water/cement ratio. Figure 14.13
gives Mohr failure envelopes for three water/cement ratios.

These results show that the properties of grouts with water/cement ratios of 0.35 to
0.4 are significantly better than those with ratios in excess of 0.5. However, Hyett et
al found that the scatter in test results increased markedly for water/cement ratios less
than 0.35. The implication is that the ideal water/cement ratio for use with cable
reinforcement lies in the range of 0.35 to 0.4.

The characteristics of grouts with different water/cement ratios are described as
follows (after Hyett et al, 1992):

w/c ratio	Characteristics at end of grout hose	Characteristics when handled
< 0.30	Dry, stiff sausage structure.	Sausage fractures when bent. Grout too dry to stick to hand. Can be rolled into balls.
0.30	Moist sausage structure. 'Melts' slightly with time.	Sausage is fully flexible. Grout will stick to hand. Easily rolled into wet, soft balls.
0.35	Wet sausage structure. Structure 'melts' away with time.	Grout sticks readily to hand. Hangs from hand when upturned.
0.4	Sausage structure lost immediately. Flows viscously under its own weight to form pancake.	Grout readily sticks to hand but can be shaken free.
0.5	Grout flows readily and splashes on impact with ground.	Grout will drip from hand - no shaking required.
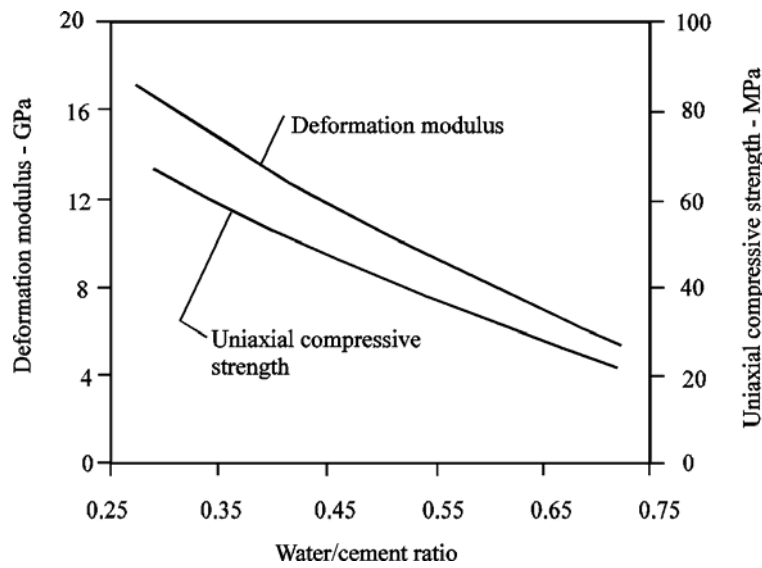
Figure 14.12: Relationship between the water/cement ratio and the average uniaxial compressive strength an deformation modulus for grouts testes at 28 days.
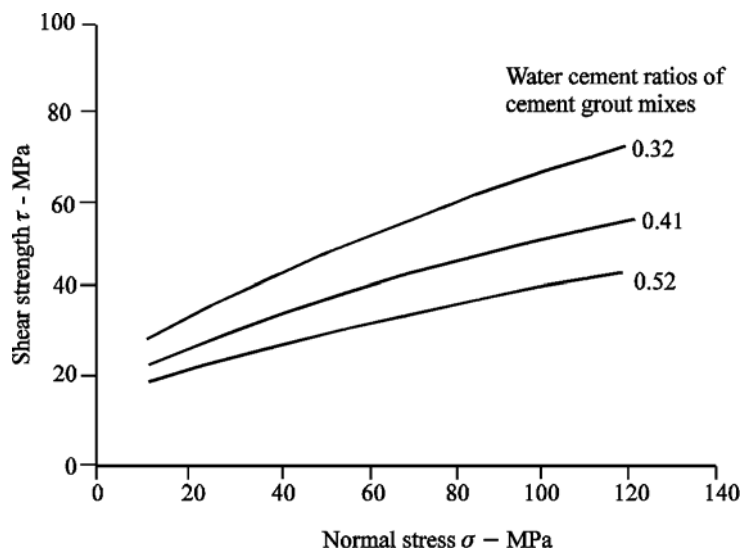
w/c ratio	σ_c MPa	constant m	constant s	Friction angle $\phi°$	Cohesion c MPa
0.32	78	3.05	1	24	25
0.41	54	2.14	1	20	19
0.52	38	1.67	1	17	14

Figure 14.13: Mohr failure envelopes for the peak strength of grouts with different water/cement ratios, tested at 28 days.

14.5.3   Cable installation

The left hand drawing in Figure 14.14 shows the traditional method of grouting a cable in an uphole. This method will be called the 'breather tube method'. The grout, usually having a water/cement ratio ≥ 0.4, is injected into the bottom of the hole through a large diameter tube, typically 19 mm diameter. The air is bled through a smaller diameter tube which extends to the end of the hole and which is taped onto the cable. Both tubes and the cable are sealed into the bottom of the hole by means of a plug of cotton waste or of quick setting mortar. As shown, the direction of grout travel is upwards in the hole and this tends to favour a grout column which is devoid of air gaps since any slump in the grout tends to fill these gaps.

Apart from the difficulty of sealing the collar of the hole, the main problem with this system is that it is difficult to detect when the hole is full of grout. Typically, the hole is judged to be full when air ceases to flow from the bleed tube. This may occur prematurely if air is vented into an open joint along the hole. In addition, a void the size of the bleed tube is likely to be left in the grout column. Therefore, it is preferable to stop grouting the borehole only when grout returns along the bleed tube. However, a viscous grout will not flow down a 9 mm bleed tube and so a larger tube is required.

An alternative method, called the 'grout tube method' is illustrated in the right hand drawing in Figure 14.14. In this case a large diameter grout injection tube extends to the end of the hole and is taped onto the cable. The cable and tube are held in place in the hole by a wooden wedge inserted into the hole collar. Note that care has to be taken to avoid compressing the grout tube between the wedge and the cable. Grout is injected to the top of the hole and is pumped down the hole until it appears at the hole collar. If a watery grout appears first at the collar of the hole, grout pumping is continued until a consistently thick grout is observed.

Provided that a very viscous mix is used (0.3 to 0.35 water/cement ratio), the grout will have to be pumped into the hole and there is little danger of slump voids being formed. However, a higher water/cement ratio mix will almost certainly result in air voids in the grout column as a result of slumping of the grout. The principal advantage of this method is that it is fairly obvious when the hole is full of grout and this, together with the smaller number of components required, makes the method attractive when compared with the traditional method for grouting plain strand cables. In addition, the thicker grout used in this method is not likely to flow into fractures in the rock, preferring instead the path of least flow resistance towards the borehole collar.

The procedure used for grouting downholes is similar to the grout tube method, described above, without the wooden wedge in the borehole collar. The grout tube may be taped to the cable or retracted slowly from the bottom of the hole as grouting progresses. It is important to ensure that the withdrawal rate does not exceed the rate of filling the hole so the air voids are not introduced. This is achieved by applying, by hand, a slight downward force to resist the upward force applied to the tube by the rising grout column. Grout of any consistency is suitable for this method but the best range for plain strand cables is between 0.3 and 0.4 water/cement ratio.

Modified cables, such as birdcage, ferruled or bulbed strand, should be grouted using a 0.4 water/cement ratio mix to ensure that the grout is fluid enough to fill the cage structure of these cables. Therefore, the breather tube method must be used for

these types of cables, since the grout flow characteristics required by the grout tube method is limited to grouts in the range of 0.3 to 0.35 water/cement ratio.

One of the most critical components in a cable installation is the grout column. Every possible care must be taken to ensure that the column contains as few air voids as possible. In the breather tube method, a large diameter breather tube will allow the return of grout as well as air. When using the grout tube method in upholes, a 0.3 to 0.35 water/cement ration grout will ensure that pumping is required to cause the grout column to flow, and this will avoid slumping of the grout in the borehole. A grout with a water/cement ratio of less than 0.3 should be avoided, since it will tend to form encapsulated air voids as it flows around the cable.
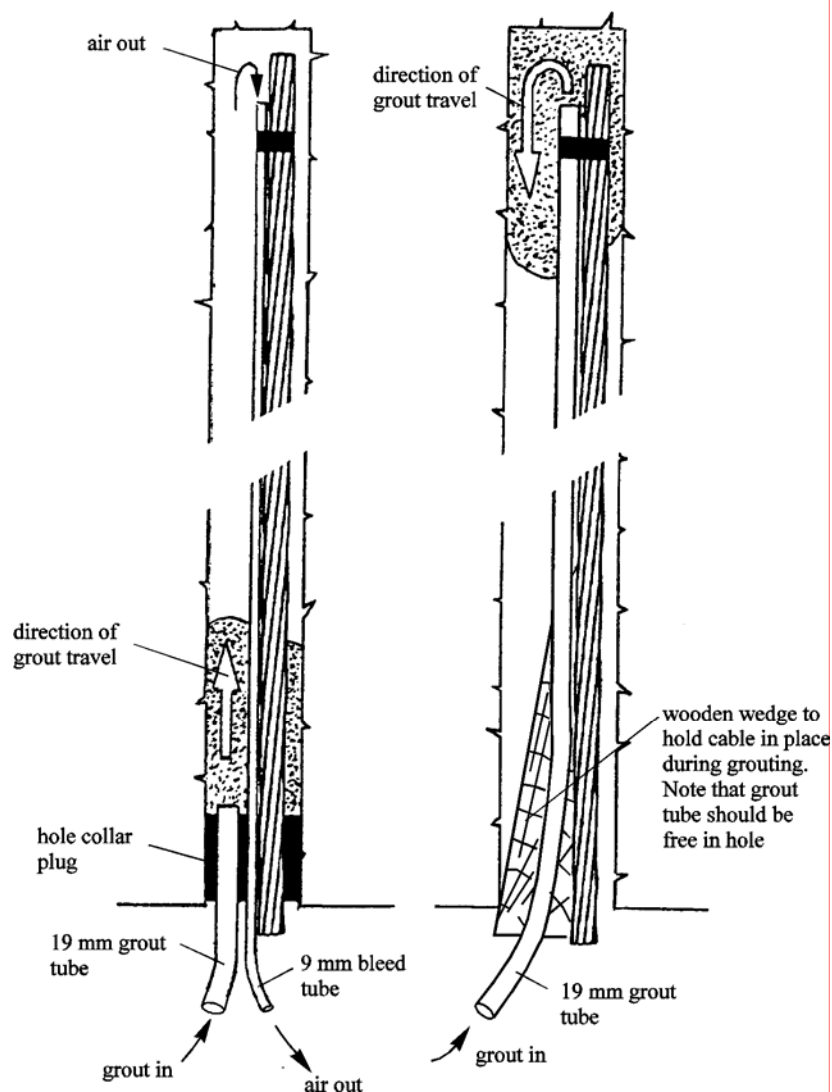
Figure 14.14: Alternative methods for grouting cables in upholes.

A hollow cable, illustrated in Figure 14.15, has been introduced by Atlas Copco and this could reduce some of the grouting problems discussed above.

Figure 14.15: Hollow cable by Atlas Copco.

14.5.4   Cables for slope reinforcement

Most of the applications described in this chapter have been related to underground excavations. However, under certain circumstances, it may also be necessary to reinforce slopes and foundations and cables have proved to be very effective in such applications.

Figure 14.16 illustrates a unit set up for drilling 140 m long 50 mm diameter holes for the installation of cables, illustrated in Figure 14.17, in a slope.

Figure 14.16: Drilling machine for the installation of 40 m long reinforcing cables in 50 mm diameter holes in a dam excavation.

Figure 14.17: 40 m long multi-strand cables with a capacity of 200 tons each being prepared for installation in a dam excavation.

These cables were installed to stabilise the slopes of a dam foundation in gneiss. Sheet jointing parallel to the surface of the steep slopes would have resulted in large scale slope instability if the excavation, which undercut these sheet joints, had not been reinforced.

The cables illustrated have an ultimate capacity of 312 tons and a working load of 200 tons. The cables were fully grouted after tensioning. The cost of materials and installation for these cables was approximately US$ 500 per metre.

15

Shotcrete support

15.1 Introduction

The use of shotcrete for the support of underground excavations was pioneered by the civil engineering industry. Reviews of the development of shotcrete technology have been presented by Rose (1985), Morgan (1992) and Franzén (1992). Rabcewicz (1969) was largely responsible for the introduction of the use of shotcrete for tunnel support in the 1930s, and for the development of the New Austrian Tunnelling Method for excavating in weak ground.

In recent years the mining industry has become a major user of shotcrete for underground support. It can be expected to make its own contributions to this field as it has in other areas of underground support. The simultaneous working of multiple headings, difficulty of access and unusual loading conditions are some of the problems which are peculiar to underground mining and which require new and innovative applications of shotcrete technology.

An important area of shotcrete application in underground mining is in the support of 'permanent' openings such as ramps, haulages, shaft stations and crusher chambers. Rehabilitation of conventional rockbolt and mesh support can be very disruptive and expensive. Increasing numbers of these excavations are being shotcreted immediately after excavation. The incorporation of steel fibre reinforcement into the shotcrete is an important factor in this escalating use, since it minimises the labour intensive process of mesh installation.

Recent trials and observations suggest that shotcrete can provide effective support in mild rockburst conditions (McCreath and Kaiser, 1992, Langille and Burtney, 1992). While the results from these studies are still too limited to permit definite conclusions to be drawn, the indications are encouraging enough that more serious attention will probably be paid to this application in the future.

15.2 Shotcrete technology

Shotcrete is the generic name for cement, sand and fine aggregate concretes which are applied pneumatically and compacted dynamically under high velocity.

15.2.1 Dry mix shotcrete

As illustrated in Figure 15.1, the dry shotcrete components, which may be slightly pre-dampened to reduce dust, are fed into a hopper with continuous agitation. Compressed air is introduced through a rotating barrel or feed bowl to convey the

materials in a continuous stream through the delivery hose. Water is added to the mix at the nozzle. Gunite, a proprietary name for dry-sprayed mortar used in the early 1900's, has fallen into disuse in favour of the more general term shotcrete.
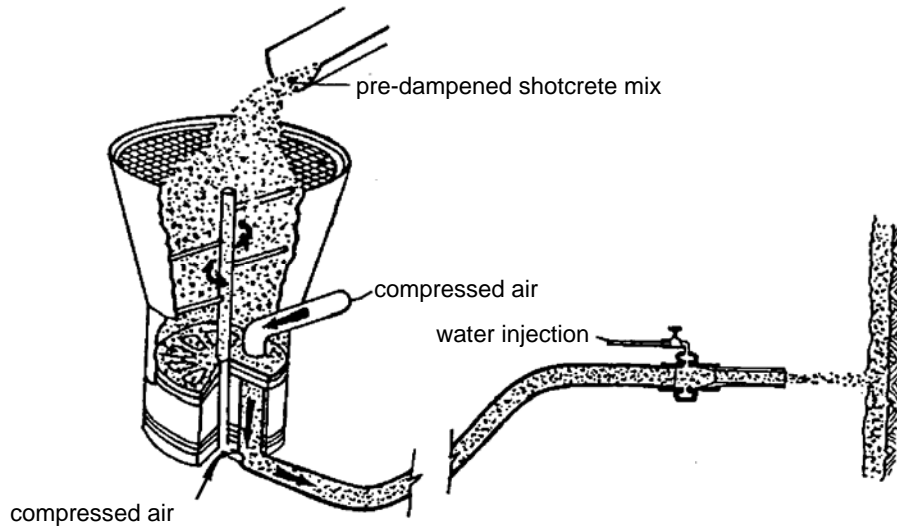
Figure 15.1: Simplified sketch of a typical dry mix shotcrete system. After Mahar et al (1975).
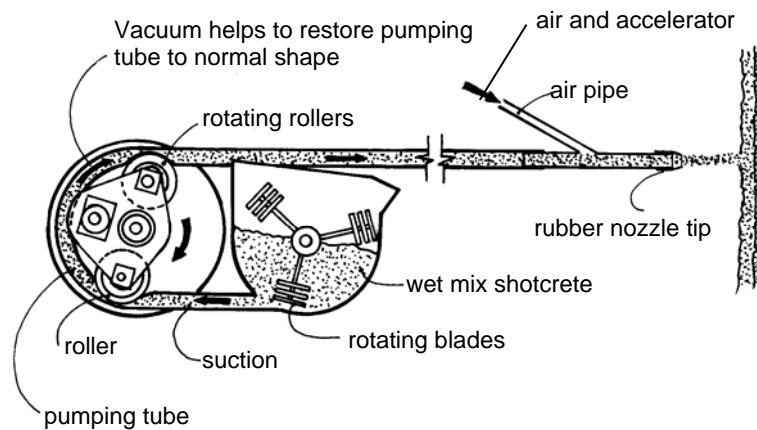
Figure 15.2: One typical type of wet mix shotcrete machine. After Mahar et al (1975).

15.2.2 Wet mix shotcrete

In this case the shotcrete components and the water are mixed (usually in a truck mounted mixer) before delivery into a positive displacement pumping unit, which then delivers the mix hydraulically to the nozzle where air is added to project the material onto the rock surface.

The final product of either the dry or wet shotcrete process is very similar. The dry mix system tends to be more widely used in mining, because of inaccessibility for large transit mix trucks and because it generally uses smaller and more compact equipment. This can be moved around relatively easily in an underground mine environment. The wet mix system is ideal for high production applications in mining and civil engineering, where a deep shaft or long tunnel is being driven and where access allows the application equipment and delivery trucks to operate on a more or less continuous basis. Decisions to use the dry or wet mix shotcrete process are usually made on a site-by-site basis.

15.2.3   *Steel fibre reinforced micro silica shotcrete*

Of the many developments in shotcrete technology in recent years, two of the most significant were the introduction of silica fume, used as a cementitious admixture, and steel fibre reinforcement.

Silica fume or micro silica is a by-product of the ferro silicon metal industry and is an extremely fine pozzolan. Pozzolans are cementitious materials which react with the calcium hydroxide produced during cement hydration. Silica fume, added in quantities of 8 to 13% by weight of cement, can allow shotcrete to achieve compressive strengths which are double or triple the value of plain shotcrete mixes. The result is an extremely strong, impermeable and durable shotcrete. Other benefits include reduced rebound, improved flexural strength, improved bond with the rock mass and the ability to place layers of up to 200 mm thick in a single pass because of the shotcrete's 'stickiness'. However, when using wet mix shotcrete, this stickiness decreases the workability of the material and superplaticizers are required to restore this workability.

Steel fibre reinforced shotcrete was introduced in the 1970s and has since gained world-wide acceptance as a replacement for traditional wire mesh reinforced plain shotcrete. The main role that reinforcement plays in shotcrete is to impart ductility to an otherwise brittle material. As pointed out earlier, rock support is only called upon to carry significant loads once the rock surrounding an underground excavation deforms. This means that unevenly distributed non-elastic deformations of significant magnitude may overload and lead to failure of the support system, unless that system has sufficient ductility to accommodate these deformations.

Typical steel fibre reinforced, silica fume shotcrete mix designs are summarised in Table 15.1. These mixes can be used as a starting point when embarking on a shotcrete programme, but it may be necessary to seek expert assistance to 'fine tune' the mix designs to suit site specific requirements. For many dry mix applications it may be advantageous to purchase pre-mixed shotcrete in bags of up to 1,500 kg capacity, as illustrated in Figure 15.3.

Figure 15.4 shows the steel fibre types which are currently available on the north American market. In addition to their use in shotcrete, these fibres are also widely used in concrete floor slabs for buildings, in airport runways and in similar concrete applications.

Wood et al (1993) have reported the results of a comprehensive comparative study in which all of the fibres shown in Figure 15.4 were used to reinforce shotcrete samples, which were then subjected to a range of tests. Plain and fibre reinforced silica fume

shotcrete samples were prepared by shooting onto vertical panels, using both wet and dry mix processes. The fibre reinforced samples all contained the same steel fibre dosage of 60 kg/m^3 (see Table 15.1). All the samples were cured under controlled relative humidity conditions and all were tested seven days after shooting.

Table 15.1: Typical steel fibre reinforced silica fume shotcrete mix designs (After Wood, 1992)

Components	Dry mix		Wet mix	
	kg./m^3	% dry materials	kg./m^3	% wet materials
Cement	420	19.0	420	18.1
Silica fume additive	50	2.2	40	1.7
Blended aggregate	1,670	75.5	1,600	68.9
Steel fibres	60	2.7	60	2.6
Accelerator	13	0.6	13	0.6
Superplasticizer	-	-	6 litres	0.3
Water reducer	-	-	2 litres	0.1
Air entraining admixture	-	-	if required	
Water	controlled at nozzle		180	7.7
Total	2,213	100	2,321	100

Figure 15.3: Bagged pre-mixed dry shotcrete components being delivered into a hopper feeding a screw conveyor, fitted with a pre-dampener, which discharges into the hopper of a shotcrete machine
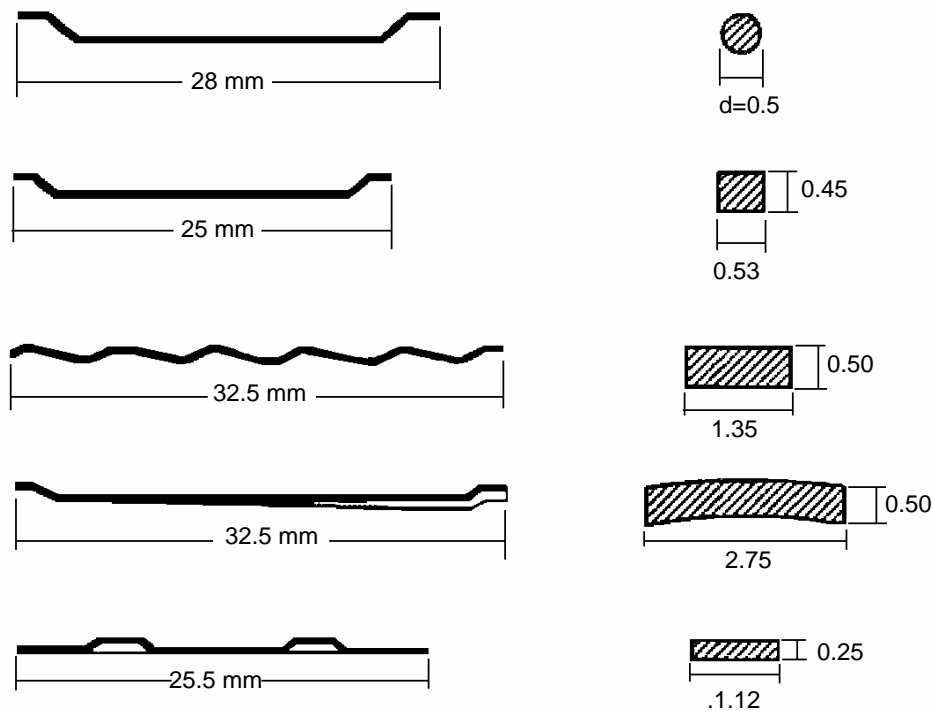
Figure 15.4. Steel fibre types available on the north American market. After Wood et al (1993). (Note: all dimensions are in mm).

These tests showed that the addition of steel fibres to silica fume shotcrete enhances both the compressive and flexural strength of the hardened shotcrete by up to 20%. A significant increase in ductility was also obtained in all the tests on fibre reinforced samples, compared with plain samples. While different fibres gave different degrees of improvement, all of the fibres tested were found to exceed the levels of performance commonly specified in north America (i.e. 7-day compressive strength of 30 MPa for dry mix, 25 MPa for wet mix and 7-day flexural strength of 4 MPa).

Kompen (1989) carried out bending tests on slabs of unreinforced shotcrete and shotcrete reinforced with 'Dramix'[1] steel fibres, shown in Figure 15.5. The shotcrete had an unconfined compressive strength, determined from tests on cubes, of 50 MPa. The results of these tests are reproduced in Figure 15.6. The peak strength of these slabs increased by approximately 85% and 185% for 1.0 and 1.5 volume % of fibres, respectively. The ductility of the fibre reinforced slabs increased by approximately 20 and 30 times for the 1.0 and 1.5 volume % of fibres, respectively.
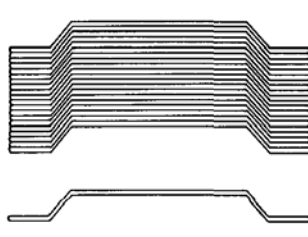
Figure 15.5: 'Dramix' steel fibres used in slab bending tests by Kompen (1989). The fibres are glued together in bundles with a water soluble glue to facilitate handling and homogeneous distribution of the fibres in the shotcrete.

---

[1] Manufactured by N.V. Bekaert S.A., B-8550 Zwevegem, Belgium.
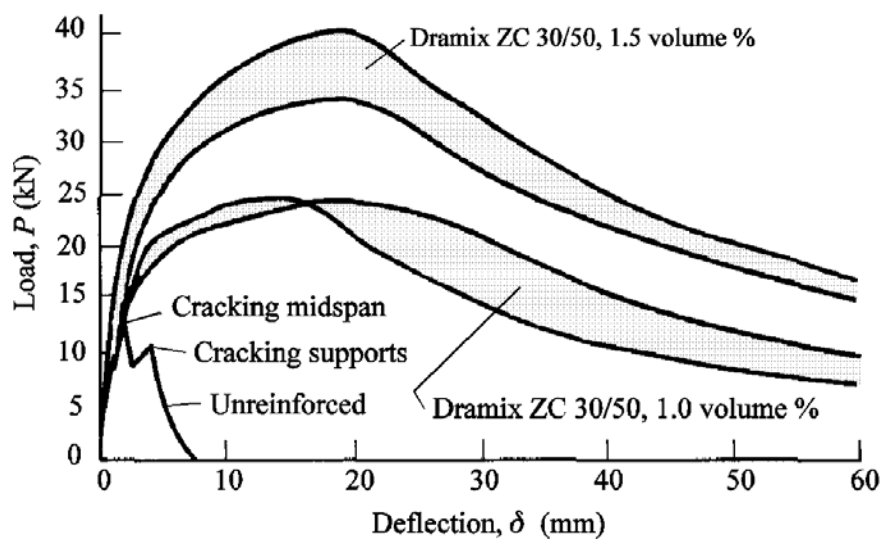
Figure 15.6: Load deflection curves for unreinforced and steel fibre reinforced shotcrete slabs tested in bending. After Kompen (1989).

15.2.4   *Mesh reinforced shotcrete*

While steel fibre reinforced shotcrete has been widely accepted in both civil and mining engineering, mesh reinforced shotcrete is still widely used and is preferred in some applications. In very poor quality, loose rock masses, where adhesion of the shotcrete to the rock surface is poor, the mesh provides a significant amount of reinforcement, even without shotcrete. Therefore, when stabilising slopes in very poor quality rock masses or when building bulkheads for underground fill, weldmesh is frequently used to stabilise the surface or to provide reinforcement. In such cases, plain shotcrete is applied later to provide additional support and to protect the mesh against corrosion.

Kirsten (1992, 1993) carried out a comprehensive set of laboratory bending tests on both mesh and fibre reinforced shotcrete slabs. The load versus deflection curves, that he obtained, were similar to those reported by Kompen, reproduced in Figure 15.6. He found that the load carrying capacity of the mesh and fibre reinforced shotcrete samples were not significantly different, but that the mesh reinforced samples were superior in bending with both point loads and uniformly distributed loads. He concluded that this was due to the more favourable location of the mesh reinforcement in the slabs subjected to bending.

Kirsten also concluded that the quality control, required to obtain a consistent dosage and uniform distribution of fibres in shotcrete, is more easily achieved in civil engineering than in mining applications. This is a reflection of the multiple working headings and the difficulties of access that are common problems associated with many mines. Under these circumstances, more reliable reinforcement will be obtained with mesh reinforced rather than fibre reinforced shotcrete. However, in large mines, in which many of the 'permanent' openings are similar to those on large civil engineering sites, these problems of quality control should not arise.

Chainlink mesh, used in many underground mining excavations to support loose rock, is not usually suitable for shotcrete reinforcement. This is because penetration of the shotcrete is inhibited by the twisted joints as illustrated in Figure 15.7. This allows air cavities to form behind the mesh and these may allow water to enter and cause corrosion of the mesh.

On the other hand, weldmesh, tightly pinned against the rock face as illuatrated in Figure 15.8, is generally ideal for shotcrete applications. Typically the weldmesh should be made from 4 mm diameter wire welded into a 100 mm x 100 mm grid. This type of mesh is strong enough for most underground applications and the sheets are light enough to he handled by one man.

Figure 15.7: Chainlink mesh, while very strong and flexible, is not ideal for shotcrete application because it is difficult for the shotcrete to penetrate the mesh.

Figure 15.8: Welded wire mesh, firmly attached to the rock surface, provides excellent reinforcement for shotcrete.

15.3 Shotcrete applications

The quality of the final shotcrete product is closely related to the application procedures used. These procedures include: surface preparation, nozzling technique, lighting, ventilation, communications, and crew training.

Shotcrete should not be applied directly to a dry, dusty or frozen rock surface. The work area is usually sprayed with an air-water jet to remove loose rock and dust from the surface to be shot. The damp rock will create a good surface on which to bond the initial layer of shotcrete paste. The nozzleman commonly starts low on the wall and moves the nozzle in small circles working his way up towards the back, or roof. Care must be taken to avoid applying fresh materials on top of rebound or oversprayed shotcrete. It is essential that the air supply is consistent and has sufficient capacity to ensure the delivery of a steady stream of high velocity shotcrete to the rock face. Shooting distances are ideally about 1 to 1.5 metres. Holding the nozzle further from the rock face will result in a lower velocity flow of materials which leads to poor compaction and a higher proportion of rebound.

A well-trained operator can produce excellent quality shotcrete manually, when the work area is well-lit and well-ventilated, and when the crew members are in good communication with each other using prescribed hand signals or voice activated FM radio headsets. However, this is a very tiring and uncomfortable job, especially for overhead shooting, and compact robotic systems are increasingly being used to permit the operator to control the nozzle remotely. Typical robotic spray booms, used for shotcrete application in underground excavations, are illustrated in Figures 15.9, 15.10 and 15.11.

Figure 15.9: A truck mounted shotcrete robot being used in a large civil engineering tunnel. Note that the distance between the nozzle and the rock surface is approximately one metre.

Figure 15.10: Compact trailer-mounted robot unit for remote controlled shotcrete application.
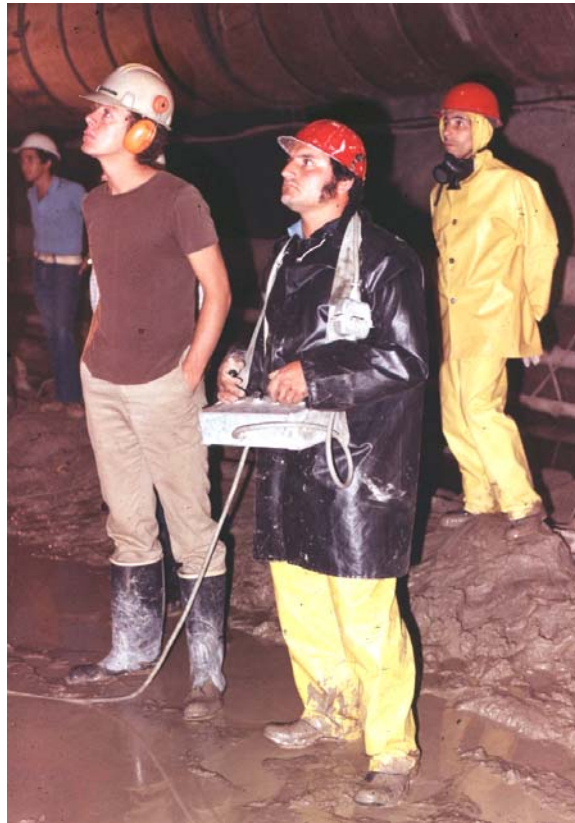
Figure 15.11: Shotcrete operator using a remotely controlled unit to apply shotcrete to a rock face in a large civil engineering excavation.
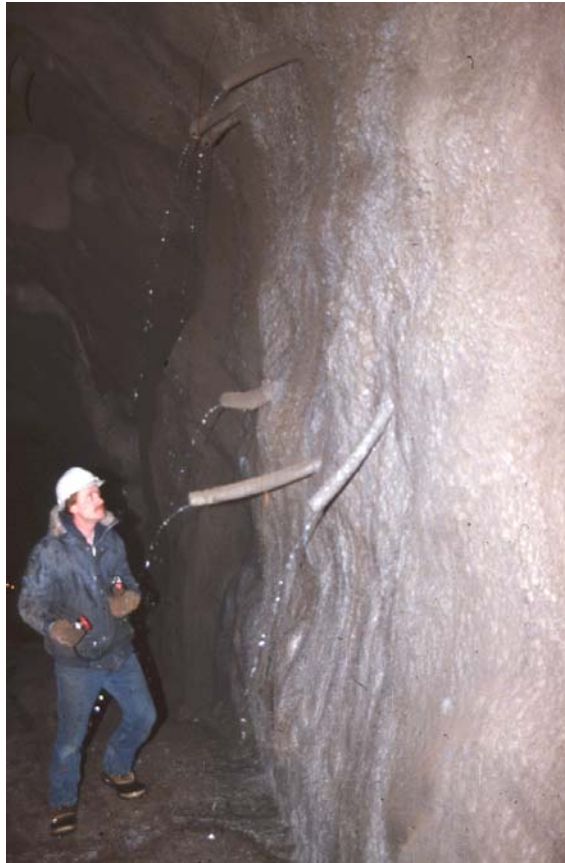
Figure 15.12: Plastic pipes used to provide drainage for a
shotcrete layer applied to a rock mass with water-bearing
joints.

When shotcrete is applied to rock masses with well-defined water-bearing joints, it is
important to provide drainage through the shotcrete layer in order to relieve high
water pressures. Drain holes, fitted with plastic pipes as illustrated in Figure 15.12,
are commonly used for this purpose. Where the water inflow is not restricted to a few
specific features, a porous fibre mat can be attached to the rock surface before the
shotcrete layer is applied. When practical to do so, the water from these drains should
be collected and directed into a drainage ditch or sump.

15.4 Design of shotcrete support

The design of shotcrete support for underground excavations is a very imprecise
process. However, one observation, which is commonly made by practical engineers
with years of experience in using shotcrete underground, is that it almost always
performs better than anticipated. There are many examples (very few of which are
documented) where shotcrete has been used as a last act of desperation in an effort to
stabilise the failing rock around a tunnel and, to most people's surprise, it has worked.

The complex interaction between the failing rock mass around an underground
opening, and a layer of shotcrete of varying thickness with properties which change
as it hardens, defies most attempts at theoretical analysis. It is only in recent years,

with the development of powerful numerical tools, that it has been possible to contemplate realistic analyses, which will explore the possible support-interaction behaviour of shotcrete. A clear understanding of shotcrete behaviour will require many more years of experience in the use of and in the interpretation of the results obtained from these programs. It is also important to recognise that shotcrete is very seldom used alone and its use in combination with rockbolts, cablebolts, lattice girders or steel sets further complicates the problem of analysing its contribution to support.

Current shotcrete support 'design' methodology relies very heavily upon rules of thumb and precedent experience. Wickham et al (1972) related the thickness of a shotcrete tunnel lining to their Rock Structure Rating (*RSR*). Bieniawski (1989) gave recommendations on shotcrete thicknesses (in conjunction with rockbolts or steel sets) for different Rock Mass Ratings (*RMR*) for a 10 m span opening. Grimstad and Barton (1993) have published an updated relating different support systems, including shotcrete and fibre reinforced shotcrete, to the Tunnelling Quality Index *Q*. Vandewalle (1990) collected various rules of thumb from a variety of sources and included them in his monograph.

Table 15.2 is a compilation of current shotcrete practice by the present author, combining all of these empirical rules and adding in my own practical experience. The reader is warned, that this table can only be used as an approximate guide when deciding upon the type and thickness of shotcrete to be applied in a specific application. Modifications will almost certainly be required to deal with local variations in rock conditions and shotcrete quality.

Table 15.2: Summary of recommended shotcrete applications in underground mining, for different rock mass conditions.

Rock mass description	*Rock mass behaviour*	*Support requirements*	*Shotcrete application*
Massive metamorphic or igneous rock . Low stress conditions.	No spalling, slabbing or failure.	None.	None.
Massive sedimentary rock. Low stress conditions.	Surfaces of some shales, siltstones, or claystones may slake as a result of moisture content change.	Sealing surface to prevent slaking.	Apply 25 mm thickness of plain shotcrete to permanent surfaces as soon as possible after excavation. Repair shotcrete damage due to blasting.
Massive rock with single wide fault or shear zone.	Fault gouge may be weak and erodible and may cause stability problems in adjacent jointed rock.	Provision of support and surface sealing in vicinity of weak fault of shear zone.	Remove weak material to a depth equal to width of fault or shear zone and grout rebar into adjacent sound rock. Weldmesh can be used if required to provide temporary rockfall support. Fill void with plain shotcrete. Extend steel fibre reinforced shotcrete laterally for at least width of gouge zone.

Massive metamorphic or igneous rock. High stress conditions.	Surface slabbing, spalling and possible rockburst damage.	Retention of broken rock and control of rock mass dilation.	Apply 50 mm shotcrete over weldmesh anchored behind bolt faceplates, or apply 50 mm of steel fibre reinforced shotcrete on rock and install rockbolts with faceplates; then apply second 25 mm shotcrete layer. Extend shotcrete application down sidewalls where required.
Massive sedimentary rock. High stress conditions.	Surface slabbing, spalling and possible squeezing in shales and soft rocks.	Retention of broken rock and control of squeezing.	Apply 75 mm layer of fibre reinforced shotcrete directly on clean rock. Rockbolts or dowels are also needed for additional support.
Metamorphic or igneous rock with a few widely spaced joints. Low stress conditions.	Potential for wedges or blocks to fall or slide due to gravity loading.	Provision of support in addition to that available from rockbolts or cables.	Apply 50 mm of steel fibre reinforced shotcrete to rock surfaces on which joint traces are exposed.
Sedimentary rock with a few widely spaced bedding planes and joints. Low stress conditions.	Potential for wedges or blocks to fall or slide due to gravity loading. Bedding plane exposures may deteriorate in time.	Provision of support in addition to that available from rockbolts or cables. Sealing of weak bedding plane exposures.	Apply 50 mm of steel fibre reinforced shotcrete on rock surface on which discontinuity traces are exposed, with particular attention to bedding plane traces.
Jointed metamorphic or igneous rock. High stress conditions.	Combined structural and stress controlled failures around opening boundary.	Retention of broken rock and control of rock mass dilation.	Apply 75 mm plain shotcrete over weldmesh anchored behind bolt faceplates or apply 75 mm of steel fibre reinforced shotcrete on rock, install rockbolts with faceplates and then apply second 25 mm shotcrete layer Thicker shotcrete layers may be required at high stress concentrations.
Bedded and jointed weak sedimentary rock. High stress conditions.	Slabbing, spalling and possibly squeezing.	Control of rock mass failure and squeezing.	Apply 75 mm of steel fibre reinforced shotcrete to clean rock surfaces as soon as possible, install rockbolts, with faceplates, through shotcrete, apply second 75 mm shotcrete layer.
Highly jointed metamorphic or igneous rock. Low stress conditions.	Ravelling of small wedges and blocks defined by intersecting joints.	Prevention of progressive ravelling.	Apply 50 mm of steel fibre reinforced shotcrete on clean rock surface in roof of excavation. Rockbolts or dowels may be needed for additional support for large blocks.
Highly jointed and bedded sedimentary rock. Low stress conditions.	Bed separation in wide span excavations and ravelling of bedding traces in inclined faces.	Control of bed separation and ravelling.	Rockbolts or dowels required to control bed separation. Apply 75 mm of fibre reinforced shotcrete to bedding plane traces before bolting.
Heavily jointed igneous or metamorphic rock, conglomerates or cemented rockfill. High stress conditions.	Squeezing and 'plastic' flow of rock mass around opening.	Control of rock mass failure and dilation.	Apply 100 mm of steel fibre reinforced shotcrete as soon as possible and install rockbolts, with face-plates, through shotcrete. Apply additional 50 mm of shotcrete if required. Extend support down sidewalls if necessary.

| Heavily jointed sedimentary rock with clay coated surfaces. High stress conditions. | Squeezing and 'plastic' flow of rock mass around opening. Clay rich rocks may swell. | Control of rock mass failure and dilation. | Apply 50 mm of steel fibre reinforced shotcrete as soon as possible, install lattice girders or light steel sets, with invert struts where required, then more steel fibre reinforced shotcrete to cover sets or girders. Forepoling or spiling may be required to stabilise face ahead of excavation. Gaps may be left in final shotcrete to allow for movement resulting from squeezing or swelling. Gap should be closed once opening is stable. |
| Mild rockburst conditions in massive rock subjected to high stress conditions. | Spalling, slabbing and mild rockbursts. | Retention of broken rock and control of failure propagation. | Apply 50 to 100 mm of shotcrete over mesh or cable lacing which is firmly attached to the rock surface by means of yielding rockbolts or cablebolts. |

16

Blasting damage in rock

16.1 Introduction

The development of rock mechanics as a practical engineering tool in both underground and surface mining has followed a rather erratic path over the past few decades. Only the most naively optimistic amongst us would claim that the end of the road has been reached and that the subject has matured into a fully developed applied science. On the other hand, there have been some real advances which only the most cynical would discount.

One of the results of the erratic evolutionary path has been the emergence of different rates of advance of different branches of the subject of rock mechanics. Leading the field are subjects such as the mechanics of slope instability, the monitoring of movement in surface and underground excavations and the analysis of induced stresses around underground excavations. Trailing the field are subjects such as the rational design of tunnel support, the movement of groundwater through jointed rock masses and the measurement of in situ stresses. Bringing up the rear are those areas of application where rock mechanics has to interact with other disciplines and one of these areas involves the influence of the excavation process upon the stability of rock excavations.

16.2 Historical perspective

By far the most common technique of rock excavation is that of drilling and blasting. From the earliest days of blasting with black powder, there have been steady developments in explosives, detonating and delaying techniques and in our understanding of the mechanics of rock breakage by explosives.

It is not the development in blasting technology that is of interest in this discussion. It is the application of this technology to the creation of excavations in rock and the influence of the excavation techniques upon the stability of the remaining rock.

As is frequently the case in engineering, subjects that develop as separate disciplines tend to develop in isolation. Hence, a handful of highly skilled and dedicated researchers, frequently working in association with explosives manufacturers, have developed techniques for producing optimum fragmentation and minimising damage in blasts. At the other end of the spectrum are miners who have learned their blasting skills by traditional apprenticeship methods, and who are either not familiar with the specialist blasting control techniques or are not convinced that the results obtained from the use of these techniques justify the effort and expense. At

fault in this system are owners and managers who are more concerned with cost than with safety and design or planning engineers who see both sides but are not prepared to get involved because they view blasting as a black art with the added threat of severe legal penalties for errors.

The need to change the present system is not widely recognised because the impact of blasting damage upon the stability of structures in rock is not widely recognised. It is the author's aim, in the remainder of this chapter, to explore this subject and to identify the causes of blast damage and to suggest possible improvements in the system.

A discussion on the influence of excavation processes upon the stability of rock structures would not be complete without a discussion on machine excavation. The ultimate in excavation techniques, which leave the rock as undisturbed as possible, is the full-face tunnelling machine. Partial face machines or roadheaders, when used correctly, will also inflict very little damage on the rock. The characteristics of tunnelling machines will not be discussed here but comparisons will be drawn between the amount of damage caused by these machines and by blasting.

16.3 Blasting damage

It appears to me, a casual reader of theoretical papers on blasting, that the precise nature of the mechanism of rock fragmentation as a result of detonation of an explosive charge is not fully understood. However, from a practical point of view, it seems reasonable to accept that both the dynamic stresses induced by the detonation and the expanding gases produced by the explosion play important roles in the fragmentation process.

Duvall and Fogelson (1962), Langefors and Khilstrom (1973) and others, have published blast damage criteria for buildings and other surface structures. Almost all of these criteria relate blast damage to peak particle velocity resulting from the dynamic stresses induced by the explosion. While it is generally recognised that gas pressure assists in the rock fragmentation process, there has been little attempt to quantify this damage.

Work on the strength of jointed rock masses suggests that this strength is influenced by the degree of interlocking between individual rock blocks separated by discontinuities such as bedding planes and joints. For all practical purposes, the tensile strength of these discontinuities can be taken as zero, and a small amount of opening or shear displacement will result in a dramatic drop in the interlocking of the individual blocks. It is easy to visualise how the high pressure gases expanding outwards from an explosion will jet into these discontinuities and cause a breakdown of this important block interlocking. Obviously, the amount of damage or strength reduction will vary with distance from the explosive charge, and also with the in situ stresses which have to be overcome by the high pressure gases before loosening of the rock can take place. Consequently, the extent of the gas pressure induced damage can be expected to decrease with depth below surface, and surface structures such as slopes will be very susceptible to gas pressure induced blast damage.

An additional cause of blast inducted damage is that of fracturing induced by release of load (Hagan (1982)). This mechanism is best explained by the analogy of dropping a heavy steel plate onto a pile of rubber mats. These rubber mats are

compressed until the momentum of the falling steel plate has been exhausted. The highly compressed rubber mats then accelerate the plate in the opposite direction and, in ejecting it vertically upwards, separate from each other. Such separation between adjacent layers explains the `tension fractures' frequently observed in open pit and strip mine operations where poor blasting practices encourage pit wall instability. McIntyre and Hagan (1976) report vertical cracks parallel to and up to 55 m behind newly created open pit mine faces where large multi-row blasts have been used.

Whether or not one agrees with the postulated mechanism of release of load fracturing, the fact that cracks can be induced at very considerable distance from the point of detonation of an explosive must be a cause for serious concern. Obviously, these fractures, whatever their cause, will have a major disruptive effect upon the integrity of the rock mass and this, in turn, will cause a reduction in overall stability.

Hoek (1975) has argued that blasting will not induce deep seated instability in large open pit mine slopes. This is because the failure surface can be several hundred metres below the surface in a very large slope, and also because this failure surface will generally not be aligned in the same direction as blast induced fractures. Hence, unless a slope is already very close to the point of failure, and the blast is simply the last straw that breaks the camel's back, blasting will not generally induce major deep-seated instability.

On the other hand, near surface damage to the rock mass can seriously reduce the stability of the individual benches which make up the slope and which carry the haul roads. Consequently, in a badly blasted slope, the overall slope may be reasonably stable, but the face may resemble a rubble pile.

In the case of a tunnel or other large underground excavation, the problem is rather different. In this case, the stability of the underground structure is very much dependent upon the integrity of the rock immediately surrounding the excavation. In particular, the tendency for roof falls is directly related to the interlocking of the immediate roof strata. Since blast damage can easily extend several metres into the rock which has been poorly blasted, the halo of loosened rock can give rise to serious instability problems in the rock surrounding the underground openings.

16.4 Damage control

The ultimate in damage control is machine excavation. Anyone who has visited an underground metal mine and looked up a bored raise will have been impressed by the lack of disturbance to the rock and the stability of the excavation. Even when the stresses in the rock surrounding the raise are high enough to induce fracturing in the walls, the damage is usually limited to less than half a metre in depth, and the overall stability of the raise is seldom jeopardised.

Full-face and roadheader type tunnelling machines are becoming more and more common, particularly for civil engineering tunnelling. These machines have been developed to the point where advance rates and overall costs are generally comparable or better than the best drill and blast excavation methods. The lack of disturbance to the rock and the decrease in the amount of support required are major advantages in the use of tunnelling machines.

For surface excavations, there are a few cases in which machine excavation can be used to great advantage. In the Bougainville open pit copper mine in Papua New

Guinea, trials were carried out on dozer cutting of the final pit wall faces. The final vertical blastholes were placed about 19 m from the ultimate bench crest position. The remaining rock was then ripped using a D-10 dozer, and the final 55 degree face was trimmed with the dozer blade. The rock is a very heavily jointed andesite, and the results of the dozer cutting were remarkable when compared with the bench faces created by the normal open pit blasting techniques.

The machine excavation techniques described above are not widely applicable in underground mining situations, and consideration must therefore be given to what can be done about controlling damage in normal drill and blast operations.

A common misconception is that the only step required to control blasting damage is to introduce pre-splitting or smooth blasting techniques. These blasting methods, which involve the simultaneous detonation of a row of closely spaced, lightly charged holes, are designed to create a clean separation surface between the rock to be blasted and the rock which is to remain. When correctly performed, these blasts can produce very clean faces with a minimum of overbreak and disturbance. However, controlling blasting damage starts long before the introduction of pre-splitting or smooth blasting.

As pointed out earlier, a poorly designed blast can induce cracks several metres behind the last row of blastholes. Clearly, if such damage has already been inflicted on the rock, it is far too late to attempt to remedy the situation by using smooth blasting to trim the last few metres of excavation. On the other hand, if the entire blast has been correctly designed and executed, smooth blasting can be very beneficial in trimming the final excavation face.

Figure 16.1 illustrates a comparison between the results achieved by a normal blast and a face created by presplit blasting in a jointed gneiss. It is evident that, in spite of the fairly large geological structures visible in the face, a good clean face has been achieved by the pre-split. It is also not difficult to imagine that the pre-split face is more stable than the section which has been blasted without special attention to the final wall condition.

Figure 16.1: Comparison between the results achieved by pre-split blasting (on the left) and normal bulk blasting for a surface excavation in gneiss.

The correct design of a blast starts with the very first hole to be detonated. In the case of a tunnel blast, the first requirement is to create a void into which rock broken by the blast can expand. This is generally achieved by a wedge or burn cut which is designed to create a clean void and to eject the rock originally contained in this void clear of the tunnel face.

In today's drill and blast tunnelling in which multi-boom drilling machines are used, the most convenient method for creating the initial void is the burn cut. This involves drilling a pattern of carefully spaced parallel holes which are then charged with powerful explosive and detonated sequentially using millisecond delays. A detailed discussion on the design of burn cuts is given by Hagan (1980).

Once a void has been created for the full length of the intended blast depth or `pull', the next step is to break the rock progressively into this void. This is generally achieved by sequentially detonating carefully spaced parallel holes, using one-half second delays. The purpose of using such long delays is to ensure that the rock broken by each successive blasthole has sufficient time to detach from the surrounding rock and to be ejected into the tunnel, leaving the necessary void into which the next blast will break.

A final step is to use a smooth blast in which lightly charged perimeter holes are detonated simultaneously in order to peel off the remaining half to one metre of rock, leaving a clean excavation surface.

The details of such a tunnel blast are given in Figure 16.2. The development of the burn cut is illustrated in Figure 16.3 and the sequence of detonation and fracture of the remainder of the blast is shown in Figure 16.4. The results achieved are illustrated in a photograph reproduced in Figure 16.5. In this particular project, a significant reduction in the amount of support installed in the tunnel was achieved as a result of the implementation of the blasting design shown in Figure 16.2.

A final point on blasting in underground excavations is that it is seldom practical to use pre-split blasting, except in the case of a benching operation. In a pre-split blast, the closely spaced parallel holes (similar to those numbered 9, 10 and 11 in Figure 16.2) are detonated before the main blast instead of after, as in the case of a smooth blast. Since a pre-split blast carried out under these circumstances has to take place in almost completely undisturbed rock which may also be subjected to relatively high induced stresses, the chances of creating a clean break line are not very good. The cracks, which should run cleanly from one hole to the next, will frequently veer off in the direction of some pre-existing weakness such as foliation. For these reasons, smooth blasting is preferred to pre-split blasting for tunnelling operations.

In the case of rock slopes such as those in open pit mines, the tendency today is to use large diameter blastholes on a relatively large spacing. These holes are generally detonated using millisecond delays which are designed to give row by row blasting. Unfortunately, scatter in the delay times of the most commonly used open pit blasting systems can sometimes cause the blastholes to fire out of sequence, and this can produce poor fragmentation as well as severe damage to the rock which is to remain to form stable slopes.

Downhole delay systems which can reduce the problems associated with the detonation of charges in large diameter blastholes are available, but open pit blasting engineers are reluctant to use them because of the added complications of laying out

the blasting pattern, and also because of a fear of cut-offs due to failure of the ground caused by the earlier firing blastholes. There is clearly a need for further development of the technology and the practical application of bench blasting detonation delaying, particularly for the large blasts which are required in open pit mining operations.
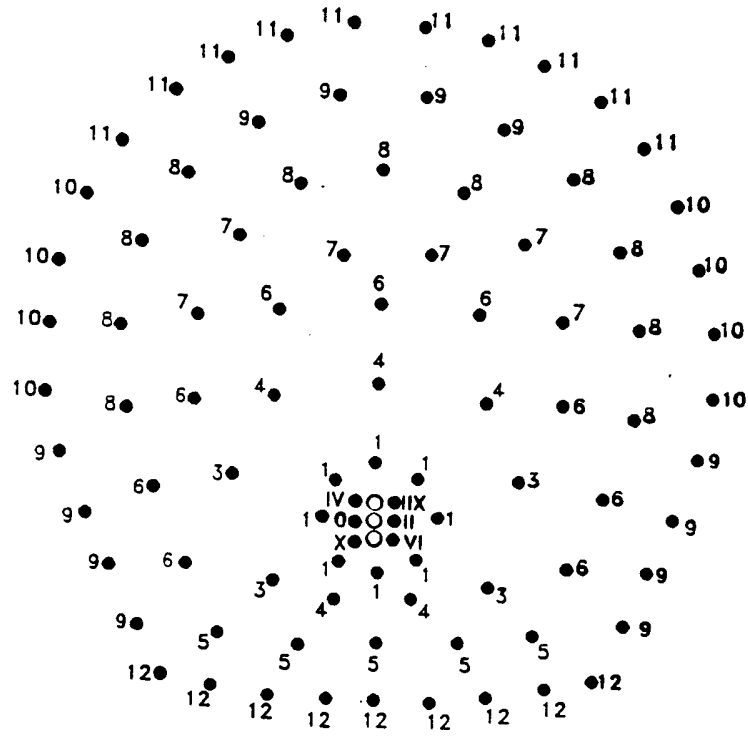
Holes	no	Dia mm	Explosives	Total wt. kg	Detonators
Burn	14	45	Gelamex 80, 18 sticks/hole	57	Millisec
Lifters	9	45	Gelamex 80, 16 sticks/hole	33	Half-sec
Perimeter	26	45	Gurit, 7 sticks/hole and Gelamex 80, 1 stick/hole	26	Half-sec
Others	44	45	Gelamex 80, 13 sticks/hole	130	Half-sec
Relief	3	75	No charge		
Total	96			246	

Figure 16.2: Blasthole pattern and charge details used by Balfour Beatty - Nuttall on the Victoria hydroelectric project in Sri Lanka. Roman numerals refer to the detonation sequence of millisecond delays in the burn cut, while Arabic numerals refer to the half-second delays in the remainder of the blast.
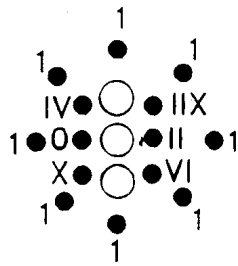
Layout of holes
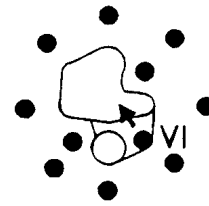
Milliscond delay VI
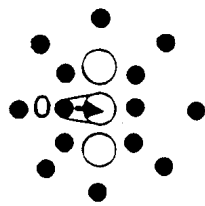
Millisecond delay 0
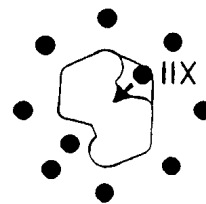
Millisecond delay IIX
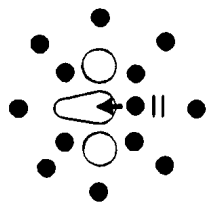
Millisecond delay II
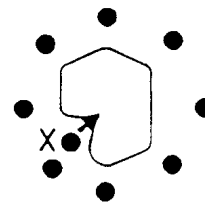
Millisecond delay X
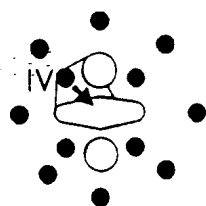
Millisecond delay IV
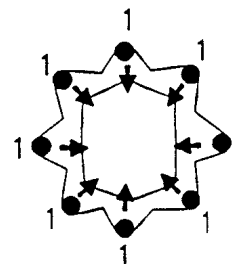
Half-second delay 1

Figure 16.3 Development of a burn cut using millisecond delays.

Half-second delay 3

Half-second delay 7

Half-second delay 4

Half-second delay 8

Half-second delay 5

Half-second delay 9

Half-second delay 6

Lifters & smooth blast
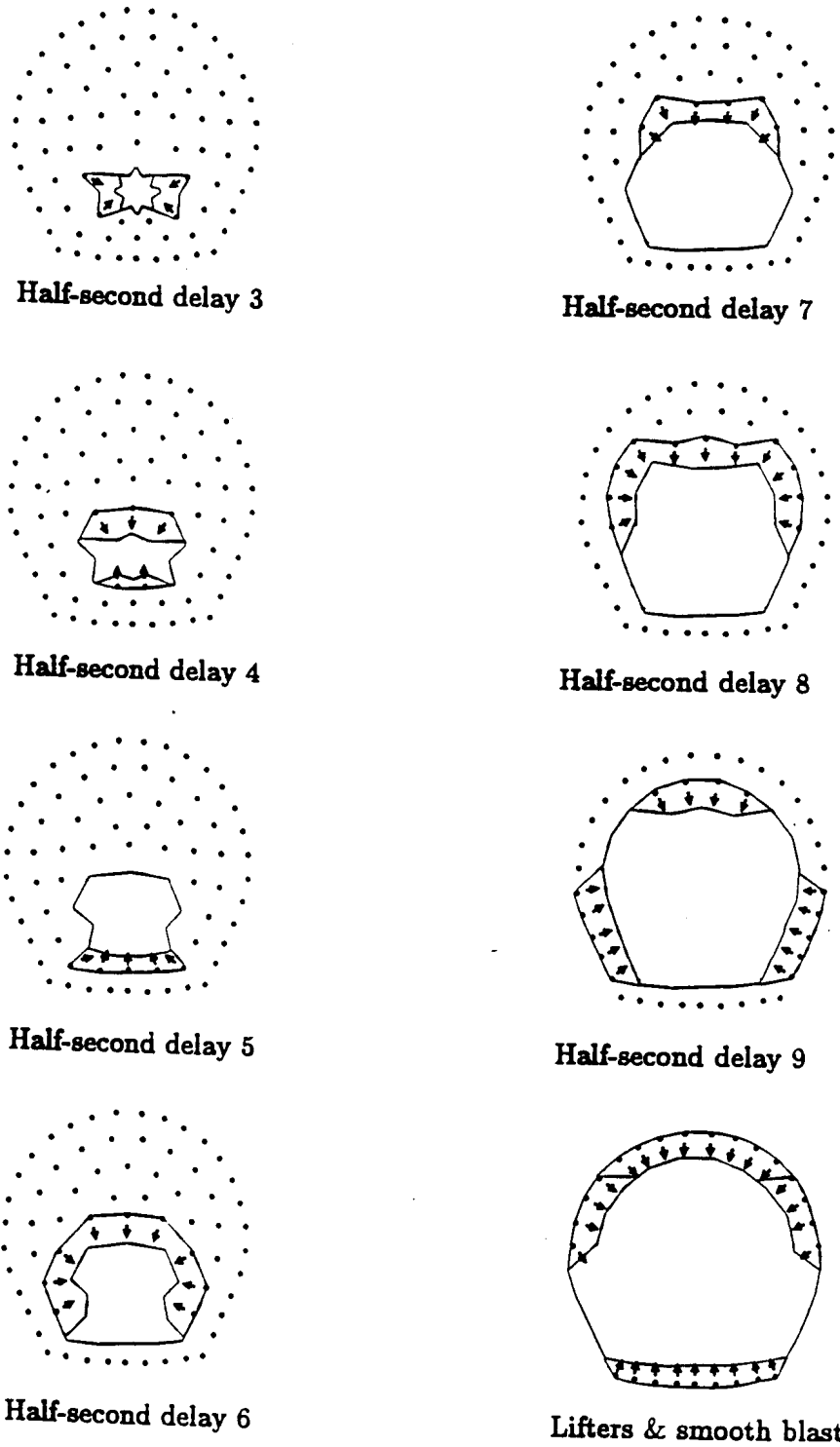
Figure 16.4: Use of half-second delays in the main blast and smooth blasting of the perimeter of a tunnel.

Figure 16.5: Results achieved using well designed and carefully controlled blasting in a 19 foot diameter tunnel in gneiss in the Victoria hydroelectric project in Sri Lanka. Photograph reproduced with permission from the British Overseas Development Administration and from Balfour Beatty - Nuttall.

16.5 Blasting design and control

While there is room for improvement in the actual techniques used in blasting, many of the existing techniques, if correctly applied, could be used to reduce blasting damage in both surface and underground rock excavation. As pointed out earlier, poor communications and reluctance to become involved on the part of most engineers, means that good blasting practices are generally not used on mining and civil engineering projects.

What can be done to improve the situation? In the writer's opinion, the most critical need is for a major improvement in communications. Currently available, written information on control of blasting damage is either grossly inadequate, as in the case of blasting handbooks published by explosives manufacturers, or it is hidden in technical journals or texts which are not read by practical blasting engineers. Ideally, what is required is a clear, concise book, which sets out the principles of blasting design and control in unambiguous, non- mathematical language. Failing this, a series of articles, in similarly plain language, published in trade journals, would help a great deal.

In addition to the gradual improvement in the understanding of the causes and control of blast damage which will be achieved by the improvement in communications, there is also a need for more urgent action on the part of engineers involved in rock excavation projects. Such engineers, who should at least be aware of

the damage being inflicted by poor blasting, should take a much stronger line with owners, managers, contractors and blasting foremen. While these engineers may not feel themselves to be competent to redesign the blasts, they may be able to persuade the other parties to seek the advice of a blasting specialist. Explosives manufacturers can usually supply such specialist services, or can recommend individuals who will assist in improving the blast design. Incidentally, in addition to reducing the blasting damage, a well designed blast is generally more efficient and may provide improved fragmentation and better muck-pile conditions at the same cost.

16.6 Conclusion

Needless damage is being caused to both tunnels and surface excavation by poor blasting. This damage results in a decrease in stability which, in turn, adds to the costs of a project by the requirement of greater volumes of excavation or increased rock support.

Tools and techniques are available to minimise this damage, but these are not being applied very widely in either the mining or civil engineering industries because of a lack of awareness of the benefits to be gained, and a fear of the costs involved in applying controlled blasting techniques. There is an urgent need for improved communications between the blasting specialists who are competent to design optimum blasting systems and the owners, managers and blasting foremen who are responsible for the execution of these designs.

Research organisations involved in work on blasting should also recognise the current lack of effective communications and, in addition to their work in improving blasting techniques, they should be more willing to participate in field-oriented programs in co-operation with industry. Not only will organisations gain invaluable practical knowledge but, by working side-by-side with other engineers, they will do a great deal to improve the general awareness of what can be achieved by good blasting practices.

17

References

Amos, A.J., A. Granero Hernandez, and R.J. Rocca. 1981. Problemas de meteorizacion del geneis en la Presa Principal del complejo hidroeléctrico Río Grande I. *Proc. VIII Cong. Geol. Arg. Actas* **2,** 123-135.

Anon. 1977. Description of rock masses for engineering purposes. Geological Society Engineering Group Working Party Report. *Q. J. Engng Geol.* **10**, 355-388.

Azzoni, A., La Barbera, G. and Zaninetti, A. 1995. Analysis and prediction of rockfalls using a mathematical model. *International Journal of Rock Mechanics and Mining Science and Geomechanics Abstracts.* Vol. 32., No. 7. pp. 709-724.

Badger, T.C. and Lowell, S. 1992. Rockfall Control Washington State. In *Rockfall Prediction and Control and Landslide Case Histories, Transportation Research Record,* National Research Council, Washington, No 1342, pp 14-19.

Bajzelj, U., Likar, J., Zigman, F., Subelj, A. and Spek, S. 1992. Geotechnical analyses of the mining method using long cable bolts. In *Rock support in mining and underground construction*, *proc. int. symp. on rock support,* Sudbury, (eds. P.K. Kaiser and D.R. McCreath)*,* 393-402. Rotterdam: Balkema.

Baker, D.G. 1991. Wahleach power tunnel monitoring. *Proc. 3rd Int. Symp. on Field Measurements in Geomechanics, Oslo, Norway*, in press.

Balmer, G. 1952. A general analytical solution for Mohr's envelope. *Am. Soc. Test. Mat.* **52**, 1260-1271.

Bandis, S.C. 1980. *Experimental studies of scale effects on shear strength, and deformation of rock joints*. Ph.D. thesis, University of Leeds.

Bandis, S.C. 1990. Mechanical properties of rock joints. In *Proc. Int. Soc. Rock Mech. symp. on rock joints,* Loen, Norway, (eds N. Barton and O. Stephansson), 125-140. Rotterdam: Balkema.

Barton, N. 1976. The shear strength of rock and rock joints. *Int. J. Rock Mech. Min. Sci. & Geomech. Abstr.* **13,** 1-24.

Barton, N. 1989. Cavern design for Hong Kong rocks. *Proc. Rock Cavern Seminar - Hong Kong* (eds A.W. Malone and P.G.D. Whiteside), pp. 179-202. London: Institution of Mining and Metallurgy

Barton, N., By, T.L., Chryssanthakis, L., Tunbridge, L., Kristiansen, J., Løset, F., Bhasin, R.K., Westerdahl, H. and Vik, G. 1992. Comparison of prediction and performance for a 62 m span sports hall in jointed gneiss. *Proc. 4th. int. rock mechanics and rock engineering conf.,* Torino. Paper 17.

Barton, N., Løset, F., Lien, R. and Lunde, J. 1980. Application of the Q-system in design decisions. In *Subsurface space,* (ed. M. Bergman) **2,** 553-561. New York: Pergamon.

Barton, N.R. 1973. Review of a new shear strength criterion for rock joints. *Engng Geol.* **7**, 287-332.

Barton, N.R. 1974. *A review of the shear strength of filled discontinuities in rock.* Norwegian Geotech. Inst. Publ. No. 105. Oslo: Norwegian Geotech. Inst.

Barton, N.R. 1976. The shear strength of rock and rock joints. *Int. J. Mech. Min. Sci. & Geomech. Abstr.* **13**(10), 1-24.

Barton, N.R. 1987. *Predicting the behaviour of underground openings in rock. Manuel Rocha Memorial Lecture*, Lisbon. Oslo: Norwegian Geotech. Inst.

Barton, N.R. and Bandis, S.C. 1982. Effects of block size on the the shear behaviour of jointed rock. *23rd U.S. symp. on rock mechanics*, Berkeley, 739-760.

Barton, N.R. and Bandis, S.C. 1990. Review of predictive capabilites of JRC-JCS model in engineering practice. In *Rock joints, proc. int. symp. on rock joints,* Loen, Norway, (eds N. Barton and O. Stephansson), 603-610. Rotterdam: Balkema.

Barton, N.R. and Choubey, V. 1977. The shear strength of rock joints in theory and practice. *Rock Mech.* **10**(1-2), 1-54.

Barton, N.R., Lien, R. and Lunde, J. 1974. Engineering classification of rock masses for the design of tunnel support. *Rock Mech.* **6**(4), 189-239.

Bétournay, M.C. 1987. A design philosophy for surface crown pillars in hard rock mines. *Bull. Canadian Inst. Min. Metall.* **80** (903), 45-61.

Bieniawski Z.T. 1989. *Engineering Rock Mass Classifications*. Wiley, New York. 251 pages.

Bieniawski, Z.T. 1967. Mechanism of brittle fracture of rock, parts I, II and III. *Int. J. Rock Mech. Min. Sci. & Geomech. Abstr.* **4**(4), 395-430.

Bieniawski, Z.T. 1973. Engineering classification of jointed rock masses. *Trans S. Afr. Inst. Civ. Engrs* **15**, 335-344.

Bieniawski, Z.T. 1974. Estimating the strength of rock materials. *J. South African Inst. Min. Metall .* **74** (8), 312-320.

Bieniawski, Z.T. 1974. Geomechanics classification of rock masses and its application in tunnelling. In *Advances in Rock Mechanics* **2** , part A: pp.27-32. Washington, D.C.: National Academy of Sciences

Bieniawski, Z.T. 1976. Rock mass classification in rock engineering. In *Exploration for rock engineering, proc. of the symp.*, (ed. Z.T. Bieniawski) **1**, 97-106. Cape Town: Balkema.

Bieniawski, Z.T. 1978. Determining rock mass deformability - experiences from case histories. *Int. J. Rock Mech. Min. Sci. & Geomech. Abstr.* **15**, 237-247.

Bieniawski, Z.T. 1979. The geomechanics classification in rock engineering applications. *Proc. 4th. congr., Int. Soc. Rock Mech.,* Montreux **2**, 41-48.

Bieniawski, Z.T. 1989. *Engineering rock mass classifications.* New York: Wiley.

Bieniawski. Z. T., 1967. Mechanism of brittle fracture of rock, parts I, II and III. *Int. J. Rock Mech. Min. Sci. & Geomech. Abstr.* **4** (4),395-30.

Bouchier, F., Dib, E. and O'Flaherty, M. 1992. Practical improvements to installation of cable bolts: progress at Campbell Mine. In *Rock support in mining and underground construction, proc. int. symp. on rock support,* Sudbury, (eds P.K. Kaiser and D.R. McCreath), 311-318. Rotterdam: Balkema.

Bowcock, J.B., Boyd, J.M., Hoek, E. and Sharp, J.C. 1976. Drakensberg pumped storage scheme, rock engineering aspects. In *Exploration for Rock Engineering* (ed. Z.T. Bieniawski) **2** , pp. 121-139. Rotterdam: Balkema

Bozzolo, D., Pamini, R. and Hutter, K. 1988. Rockfall analysis - a mathematical model and its test with field data. *Proc. 5th International Symposium on Landslides, Lusanne.* July 1988, Vol. 1, pp. 555-560.

Brady, B.H.G. and Brown, E.T. 1985. *Rock mechanics for underground mining*. London: Allen and Unwin.

Brand, E.W. 1988. Special Lecture: Landslide risk assessment in Hong Kong. *Proc. 5th International Symposium on Landslides, Lusanne.* July 1988, Vol. 2, pp. 1059-1074.

Brawner, C.O. and Hoek, E. 1977. Design, Construction and Maintenance of rock slopes on highway projects. *Proc. VIIIth International Road Federation World Meeting, Tokyo.* October, 1977,

British Standard Code of Practice, 1987. BS 8081, *Ground Anchorage*, 89-115.

Brown E.T., Bray J.W., Ladanyi B. and Hoek E. 1983. Characteristic line calculations for rock tunnels. *J. Geotech. Engng Div., Am. Soc. Civ. Engrs* **109**, 15-39.

Brown, A. 1982. The influence and control of groundwater in large slopes. In *Stability in Surface Mining* (ed. C.O. Brawner), pp. 19-41. New York: Society of Mining Engineers, AIME

Brown, E.T. 1970. Strength of models of rock with intermittent joints. *J. Soil Mech. Foundn Div., ASCE* **96**, SM6, 1935-1949.

Brown, E.T. 1987. Introduction. *Analytical and computational methods in engineering rock mechanics*, (ed. E.T. Brown), 1-31. London: Allen and Unwin.

Brown, E.T. and Bray, J.W. 1982. Rock-support interaction calculations for pressure shafts and tunnels. In *Rock Mechanics: Caverns and Pressure Shafts* (ed. W. Wittke) **2**, pp. 555-565. Rotterdam: Balkema

Brown, E.T. and Ferguson, G.A. 1979. Progressive hanging wall caving at Gath's mine, Rhodesia. *Trans. Instn Min. Metall. (Section A: Min. industry)* **88**, A92-105.

Brown, E.T. and Hoek, E. 1978. Trends in relationships between measured rock in situ stresses and depth. *Int. J. Rock Mech. Min. Sci. & Geomech. Abstr.* **15**, 211-215.

Brown, E.T., Bray, J.W., Ladanyi, B. and Hoek, E. 1983. Characteristic line calculations for rock tunnels. *J. Geotech. Engng Div., ASCE* **109**, 15-39.

Bucky, P.B. 1931. Use of models for the study of mining problems. A*m. Inst. Min. Metall. Engrs*, *Technical Publication* 425.

Bunce, C.M. 1994. Risk Analysis for Rock Fall on Highways. *MSc thesis submitted to the Department of Civil Engineering, University of Alberta, Canada.* 129 pages.

Bywater, S. and Fuller, P.G. 1984. Cable support for lead open stope hanging walls at Mount Isa Mines Limited. In *Rock bolting: theory and application in mining and underground construction*, (ed. O. Stephansson), 539-556. Rotterdam: Balkema.

Carter, T.G. 1992. A new approach to surface crown pillar design. *Proc. 16th. Canadian Rock Mechanics Symposium, Sudbury,* 75-83.

Carter, T.G. 1992. Prediction and uncertainties in geological engineering and rock mass characterization assessments. *Proc. 4th. int. rock mechanics and rock engineering conf.,* Torino. Paper 1.

Chan, Y.C., Chan C.F. and Au S.W.C., 1986. Design of a boulder fence in Hong Kong. *Conf. On Rock Engineering and Excavation in an Urban Environment.* Hong Kong: Institution of Mining & Metallurgy.

Cheng, Y. 1987. New development in seam treatment of Feitsui arch dam foundation. *Proc. 6th Cong. ISRM, Montreal*, 319-326.

Cheng, Y. and Liu, S.C. 1990. Power caverns of the Mingtan Pumped Storage Project, Taiwan. In *Comprehensive Rock Engineering* (ed. J.A. Hudson) **5**, 111-132

Clegg, I.D. and Hanson, D.S. 1992. Ore pass design and support at Falconbridge Limited. In *Rock support in mining and underground construction, proc. int. symp. on rock support*, Sudbury, (eds P.K. Kaiser and D.R. McCreath), 219-225. Rotterdam: Balkema.

Clifford, R.L. 1974. Long rockbolt support at New Broken Hill Consolidated Limited. *Proc. Aus. Inst. Min. Metall.,* No. 251, 21-26.

Clough, R.W. 1960. The finite element method in plane stress analyses. *Proc. 2nd. ASCE Conference on Electronic Computation*, *Pittsburgh* , 345-378.

Coates, D. 1966. *Rock Mechanics Principles* . Ottawa: Dept. Mines and Technical Surveys

Cook, N.G.W. (1965) The failure of rock. *Int. J. Rock Mech. Min. Sci. Geomech. Abstr.* **2**, 389-403.

Cording, E.J. and Deere, D.U. 1972. Rock tunnel supports and field measurements. *Proc. North American rapid excav. tunneling conf.,* Chicago, (eds. K.S. Lane and L.A. Garfield) **1**, 601-622. New York: Soc. Min. Engrs, Am. Inst. Min. Metall. Petrolm Engrs.

Cording, E.J., Hendron, A.J. and Deere, D.U. 1971. Rock engineering for underground caverns*. Proc. Symp. on Underground Rock Chambers*, *1971* , pp. 567-600. New York: American Society of Civil Engineers

Coulomb, C.A. 1776. Essai sur une application des regles de maximis et minimis a quelques problemes de statique, relatifs a l'architecture*. Memoires de Mathematique & de Physique* **7** , 343- 82.

Crouch, S.L. and Starfield, A.M. 1983*. Boundary element methods in solid mechanics* . London: Allen and Unwin

Cummings, R.A., Kendorski, F.S. and Bieniawski, Z.T. 1982. *Caving rock mass classification and support estimation*. U.S. Bureau of Mines Contract Report #J0100103. Chicago: Engineers International Inc.

Cundall, P.A. 1971. A computer model for simulating progressive large scale movements in blocky rock systems. In.*Rock Fracture , Proc. Symp. ISRM, Nancy* **1,** Paper 2-8.

Daeman, J.J.K. 1977. Problems in tunnel support mechanics. *Underground Space* **1** , 163-172.

Davis, W.L. 1977. Initiation of cablebolting at West Coast Mines, Rosebury. *Proc. Aust. Inst. Min. Metall. conf.,* Tasmania, 215-225.

Deere, D.U. 1989. *Rock quality designation (RQD) after 20 years*. U.S. Army Corps Engrs Contract Report GL-89-1. Vicksburg, MS: Waterways Experimental Station.

Deere, D.U. and Deere, D.W. 1988. The rock quality designation (RQD) index in practice. In *Rock classification systems for engineering purposes,* (ed. L. Kirkaldie)*,* ASTM Special Publication 984, 91-101. Philadelphia: Am. Soc. Test. Mat.

Deere, D.U. and Miller, R.P. 1966. *Engineering classification and index properties of rock*. Technical Report No. AFNL-TR-65-116. Albuquerque, NM: Air Force Weapons Laboratory.

Deere, D.U., Hendron, A.J., Patton, F.D. and Cording, E.J. 1967. Design of surface and near surface construction in rock. In *Failure and breakage of rock, proc. 8th U.S. symp. rock mech.*, (ed. C. Fairhurst), 237-302. New York: Soc. Min. Engrs, Am. Inst. Min. Metall. Petrolm Engrs.

Diederichs, M.S., Pieterse, E., Nosé, J. and Kaiser, P.K. 1993. A model for evaluating cable bond strength: an update. *Proc. Eurock '93,* Lisbon*.* (in press).

Dorsten, V., Frederick, F.H. and Preston, H.K. 1984. Epoxy coated seven-wire strand for prestressed concrete. *Prestressed Concrete Inst. J.* **29**(4), 1-11.

Doruk, P. 1991. *Analysis of the laboratory strength data using the original and modified Hoek-Brown failure criteria.* MASc thesis, Dept. Civil Engineering, University of Toronto.

Duncan Fama, M.E. 1993. Numerical modelling of yield zones in weak rocks. In *Comprehensive rock engineering*, (ed. J.A. Hudson) **2**, 49-75. Oxford: Pergamon.

Duvall, W.I. and Fogelson, D.E. 1962. Review of criteria for estimating damage to residences from blasting vibrations . *U.S. Bur. Mines Rep. Invest.* 5986. 19 pages.

Endersbee, L.A. and Hofto, E.O. 1963. Civil engineering design and studies in rock mechanics for Poatina underground power station, Tasmania. *J. Instn. Engrs Australia* **35** , 187- 209.

Engelder, T. and Sbar, M.L. 1984. Near-surface in situ stress: introduction. *J. Geophys. Res*. **89**, 9321-9322. Princeton, NJ: Princeton University Press.

Ewy, R.T. and Cook, N.G.W. 1990. Deformation and fracture around cylindrical openings in rock. Parts I & II. *Int. J. Rock Mech. Min. Sci. Geomech. Abstr.* **27**, 387-427.

Fabjanczyk, M.W. 1982. Review of ground support practice in Australian underground metalliferous mines. *Proc. Aus. Inst. Min. Metall. conf.,* Melbourne, 337-349. Melbourne: Aust. Inst. Min. Metall.

Fairhurst, C. and Cook. N.G.W., 1966. The phenomenon of rock splitting parallel to a free surface under compressive stress. *Proc. 1st. Cong. ISRM, Lisbon* **1,** 687-692

Farmer, I.W., and Shelton, P.D. 1980. Review of underground rock reinforcement systems. *Trans. Instn Min. Metall. (Sect. A: Min. industry)* **89** , A68-83.

Feat-Smith, I. 1982. Survey of rock tunnelling machines available for mining projects. *Trans. Instn Min. Metall. (Sect. A: Min. industry*) **91** , A23-31.

Federal Highways Administration. 1993. *Rockfall Hazard Rating System, Participants Manual for NHI Course No. 130220.* Publication No. FHWA SA-93-057.

Fell, R. 1994. Landslide risk assessment and acceptable risk. *Canadian Geotechnical Journal.* Vol. 31. pp. 261-272

Fenner, R. 1938. Untersuchungen zur Erkenntnis des Gebirgsdruckes. *Glukauf* **74**, 681-695, 705-715.

Fookes, P.G. and Sweeney, M. 1976. Stabilisation and control of local rockfalls and degrading of slopes. *Quarterly J. Engineering Geology.* Vol. 9, pp 37-55.

Franklin, J.A. and Hoek, E. 1970. Developments in triaxial testing equipment. *Rock Mech.* **2,** 223-228. Berlin: Springer-Verlag.

Franzén, T. 1992. Shotcrete for underground support - a state of the art report with focus on steel fibre reinforcement. In *Rock support in mining and underground construction, proc. int. symp. rock support,* Sudbury, (eds P.K. Kaiser and D.R. McCreath), 91-104. Rotterdam: Balkema.

Freeze, A.R. and Cherry, J.A. 1979. *Groundwater* . Englewood Cliffs, NJ: Prentice-Hall 604 pages

Fuller, P.G. 1981. Pre-reinforcement of cut and fill stopes. In *Application of rock mechanics to cut and fill mining,* (eds O. Stephansson and M.J. Jones), 55-63. London: Instn Min. Metall.

Fuller, P.G. 1983. The potential for support of long hole open stopes with grouted cables. *Proc. 5th. Int. Cong. for Rock Mechanics, Melbourne* **2** , D39-D44. Rotterdam: Balkema

Fuller, P.G. 1984. Cable support in mining - a keynote lecture. In *Rock bolting: theory and application in mining and underground construction,* (ed. O. Stephansson), 511-522. Rotterdam: Balkema.

Gane, P.G., Hales, A.L. and Oliver, H.A. 1946. A seismic investigation of Witwatersrand earth tremors. *Bull. Seism. Soc. Am.* **36** , 49-80.

Garford Pty Ltd. 1990. *An improved, economical method for rock stabilisation*. 4p. Perth.

Greenwald, H.P., Howarth, H.C. and Hartman, I. 1939. Experiments on the strength of small pillars of coal in the Attsburg bed. *U.S. Bureau of Mines Tech. Rep.* No. 605.

Griffith, A.A. 1921. The phenomenon of rupture and flow in solids. *Phil. Trans. Roy. Soc., London* **A221** , 163-198.

Griffith, A.A. 1924. Theory of rupture. *Proc. 1st congr. applied mechanics*, Delft, 55-63. Delft: Technische Bockhandel en Drukkerij.

Griggs, D.T. 1936. Deformation of rocks under high confining pressures. *J. Geol.* **44** , 541-577.

Grimstad, E. and Barton, N. 1993. Updating the Q-System for NMT. *Proc. int. symp. on sprayed concrete - modern use of wet mix sprayed concrete for underground support*, Fagernes, (eds Kompen, Opsahl and Berg). Oslo: Norwegian Concrete Assn.

Hagan, T.N. 1980. Understanding the burn cut - a key to greater advance rates. *Trans. Instn. Min. Metall. (Sect. A: Min. Industry)* , **89**, A30-36.

Hagan, T.N. 1982. Controlling blast-induced cracking around large caverns. *Proc. ISRM Symp., Rock Mechanics Related to Caverns and Pressure Shafts* , *Aachen, West Germany*.

Haimson B.C. 1978. The hydrofracturing stress measuring method and recent field results. *Int. J. Rock Mech. Min. Sci. & Geomech. Abstr.* **15** , 167-178.

Hammett, R.D. and Hoek, E. 1981. Design of large underground caverns for hydroelectric projects, with reference to structurally controlled failure mechanisms. *Proc. American Soc. Civil Engrs. Int. Conf. on Recent Developments in Geotechnical Engineerign for Hydro Projects. pp.* 192-206. New York: ASCE

Harr, M.E. 1987. *Reliability-based design in civil engineering.* New York: McGraw-Hill.

Hatzor, Y. and Goodman, R.E. 1992. Application of block theory and the critical key block concept in tunneling; two case histories. In *Proc. Int. Soc. Rock Mech. conf. on fractured and jointed rock masses,* Lake Tahoe, California, 632-639.

Hatzor. Y. and Goodman. R.E. 1993. Determination of the 'design block' for tunnel supports in highly jointed rock. In *Comprehensive Rock Engineering, Principles, Practice and Projects.* (ed. J.A. Houson) **2,** 263-292. Oxford: Pergamon

Herget, G. 1988. *Stresses in rock.* Rotterdam: Balkema.

Heyman, J. 1972. *Coulomb's Memoir on Statics* . Cambridge: at the University Press

Hoek E and Brown E.T. 1988. The Hoek-Brown failure criterion - a 1988 update. *Proc. 15th Canadian Rock Mech. Symp.* (ed. J.H. Curran), pp. 31-38. Toronto: Civil Engineering Dept., University of Toronto

Hoek E. and Brown E.T. 1980. *Underground Excavations in Rock* . London: Institution of Mining and Metallurgy 527 pages

Hoek, E. 1965. *Rock fracture under static stress conditions.* PhD Thesis , Univ. Cape Town

Hoek, E. 1968. Brittle failure of rock. *In Rock Mechanics in Engineering Practice* . (eds K.G. Stagg and O.C. Zienkiewicz) , pp. 99-124. London: Wiley

Hoek, E. 1975. Influence of drilling and blasting on the stability of slopes in open pit mines and quarries. *Proc. Atlas Copco Bench Drilling Days Symp., Stockholm, Sweden.*

Hoek, E. 1982. Geotechnical considerations in tunnel design and contract preparation. *Trans. Instn Min. Metall. (Sect. A: Min. industry)* **91** , A101-109.

Hoek, E. 1983. Strength of jointed rock masses, 23rd. Rankine Lecture. *Géotechnique* **33**(3), 187-223.

Hoek, E. 1986. Rockfall: a computer program for predicting rockfall trajectories. Unpublished internal notes, Golder Associates, Vancouver.

Hoek, E. 1989. A limit equilibrium analysis of surface crown pillar stability. In *Surface crown pillar evaluation for active and abandoned metal mines,* (ed. M.C. Betourney), 3-13. Ottawa: Dept. Energy, Mines & Resources Canada.

Hoek, E. 1990. Estimating Mohr-Coulomb friction and cohesion values from the Hoek-Brown failure criterion. *Intnl. J. Rock Mech. & Mining Sci. & Geomechanics Abstracts.* **12**(3), 227-229.

Hoek, E. 1994. Strength of rock and rock masses, *ISRM News Journal,* **2**(2), 4-16.

Hoek, E. and Bray, J.W. 1981. *Rock Slope Engineering* . 3rd edn. London: Institution of Mining and Metallurgy 402 pages

Hoek, E. and Brown, E.T. 1980b. Empirical strength criterion for rock masses. *J. Geotech. Engng Div.*, *ASCE* **106**(GT9), 1013-1035.

Hoek, E. and Brown, E.T. 1988. The Hoek-Brown failure criterion - a 1988 update. In *Rock engineering for underground excavations*, *proc. 15th Canadian rock mech. symp.*, (ed. J.C. Curran), 31-38. Toronto: Dept. Civ. Engineering, University of Toronto.

Hoek, E. and Brown, E.T. 1997. Practical estimates or rock mass strength. *Intnl. J. Rock Mech. & Mining Sci. & Geomechanics Abstracts.* **34**(8), 1165-1186.

Hoek, E. and Moy, D. 1993. Design of large powerhouse caverns in weak rock. In *Comprehensive rock engineering,* (ed. J.A. Hudson) **5**, 85-110. Oxford: Pergamon.

Hoek, E., and Brown, E.T. 1980a. *Underground excavations in rock*. London: Instn Min. Metall.

Hoek, E., Kaiser, P.K. and Bawden. W.F. 1995. *Support of underground excavations in hard rock.* Rotterdam: Balkema

Hoek, E., Wood, D. and Shah, S. 1992. A modified Hoek-Brown criterion for jointed rock masses. *Proc. rock characterization, symp. Int. Soc. Rock Mech.: Eurock '92*, (ed. J.A. Hudson)*, 209-214. London: Brit. Geol. Soc.

Holland, C.T. and Gaddy. F.L. 1957. Some aspects of permanent support of overburden on coal beds. *Proc. W. Virginia Coal Mining Inst*. 43-66.

Holmberg, R. and Persson, P-A. 1980. Design of a tunnel perimeter blasthole pattern to prevent rock damage. *Trans. Instn Min. Metall. (Sect. A: Min. industry)* **89** , A37-40.

Hungr, O. and Evans, S.G. 1989. Engineering aspects of rockfall hazard in Canada. Geological Survey of Canada, Open File 2061, 102 pages.

Hunt, R.E. 1984. Slope failure risk mapping for highways: Methodology and case history. In *Rockfall prediction and Control and Landslide Case Histories.* Transportation Research Record, National Research Council, Washington, No. 1343. pp. 42-51.

Hunt, R.E.B. and Askew, J.E. 1977. Installation and design guidelines for cable dowel ground support at ZC/NBHC. *Proc. Underground Operators Conference, Broken Hill* , 113-22.

Hutchins, W.R., Bywater, S., Thompson, A.G. and Windson, C.R. 1990. A versatile grouted cable dowel reinforcing system for rock. *Proc. Aus. Inst. Min. Metall.* **1**, 25-29.

Hutchinson, D.J. and Diederichs, M.S. 1996. *Cablebolting in underground mines.* Vancouver: Bitech

Hyett, A.J., Bawden, W.F. and Coulson, A.L. 1992. Physical and mechanical properties of normal Portland cement pertaining to fully grouted cable bolts. In *Rock support in mining and underground construction*, *proc. int. symp. rock support,* Sudbury, (eds. P.K. Kaiser and D.R. McCreath), 341-348. Rotterdam: Balkema.

Hyett, A.J., Bawden, W.F. and Reichert, R.D. 1992. The effect of rock mass confinement on the bond strength of fully grouted cable bolts. *Int. J. Rock Mech. Min. Sci. & Geomech. Abstr*. **29**(5), 503-524.

Hyett, A.J., Bawden, W.F., Powers, R. and Rocque, P. 1993. The nutcase cable. In *Innovative mine design for the 21st century,* (eds W.F. Bawden and J.F. Archibald), 409-419. Rotterdam: Balkema.

Ide, J.M. 1936. Comparison of statically and dynamically determined Young's modulus of rock. *Proc. Nat. Acad. Sci.* **22** , 81- 92.

Iman, R.L., Davenport, J.M. and Zeigler, D.K. 1980. *Latin Hypercube sampling (A progam user's guide).* Technical Report SAND79-1473. Albuquerque, New Mexico: Sandia Laboratories.

Imrie, A.S. 1983. Taming the Downie Slide. *Canadian Geographic* **103**.

Imrie, A.S., D.P. Moore and E.G. Enegren. 1992. Performance and maintenance of the drainage system at Downie Slide. *Proc. 6th Int. Symp. on Landslides, Christchurch, New Zealand*, in press.

International Society for Rock Mechanics Commission on Standardisation of Laboratory and Field Tests. 1978. Suggested methods for the quantitative description of discontinuities in rock masses. *Int. J. Rock Mech. Min. Sci. & Geomech. Abstr.* **15**, 319-368.

International Society for Rock Mechanics. 1981. *Rock characterisation, testing and monitoring - ISRM suggested methods.* Oxford: Pergamon.

Jaeger, C. 1972. *Rock Mechanics and Engineering* . Cambridge: at the University Press 417 pages

Jaeger, J.C. 1971. Friction of rocks and stability of rock slopes. The 11th Rankine Lecture. *Géotechnique* **21**(2), 97-134.

Jaeger, J.C. and Cook, N.G.W. 1969. *Fundamentals of Rock Mechanics* . London: Chapman and Hall.

Jirovec. P. 1978. Wechselwirkung zwischen anker und gebirge. *Rock Mech.* Suppl. 7, 139-155.

John, K.W. 1968. Graphical stability analyses of slopes in jointed rock. *Proc. Soil Mech. Fndn Div.*, ASCE , SM2, paper no. 5865.

Kaiser, P.K., Hoek, E. and Bawden, W.F. 1990. A new initiative in Canadian rock mechanics research. *Proc. 31st US rock mech. symp.*, Denver, 11-14.

Kaiser, P.K., Yazici, S. and Nosé, J. 1992. Effect of stress change on the bond strength of fully grouted cables. *Int. J. Rock Mech.. Min. Sci. Geomech. Abstr.* **29**(3), 293-306.

Kemeny, J.M. and Cook, N.G.W. 1987. Crack models for the failure of rock under compression. In *Proc. 2nd int. conf. on constitutive laws for engineering materials, theory and applications*, (eds C.S. Desai, E. Krempl, P.D. Kiousis and T. Kundu) 1, 879-887. Tucson, AZ: Elsevier.

Kendorski, F., Cummings, R., Bieniawski, Z.T. and Skinner, E. 1983. Rock mass classification for block caving mine drift support. *Proc. 5th congr. Int. Soc. Rock Mech.*, Melbourne, B51-B63. Rotterdam: Balkema.

King, L.V. 1912. On the limiting strength of rocks under conditions of stress existing in the earth's interior. *J. Geol.* **20** , 119- 138.

Kirsch, G., 1898. Die theorie der elastizitat und die bedurfnisse der festigkeitslehre. *Veit. Deit. Ing.* **42** (28), 797-807.

Kirsten, H.A.D. 1992. Comparative efficiency and ultimate strength of mesh- and fibre-reinforced shotcrete as determined from full-scale bending tests. *J. S. Afr. Inst. Min. Metall*. Nov., 303-322.

Kirsten, H.A.D. 1993. Equivalence of mesh- and fibre-reinforced shotcrete at large deflections. *Can. Geotech. J.* **30**, 418-440.

Kompen, R. 1989. Wet process steel fibre reinforced shotcrete for rock support and fire protection, Norwegian practice and experience. In *Proc. underground city conf.*, Munich, (ed. D. Morfeldt), 228-237.

Ladanyi, B. and Archambault. G. 1970. Simulation of shear behaviour of a jointed rock mass. In *Rock mechanics - Theory and Practice, Proc. 11th Symp. on Rock Mechanics, Berkeley, 1969* , pp.105-25. New York: Society of Mining Engineers, AIME

Lajtai, E.Z. 1982. *The fracture of Lac du Bonnet granite*. Contract Report. Pinawa, Ontario: Atomic Energy of Canada.

Lajtai, E.Z. and Lajtai, V.N. 1975. The collapse of cavities. *Int. J. Rock Mech. Min. Sci. Geomech. Abstr.* **12,** 81-86.

Lang, T.A. 1961. Theory and practice of rockbolting. *Trans Amer. Inst. Min. Engrs* **220**, 333-348.

Langefors, U. and Khilstrom, B. 1973. *The modern technique of rock blasting* . 2nd edn. New York: Wiley. 405 pages

Langille, C.C. and Burtney, M.W. 1992. Effectiveness of shotcrete and mesh support in low energy rockburst conditions at INCO's Creighton mine. In *Rock support in mining and underground construction, proc. int. symp. rock support,* Sudbury, (eds. P.K. Kaiser and D.R. McCreath), 633-638. Rotterdam: Balkema.

Lappalainen, P., Pulkkinen, J. and Kuparinen, J. 1984. Use of steel strands in cable bolting and rock bolting. In *Rock bolting: theory and application in mining and underground construction*, (ed. O. Stephansson), 557-562. Rotterdam: Balkema.

Lau. J. S. O. and Gorski. B. 1991. *The post failure behaviour of Lac du Bonnet grey granite.* CANMET Divisional Report MRL 91-079(TR). Ottawa: Dept. Energy Mines and Resources, Canada.

Laubscher, D.H. 1977. Geomechanics classification of jointed rock masses - mining applications. *Trans. Instn. Min. Metall.* **86**, A1-8.

Laubscher, D.H. 1984. Design aspects and effectiveness of support systems in different mining conditions. *Trans Instn. Min. Metall.* **93**, A70 - A82.

Laubscher, D.H. and Taylor, H.W. 1976. The importance of geomechanics classification of jointed rock masses in mining operations. In *Exploration for rock engineering*, (ed. Z.T. Bieniawski) **1**, 119-128. Cape Town: Balkema.

Laubscher, D.M. and Page, C.H. 1990. The design of rock support in high stress or weak rock environments. *Proc. 92nd Can. Inst. Min. Metall. AGM*, Ottawa, Paper # 91.

Lauffer, H. 1958. Gebirgsklassifizierung für den Stollenbau. *Geol. Bauwesen* **24**(1), 46-51.

Leeman, E.R. and Hayes, D.J. 1966. A technique for determining the complete state of stress in rock using a single borehole. *Proc. 1st Cong. Int. Soc. Rock Mech, Lisbon* **2** , 17-24.

Lewis, M.R. and D.P. Moore. 1989. Construction of the Downie Slide and Dutchman's Ridge drainage adits. *Canadian Tunnelling* (ed. Z. Eisenstein), 163-172. Vancouver: Bi-Tech

Lin, D and Fairhurst, C. 1988. Static analysis of the stability of three-dimensional blocky systems around excavations in rock. *Int. J. Rock Mech. Min. Sci. & Geomech. Abstr.* **25** (3), 139-147.

Liu, S.C., Y. Cheng and C.T. Chang. 1988. Design of the Mingtan cavern. *Proc .symp. ISRM. on Rock Mech. and Power Plants, Madrid*, 199-208.

Londe, P. 1965. Une methode d'analyse a trois dimensions de la stabilite d'une rive rocheuse. *Annales des Ponts et Chaussees* **135** (1), 37-60.

Londe, P., Vigier, G. and Vormeringer, R. 1969. The stability of rock slopes, a three-dimensional study. *J. Soil Mech. Foundns Div., ASCE* **95** (SM 1), 235-262.

Londe, P., Vigier, G. and Vormeringer, R. 1970. Stability of slopes - graphical methods. *J. Soil Mech. Fndns Div., ASCE* **96** (SM 4), 1411-1434.

Lorig, L.J. and Brady, B.H.G. 1984. A hybrid computational scheme for excavation and support design in jointed rock media. In *Design and performance of underground excavations*, (eds E.T. Brown and J.A. Hudson), 105-112. London: Brit. Geotech. Soc.

Løset, F. 1992. Support needs compared at the Svartisen Road Tunnel. *Tunnels and Tunnelling,* June.

Lottes, G. 1972. The development of European pumped-storage plants. *Water Power* **24** , 22-33.

Love, A.E.H. 1927. *A treatise on the mathematical theory of elasticity*. New York: Dover.

Lutton, R.J., Banks, D.C. and Strohm, W.E. 1979. Slides in the Gaillard Cut, Panama Canal Zone. In *Rockslides and Avalanches* (ed. B. Voight) **2** , pp. 151-224. New York: Elsevier

Mahar, J.W., Parker, H.W. and Wuellner, W.W. 1975. *Shotcrete practice in underground construction*. US Dept. Transportation Report FRA-OR&D 75-90. Springfield, VA: Nat. Tech. Info. Service.

Marachi, N.D., Chan, C.K. and Seed, H.B. 1972. Evaluation of properties of rockfill materials. *J. Soil Mechs. Fdns. Div. ASCE* **98**(SM4), 95-114.

Marshall, D. 1963. Hangingwall control at Willroy. *Can. Min. Metall. Bull*. **56**, 327-331.

Martin, C.D. 1990. Characterizing in situ stress domains at the AECL Underground Research Laboratory. *Can. Geotech. J.* **27**, 631-646.

Martin, C.D. 1993. *The strength of massive Lac du Bonnet granite around underground openings*. Ph.D. thesis, Winnipeg, Manitoba: Dept. Civil Engineering, University of Manitoba.

Martin, C.D. and Simmons, G.R. 1992. The Underground Research Laboratory, an opportunity for basic rock mechanics. *ISRM News Journal* **1**(1), 5-12.

Masur, C.I. and Kaufman, R.I. 1962. Dewatering. In *Foundation Engineering* (ed. G.A. Leonards), pp. 241-350. New York: McGraw- Hill

Mathews, K.E. and Edwards, D.B. 1969. Rock mechanics practice at Mount Isa Mines Limited, Australia. *Proc. 9th Commonwealth min. metall. congr.,* Paper 32. London: Instn Min. Metall.

Mathews, K.E., Hoek, E., Wyllie, D.C. and Stewart, S.B.V. 1981. *Prediction of stable excavations for mining at depth below 1000 metres in hard rock*. CANMET Report DSS Serial No. OSQ80-00081, DSS File No. 17SQ.23440-0-9020. Ottawa: Dept. Energy, Mines and Resources.

Mathews, S.M., Tillman, V.H. and Worotnicki, G. 1983. A modified cablebolt system for support of underground openings. *Proc. Aust. Inst. Min. Metall. annual conf.,* Broken Hill. 243-255.

Matthews, S.M., Thompson, A.G., Windsor, C.R. and O'Bryan, P.R. 1986. A novel reinforcing system for large rock caverns in blocky rock masses. In *Large rock caverns,* (ed. K.H.O. Saari) **2,** 1541-1552. Oxford: Pergamon.

McCreath, D.R. and Kaiser, P.K. 1992. Evaluation of current support practices in burst-prone ground and preliminary guidelines for Canadian hardrock mines. In *Rock support in mining and underground construction, proc. int. symp. rock support,* Sudbury, (eds P.K. Kaiser and D.R. McCreath), 611-619. Rotterdam: Balkema.

McIntyre, J.S. and Hagan, T.N. 1976. The design of overburden blasts to promote highwall stability at a large strip mine. *Proc. 11th Canadian Rock Mech. Symp. , Vancouver.*

McMahon, B.K. 1971. A statistical method for the design of rock slopes. *Proc. 1st Australia-New Zealand Conf. on Geomechanics, Melbourne* **1** , 314-321.

McMahon, B.K. 1975. Probability of failure and expected volume of failure in high rock slopes. *Proc. 2nd Aust.-New Zealand Conf. on Geomech., Brisbane*.

Merritt, A.H. 1972. Geologic prediction for underground excavations. *Proc. North American. rapid excav. tunneling conf.*, Chicago, (eds K.S. Lane and L.A. Garfield) **1,** 115-132. New York: Soc. Min. Engrs, Am. Inst. Min. Metall. Petrolm Engrs.

Moore, D.P., A.S. Imrie and D.G. Baker. 1991. Rockslide risk reduction using monitoring. *Proc. Can. Dam Safety Assoc. Annual Meeting, Whistler, British Columbia*, in press.

Moretto, O. 1982. Mecánica de rocas en el complejo hidroeléectrico Río Grande No. 1. *Proc. Primer. Cong. Sudamericano de Mecánica de Rocas, Bogotá, Colombia.*

Morgan, D.R. 1993. Advances in shotcrete technology for support of underground openings in Canada.In *Shotcrete for underground support V*, *proc. engineering foundation conf.*, Uppsala, (eds J.C. Sharp and T. Franzen), 358-382. New York: Am. Soc. Civ. Engrs.

Morgan, G.C. 1991. Qualification of risks from slope hazards. In *Landslide Hazards in the Canadian Cordillera.* Geological Association of Canada, Special Publication.

Morgan, G.C., Rawlings, G.E. and Sobkowicz, J.C. 1992. Evaluation of total risk to communities from large debris flows. *Geotechnical and Natural Hazards,* Vancouver Geotechnical Society and Canadian Geotechnical Society, Vancouver, BC, Canada, May 6-9, 1992, pp. 225—236.

Morgenstern, N.R. 1991. Limitations of stability analysis in geo-technical practice. *Geotecnia* **61**: 5-19.

Morrison, R.G.K. 1942. Report on the rockburst situation in Ontario mines. *Trans. Can. Inst. Min. Metall.* **45** .

Morrison, R.G.K. 1976. *A philosophy of ground control: a bridge between theory and practice .* rev. edn. Montreal: Department of Mining and Metallurgical Engineering, McGill University 182 pages

Morriss, P. and Stoter, H.J. 1983. Open-cut slope design using probabilistic methods. *Proc. 5th. Cong. ISRM., Melbourne* **1** , C107-C113. Rotterdam: Balkema

Moy D., Hsieh C.S. and Li, H.C. 1990. The introduction of steel fiber shotcrete to underground cavern support in Taiwan. *Shotcrete for Underground Support, Proc. of the Engineering Foundation Conf. on Shotcrete* V , *Uppsala, Sweden.* in press

Moy, D. and Hoek, E. 1989. Progress with the excavation and support of the Mingtan power cavern roof. *Proc. Rock Cavern Seminar - Hong Kong* (eds A.W. Malone and P.G.D. Whiteside), pp. 235-245. London: Institution Mining and Metallurgy

Muller, J. 1979. Josef Stini. Contributions to engineering geology and slope movement investigations. In *Rockslides and Avalanches* (ed. B. Voight), Part 2, pp. 95-109. New York: Elsevier

Muskhelishvili, N.I. 1953. *Some basic problems of the mathematical theory of elasticity.* 4th edn, translated by J.R.M. Radok. Gronigen: Noordhoff.

Nguyen, V. U. and Chowdhury, R.N. 1985. Simulation for risk analysis. *Geotechnique* **35**(1), 47-58.

Nickson, S.D. 1992. *Cable support guidelines for underground hard rock mine operations.* MASc. thesis, Dept. Mining and Mineral Processing, University of British Columbia.

Nielsen, N.M., Hartford, D.N.D. and MacDonald. 1994. Selection of tolerable risk criteria for dam safety decision making. *Proc. 1994 Canadian Dam Safety Conference, Winnipeg, Manitoba.* Vancouver: BiTech Publishers, pp 355-369.

Obert, L and Duvall, W.I. 1967. *Rock Mechanics and the Design of Structures in Rock .* New York: Wiley 65 pages

Ortlepp, D.W. 1992. The design of the containment of rockburst damage in tunnels - an engineering approach. In *Rock support in mining and underground construction, proc. int. symp. on rock support,* Sudbury, (eds P.K. Kaiser and D.R. McCreath), 593-609. Rotterdam: Balkema.

Ortlepp, D.W. and Gay, N.C. 1984. Performance of an experimental tunnel subjected to stresses ranging from 50 MPa to 230 MPa. *Proc. symp. ISRM on Design and Performance of Underground Excavations, Cambridge.* pp.337-346. London: British Geotechnical Society

Ortlepp, W. D.1993. Invited lecture: The design of support for the containment of rockburst damage in tunnels - an engineering approach. In *Rock support in mining and*

underground construction, proc. int. symp. on rock support, Sudbury,(eds P.K. Kaiser and D.R. McCreath), 593-609. Rotterdam: Balkema.

Ortlepp, W.D., 1993. A philosophical consideration of support requirements in civil and mining tunnels. In *TUNCON '93, Proc. symp. Aspects of Control in Tunnelling, Johannesburg.* 49-54.

Otter, J.R.H., Cassell, A.C. and Hobbs, R.E. 1966. Dynamic relaxation. *Proc. Instn Civ. Engrs* **35**, 633-665.

Pacher, F., Rabcewicz, L. and Golser, J. 1974. Zum der seitigen Stand der Gebirgsklassifizierung in Stollen-und Tunnelbau. *Proc. XXII Geomech. colloq.,* Salzburg, 51-58.

Palmström, A. 1982. The volumetric joint count - a useful and simple measure of the degree of rock jointing. *Proc. 4th congr. Int. Assn Engng Geol.*, Delhi **5**, 221-228.

Patton, F.D. 1966. Multiple modes of shear failure in rock. *Proc. 1st congr. Int. Soc. Rock Mech.*, Lisbon **1**, 509-513.

Pearce G.E. 1988. Report on the Proc. 5th Int. Tunnelling Symp., Tunnelling 88, *Trans Instn Min. Metall. (Sect. A: Min. industry)* **97** , A149-159.

Pelli, F., Kaiser, P.K. & Morgenstern, N.R. 1991. An interpretation of ground movements recorded during construction of the Donkin-Morien tunnel. *Can. Geotech. J.* **28**(2), 239-254

Pierson, L.A., Davis, S.A. and Van Vickle, R. 1990. Rockfall Hazard Rating System Implementation Manual. Federal Highway Administration (FHWA) Report FHWA-OR—EG-90-01. FHWA, U.S. Department of Transportation.

Pine. R.J. 1992. Risk analysis design applications in mining geomechanics. *Trans. Inst. Min. Metall.* (Sect.A) **101,** 149-158.

Potvin, Y. 1988. *Empirical open stope design in Canada*. Ph.D. thesis, Dept. Mining and Mineral Processing, University of British Columbia.

Potvin, Y. and Milne, D. 1992. Empirical cable bolt support design. In *Rock Support in mining and underground construction, proc. int. symp. on rock support*, Sudbury, (eds P.K. Kaiser and D.R. McCreath), 269-275. Rotterdam: Balkema.

Potvin, Y., Hudyma, M.R. and Miller, H.D.S. 1989. Design guidelines for open stope support. *Bull. Can. Min. Metall.* **82**(926), 53-62.

Priest, S.D. and E.T. Brown. 1983. Probabilistic stability analysis of variable rock slopes. *Trans. Inst. Min. Metall.*(Sect. A*)* **92**: 1-12.

Rabcewicz, L. 1969. Stability of tunnels under rock load. *Water Power* **21**(6-8) 225-229, 266-273, 297-304.

Read, J.R.L. and Lye, G.N. 1983. Pit slope design methods, Bougainville Copper Limited open cut. *Proc. 5th Cong. ISRM., Melbourne* pp. C93-C98. Rotterdam: Balkema.

Riemer, W., Pantzartzis, P., Krapp, L. and Scourtis. C.. Investigation and monitoring of landslides at the Polyphyton project in Greece. *Proc. Intnl. Symposium on Landslides, Trondheim.* 1996

Ritchie, A.M., 1963. The evaluation of rockfall and its control. *Highway Record.* Vol 17.

Ritter, W. 1879. *Die Statik der Tunnelgewölbe.* Berlin: Springer.

Robbins, R.J. 1976. Mechanized tunnelling - progress and expectations: 12th Sir Julius Werhner Memorial Lecture. In *Tunnelling '76* (ed. M.J. Jones), xi-xx. London: Institution Mining and Metallurgy

Rose, D. 1985. Steel fibre reinforced shotcrete for tunnel linings: the state of the art. *Proc. North American rapid excav. tunneling conf.* **1***,* 392-412. New York: Soc. Min. Engrs, Am. Inst. Min. Metall. Petrolm Engrs.

Rosenbleuth, E. 1981. Two-point estimates in probabilities*. J. Appl. Math. Modelling* **5**, October, 329-335.

Salamon, M.D.G. 1974. Rock mechanics of underground excavations. In *Advances in rock mechanics , Proc. 3rd Cong.ISRM., Denver* **1B** , pp.951-1009. Washington, DC: National Academy of Sciences

Salamon, M.D.G. and Munro, A.H. 1967. A study of the strength of coal pillars. *J. S. Afr. Inst. Min. Metall.* **65** , 55- 67.

Salamon. M.D.G. and Oravecz. K.I. 1976. *Rock mechanics in coal mining.* Johannesburg: Chamber of Mines of South Africa. 119 pages

Sarma, S.K. 1979. Stability analysis of embankments and slopes. *J. Geotech. Eng. Div., ASCE.* **105** (GT12), 1511- 1524.

Savin, G.N. 1961. *Stress concentrations around holes.* London: Pergamon.

Schmuck, C.H. 1979. Cable bolting at the Homestake gold mine. *Mining Engineering,* December, 1677-1681.

Scott, J.J. 1976. Friction rock stabilizers - a new rock reinforcement method. In *Monograph on rock mechanics applications in mining*, (eds W.S. Brown, S.J. Green and W.A. Hustrulid), 242-249. New York: Soc. Min. Engrs, Am. Inst. Min. Metall. Petrolm Engrs.

Scott, J.J. 1983. Friction rock stabilizer impact upon anchor design and ground control practices. In *Rock bolting: theory and application in underground construction*, (ed. O. Stephansson), 407-418. Rotterdam: Balkema.

Serafim, J.L. and Pereira, J.P. 1983. Consideration of the geomechanical classification of Bieniawski. *Proc. int. symp. on engineering geology and underground construction*, Lisbon **1**(II), 33-44.

Shah, S. 1992. *A study of the behaviour of jointed rock masses.* Ph.D. thesis, Dept. Civil Engineering, University of Toronto.

Sharp, J.C., Smith, M.C.F., Thoms, I.M. and Turner, V.D. 1986. Tai Koo Cavern, Hong Kong - performance of a large metro excavation in a partially weathered rock mass. *In Large Rock Caverns* (ed. K.H.O. Saari). **1** , pp. 403-423. Oxford: Pergamon

Sheory, P.R. 1994. A theory for in situ stresses in isotropic and transversely isotropic rock. *Int. J. Rock Mech. Min. Sci. & Geomech. Abstr.* **31**(1), 23-34.

Shi G.H. and Goodman R.E. 1989. The key blocks of unrolled joint traces in developed maps of tunnel walls. *Int. J. Numerical and Analytical Methods in Geomechanics* **13** , 131-158.

Shi G.H. and Goodman, R.E. 1981. A new concept for support of underground and surface excavations in discontinuous rocks based on a keystone principle. In *Rock mechanics from Research to Applications, Proc. 22nd. U.S. Symp. for Rock Mechanics, Cambridge.* pp. 290- 296. Cambridge, Mass.: Massachusetts Institute for Technology

Silveira, A.F. 1990. Some considerations on the durability of dams. *Water Power and Dam Construction*, 19-28.

Soos, I.G.K. 1979. Uplift pressures in hydraulic structures. *Water Power and Dam Construction.* **31**(5) 21-24.

Spang, R.M. and Rautenstrauch, R.W. 1988. Empirical and mathematical approaches to rockfall prediction and their practical applications. *Proc. 5th International Symposium on Landslides, Lusanne.* Vol. 2. 1237-1243.

Startzman, R.A. and Wattenbarger, R.A. 1985. An improved computation procedure for risk analysis problems with unusual probability functions. *Proc. symp. Soc. Petrolm Engrs hydrocarbon economics and evaluation,* Dallas.

Stillborg, B. 1994. *Professional users handbook for rock bolting,* 2nd edn. Clausthal-Zellerfeld: Trans Tech Publications.

Svanholm, B.O., Persson, P-A. and Larsson. B. 1977. Smooth blasting for reliable underground openings. In *Storage in excavated rock caverns, Rockstore 77: Storage* (ed. M. Bergman) **3** , pp. 573-579. Oxford: Pergamon

Talobre, J. 1957. *La mecanique des roches* . Paris: Dunod

Tatchell, G.E. 1991. Automatic data acquisition systems for monitoring dams and landslides. *Proc. 3rd Int. symp. on Field Measurements in Geomechanics, Oslo, Norway.* in press.

Terzaghi, K. 1925. Erdbaumechanik auf Bodenphysikalischer Grundlage. Vienna: Franz Deuticke.

Terzaghi, K. 1936. Presidential Address. *Proc. 1st Int. Conf. for Soil Mechanics and Foundations Engineering, Cambridge, Mass*. **1** , 22-3.

Terzaghi, K. 1945. Stress conditions for the failure of saturated concrete and rock. *Proc. Am. Soc. Test. Mater.* **45** , 777-801.

Terzaghi, K. 1946. Rock defects and loads on tunnel supports. In *Rock tunneling with steel supports,* (eds R. V. Proctor and T. L. White) **1**, 17-99. Youngstown, OH: Commercial Shearing and Stamping Company.

Terzaghi, K. and Richart, F.E. 1952. Stresses in rock about cavities. *Geotechnique* **3**, 57-90.

Terzaghi, R. and Voight, B. 1979. Karl Terzaghi on rockslides: the perspective of a half-century. In *Rockslides and Avalanches* (ed. B. Voight), Part 2, pp. 111-131. New York: Elsevier

Thorn, L.J. and Muller, D.S. 1964. Prestressed roof support in underground engine chambers at Free State Geduld Mines Ltd. *Trans. Assn Mine Mngrs S. Afr.*, 411-428.

Tyler, D.B., Trueman, R.T. and Pine, R.J. 1991. Rockbolt support design using a probabilistic method of key block analysis. In *Rock mechanics as a multidisciplinary science*, (ed. J.C. Roegiers), 1037-1047. Rotterdam: Balkema.

Tyler. D.B., Trueman. R. and Pine. R.J. 1991. Rockbolt support design using a probabilistic method of key block analysis. *Proc. 32nd U.S. Symp. Rock Mechanics, Norman, Oklahoma,* 1037-47.

Vandewalle, M. 1993. *Dramix: Tunnelling the world.* 3rd edn. Zwevegem, Belgium: N.V. Bekaert S.A.

Vanmarcke, E.H. 1980. Probalistic analysis of earth slopes. *Engineering Geology* **16**: 29-50.

Varnes, D.J. 1984. Landslide hazard zonation: a review of principles and practice. *Natural Hazards 3.* UNESCO, Paris, 63 pages.

Vogele, M., Fairhurst, C. and Cundall, P.A. 1978. Analysis of tunnel support loads using a large displacement, distinct block model. In *Storage in excavated rock caverns* (ed. M. Bergman) **2**, pp. 247-252. Oxford: Pergamon

von Karman. Th. 1911. Festigkeitsversuche unter allseitigem Druck. *Zeit d Ver Deutscher Ing.* **55** , 1749-1757.

von Kimmelmann, M.R., Hyde, B. and Madgwick, R.J. 1984. The use of computer applications at BCL Limited in planning pillar extraction and the design of mine layouts. In *Design and performance of underground excavations*, (eds E.T. Brown and J.A. Hudson), 53-64. London: Brit. Geotech. Soc.

VSL Systems Ltd. 1982. Slab post tensioning. 12p. Switzerland.

Warburton, P.M. 1981. Vector stability analysis of an arbitrary polyhedral block with any number of free faces. *Int. J. Rock Mech. Min. Sci. & Geomech. Abstr.* **18** , 415-427.

Whitman. R.V. 1984. Evaluating calculated risk in geotechnical engineering. *J. Geotech. Enng, ASCE* **110**(2), 145-186.

Wickham, G.E., Tiedemann, H.R. and Skinner, E.H. 1972. Support determination based on geologic predictions. In *Proc. North American rapid excav. tunneling conf.*, Chicago, (eds K.S. Lane and L.A. Garfield), 43-64. New York: Soc. Min. Engrs, Am. Inst. Min. Metall. Petrolm Engrs.

Windsor, C.R. 1990. *Ferruled strand.* Unpublished memorandum. Perth: CSIRO.

Windsor, C.R. 1992. Cable bolting for underground and surface excavations. In *Rock support in mining and underground construction, proc. int. symp. on rock support*, Sudbury, (eds P.K. Kaiser and D.R. McCreath), 349-376. Rotterdam: Balkema.

Wittke, W.W. 1965. Method to analyse the stability of rock slopes with and without additional loading. (in German) *Felsmechanik und Ingerieurgeologie* , Supp. 11, **30** , 52-79. English translation in Imperial College Rock Mechanics Research Report , no. 6, July 1971.

Wood, D.F. 1992. Specification and application of fibre reinforced shotcrete. In *Rock support in mining and underground construction, proc. int. symp. on rock support*, Sudbury, (eds. P.K. Kaiser and D.R. McCreath), 149-156. Rotterdam: Balkema.

Wood, D.F., Banthia, N. and Trottier, J-F. 1993. A comparative study of different steel fibres in shotcrete. *In Shotcrete for underground support VI,* Niagara Falls, 57-66. New York: Am. Soc. Civ. Engrs.

Worotnicki, G. and Walton, R.J. 1976. Triaxial 'hollow inclusion' gauges for determination of rock stresses in situ. *Proc symp. ISRM on Investigation of Stress in Rock, Sydney* . Supplement 1-8. Sydney: Institution of Engineers, Australia .

Yazici, S. and Kaiser, P.K. 1992. Bond strength of grouted cable bolts. *Int J. Rock Mech. Min. Sci. & Geomech. Abstr*. **29**(3), 279-292.

Zheng, Z., Kemeny, J. and Cook, N.G.W. 1989. Analysis of borehole breakouts. *J. Geophys. Res*. **94**(B6), 7171-7182.

Zoback, M. L. 1992. First- and second-order patterns of stress in the lithosphere: the World Stress Map Project. *J. Geophys. Res*. **97**(B8), 11761-11782.